

Department of

Civil Engineering

College of Engineering

The University of Iowa

Iowa City, Iowa

Consolidation of Loess

by

Harrison Kane

Final Report

Research Project HR-144

Iowa State Highway Commission

Report No. 71-2

July 1971

CONSOLIDATION OF LOESS

by

Harrison Kane
Professor of Civil Engineering
The University of Iowa

Final Report
Research Project HR-144
Iowa State Highway Commission

The opinions, findings and conclusions expressed
in this publication are those of the author
and not necessarily those of the
Iowa State Highway Commission

REPORT 71-2

DEPARTMENT OF CIVIL ENGINEERING
THE UNIVERSITY OF IOWA
IOWA CITY, IOWA

July, 1971

FOREWORD

This is the final report on the research performed in the Department of Civil Engineering at the University of Iowa for the Iowa State Highway Commission under Research Project HR-144. The principal investigator was assisted by Mr. Altaf ur Rahman and Mr. Bharat Mathur, Graduate Research Assistants.

ABSTRACT

Effective stress paths for a loessial soil subject to collapse during confined compression have been determined from the results of a testing program consisting of (1) confined compression tests on natural samples of loess with initial water contents ranging from air-dry to saturation, (2) negative pore-water pressure measurements to -300 psi during these tests, and (3) K_0 -tests in which the lateral stress ratio was measured for one-dimensional strain.

Before collapse, K_0 was found to average 0.23, an extremely low value for a loose soil, whereas after collapse, K_0 increased to 0.54, which is consistent with values for other soils. Because of the low K_0 -values before collapse, the effective stress path for loading in confined compression initially approaches the failure envelope. At collapse the stress path intersects the failure envelope and thereafter it changes direction as a consequence of the higher K_0 -value after collapse.

From the stress path interpretation of the results, it is demonstrated that the collapse mechanism of loess in confined compression and during wetting is a shear phenomenon and subject to analysis in terms of effective stresses.

TABLE OF CONTENTS

<u>Chapter</u>		<u>Page</u>
1.	INTRODUCTION	1
1.1	General Nature of the Problem	1
1.2	Properties of Loess	1
1.3	Behavior of Loess Under Compression	2
1.4	Scope of This Study	4
2.	SOIL INDEX PROPERTIES AND SAMPLING PROCEDURES	6
2.1	Soil Index Properties	6
2.2	Sampling and Preparation of Test Specimens	6
3.	LABORATORY TESTS	11
3.1	Introduction	11
3.2	Confined Compression Tests	11
3.3	K_o - Tests	50
3.4	Triaxial Compression Tests	52
4.	DISCUSSION OF TEST RESULTS	56
4.1	General Comparisons	56
4.2	Volume Changes and Strains	58
4.3	Pore-Water Pressures	63
4.4	Special Tests	70
4.5	Summary	72

TABLE OF CONTENTS (Continued)

<u>Chapter</u>		<u>Page</u>
5.	ANALYSIS OF MECHANICAL BEHAVIOR . . .	76
5.1	Introduction	76
5.2	Effective Stresses	78
5.3	Effective Stresses at Collapse During Confined Compression	81
5.4	Effective Stress Paths	89
6.	SUMMARY AND CONCLUSIONS	102
6.1	Summary	102
6.2	Conclusions	103
APPENDIX I.	REFERENCES	106
APPENDIX II.	NOTATION	108
APPENDIX III.	CONFINED COMPRESSION TEST RESULTS	110
APPENDIX IV.	K_0 -TEST REPORT	137

LIST OF TABLES

<u>Table</u>	<u>Page</u>
2.1 Soil Index Properties	7
3.1 Summary of Confined Compression Tests	47
3.2 Summary of Special Consolidation Tests	49
3.3 Summary of K_o -Tests	53
3.4 Summary of Triaxial Compression Tests	54
4.1 Strains Due to Wetting	73

LIST OF FIGURES

<u>Figure</u>	<u>Page</u>
2.1 Grain Size Distribution, Oakdale Loess	8
3.1 Confined Compression Cell	13
3.2 Effect of Entrapped Air on Pressure Response Time	16
3.3 Results of Confined Compression Test No. 3	22
3.4 Results of Confined Compression Test No. 4	23
3.5 Results of Confined Compression Test No. 5	24
3.6 Results of Confined Compression Test No. 6	25
3.7 Results of Confined Compression Test No. 7	26
3.8 Results of Confined Compression Test No. 11. . . .	27
3.9 Results of Confined Compression Test No. 13. . . .	28
3.10 Results of Confined Compression Test No. 14. . . .	29
3.11 Results of Confined Compression Test No. 15. . . .	30
3.12 Results of Confined Compression Test No. 16. . . .	31
3.13 Results of Confined Compression Test No. 17. . . .	32
3.14 Results of Confined Compression Test No. 18. . . .	33
3.15 Results of Confined Compression Test No. 19. . . .	34
3.16 Results of Confined Compression Test No. 20. . . .	35
3.17 Results of Confined Compression Test No. 21. . . .	36
3.18 Results of Confined Compression Test No. 22. . . .	37
3.19 Results of Confined Compression Test No. 23. . . .	38

LIST OF FIGURES (Continued)

<u>Figure</u>		<u>Page</u>
3.20	Results of Confined Compression Test No. 24. . .	39
3.21	Results of Confined Compression Test No. S1. . .	40
3.22	Results of Confined Compression Test No. S2. . .	41
3.23	Results of Confined Compression Test No. S3. . .	42
3.24	Results of Confined Compression Test No. S4. . .	43
3.25	Results of Confined Compression Test No. S5. . .	44
3.26	Results of Confined Compression Test No. S6. . .	45
3.27	Results of Confined Compression Test No. S7. . .	46
3.28	Definition of Collapse Stress σ_{vc}	51
3.29	Failure Envelope for Oakdale Loess Based on Total Stresses	55
4.1	Comparison of Confined Compression Test Results .	57
4.2	Relations From Confined Compression Tests . . .	59
4.3	Stress-Strain Curves for Confined Compression Tests Nos. 14, 21, and 22	61
4.4	Comparison of $(\sigma_v)_2$ with σ_{vc}	62
4.5	Relation Between Initial Pore-Water Pressure and Water Content	64
4.6	Pore-Water Pressure vs Degree of Saturation During Confined Compression	65
4.7	Pore-Water Pressure vs Vertical Stress During Confined Compression.	67
4.8	Pore-Water Pressure vs Collapse Stress	69
4.9	Comparison of Special With Basic Confined Compression Tests	71

LIST OF FIGURES (Continued)

<u>Figure</u>		<u>Page</u>
4.10	Compressive Strains Due to Wetting	74
5.1	Stress Path for Confined Compression	77
5.2	Relations Between x and S_r	80
5.3	Failure Envelope for Oakdale Loess Based on Effective Stresses	83
5.4	Procedure for Determining the Pore Pressure u	85
5.5	x vs S_r for Oakdale Loess Based on Individual Test r Results	87
5.6	x vs S_r for Oakdale Loess Based on Average Test r Results	88
5.7	Effective Stress Paths for Confined Compression of Loess	90
5.8	Effective Stress Path for Confined Compression Test No. 7	93
5.9	Effective Stress Path for Confined Compression Test No. 9	94
5.10	Effective Stress Path for Confined Compression Test No. 11	95
5.11	Effective Stress Path for Confined Compression Test No. 12	96
5.12	Effective Stress Path for Confined Compression Test No. 14	97
5.13	Effective Stress Path for Confined Compression Test No. S2	98
5.14	Effective Stress Path for Confined Compression Test No. S1	99
5.15	Effective Stress Path for Confined Compression Test No. S5	100

CHAPTER 1

INTRODUCTION

1.1 General Nature of the Problem

Foundations and embankments supported on loess have been known to undergo large settlements. It has been recognized that these settlements are the result of a collapse of the loose structure of the natural soil. The degree of uncertainty associated with predictions of this collapse is illustrated by the fact that there were six empirical criteria for determining susceptibility to collapse described at a recent state of the art session (Northey, 1969).

This research has been undertaken to study and describe, quantitatively, the mechanisms involved in the collapse phenomenon. Supporting data incorporates two quantities which have not previously been measured in this context: the negative pore-water pressure and the lateral stress ratio, both measured during confined compression.

1.2 Properties of Loess

Loess is a wind-deposited sediment transported from the flood plains of glacial rivers. The natural, undisturbed loess is a loose, open-structured soil composed of silt particles separated by clay coatings or aggregates of clay particles (Larionov, 1965; Gibbs and Holland, 1960). A typical midwestern loess has a clay content of 10% to 30%,

with water contents from 5% to 30% and densities from 70 pcf to 90 pcf (Sheeler, 1968). The significant properties in this study are (1) the low natural density which permits the occurrence of large volume changes, (2) the bond strength provided by the clay coatings, and (3) the changes in this bond strength that occur with changes in water content.

Compression of loess occurs when the stress between particles exceeds the bond strength provided by the clay coatings. This may be caused by an increase in stress due to an applied load, or by a decrease in strength due to swelling and softening of the clay binder after wetting. The loss of strength on wetting has been recognized for some time (e.g. Holz and Gibbs, 1951). A recent description of this behavior has been given by V. G. Berenzantzev, et al. (1969). In this paper the subsidence deformation below a foundation is shown to occur in a zone where the shear strength has decreased as a result of wetting to the level of the existing shear stresses. The amount of settlement depends also on the water content before wetting. Studies by Bally (1961) demonstrated large compressive strains upon wetting of air-dry loess but small strains for the same soil at an initial water content of 24%. Similar observations have been made by others.

1.3 Behavior of Loess Under Compression

The significant variables which are involved in the above phenomena are:

- Initial variables:
- a. Structure
 - b. Clay percentage
 - c. Void ratio
 - d. Water content
 - e. Negative pore-water pressure
 - f. Pore-air pressure

Variables during compression:

- a. Applied stress
- b. Void ratio
- c. Water content
- d. Negative pore-water pressure
- e. Pore-air pressure

The concept of an effective stress (Bishop, 1960) has been used to explain the behavior of partly saturated soils (Bishop and Blight, 1963; Burland, 1965). The effective stress is expressed as a function of the applied stress, the pore-water pressure, and the pore-air pressure. Interpretations in terms of effective stresses normally separate shear strength and volume change behavior (Bishop and Blight, 1963). In the case of isotropic compression no external shear is applied and this test has been used in studies of effective stresses for volume change. Actually, volume changes in loess are accompanied by the shifting of particles with respect to each other and shearing stresses between the particles develop whether or not an external stress difference is applied. An isotropic change in the effective stress may also be caused by changes in pore-water pressure; for example, wetting will increase the pore-water pressure and thus decrease the effective stress. This would normally be expected to produce a volume expansion but, as previously noted, in the case of loess wetting can cause a collapse of the soil structure and

a decrease in volume. Because of this, the general applicability of effective stresses to the behavior of partly saturated soils has been questioned (Burland, 1965).

For the study of the collapse behavior of loess, a confined compression test has several advantages over the isotropic compression test. In the former, shear stresses develop as a result of the difference between the applied vertical and horizontal stresses. The magnitude of these shear stresses can be determined and related to the measured volume changes and the shear strength. There are two additional advantages to the confined compression test. First the mechanics of applying the loads and measuring the volume change are simpler and second, the stress conditions more nearly duplicate a real field loading condition. For these reasons, the confined compression test was chosen for this study.

1.4 Scope of this Study

The purpose of this research is to describe the mechanisms involved with the confined compression of loess before, during, and after the collapse of the soil's natural structure. Knowledge of these mechanisms will assist the soils engineer in arriving at design decisions for foundations on loess. For example, it will be possible for the engineer to make a reasonable estimate of whether or not large settlements of an embankment or structure supported on loess will occur during loading or during subsequent natural changes in water content.

To provide the data for interpreting the behavior of the soil, two special types of tests were run: (1) confined compression tests in which the negative pore-water pressure was measured during the course of the tests utilizing a specially constructed cell, and (2) a special series of tests in which the lateral stress ratio (the ratio of the horizontal to the vertical stress) was measured in a triaxial compression cell under a zero-lateral-strain condition (K_0 -tests).

All of the tests have been run on samples from a single site and the properties of the soil are presented in Chapter 2. The equipment, test procedures, and test results for the confined compression tests, K_0 -tests, and strength tests are given in Chapter 3 and the results and interrelationships among the various measured quantities are discussed in Chapter 4.

In Chapter 5, the mechanical behavior of the soil is analyzed. The results of this analysis lead to quantitative effective stress paths for the confined compression tests which provide a new insight into the collapse phenomenon. In the final chapter, the work is summarized and the conclusions are presented.

Four appendices are included. In Appendices I and II, the references and notation are listed. The detailed results from each of the confined compression tests are tabulated in Appendix III to support the interpretations in the body of this report. Finally, Appendix IV is a detailed report on the K_0 -tests which were conducted as a separate study. The key results from this appendix are summarized in Chapter 3.

CHAPTER 2

SOIL INDEX PROPERTIES AND SAMPLING PROCEDURES

2.1 Soil Index Properties

The undisturbed soil samples were obtained from a road cut in a loess deposit on the Oakdale campus of the University of Iowa, just west of Iowa City. Index properties for the Oakdale loess are listed in Table 2.1 and the grain size distribution curve is shown in Fig. 2.1.

For comparison, Table 2.1 also lists the range in index properties for loess in Iowa as summarized by Sheeler (1968). The natural dry density of the Oakdale loess is relatively high for loessial soils in Iowa. Densities in east-central Iowa from 80 pcf to 90 pcf have been reported by Lyon, Handy, and Davidson (1954) and, as noted in Table 2.1, densities as low as 66 pcf have been measured. On the basis of the comparison to Table 2.1, the Oakdale loess is described as a relatively dense, silty loess of low plasticity.

2.2 Sampling and Preparation of Test Specimens

Hand-carved blocks of soil, 8 in. by 10 in. by 10 in. were removed from the test pit, wrapped in plastic, and transported directly to the laboratory by automobile. Upon arrival at the laboratory, the blocks were divided into smaller samples 2 in. thick by 4 in. in diameter for the consolidation test specimens, and 5 in. in length by 3 in. in

TABLE 2.1 SOIL INDEX PROPERTIES

	<u>Oakdale Loess</u>	<u>Range for Loess in Iowa^a</u>
Liquid Limit	27	24-53
Plastic Limit	23	17-29
Plasticity Index	4	3-34
Specific Gravity	2.72	2.68-2.72
Percentage Clay		
Less than 0.005 mm	17	
Less than 0.002 mm	13	12-42
Activity ^b	0.50	
Natural Dry Density pcf		
Range	90.4 to 92.5	
Average	91	66-99
Natural Void Ratio		
Range	0.800 to 0.940	
Average	0.861	
Natural Water Content, %		
Range	21.2 to 22.9	
Average	22	

^aSheeler (1968)

^bActivity = plasticity index / (% 0.002 mm clay - 5%)
(Seed, H.B. et al, 1962)

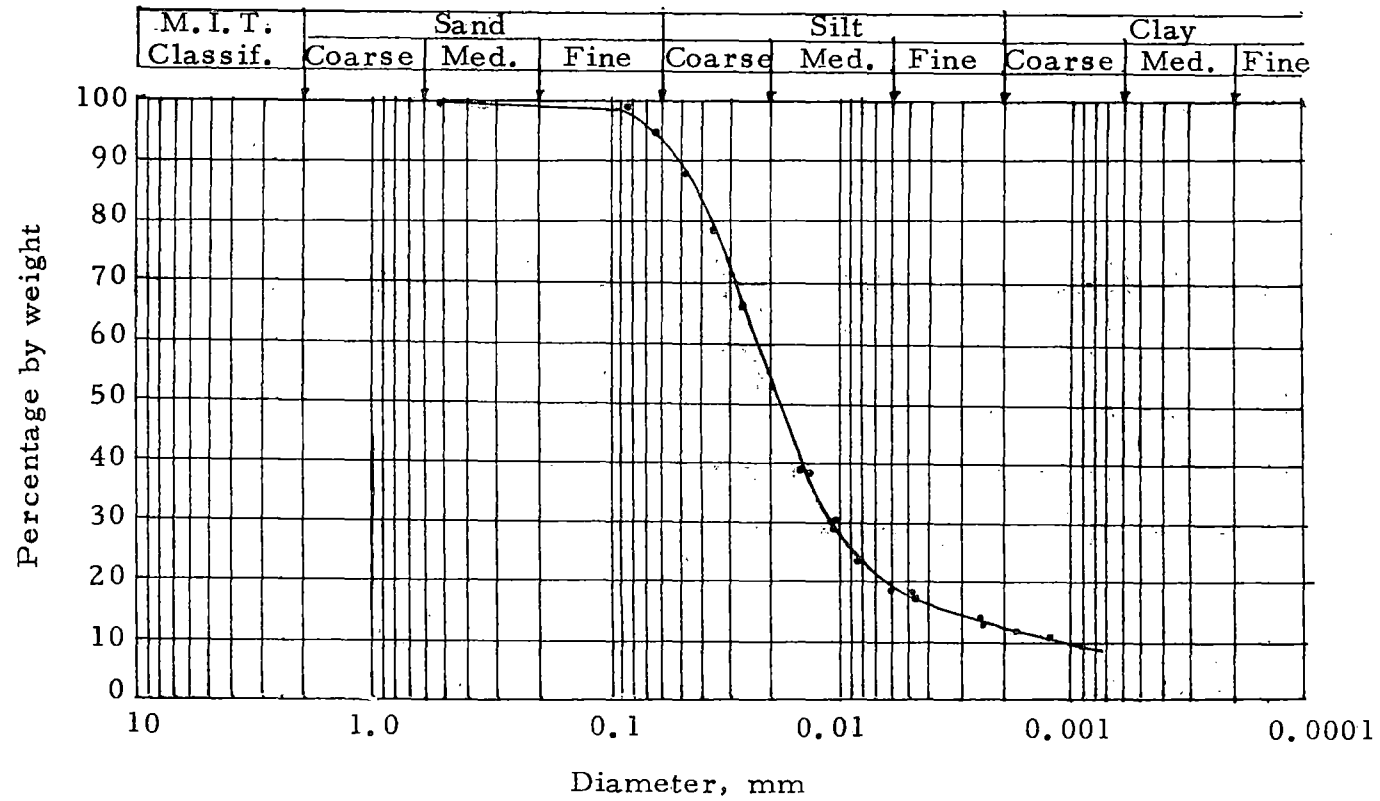


Fig. 2.1 Grain Size Distribution, Oakdale Loess

diameter for the triaxial test specimens. The water content of each sample was determined and the samples were wrapped in aluminum foil and then dipped several times into molten paraffin. Finally, they were placed in a plastic bag and the weight of the entire package was recorded to permit a check on the moisture loss if desired. The samples were stored in a moist room until needed for testing. Numerous checks on the water contents showed no measurable loss in water from the samples prepared and stored in this manner.

The confined compression testing program required structurally undisturbed specimens with a range in water contents, nominally 4%, 8%, 12%, 16%, 20%, 24%, and 28%. Since the natural water content was about 22%, the specimens had to be wetted or dried to achieve the desired water contents before trimming to test specimen size.

The alteration of the water content was accomplished in the following manner. To achieve a water content of 28%, the sample as stored at its natural water content was unwrapped and wetted by spraying the surface with a measured quantity of water. The sample was then rewrapped and placed in a moist chamber for several days to permit the dispersal of the water throughout the soil. This process was repeated until the water content of the sample, estimated from the sample's wet weight and its original weight and water content, was the desired 28%. The sample was then trimmed into the consolidation ring for testing. The water contents of the specimen and the trimmings were compared

to check the uniformity of water distribution in the sample and in all cases the differences were less than 1%.

Water contents below the natural water content were achieved by permitting the surface of the sample to air-dry for several hours, during which time the sample was weighed periodically to determine the weight of water evaporated. The sample was then stored in the moist chamber to permit the remaining soil moisture to redistribute itself. This process was repeated until the desired water content was reached. It was found that air-drying the samples too rapidly produced cracks which required discarding the sample. The modified water contents were in general within 2% of the desired nominal water content.

CHAPTER 3

LABORATORY TESTS

3.1 Introduction

Four types of tests were run on the undisturbed specimens of loess to determine the stress-strain and strength properties. These tests included a basic series of confined compression tests with the measurement of negative pore-water pressures, a special series of confined compression tests in which the water content was altered by measured amounts during the test, confined compression tests with the measurement of lateral stresses, and drained triaxial compression tests.

The test procedures and results are presented in this chapter.

3.2 Confined Compression Tests

3.2.1 Equipment. Special equipment was designed and constructed to permit the measurement of negative pore-water pressures in the partially saturated specimens of loess while the soil was undergoing compression under standard consolidation test loading. The equipment included three major components: a confined compression cell in which the specimen was placed during compression, a control panel board which permitted application and measurement of nitrogen gas under pressure, and instrumentation for measuring the pressures and deformations during compression.

The confined compression cell is shown in Fig. 3.1. The three main parts are the base, the cylinder, and the top. The base and top are machined from stainless steel and the cylinder is a section of 5-inch diameter aluminum pipe. A fine-grained porous stone with a rated bubbling pressure of 225 psi is sealed into the base. Two small-diameter ports enter through the bottom of the base to the lower surface of the stone. One port is fitted with a valve and a supply of deaired water confined in a control cylinder capable of forcing measured quantities of water through the stone into the soil. A 150-psi pressure transducer is mounted at the other port. The cell top encloses the top of the cylinder. A 1/2-inch diameter loading ram is guided through the top by a ball-bushing and teflon seals provide a low-friction seal. The top is connected to the base by four bolts extending from the base to the top outside the cylinder. Accurate alignment of the loading ram is assured by the machined cylinder ends.

The soil specimen is carved into a standard consolidation ring, 2.5 in. in diameter by 0.75 in. thick. The ring is located centrally in the base by three lugs and held in place by a collar. The load from the loading ram is transmitted to the soil by the loading cap and stone. The ring, collar, and loading cap are standard consolidation cell components.

For applying the cell pressure and for deairing procedures three additional entries to the cell are provided: a nitrogen connection through the top for applying pressure during deairing, a similar connection

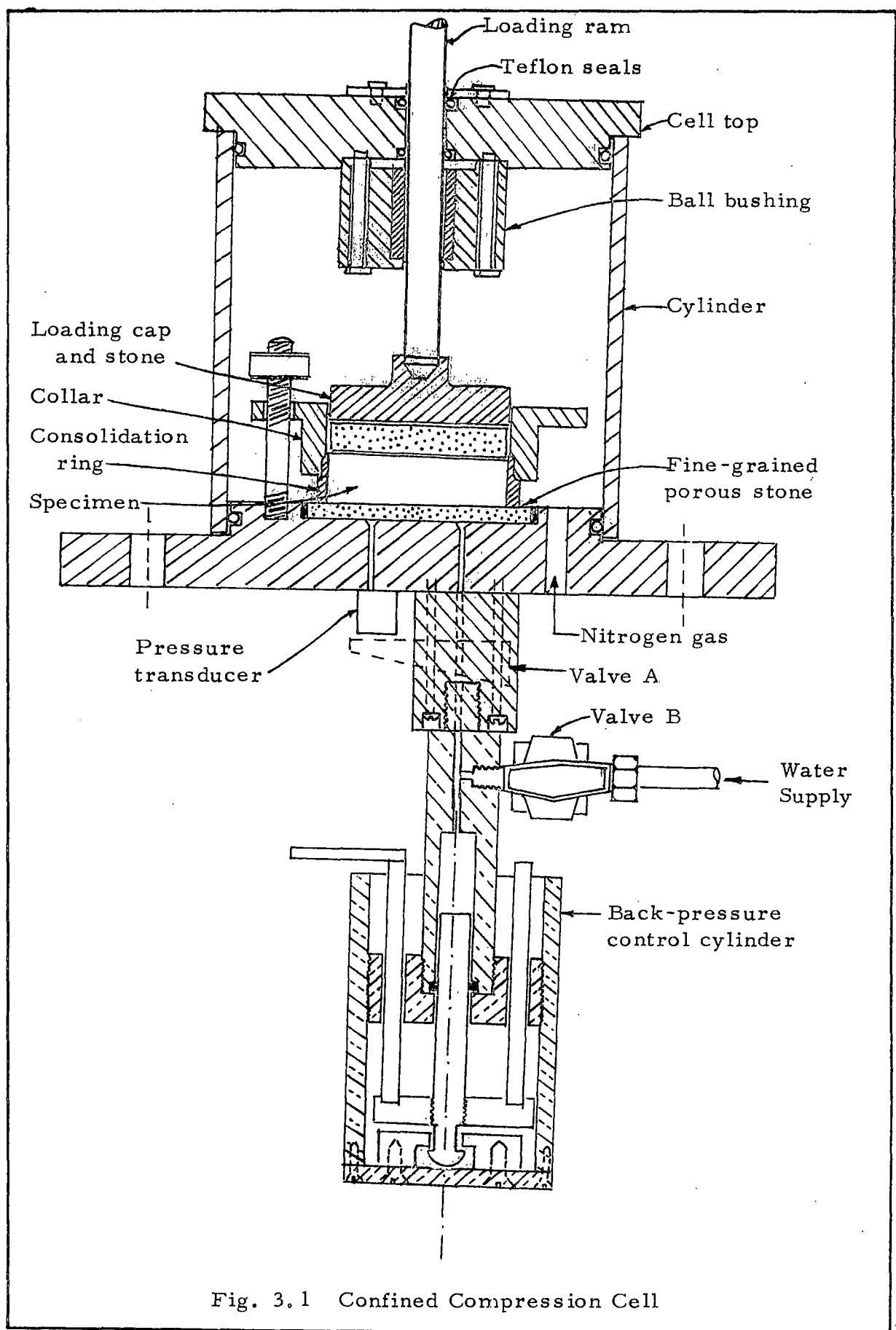


Fig. 3.1 Confined Compression Cell

through the base for filling and draining the cylinder in the deairing operation.

Nitrogen gas under pressure was obtained from cylinders of the compressed gas. A regulating valve on the cylinder reduced the pressure to a maximum of 300 psi. This pressure was further reduced and maintained at a desired level by a precision pressure regulator mounted on a panel board along with a 300-psi bourdon gage for measuring the output pressure to the cell.

During operation the stone in the base and the ports below the stone were saturated with water. The pressure in this water was measured by a 150-psi pressure transducer mounted directly on the base. The transducer was read on a Sanborn strip chart recorder. The compression of the soil specimen during loading was measured with a dial indicator reading 0.0001 in.

The confined compression cell was mounted in a consolidation test machine having dead-weight loading at a lever ratio of 10 to 1. The base of the cell was bolted to the test machine and the desired loads were applied to the top of the ram through the lever system.

3.2.2 Deairing. The measurement of the pore-water pressure requires that the system of voids in and below the fine ceramic porous stone be completely saturated and act as a closed system. To insure saturation it was necessary to follow a special deairing procedure before each test. This procedure is described in the following paragraphs.

Freshly deaired distilled water was introduced into the cell through an inlet in the base to a level approximately four inches above the stone. With valves A and B open, a nitrogen pressure of 150 psi was applied to the top of the water in the cell. Under this pressure the deaired water was forced through the stone and valve B. Most of the trapped air could be removed by flushing the water through the system in this manner. To remove the remaining air it was necessary to close valve B and permit the full 150 psi pressure to build up in the water below the stone. Under this pressure, the trapped air below the stone dissolved in the water and diffused through the stone into the volume of water above the stone. After a one hour period, the water above the stone was drained off, replaced with freshly deaired water and the procedure was repeated.

The completeness of deairing was determined by the output of the pressure transducer below the stone. Fig. 3.2 shows the increase in pressure below the stone as a function of the time after valve A is closed. Fig. 3.2a indicates that there is air trapped in the system below the stone because the pressure builds up slowly as a result of the compressibility of the air. When all the air has been removed, the pressure buildup is almost immediate as shown in Fig. 3.2b.

3.2.3 Initial negative pore-water pressure measurements. The measurement of the negative pore-water pressures has been made using a technique known as the axis translation technique (Olson and

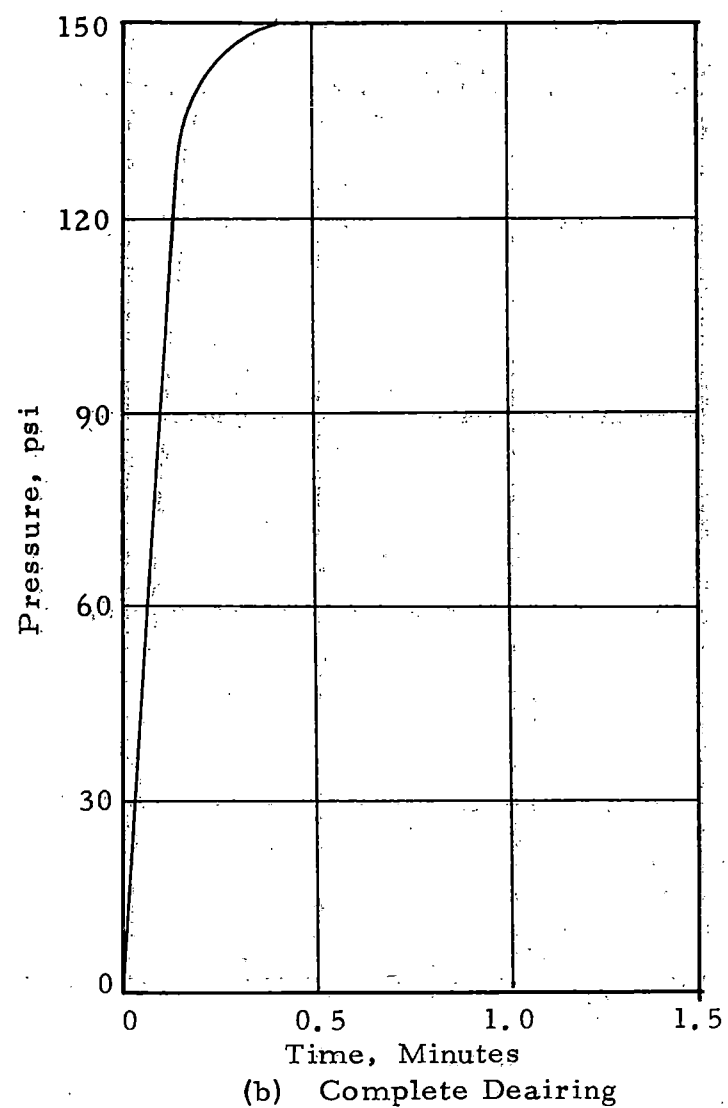
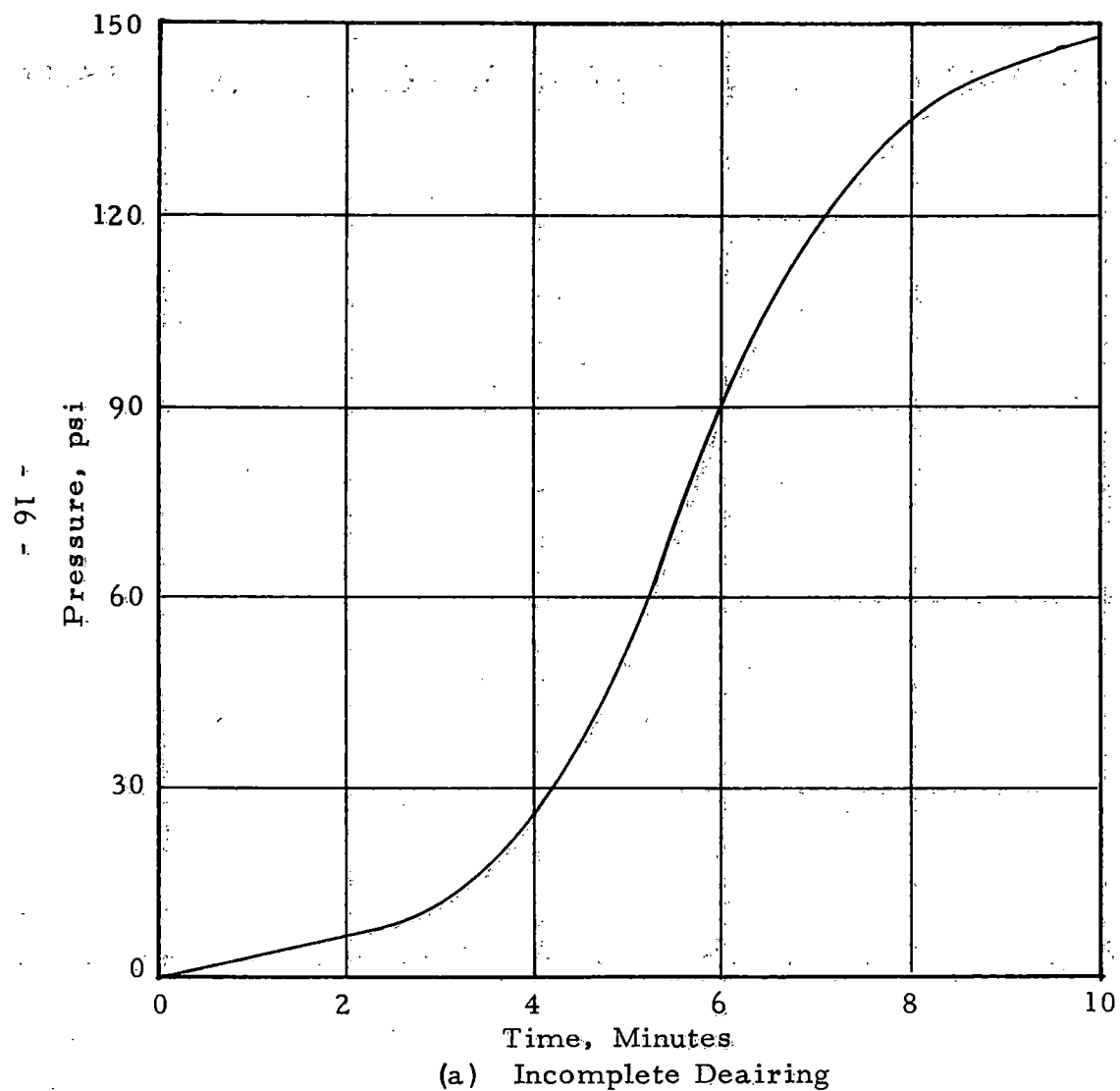


Fig. 3.2 Effect of Entrapped Air on Pressure Response Time

Langfelder, 1965). This technique works in the following manner. If a partly saturated specimen of soil is placed on the fine ceramic porous stone shown in Fig. 3.1, the capillary suction in the soil will tend to draw the water out of the porous stone. With valve A closed and the voids in and below the stone completely saturated, the water below the stone is in a closed system. Thus the water pressure below the stone will become equal to the pore-water pressure in the soil with a negligible flow.

However, if the pore-water pressure is below -10 to -15 psi, cavitation will occur and the system below the stone will no longer behave as a closed system. This condition is avoided in the axis translation method by placing the soil and the porous stone in a closed chamber. A positive gas pressure applied in the cell cancels the negative pore-water pressure in the pore fluid. The negative pore-water pressure in the soil, therefore, is equal to the measured water pressure below the stone minus the gas pressure in the cell.

In order to determine the initial negative pore-water pressure, an undisturbed soil sample at the desired moisture content was carved into the consolidation ring. The soil and the consolidation ring were weighed and the trimmings used to check the nominal moisture content. The cell was prepared by removing the top and cylinder and wiping the excess water off the porous stone after having closed valve A. A small negative water pressure developed immediately in the water below the

stone as a result of evaporation and the formation of menisci on the surface of the stone. This pressure was monitored on the Sanborn recorder. Next the sample was placed on the stone and the collar placed around the consolidation ring and secured with three nuts. A circle of filter paper was placed on top of the sample and the loading cap and stone were put into position. Following these steps the cell was assembled and the top secured to the base by means of the bolts extending from the top to the base. The above work in general took less than two minutes to complete. With the cell assembled it was then possible to apply nitrogen pressure in the cell. The applied cell pressure tends to cancel the measured negative water pressure and the cell pressure was continually adjusted to maintain a pressure of zero in the water below the stone.

Finally, a seating load of $1/32$ tsf was applied to the soil specimen and an additional load was applied to the top of the loading ram to compensate for the cell pressure acting upwards on the bottom of the ram. These loads were generally in place six minutes after the start of the tests.

As the pressure in the soil and in the stone equalizes, the measured pressure below the stone tends to become negative. As noted above, the negative pressure was compensated by increasing the cell pressure. This was done at one minute intervals for the first ten

minutes, two minute intervals for the next ten minutes, and every ten minutes thereafter. In some cases the applied cell pressure overshot the trial negative pore-water pressure and a positive pressure was recorded in the water below the stone. Care was taken not to reduce the cell pressure, except at the end of the test, because it was observed during preliminary testing that air bubbles formed on reducing the cell pressure, thus introducing undesired air in the water below the stone.

Equilibrium was reached when there was no change in cell pressure and water pressure below the stone for a period of ten minutes or more. At this time the initial negative pore-water pressure was computed as the difference between the cell pressure and the pressure below the stone if any.

3.2.4 Procedures during consolidation. A loading sequence of 1/2, 1, 2, 4, 8, 16, and 32 tsf was used for soils at or wetter than a water content of 16 percent. The 1/2 tsf load was omitted for soils with water contents less than 16 percent. The compression of the specimen was measured with a 0.0001-inch dial indicator. For each load the compression, the cell pressure, and the water pressure below the stone were recorded at time intervals of 1/2, 1, 2, 4, 8, 15, 30 and 60 minutes. At the end of sixty minutes the next load was applied.

Unloading was accomplished by reducing the load from 32 tsf to 8, 2, 1/2, and 0 tsf. The 1/2 tsf step was omitted for the drier

soils. When the load was removed, the valves below the stone were opened, the soil pressure reduced to zero, and the cell disassembled. The weight of the specimen and the ring after the test was recorded. The specimen was then removed from the ring, weighed, and the water content determined.

3.2.5 Special tests. In this test series the water content of the soil was increased while the soil was under constant load; during this process the compression of the specimen and changes in pore-water pressure were measured. The increase in water content was accomplished through the use of the back pressure control cylinder shown in Fig. 3.1. The control cylinder was initially filled with deaired water. With valve B closed and valve A open, water may be forced into the soil sample by rotating the control cylinder (0.100 cc of water are displaced per rotation). The volume of the water is known from the number of rotations of the control cylinder. Three rotations of the control cylinder increased the water content of the specimen by about 0.25%.

The test procedure was similar to that described above. Loading was increased to the desired level with valve A closed. After equilibrium was achieved under this load, the water content was increased. This was accomplished by first closing valve B and then opening valve A. Next the control cylinder was rotated slowly by three turns and the soil allowed to absorb the displaced water. After two hours the

compression dial indicator was read, the cell pressure and water pressure were recorded, and then the control cylinder was rotated another three turns. This process was repeated until the desired number of turns was made to achieve the required water content. At this point the pressures were permitted to equalize for 24 hours after which period the compression dial reading and pore pressures were recorded again. The remaining loading increments were then added and the test completed as in the basic series.

3.2.6 Test results. The results of the basic and special confined compression tests, with various parameters computed at each test stage, are presented in Appendix III. The results are shown graphically in Figs. 3.3 to 3.27. These figures are four-variable plots of void ratio, log stress, water content, and negative pore-water pressure. The manner in which each of these parameters varies during the tests may be observed in these figures.

Certain key parameters from each test have been determined and these are summarized in Tables 3.1 and 3.2 for the basic and special tests respectively. The tables list the initial ($\sigma_v = 0$) and final ($\sigma_v = 444$ psi) values of water content, void ratio, degree of saturation, and negative pore-water pressure. In the case of specimens with initial water contents less than 10%, the initial negative pore-water pressure is for the first load increment rather than for $\sigma_v = 0$. These values are

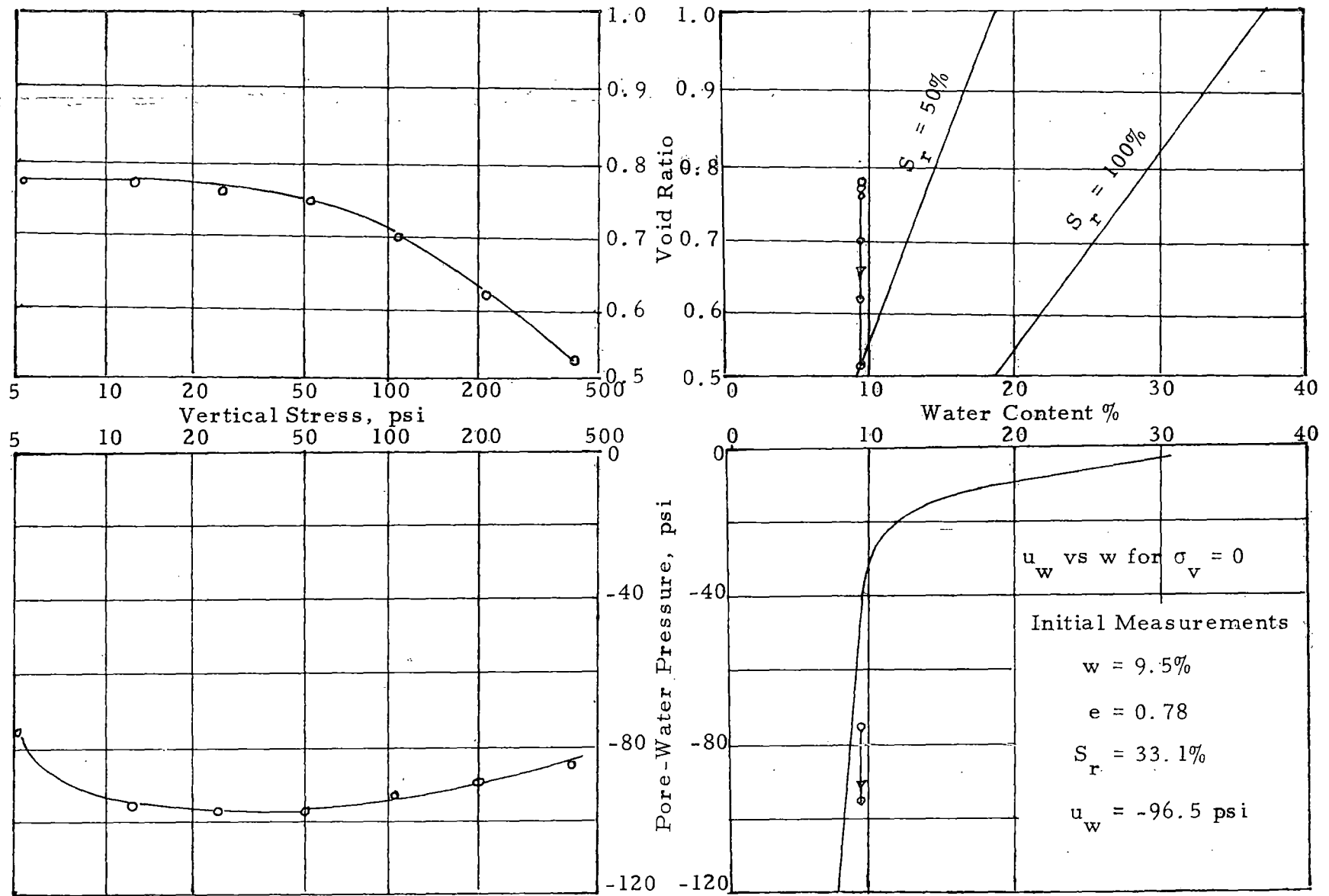


Fig. 3.3 Results of Confined Compression Test No. 3

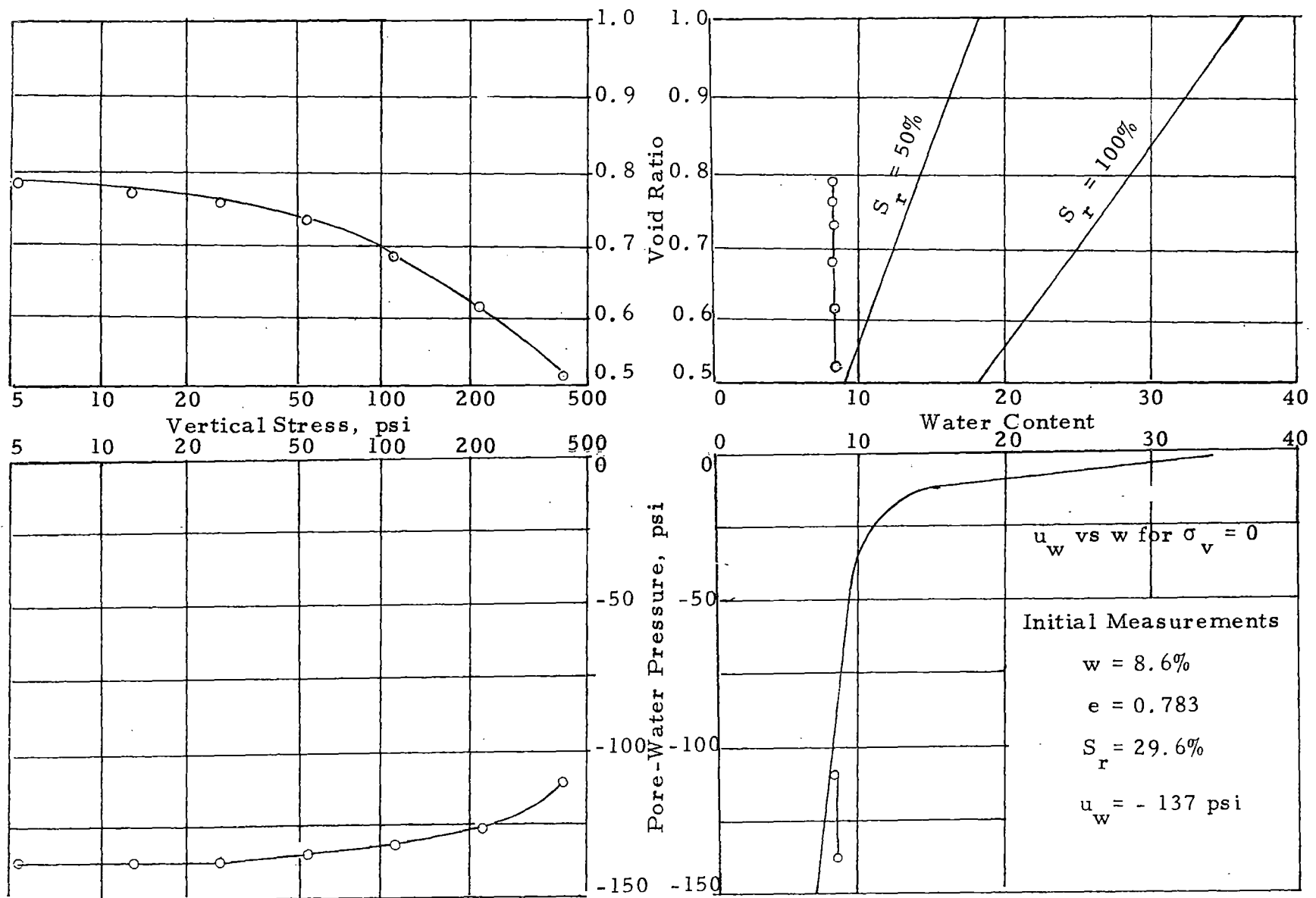


Fig. 3.4 Results of Confined Compression Test No. 4

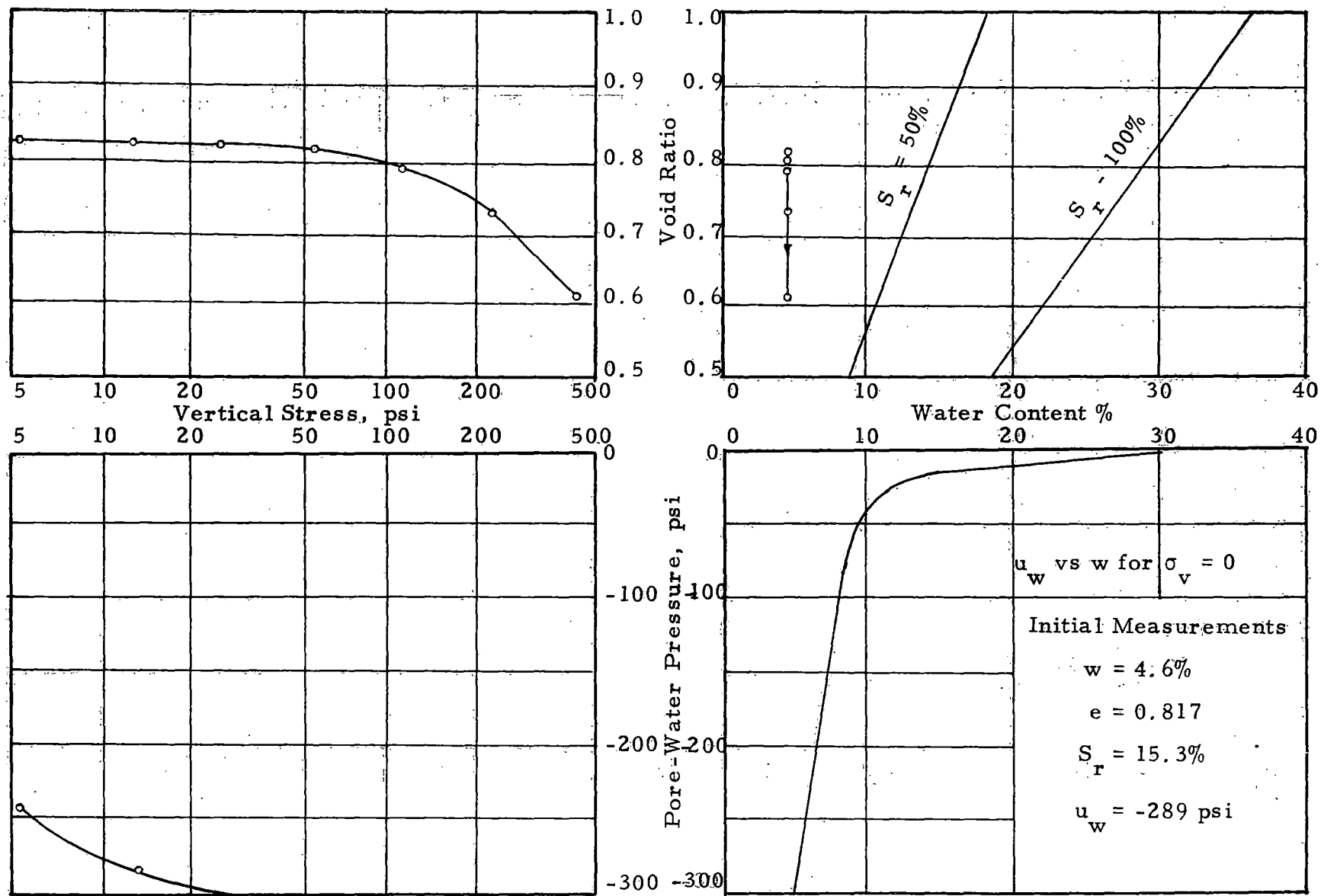


Fig. 3.5 Results of Confined Compression Test No. 5

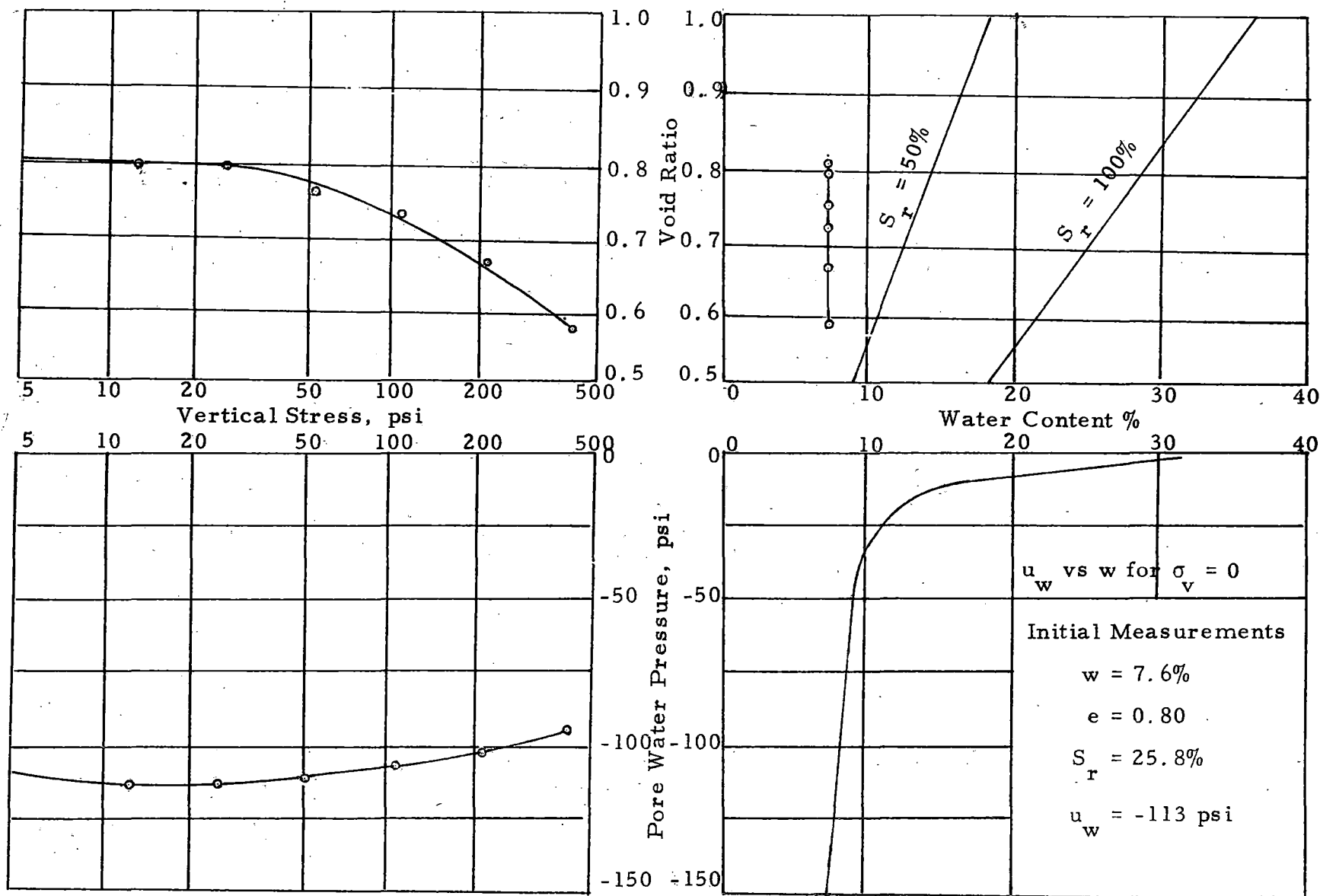


Fig. 3.6 Results of Confined Compression Test No. 6

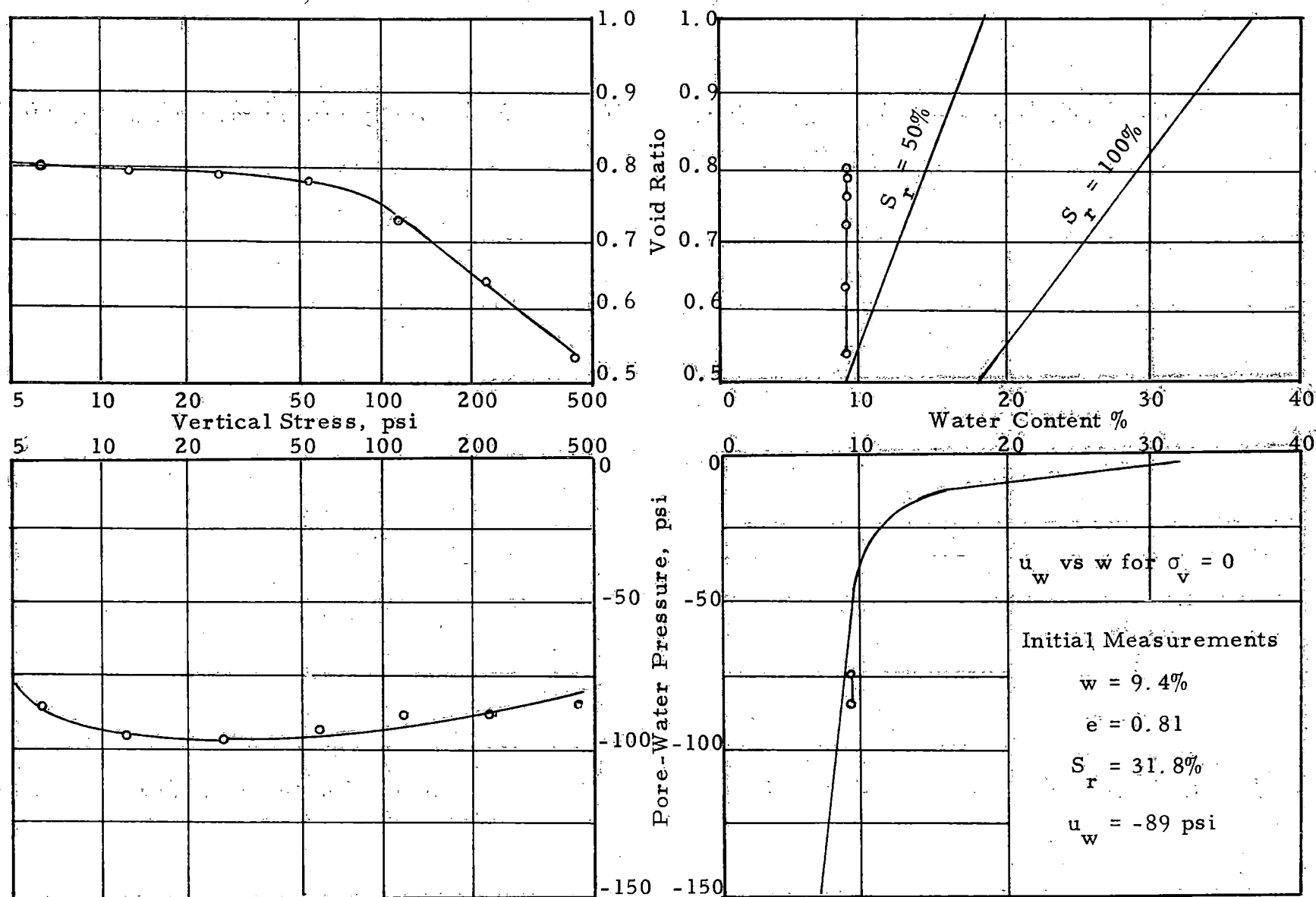


Fig. 3.7 Results of Confined Compression Test No. 7

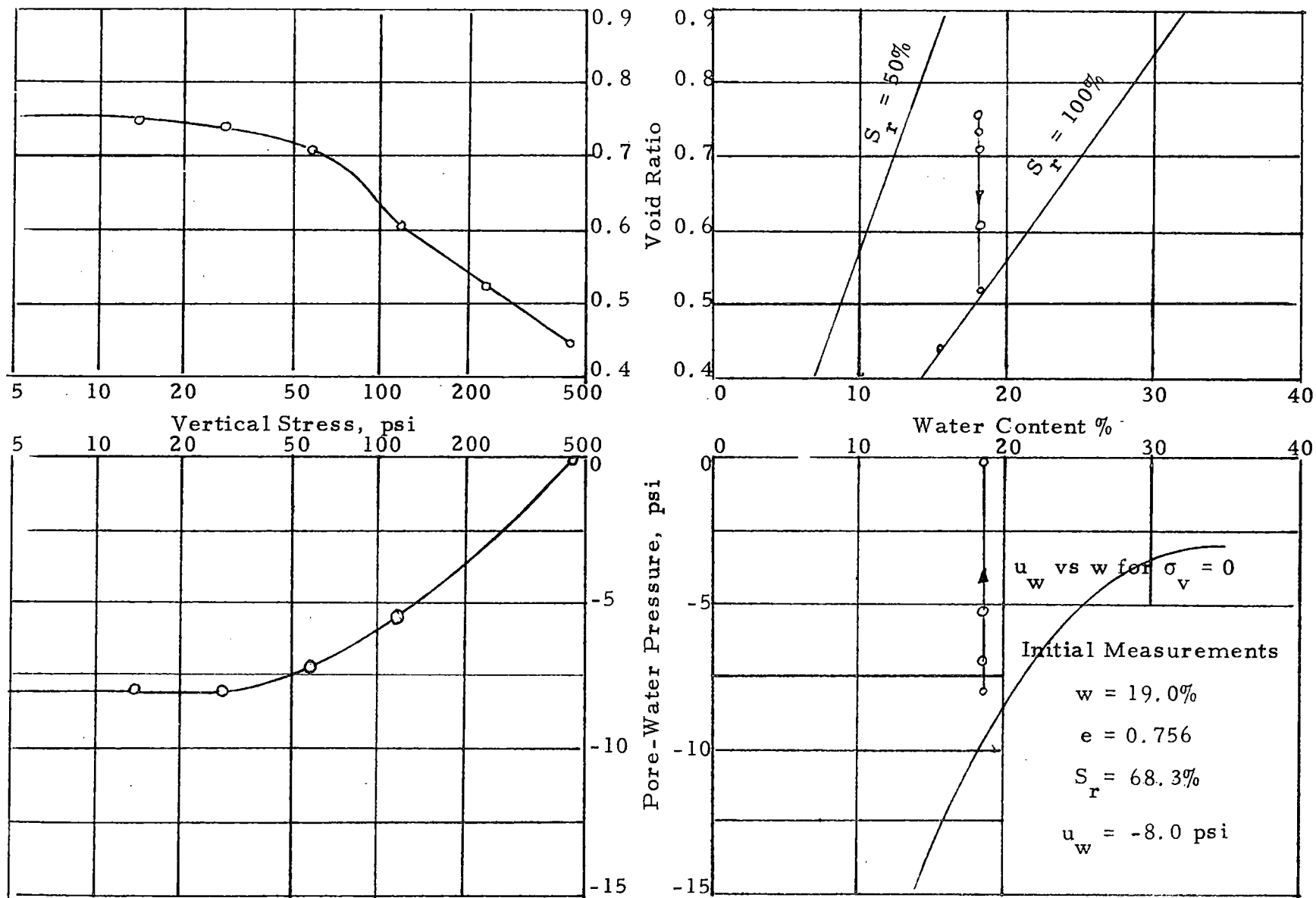


Fig. 3.8 Results of Confined Compression Test No. 11

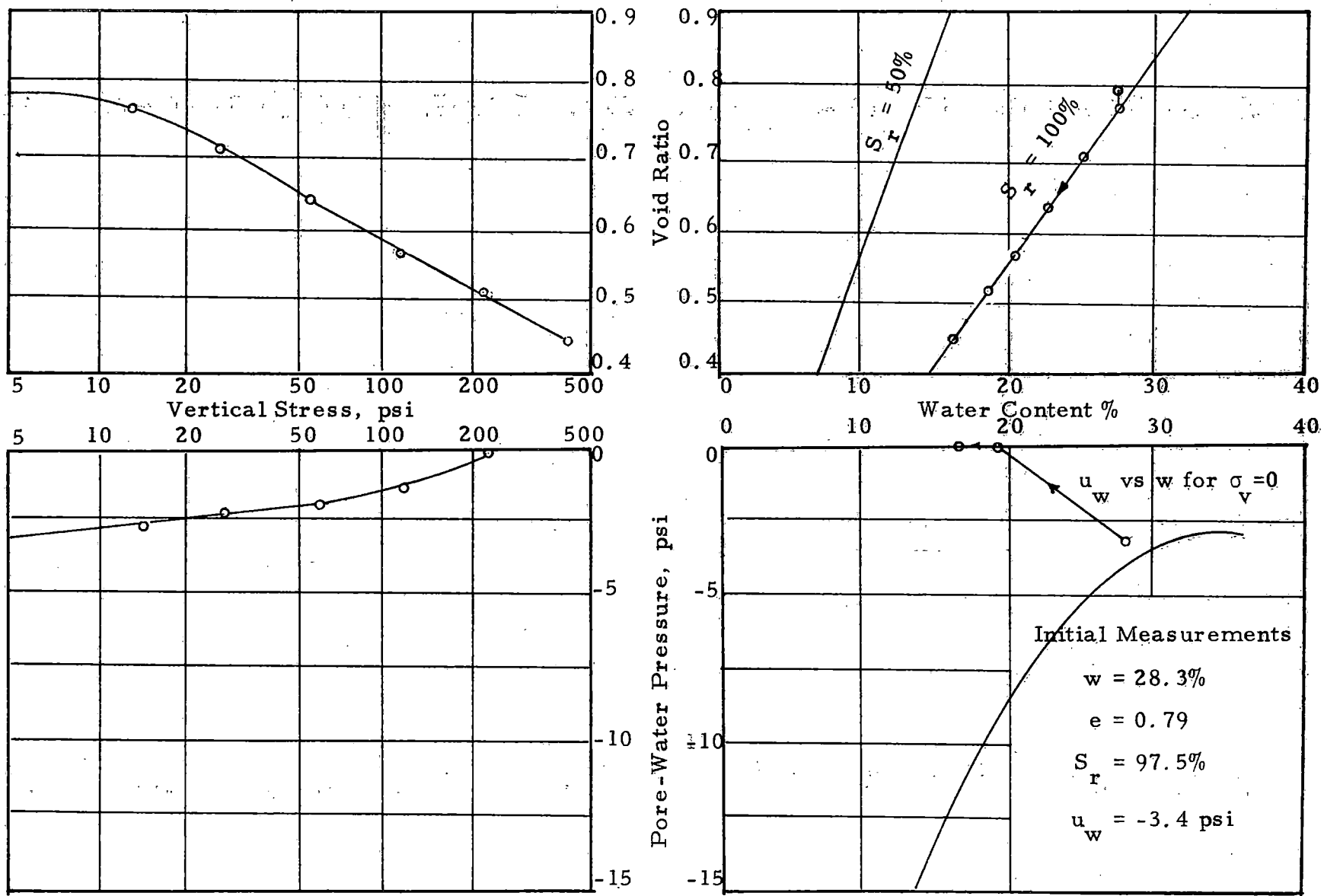


Fig. 3.9 Results of Confined Compression Test No. 13

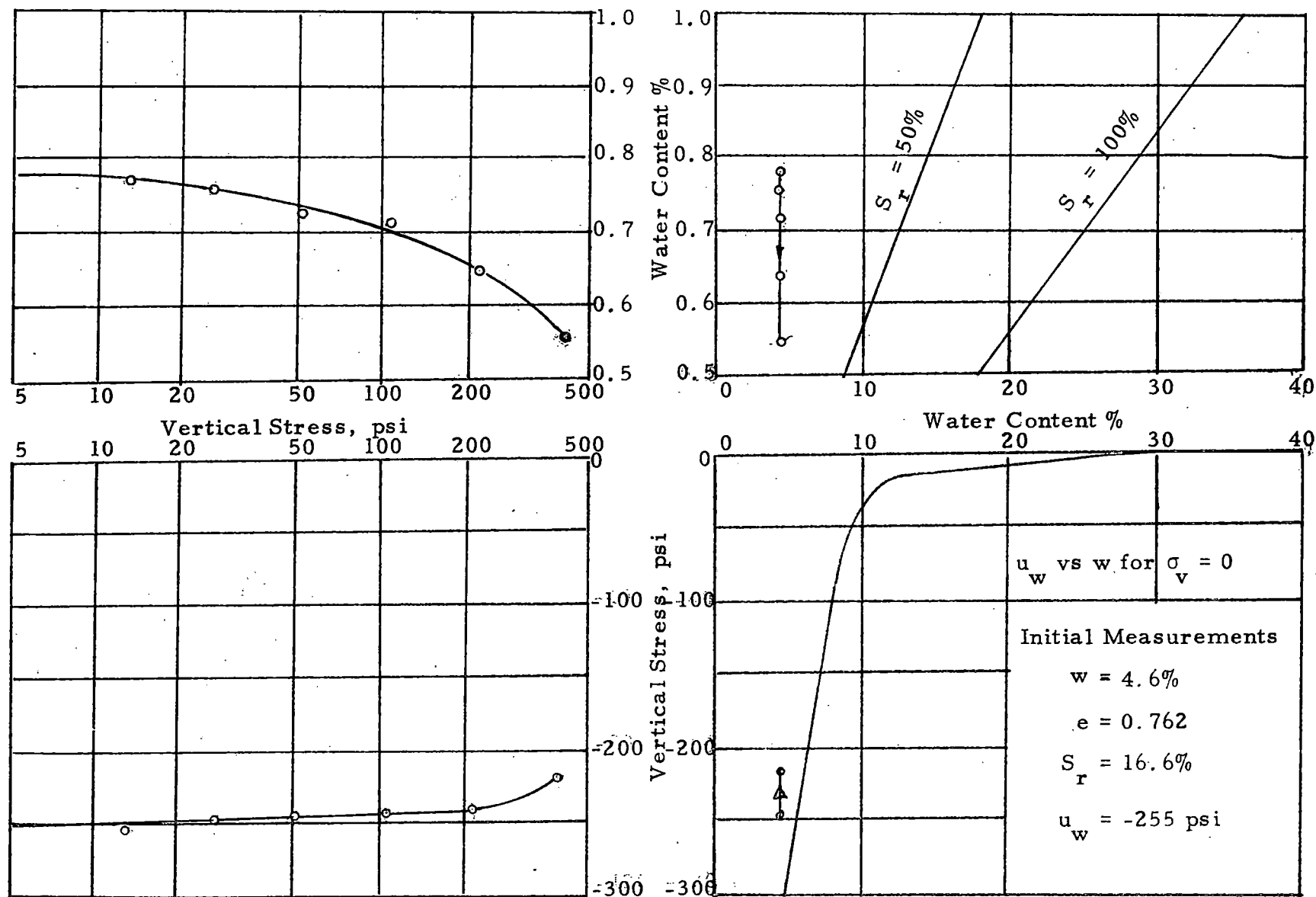


Fig. 3.10 Results of Confined Compression Test No. 14

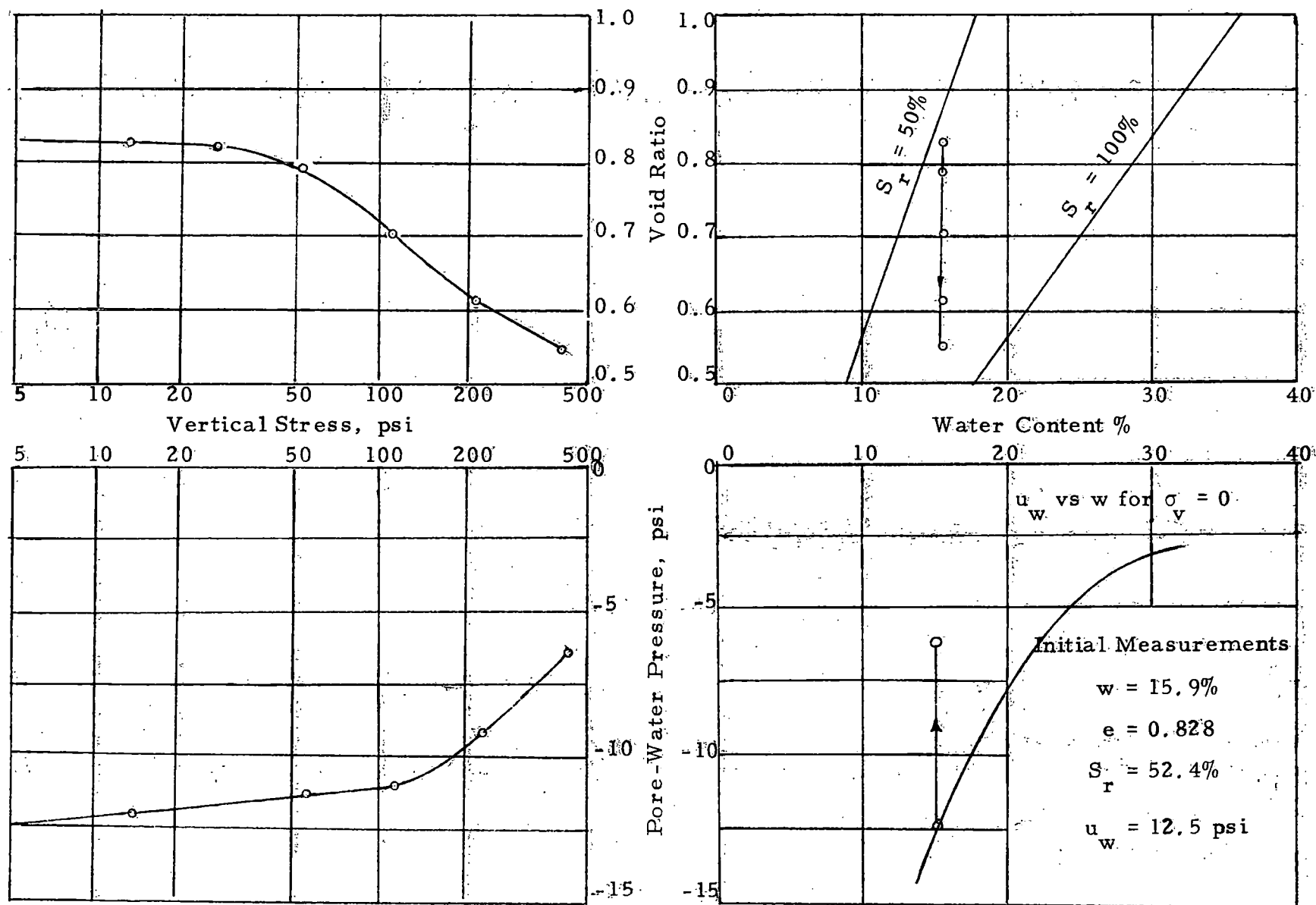


Fig. 3.11. Results of Confined Compression Test No. 15.

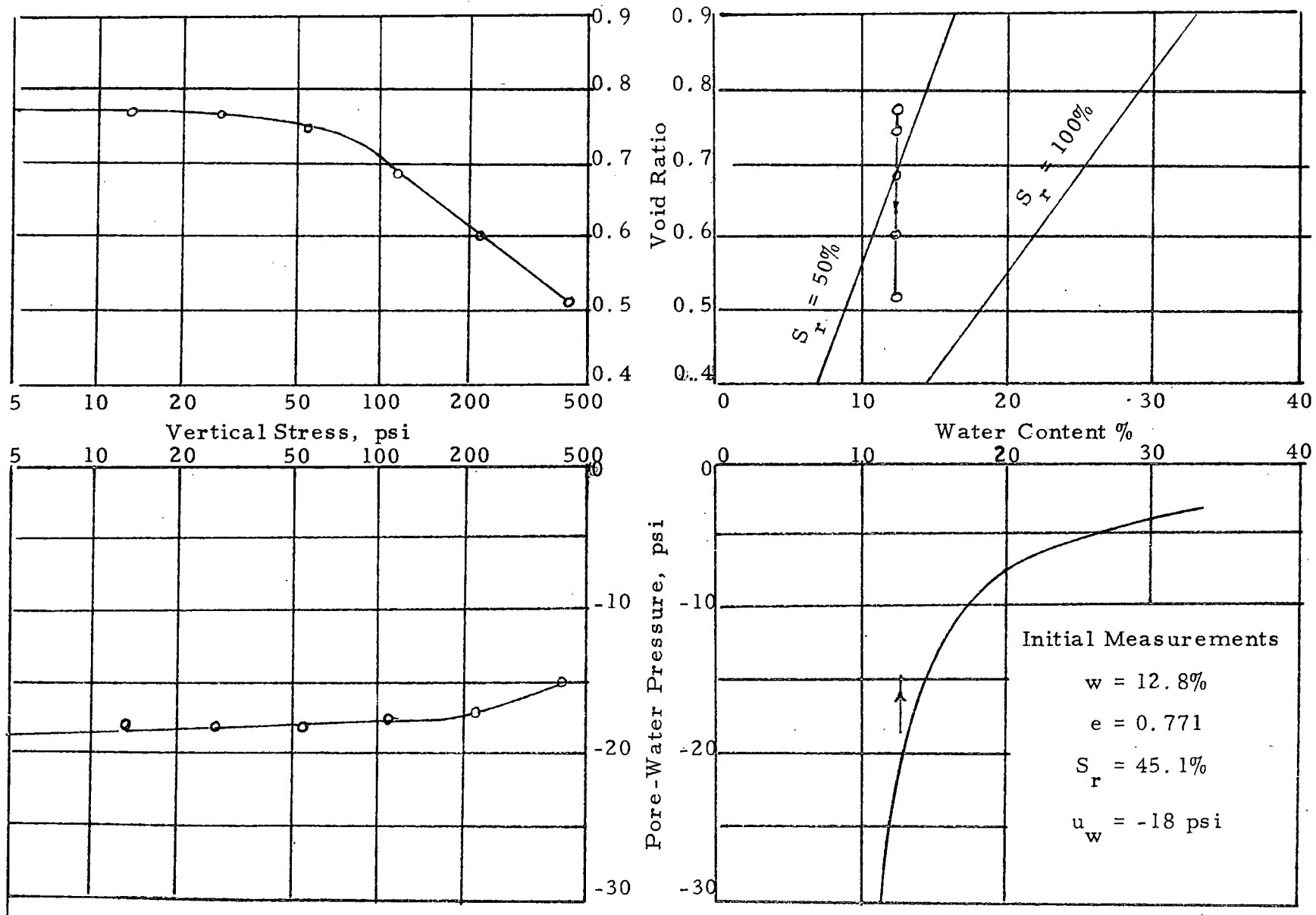


Fig. 3.12 Results of Confined Compression Test No. 16

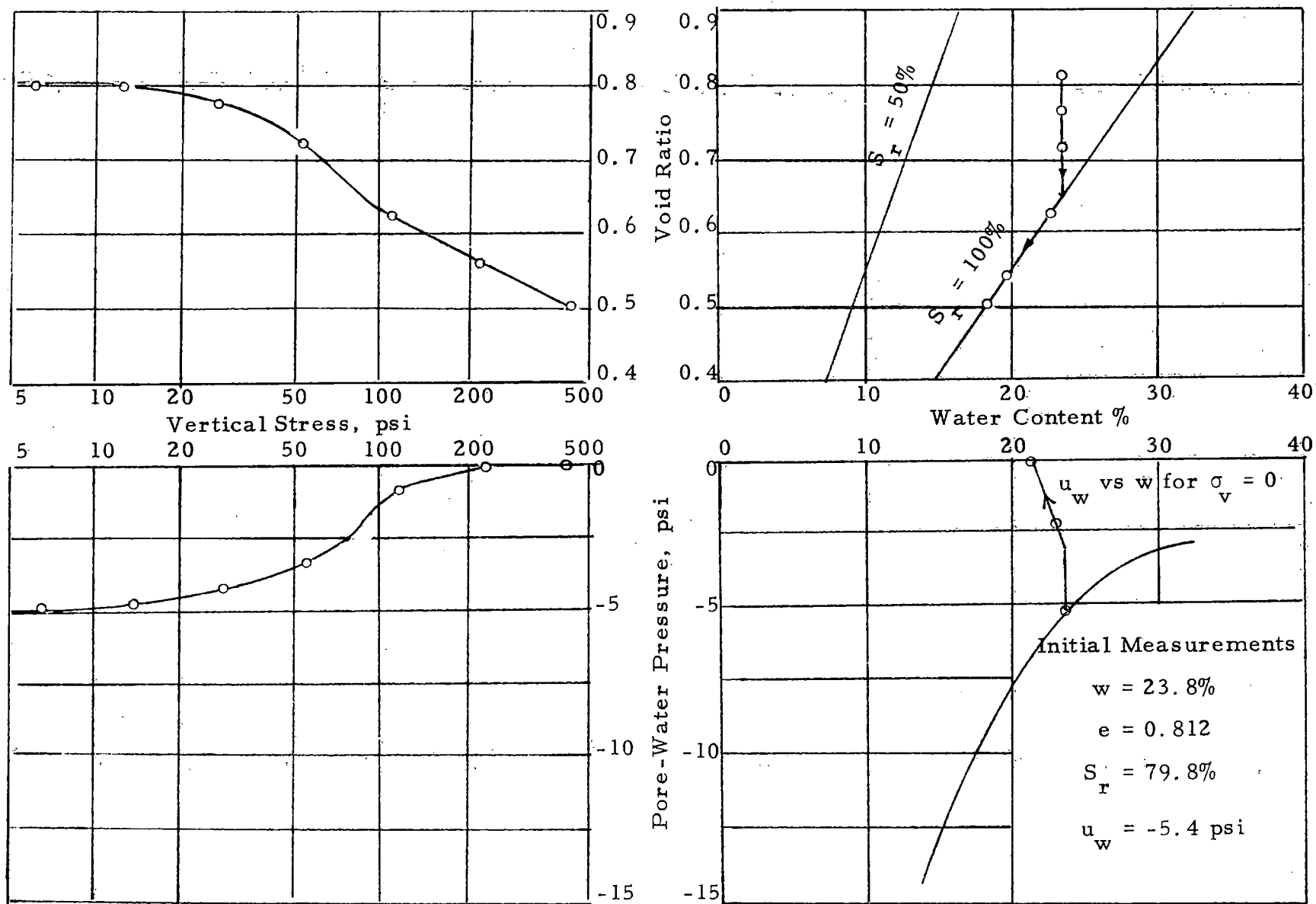


Fig. 3.13 Results of Confined Compression Test No. 17.

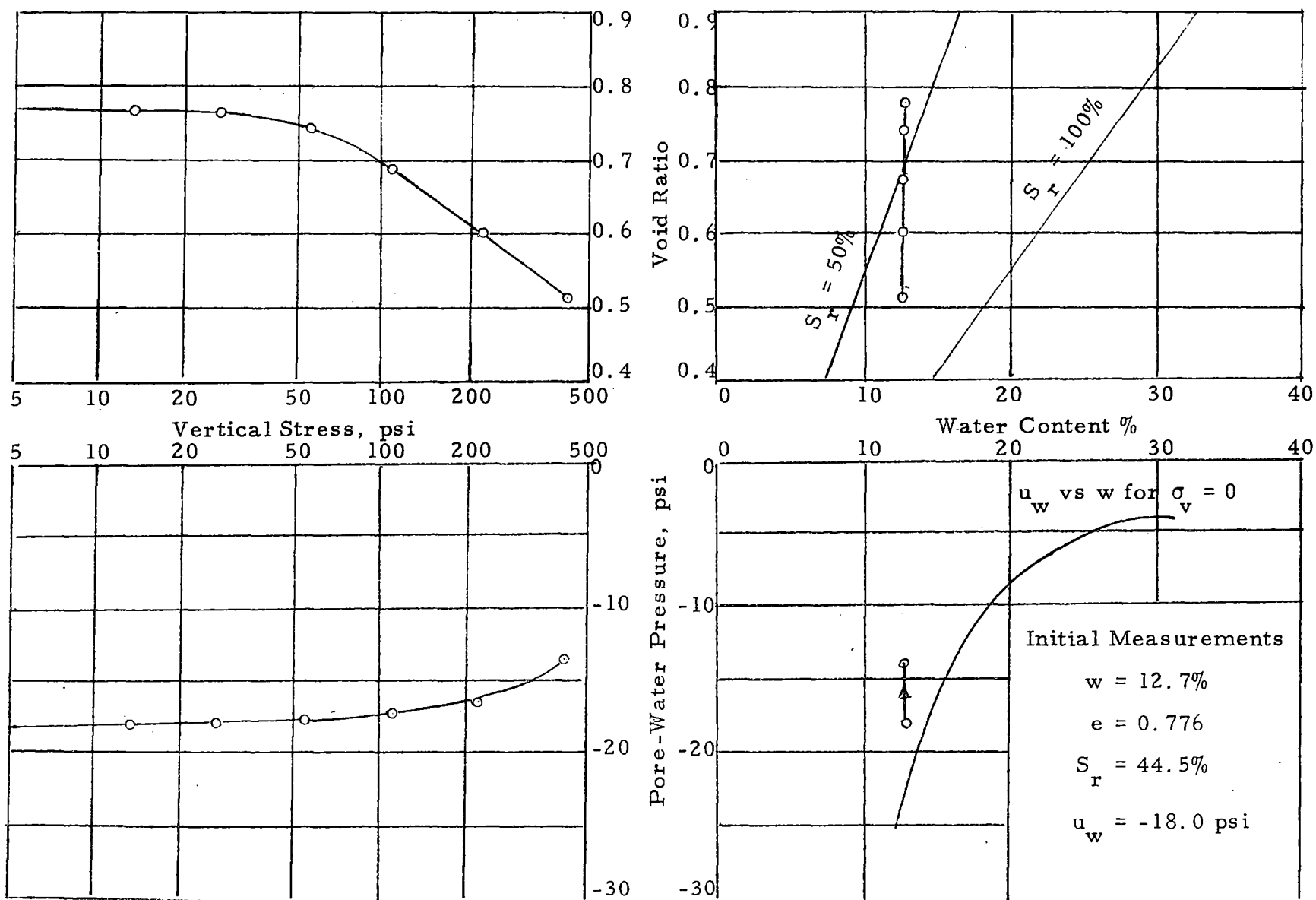


Fig. 3.14 Results of Confined Compression Test No. 18

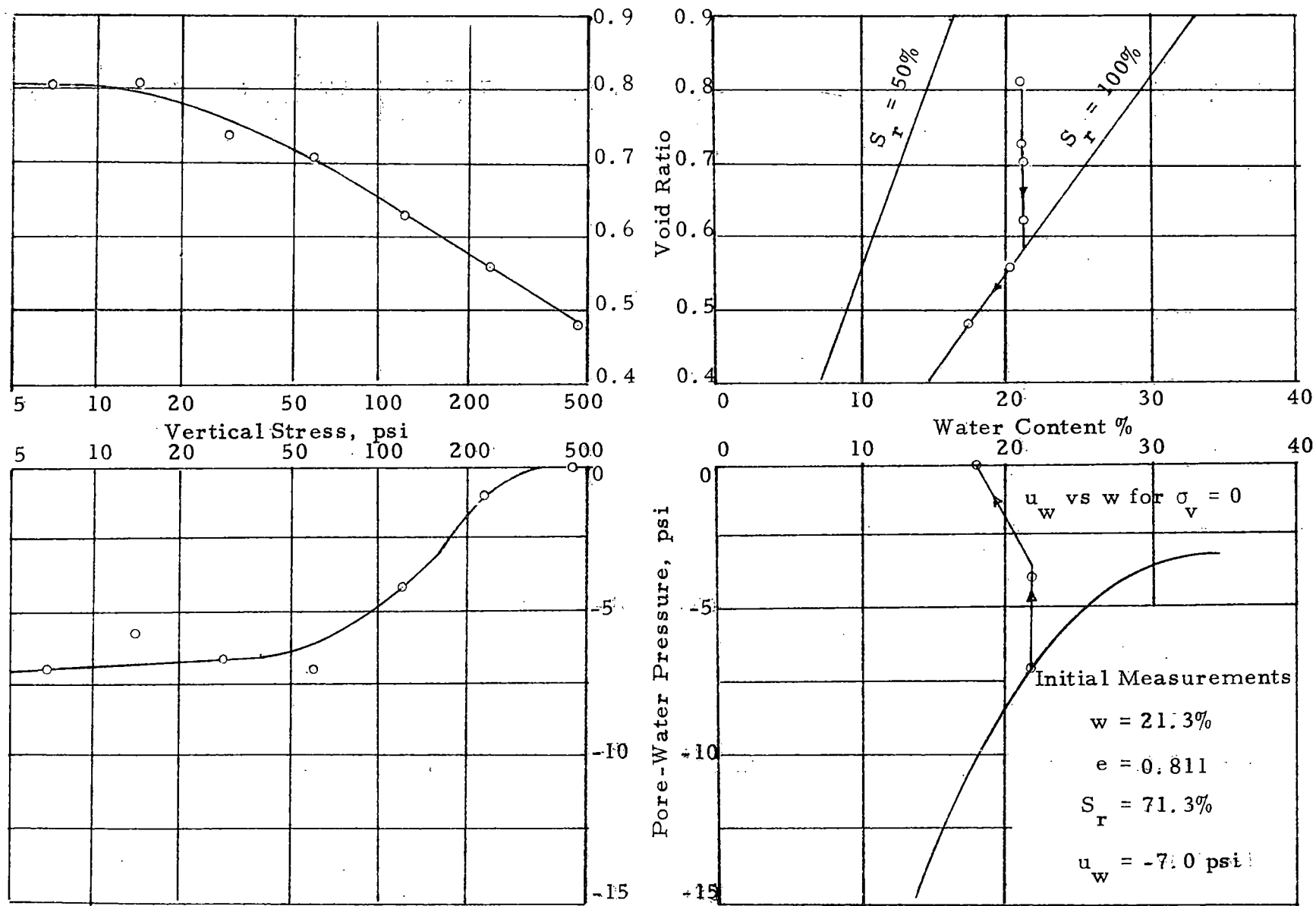


Fig. 3.15 Results of Confined Compression Test No. 19

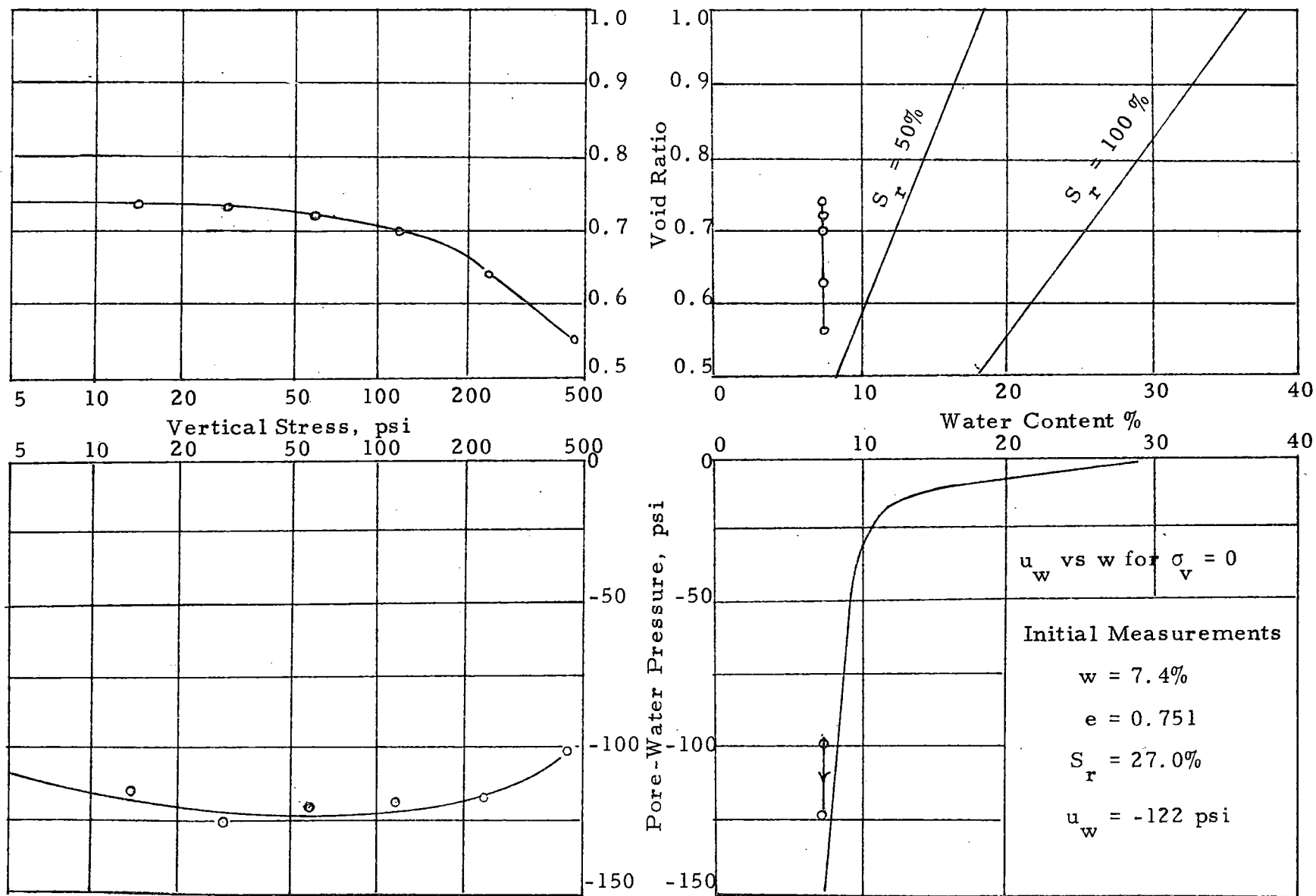


Fig. 3.16 Results of Confined Compression Test No. 20

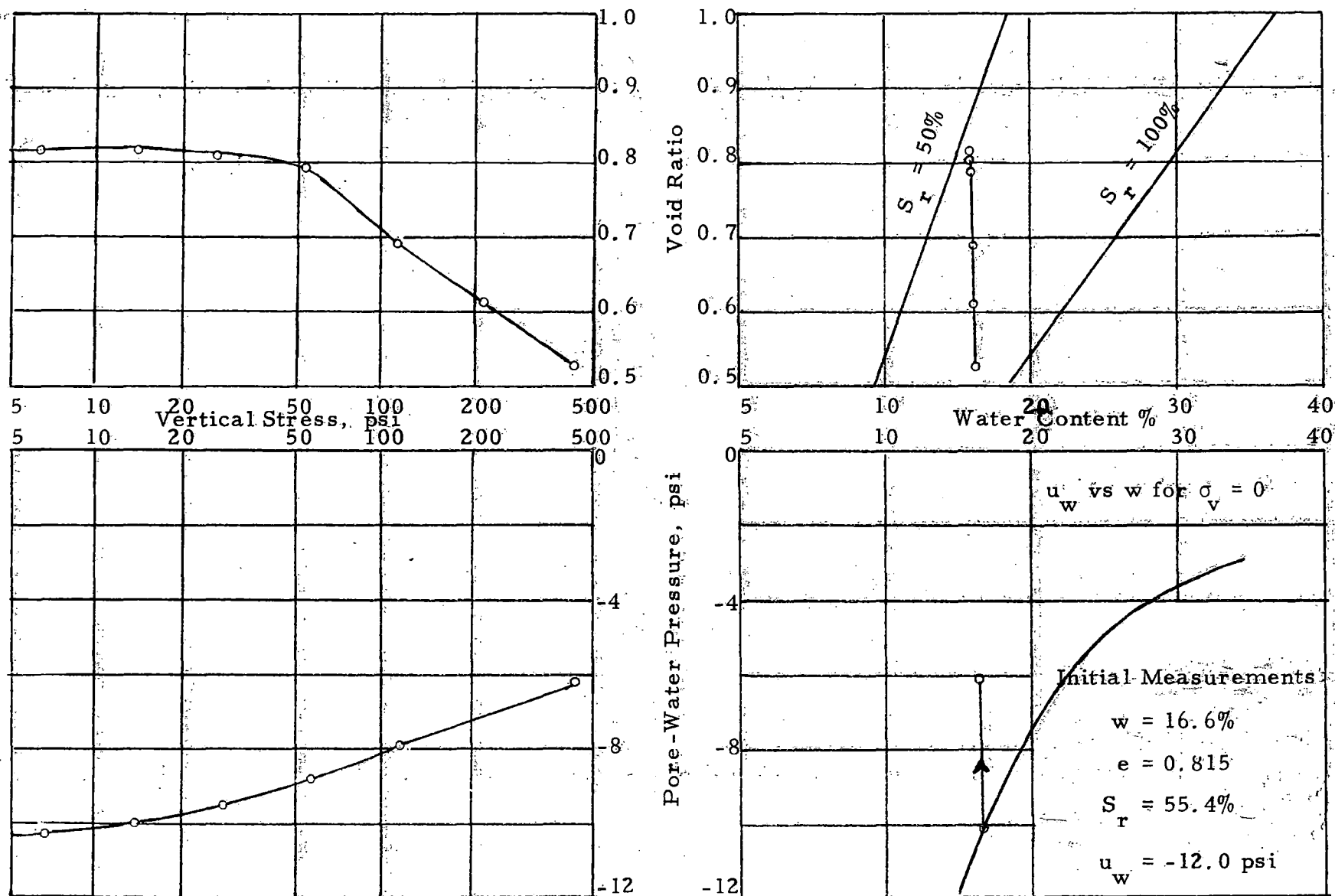


Fig. 3.17 Results of Confined Compression Test No. 21

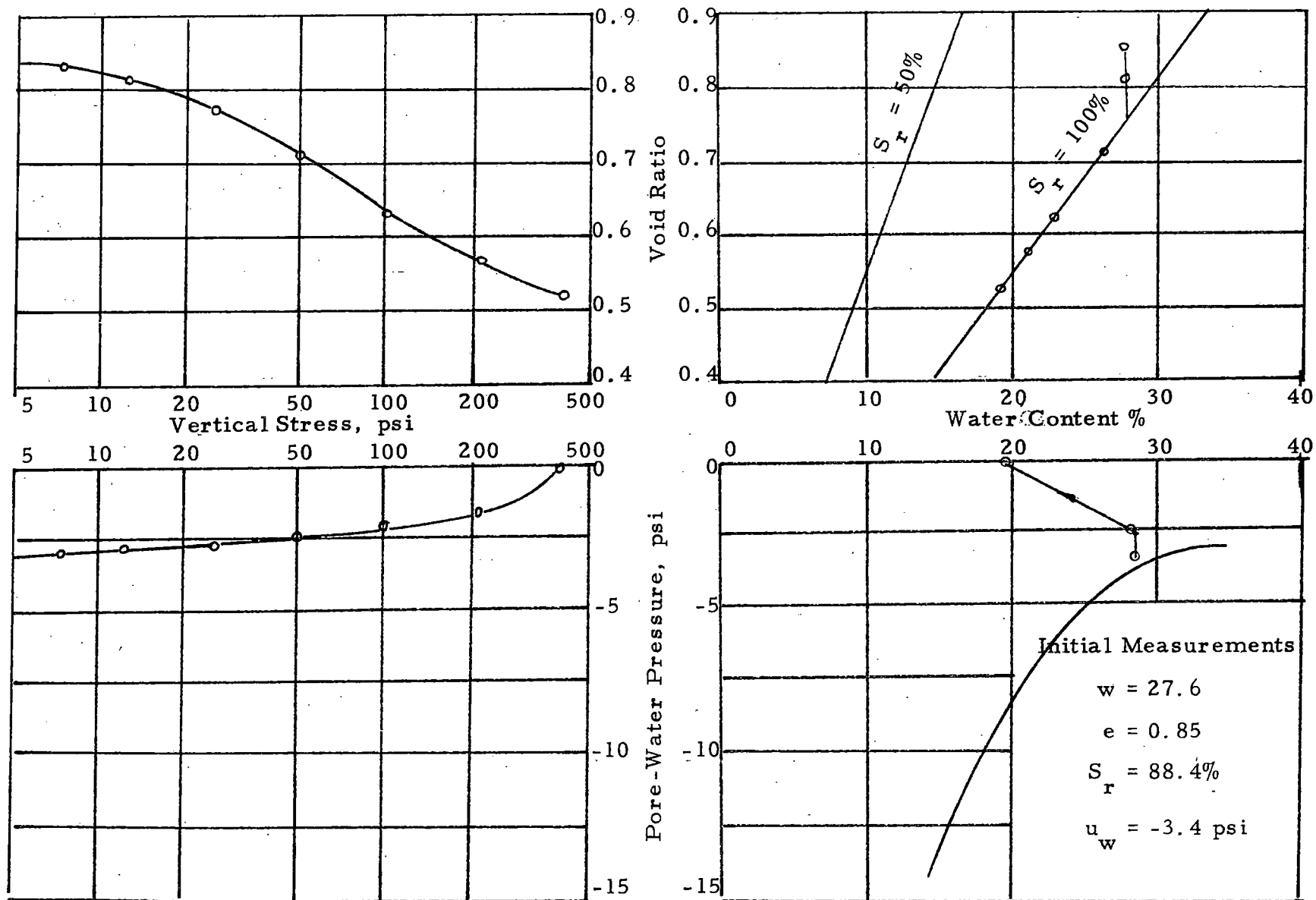


Fig. 3.18 Results of Confined Compression Test No. 22

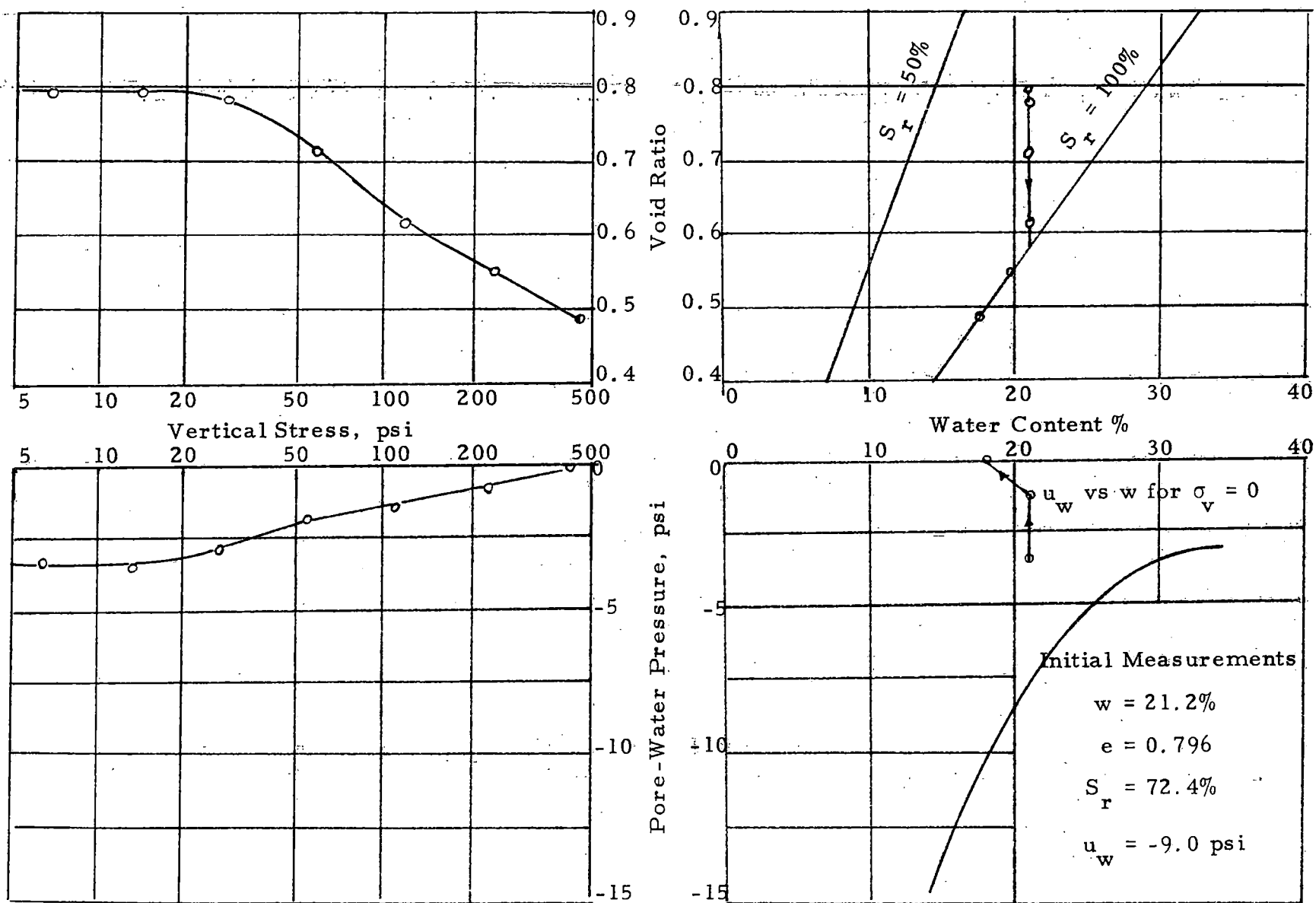


Fig. 3.19 Results of Confined Compression Test No. 23

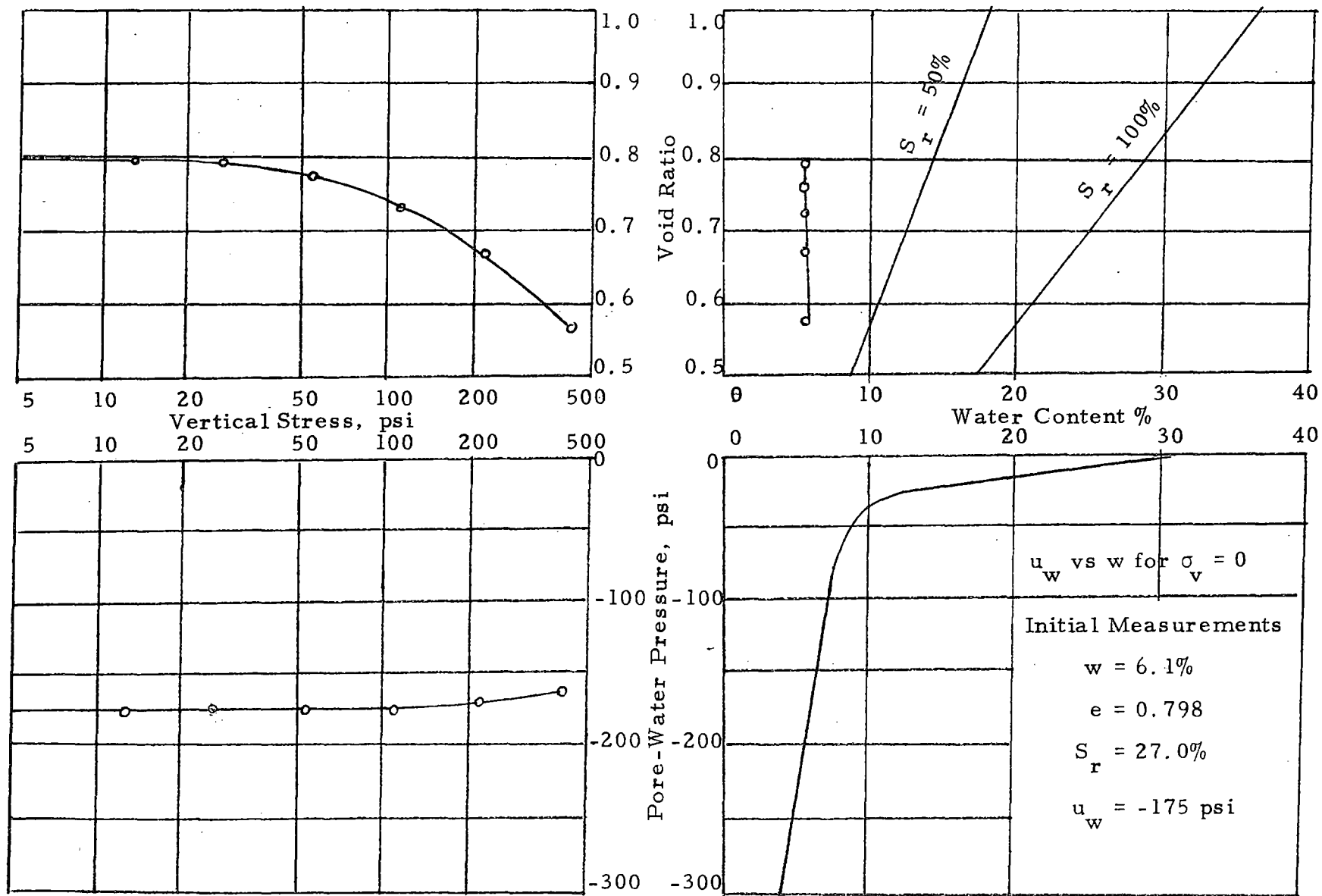


Fig. 3.20 Results of Confined Compression Test No. 24

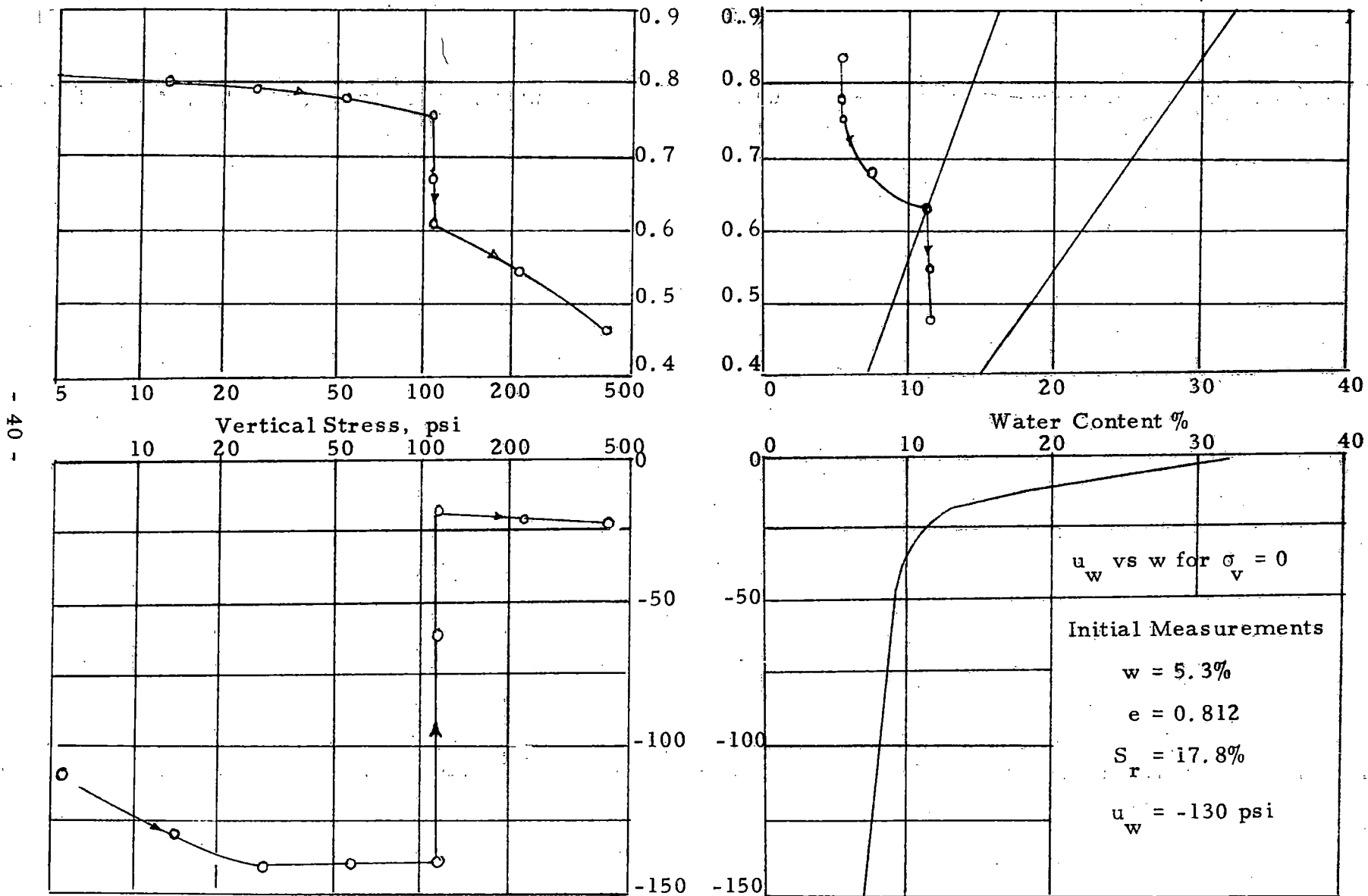


Fig. 3.21 Results of Confined Compression Test No. S1

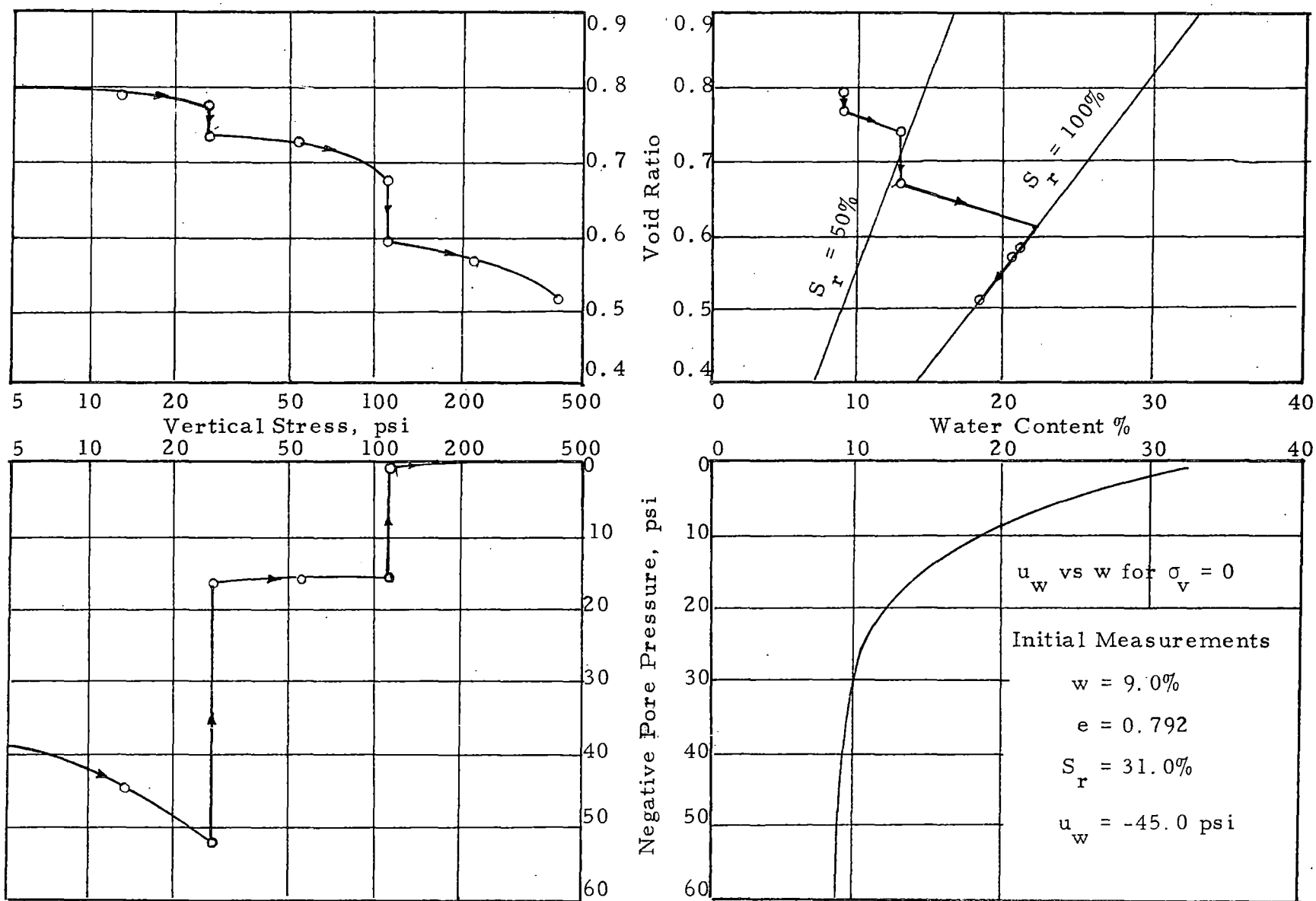


Fig. 3.22 Results of Confined Compression Test No. S2

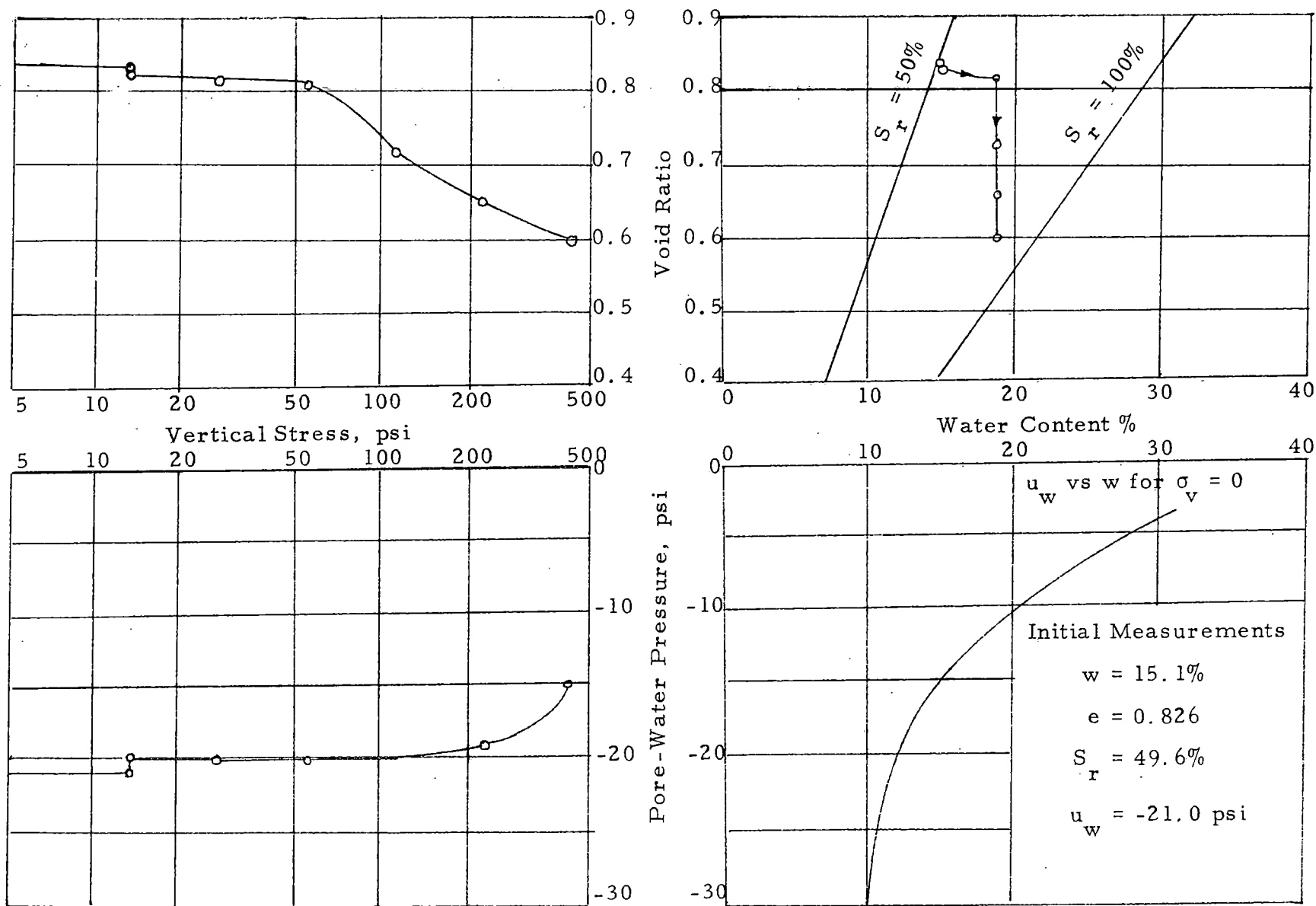


Fig. 3.23 Results of Confined Compression Test No. S3

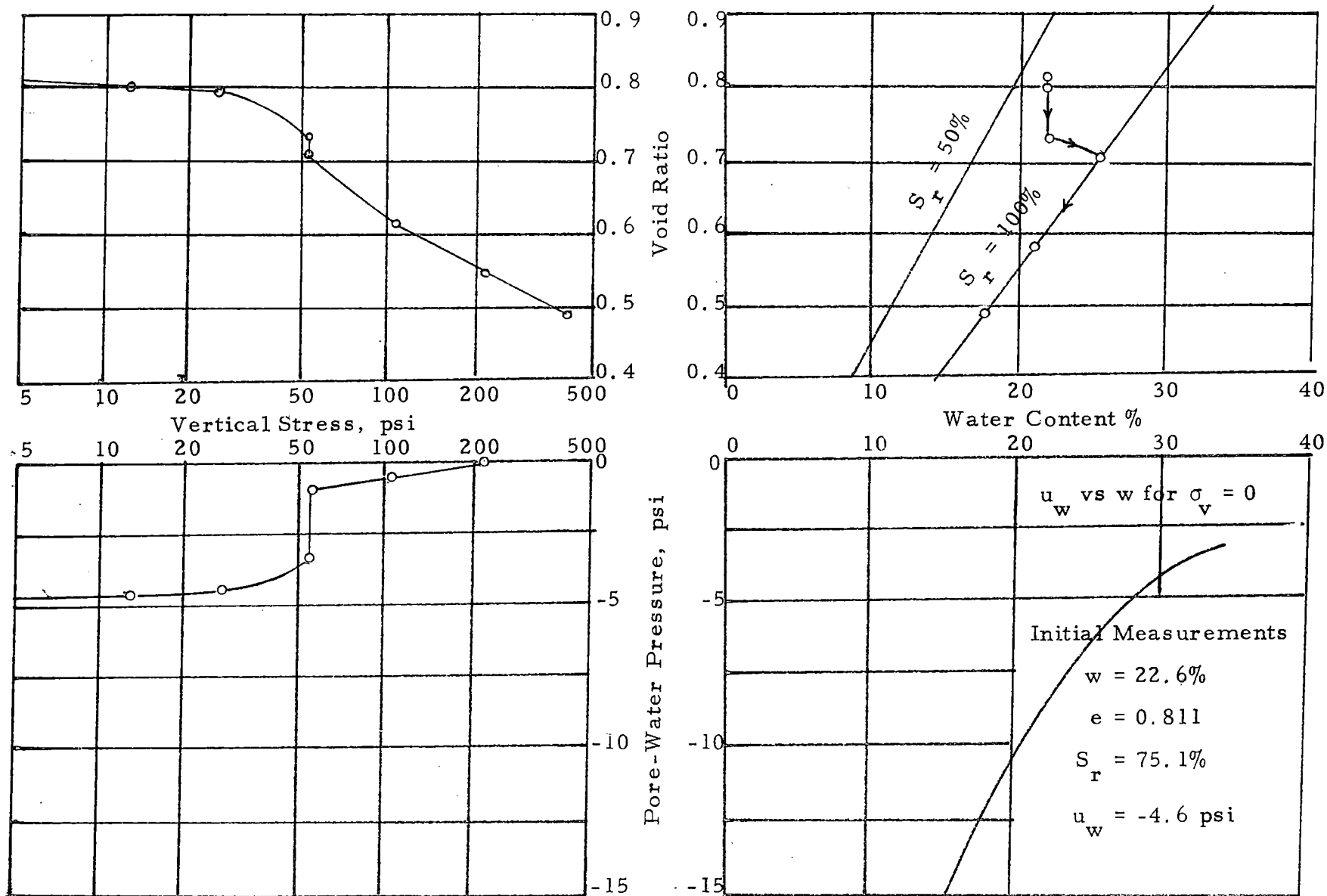


Fig. 3.24 Results of Confined Compression Test No. S4

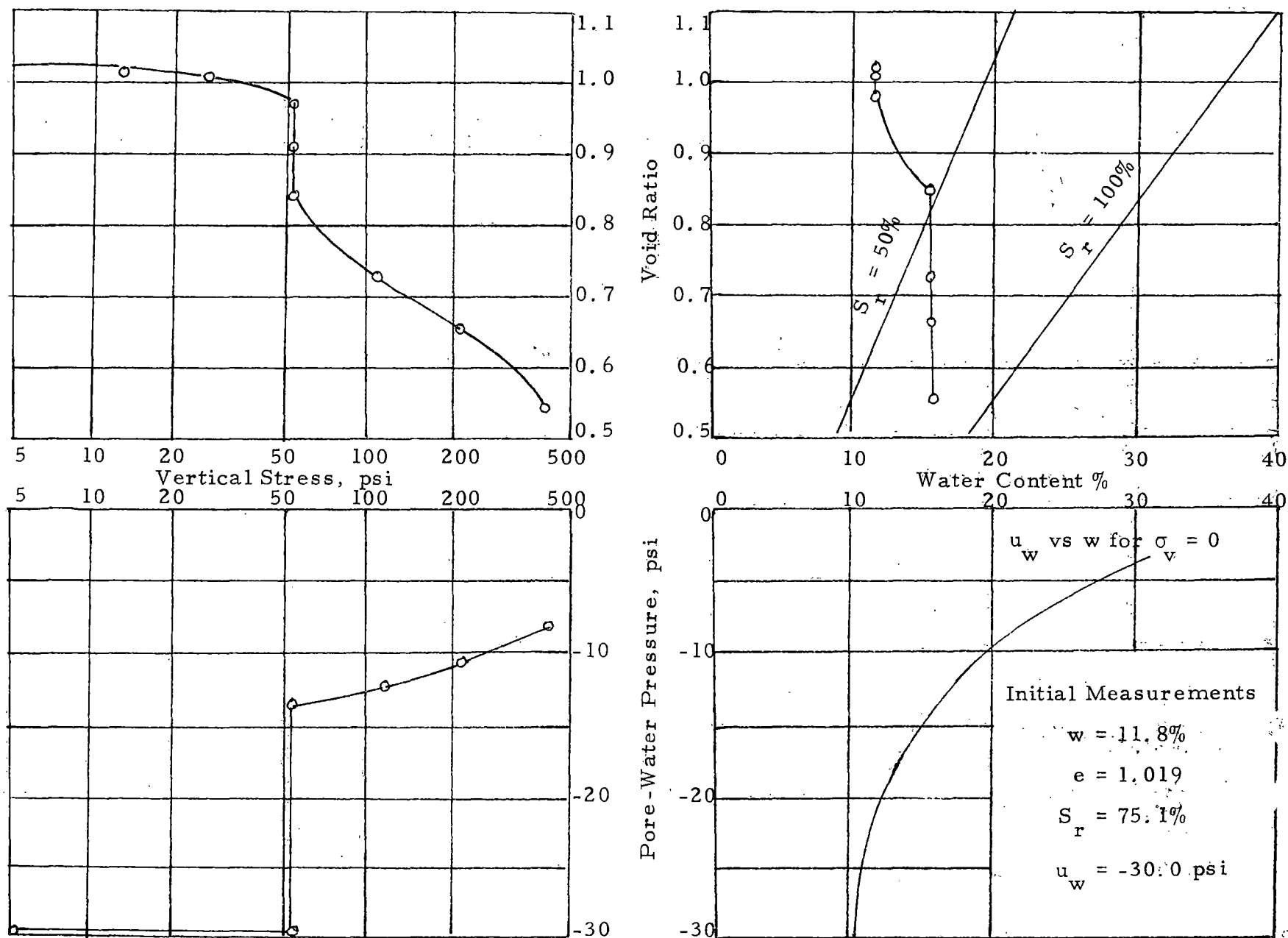


Fig. 3.25 Results of Confined Compression Test No. S-5

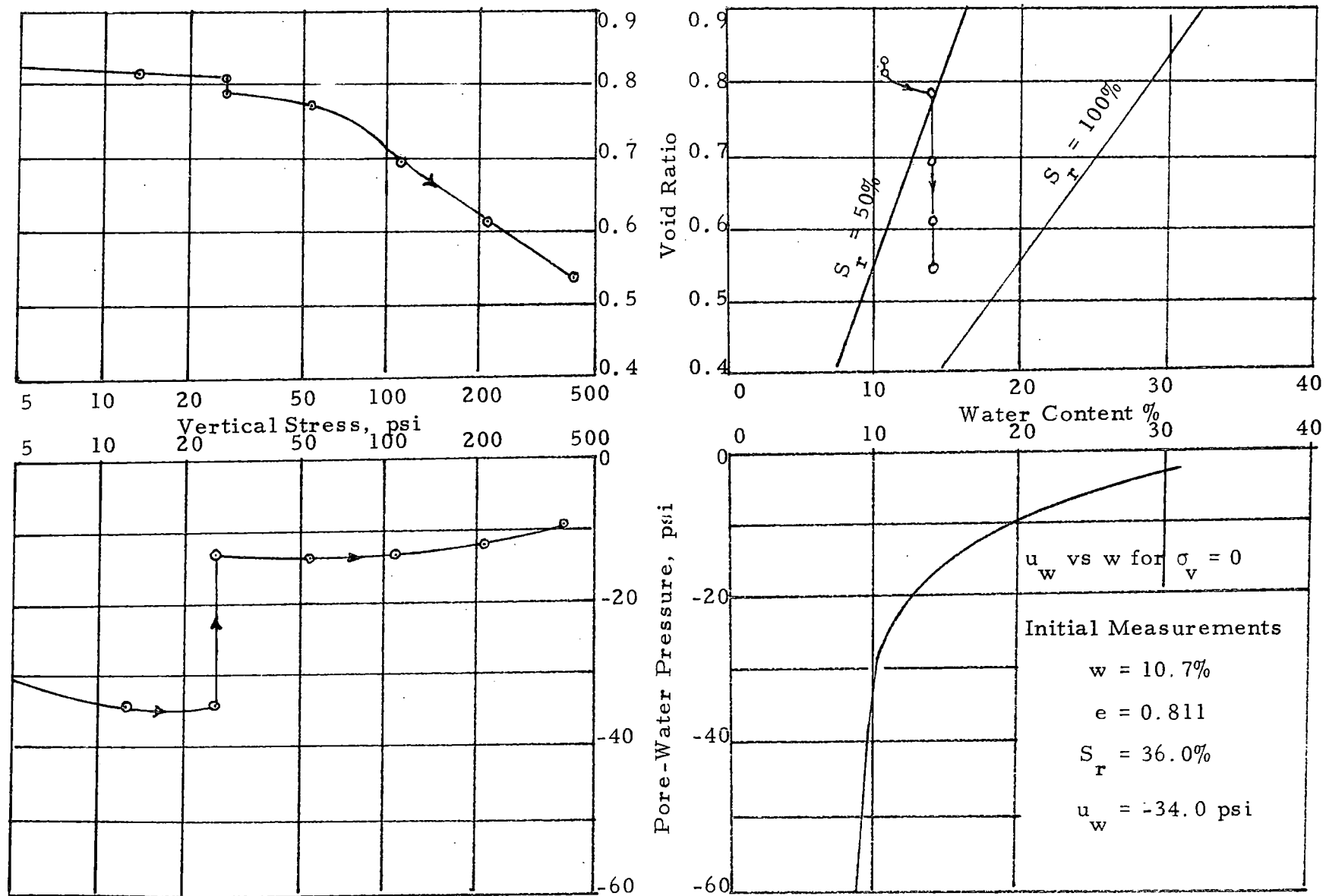


Fig. 3.26 Results of Confined Compression Test No. S6

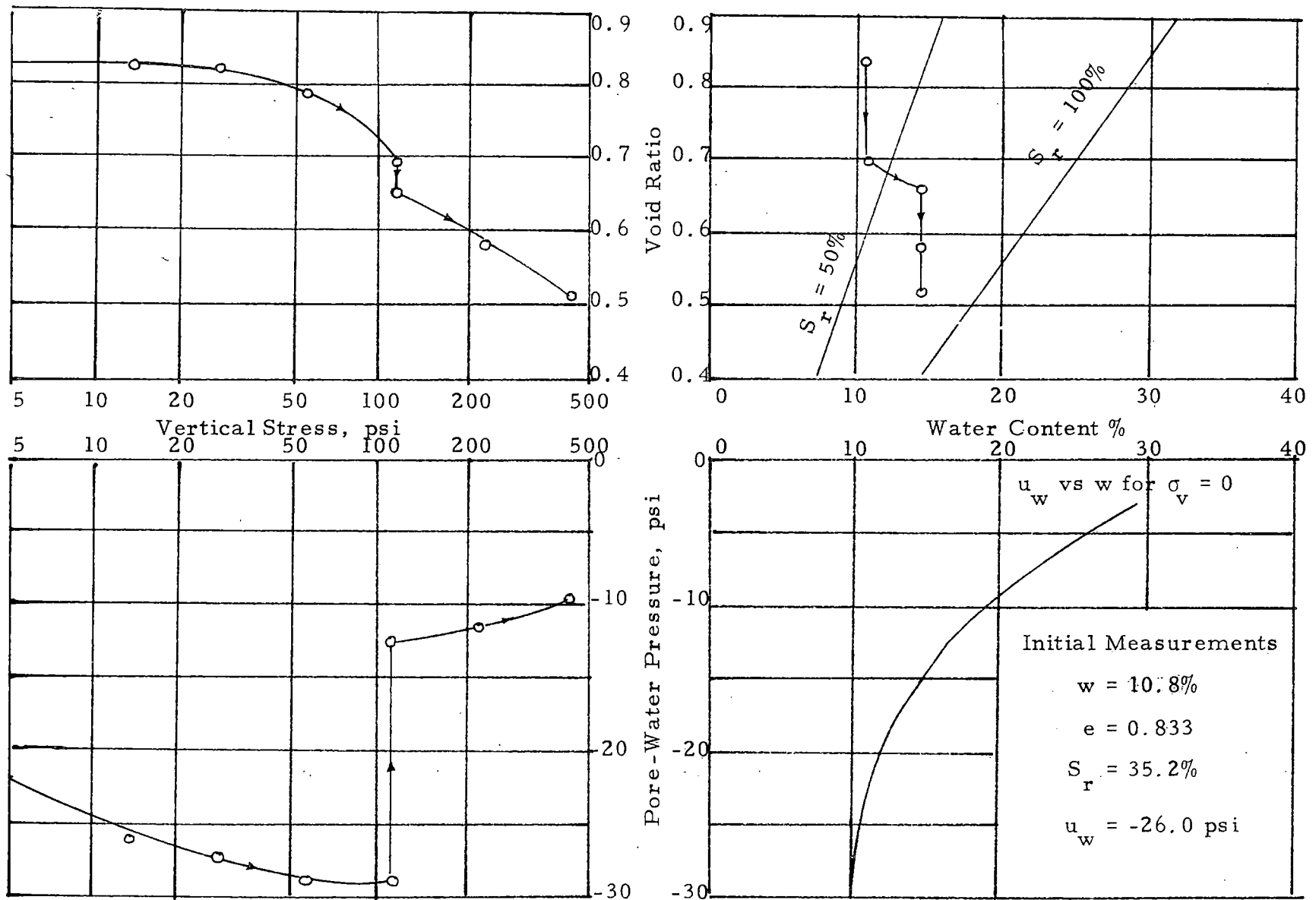


Fig. 3.27 Results of Confined Compression Test No. S7

TABLE 3.1 SUMMARY OF CONFINED COMPRESSION TESTS

1. Test No.		5	14	24	20	6	4	7	3	18
<u>INITIAL MEASUREMENTS</u>										
2. Water content	w_i %	4.6	4.6	6.1	7.4	7.6	8.6	9.4	9.5	12.7
3. Void ratio	e_i	0.817	0.762	0.798	0.751	0.801	0.783	0.805	0.780	0.776
4. Degree of saturation	S_{ri} %	15.3	16.6	20.8	27.0	25.8	29.6	31.8	33.1	44.5
5. Pore-water pressure	u_w psi	-289	-255	-175	-122	-113	-137	-89.0	-96.5	-18.0
<u>FINAL MEASUREMENTS</u> ($\sigma_v = 444$ psi)										
6. Water content	w %	4.6	4.6	6.1	7.4	7.6	8.6	9.4	9.5	12.7
7. Void ratio	e	0.604	0.551	0.574	0.566	0.575	0.530	0.553	0.523	0.525
8. Degree of saturation	S_r %	20.7	22.9	28.8	35.8	36.0	43.8	46.2	49.3	65.8
9. Pore-water pressure	u_w psi	-300	-231	-160	-98	-95	-110	-86.2	-84.2	-13.5
<u>STRESS-STRAIN PARAMETERS</u>										
10. Maximum compression index, C_c		0.394	0.296	0.318	0.297	0.305	0.299	0.319	0.279	0.293
11. σ_{vc} (Fig. 3.28)	psi	90.5	78.8	71.7	88.8	93.6	72.4	80.6	76.1	48.6
12. $(\sigma_v)_2$	psi	120.7	86.1	74.4	113.3	51.4	45.3	72.6	45.7	70.1

TABLE 3.1 SUMMARY OF CONFINED COMPRESSION TESTS (Contd.)

1. Test No.		16	15	21	11	19	23	17	22	13
<u>INITIAL MEASUREMENTS</u>										
2. Water content	w_i %	12.8	15.9	16.6	19.0	21.3	21.2	23.8	27.6	28.3
3. Void ratio	e_i	0.771	0.828	0.815	0.756	0.811	0.796	0.812	0.850	0.789
4. Degree of saturation	S_{ri} %	45.1	52.4	55.4	68.3	71.3	72.4	79.8	88.4	97.5
5. Pore-water pressure	u_w psi	-18.0	-12.5	-12.0	-8.0	-7.0	-9.0	-5.4	-3.4	-3.4
<u>FINAL MEASUREMENTS</u> ($\sigma_v = 444$ psi)										
6. Water content	w %	12.8	15.9	16.6	16.7	18.2	17.9	18.8	19.2	16.8
7. Void ratio	e	0.517	0.555	0.526	0.455	0.494	0.488	0.510	0.522	0.458
8. Degree of saturation	S_r %	67.3	78.2	85.7	100	100	100	100	100	100
9. Pore-water pressure	u_w psi	-14.9	-6.4	-6.2	0	0	0	0	0	0
<u>STRESS-STRAIN PARAMETERS</u>										
10. Maximum compression index, C_c		0.279	0.309	0.316	0.340	0.262	0.335	0.320	0.248	0.241
11. σ_{vc} (Fig. 3.28)	psi	51.1	46.3	50.0	44.2	37.8	24.6	39.2	20.4	17.1
12. $(\sigma_v)_2$	psi	68.1	58.9	62.5	43.5	20.0	37.6	34.7	15.3	18.1

TABLE 3.2 SUMMARY OF SPECIAL CONSOLIDATION TESTS

Test No.		S1	S2		S3	S4	S5	S6	S7
<u>INITIAL MEASUREMENTS</u>									
Water content	w %	5.3	9.0		15.1	22.4	11.8	10.7	10.8
Void ratio	e	0.812	0.792		0.826	0.811	1.019	0.811	0.833
Degree of saturation	S _r %	17.8	31.0		49.6	75.1	31.5	36.0	35.2
Pore-water pressure	u _w psi	-130	-45.0		-21.0	-4.6	-30.0	-34.0	-26.0
<u>AT WETTING</u>									
Vert. str. during wetting, psi		111.1	27.8	111.1	13.9	55.6	55.6	27.8	111.1
Water cont. before wetting, %		5.3	9.0	13.0	15.1	22.4	11.8	10.7	10.8
Water cont. after wetting, %		11.0	13.0	29.0	19.0	25.4	15.5	14.5	14.5
Void ratio before wetting		0.755	0.776	0.671	0.825	0.732	0.978	0.802	0.697
Void ratio after wetting		0.610	0.738	0.597	0.821	0.710	0.846	0.787	0.659
Pore-water pres. before wetting	psi	-137	-52.0	-16.2	-20.7	-3.4	-30.0	-34.0	-28.6
Pore-water pres. after wetting	psi	-19.5	-17.0	-0.8	-19.8	-0.9	-13.6	-13.6	-12.6
<u>FINAL MEASUREMENTS</u> ($\sigma_v = 444$ psi)									
Water content	%	11.0	21.5		19.0	18.2	15.5	14.5	14.5
Void ratio	e	0.468	0.516		0.597	0.496	0.553	0.54	0.517
Degree of saturation	S _r %	31.0	100		68.7	100	58.0	54.0	56.8
Pore-water pressure	u _w psi	-22.9	0		-14.7	0	-8.0	-9.6	-10.0

slightly smaller (more negative) than those for $\sigma_v = 0$ and are believed to be more reliable because of the improved seating under the higher load.

Table 3.1 also lists for the basic tests the maximum compression index C_c , which is the steepest slope of the void ratio - $\log \sigma_v$ curve, as well as two other parameters which are used in subsequent analyses. These parameters are a stress σ_{vc} defined on the basis of the change in compression index in Fig. 3.28, and the stress when the vertical compressive strain is 2%, $(\sigma_v)_2$.

Table 3.2 lists for the special tests the stress level at which the water content was increased, and the water contents, void ratios, and pore-water pressures before and after wetting.

3.3 K_o - Tests

3.3.1 Description. A series of tests designated as K_o -tests was run to supplement the confined compression tests previously described. In these tests, the lateral stress was measured during confined compression. Detailed descriptions of the scope, equipment, procedures, and results of this supplementary study are included in Appendix IV. A brief summary of the pertinent procedures and results is presented here.

The K_o - tests were run in a standard triaxial cell on specimens having diameters of 1.5 in. and heights of 3 in. Lateral strains were

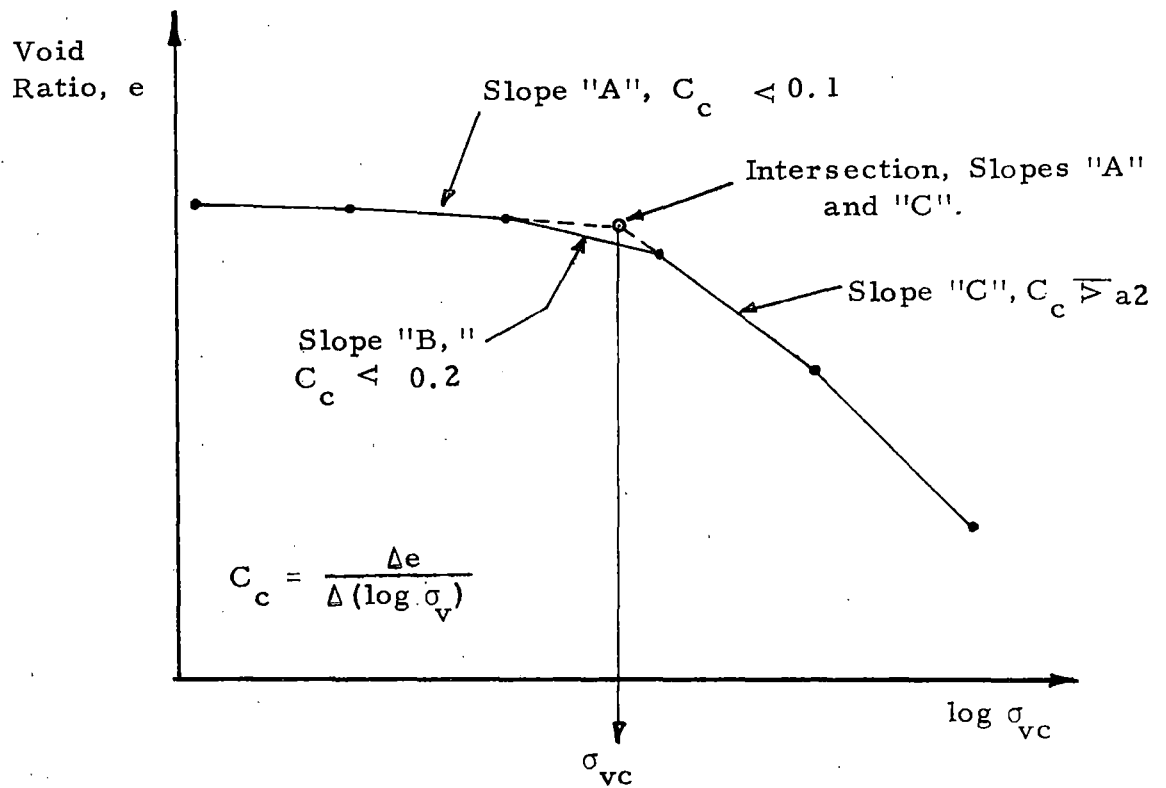


Fig. 3.28 Definition of Collapse Stress σ_{vc}

detected by means of a specially designed lateral-strain indicator. The test was set up in the same manner as a standard triaxial compression test with a zero cell pressure. The axial stress was then increased and the cell pressure was increased as necessary to maintain zero lateral strain. All specimens were undisturbed, and at their natural water contents.

3.3.2 Summary of results. The ratio of the lateral to axial stress is defined as K_o , the lateral stress ratio at rest. Before the collapse of the soil structure, which occurred at axial strains of 1% to 4%, the average value of K_o was 0.23. After collapse, K_o increased to 0.54.

Individual test values leading to these averages are given in Table 3.3.

3.4 Triaxial Compression Tests

Consolidated-drained triaxial compression tests were run on undisturbed samples at their natural water content and these tests are also described in detail in Appendix IV. The pertinent results are tabulated in Table 3.4 and the modified Mohr-Coulomb diagram based total stresses is shown in Fig. 3.29.

TABLE 3.3 SUMMARY OF K_o -TESTS

1. Test No.	1	2	3	H-1	H-2	H-3	Average
<u>INITIAL MEASUREMENTS</u>							
2. Water content %	22.6	21.5	22.9	22.6	22.7	23.0	--
3. Void ratio	0.883	0.862	0.851	0.871	0.848	0.833	--
4. Degree of saturation %	69.3	67.5	73.1	70.2	72.6	74.8	--
<u>LATERAL STRESS RATIO, K_o</u>							
5. Before collapse	0.25	0.22	0.15	0.23	0.33	0.17	0.23
6. After collapse	0.52	0.56	0.54	0.54	0.56	0.50	0.54

TABLE 3.4 SUMMARY OF TRIAXIAL COMPRESSION TESTS

Test No.	Initial			After consolidation			$(\sigma_v - \sigma_h)_f$ psi
	Water Content %	Void ratio	Degree of Saturation %	Cell Pressure psi	Void ratio	Degree of Saturation %	
(1)	(2)	(3)	(4)	(5)	(6)	(7)	(8)
1	23.4	0.817	77.9	0	0.817	77.9	15.6
2	23.3	0.841	75.4	5	0.835	76.4	24.4
3	23.2	0.856	73.6	10	0.845	74.6	27.3
4	23.5	0.896	71.3	15	0.887	72.0	34.8
5	23.4	0.842	75.5	20	0.838	75.9	40.0
6	23.4	0.868	73.2	30	0.838	75.8	57.9
7	24.0	0.856	76.3	40	0.822	79.5	73.6
8	23.3	0.862	73.5	60	0.757	83.7	110.1
9	23.2	0.819	77.1	100	0.695	90.9	200.0
10	23.5	0.837	76.5	140	0.661	96.9	274.0

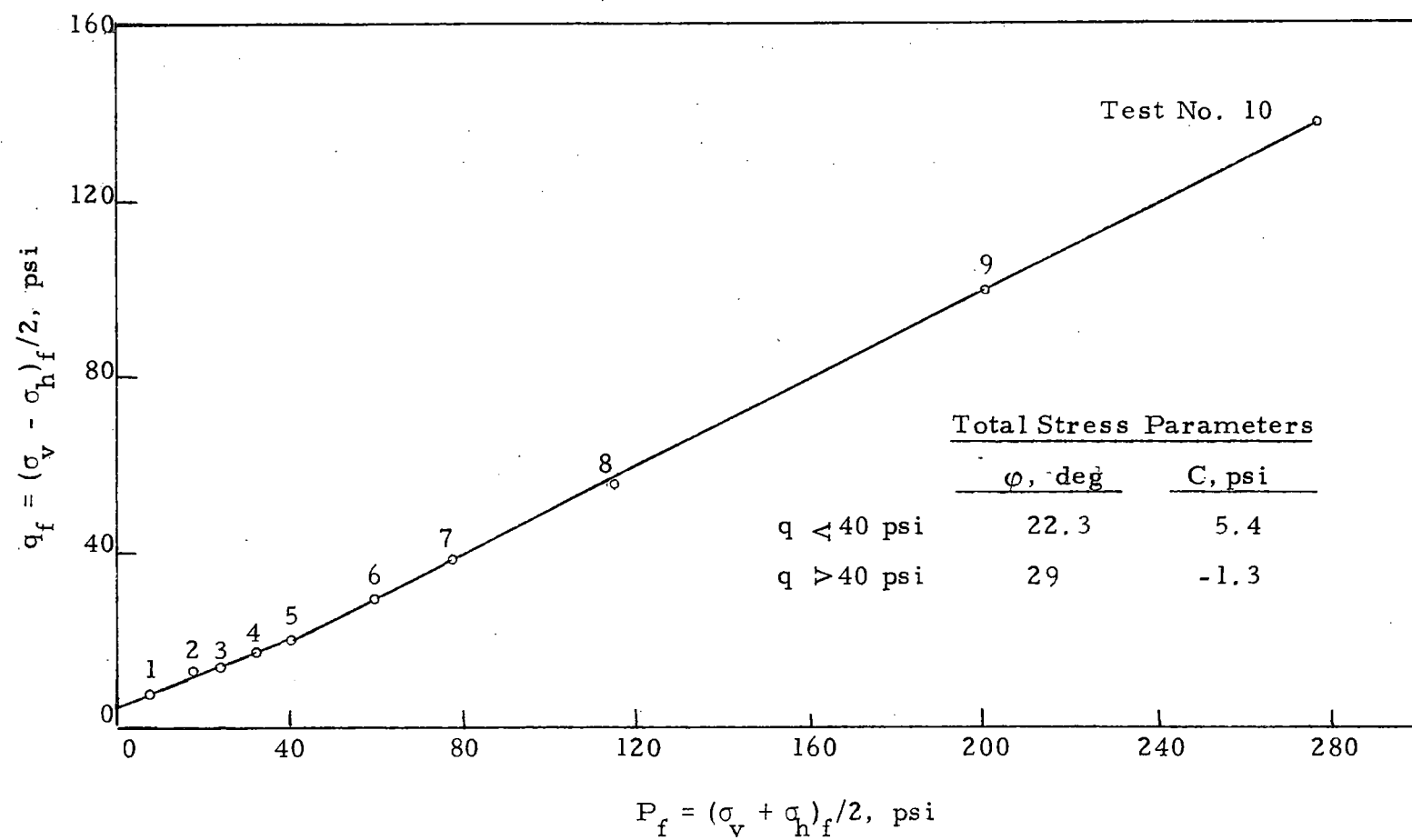


Fig. 3.29 Failure Envelope for Oakdale Loess Based on Total Stresses

CHAPTER 4

DISCUSSION OF TEST RESULTS

4.1 General Comparisons

Six specimens have been selected to illustrate the trends in the data. The test results for these specimens are presented in Fig. 4.1, a four-variable plot of log stress, void ratio, water content, and negative pore-water pressure. The specimens had initial water contents ranging from 4.6% to 28.3% and approximately the same initial void ratio.

The void ratio-log stress plots in Fig. 4.1 (a) show that the wetter specimens were more compressible than the drier specimens which is, of course, to be expected. The stress level at which the curve steepens for the driest specimen is nearly ten times that for the wettest specimen.

The void ratio-water content plots in Fig. 4.1 (b) show lines for 50% and 100% saturation and the change in degree of saturation of the sample during the course of the tests may be observed. The water content remained constant during the compression of the dry specimens. For these specimens the degree of saturation increased as a result of the reduced volume of voids but the specimens remained partially saturated. On the other hand, the wettest two specimens became 100% saturated during compression and the further reduction in voids caused water

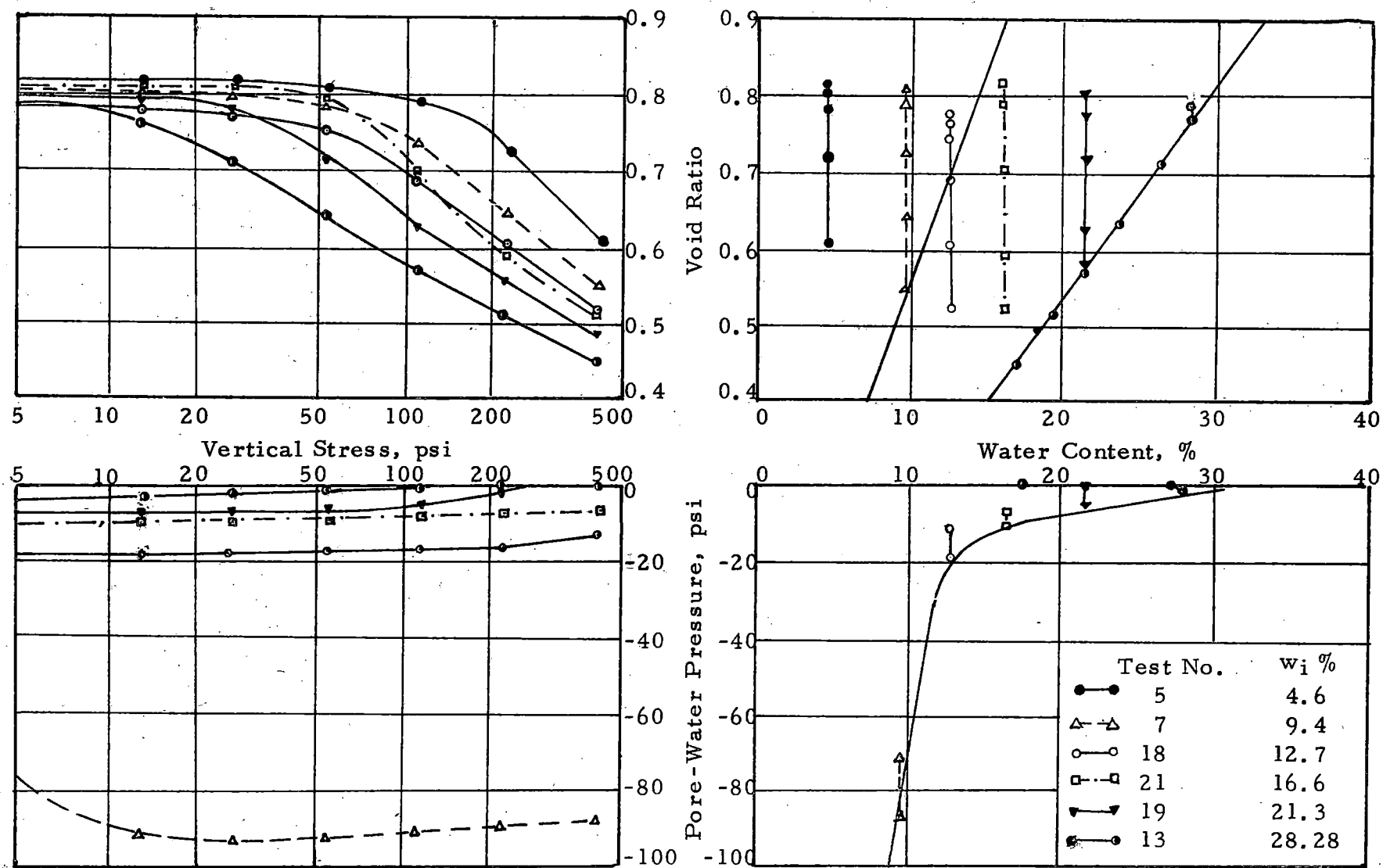


Fig. 4.1 Comparison of Confined Compression Test Results

to be expelled from the specimen and a consequent decrease in water content.

More detailed comparisons of the stress-strain and -volumetric relations, and the pore-water pressures (Fig. 4.1 (c) and (d)), before and during compression, are considered in the following sections.

4.2 Volume Changes and Strains

4.2.1 Void ratio-log stress relations. The void ratio-log stress curves may be compared by the use of two parameters, the stress at which the curve changes from a flat to a steep slope, and the slope of the steepest part of the curve. The latter slope is designated here as the maximum compression index C_c and values have been listed in Table 3.1.

Fig. 4.2 (a) shows the maximum C_c plotted against initial water content. The points are scattered above and below a value of 0.3 with values tending to be higher at lower water contents.

The stress σ_{vc} at which the void ratio-log stress curve changes from a flat to a steep slope was determined by use of the criterion given in Fig. 3.28. This criterion defines the steep slope "C" as one with C_c equal to 0.2 or more. In all cases the flat slopes "A" had C_c values smaller than 0.1. The values of σ_{vc} are listed in Table 3.1 for each test and plotted against the initial water content in Fig. 4.2 (b). The plot shows a nearly linear decrease in σ_{vc} with increasing initial water content. The least square equation for this line is

$$\sigma_{vc} \text{ (psi)} = 100.5 - 3.01 w \text{ (\%)} \quad (\text{Eq. 4.1})$$

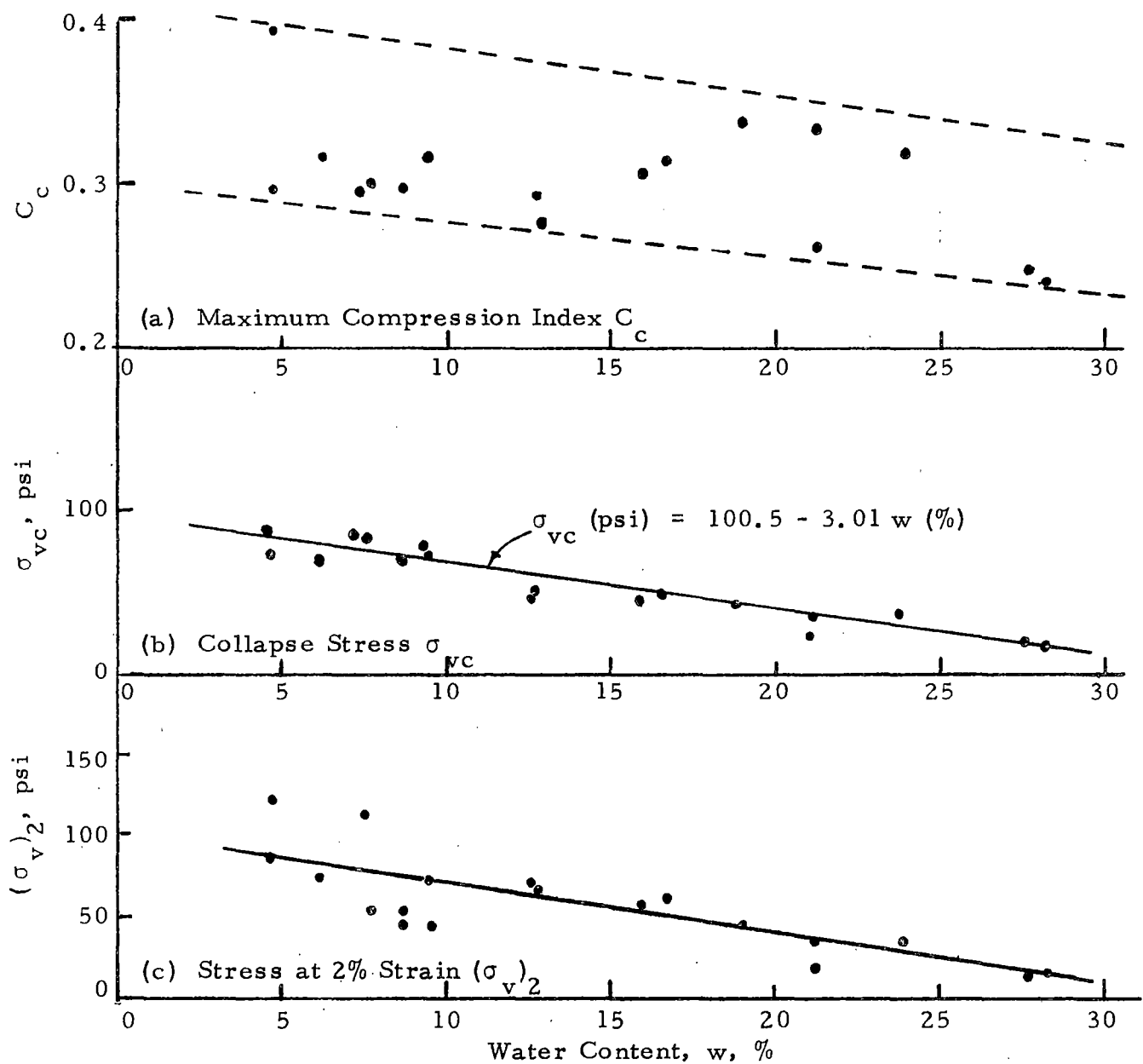


Fig. 4.2 Relations From Confined Compression Tests

4.2.2 Stress-strain relations. The stress-strain relations are to some extent obscured by void ratio-log stress curves. An arithmetic plot of strain versus stress for three typical tests is presented in Fig. 4.3. The curve for Test 21 shows a significant increase in compressibility in the stress interval between 55 psi and 110 psi. Thereafter the soil becomes stiffer with increasing stress. This increased compressibility signifies the collapse of the open structure of the natural soil. The K_o -tests demonstrated a similar collapse occurring between axial strains of 1% and 4%. Evidence that a structural change is involved was provided by the increase in K_o -values from 0.23 before collapse to 0.54 after collapse (Table 3.3).

The collapse effect is less pronounced for Tests 14 and 22, which are also shown in Fig. 4.3, and it is difficult to determine a stress at which collapse occurs. The values of σ_{vc} previously determined are indicated in the figure and lie either within or immediately ahead of the steep part of the curves. The strains which correspond to σ_{vc} are within the 1% to 4% bracket observed for collapse in the K_o -tests and, for comparison with σ_{vc} , the stresses at 2% strain $(\sigma_v)_2$ have been determined. These values are listed in Table 3.1 and plotted against water content in Fig. 4.2 (c). It is evident that a considerably greater scatter exists for $(\sigma_v)_2$ than for σ_{vc} .

A direct comparison between σ_{vc} and $(\sigma_v)_2$ is shown in Fig. 4.4. The conclusion from this figure is that σ_{vc} is representative of the stress

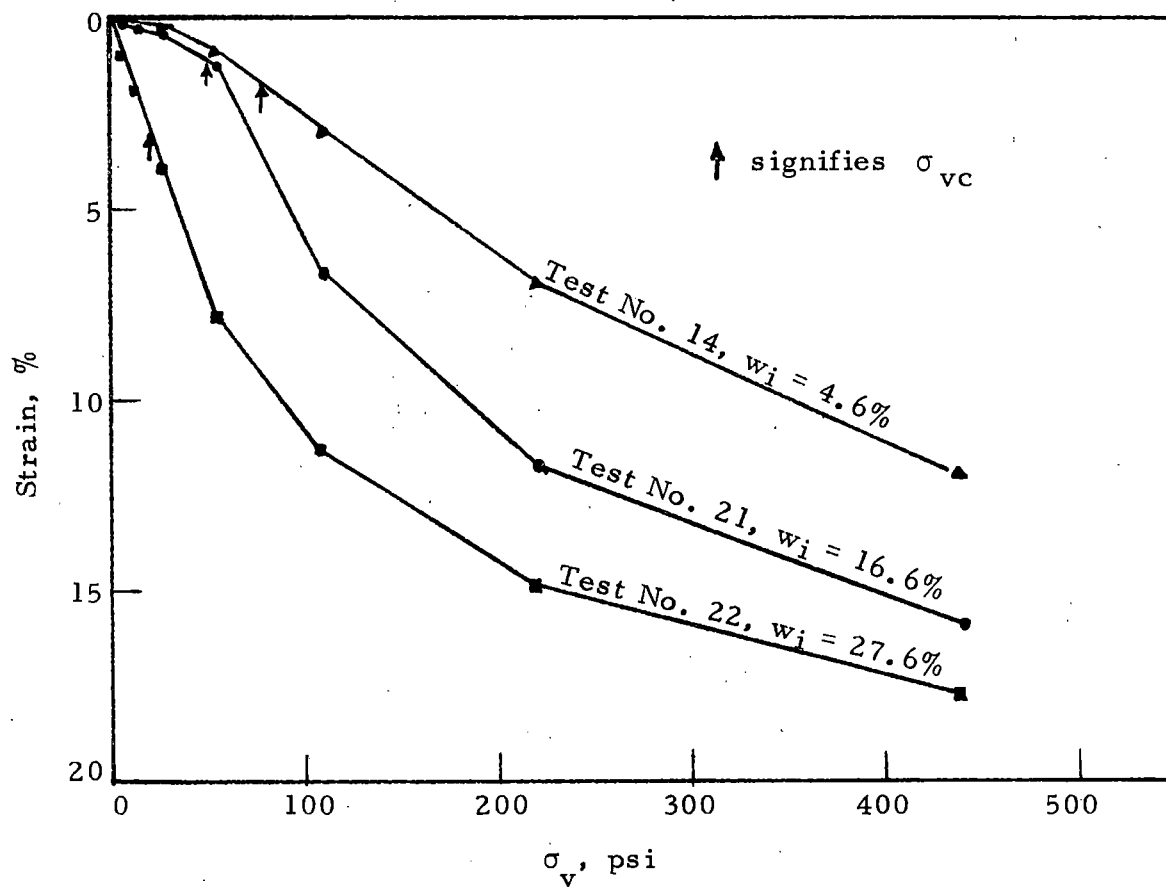


Fig. 4.3 Stress-Strain Curves for Confined Compression Tests No. 14, 21, and 22

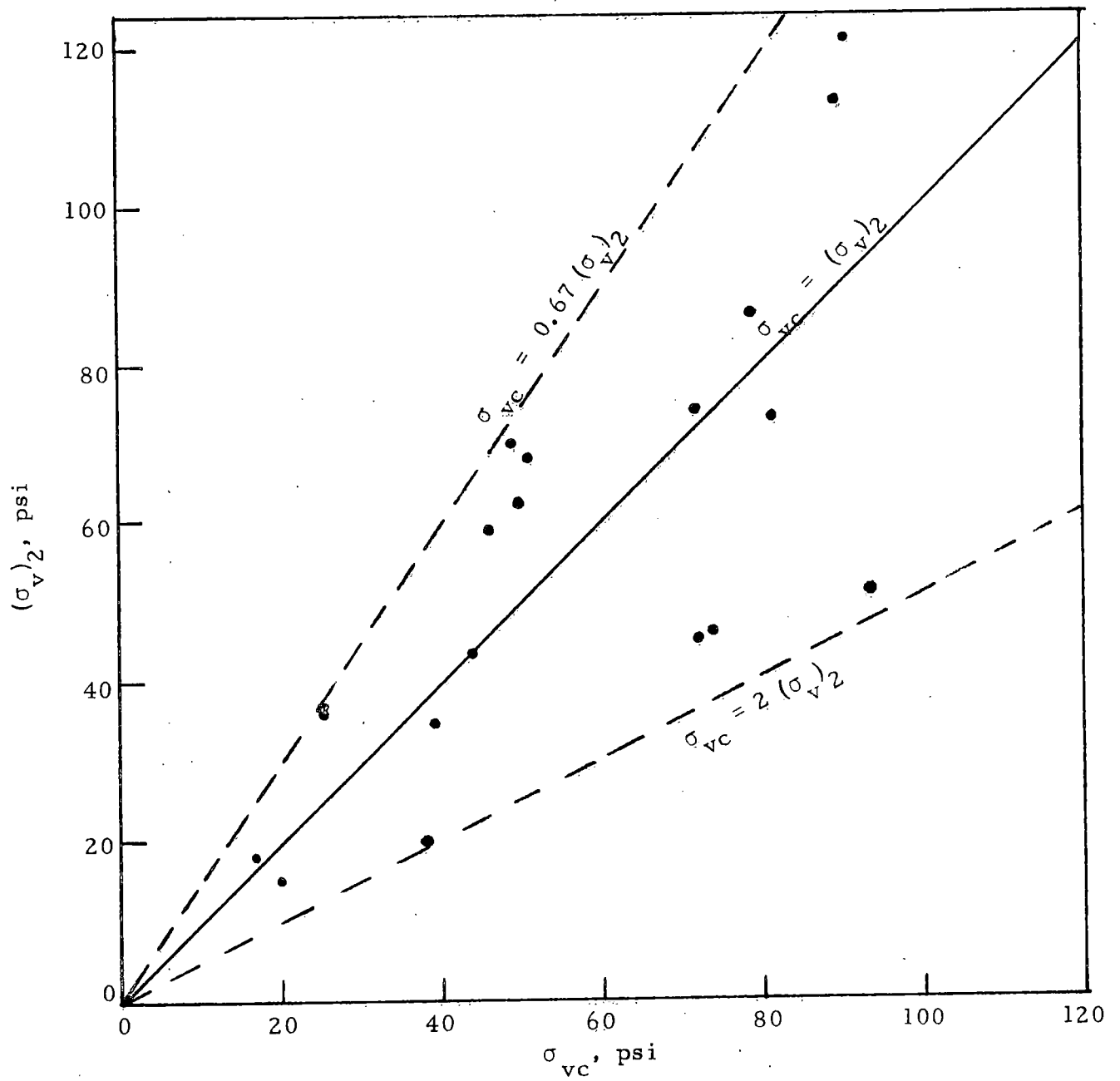


Fig. 4.4 Comparison of $(\sigma_v)_2$ with σ_{vc}

at a strain of 2% though a wide variation exists. The variation is at least in part due to the fact that the strains are based on the original thickness and seating errors are included in the determination of $(\sigma_v)_2$. On the other hand σ_{vc} is based on the incremental slope of the void ratio-log stress curve and therefore is independent of seating errors. The use of the geometric loading increments is also ill-suited to the detailed study of stress-strain relations because of the wide spacing of data points.

4.3 Pore-Water Pressures

The initial pore-water pressures given in Tables 3.1 and 3.2 are plotted against initial water content in Fig. 4.5. The curve drawn through the data points has the equation

$$u_w \text{ (psi)} = - \left(\frac{44}{w\%} \right)^{2.6} \quad (\text{Eq. 4.2})$$

This equation is limited to the pressure range between 3 psi and 300 psi. Twenty of the twenty-five measured pressures are within 33% of the value given by this equation.

For a given water content, the negative pore-water pressure is independent of the degree of saturation except when S_r exceeds 85% or 90%. This is shown in Fig. 4.6 where the pore-water pressure is plotted against degree of saturation for representative tests. For each test, the water content is constant, but the degree of saturation increases as a result of the reduction in voids during compression. The approximately horizontal curves show that the pore-water pressure does not change

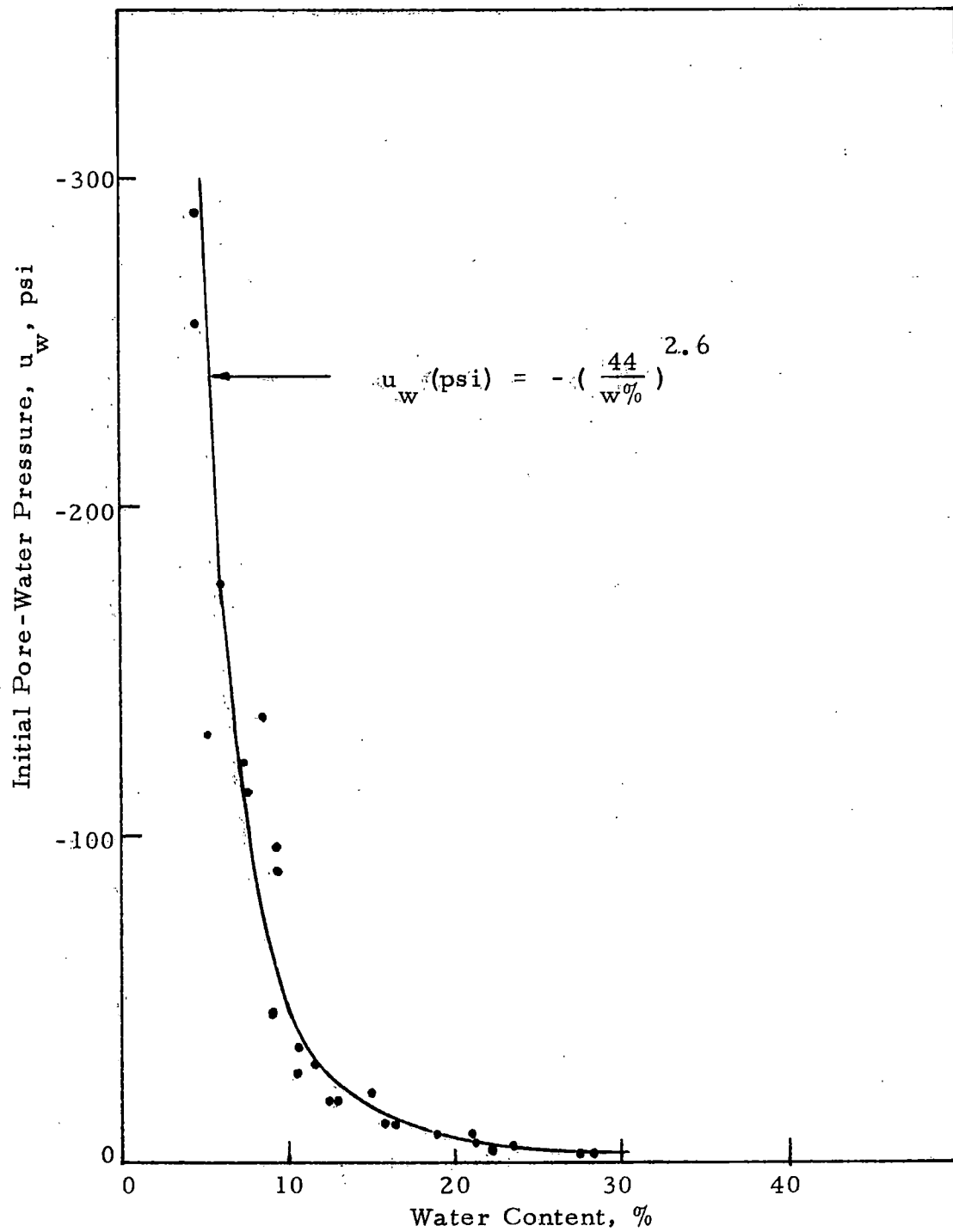


Fig. 4.5 Relation Between Initial Pore-Water Pressure and Water Content

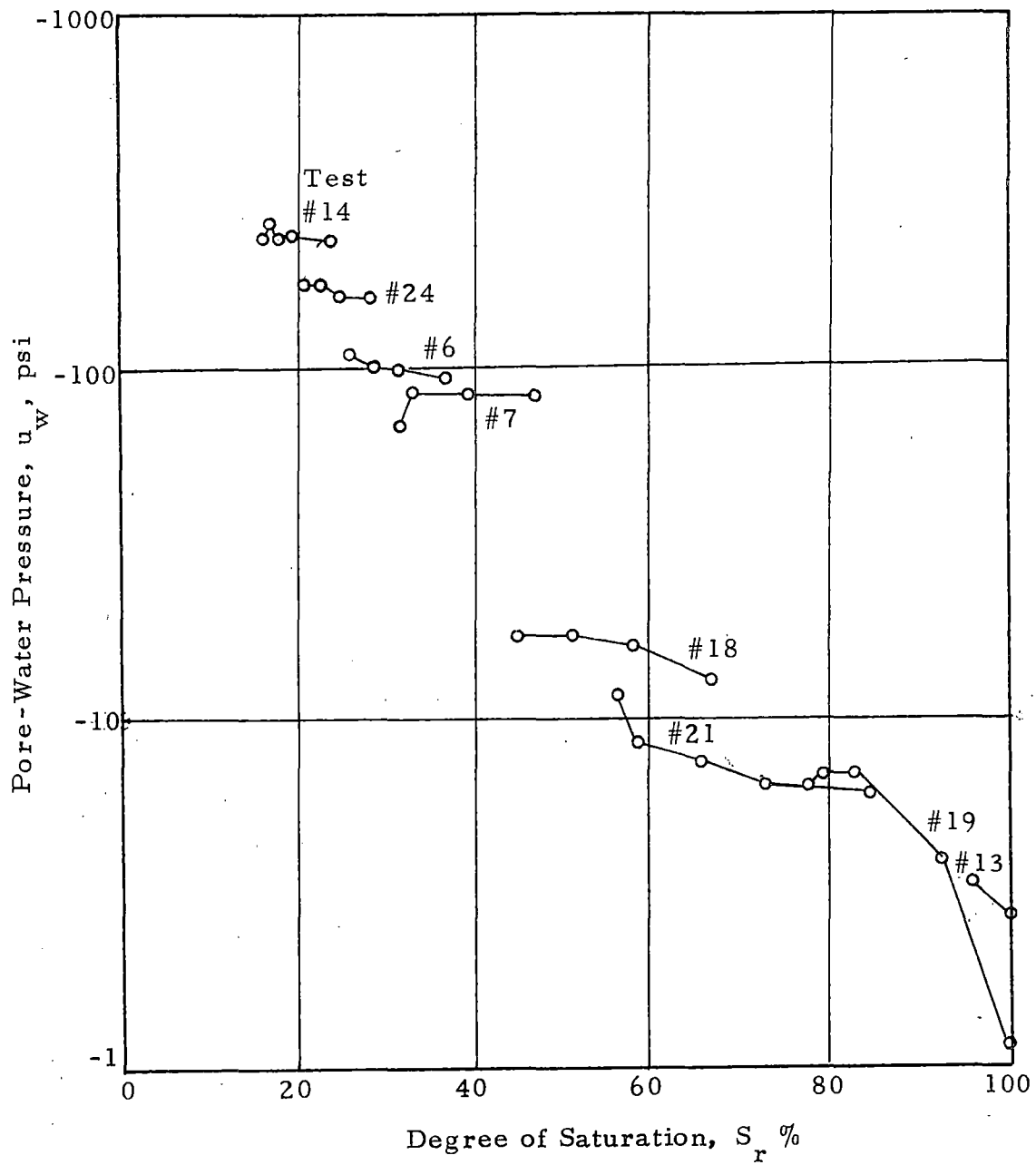


Fig. 4.6 Pore-Water Pressure vs Degree of Saturation During Confined Compression

during this process. The independence of pore-water pressure from degree of saturation may be explained as follows. The clay content is distributed as coatings on larger particles or as aggregates of clay particles. The water in the soil is dispersed in the clay voids and on the surface of the larger particles. The clay voids do not change in volume with changes in voids of the whole soil and thus the shapes of the menisci, and the pore-water pressures, are independent of the total volume of voids. When the degree of saturation exceeds 90%, however, the volume of air is at a point where a further reduction in the voids causes the larger pores to become saturated and the pore water pressure increases. At a degree of saturation of 100%, the water fills the voids and further compression is accompanied by the expulsion of water from the soil. For this saturated state, the pore-water pressure will be zero when consolidation is complete.

The negative pore-water pressure is also independent of the applied vertical stress and the resulting shear stresses. This is shown by the plot of pore-water pressure versus vertical stress in Fig. 4.7. Changes in measured pore-water pressure are not significant except when the vertical stress in the wetter specimens exceeds 110 psi, but for these cases the specimens are approaching saturation.

This behavior was not anticipated. Shearing strains on an undrained saturated clay specimen in general will cause a change in pore-water pressure. In normally-consolidated clays the pore-water pressure

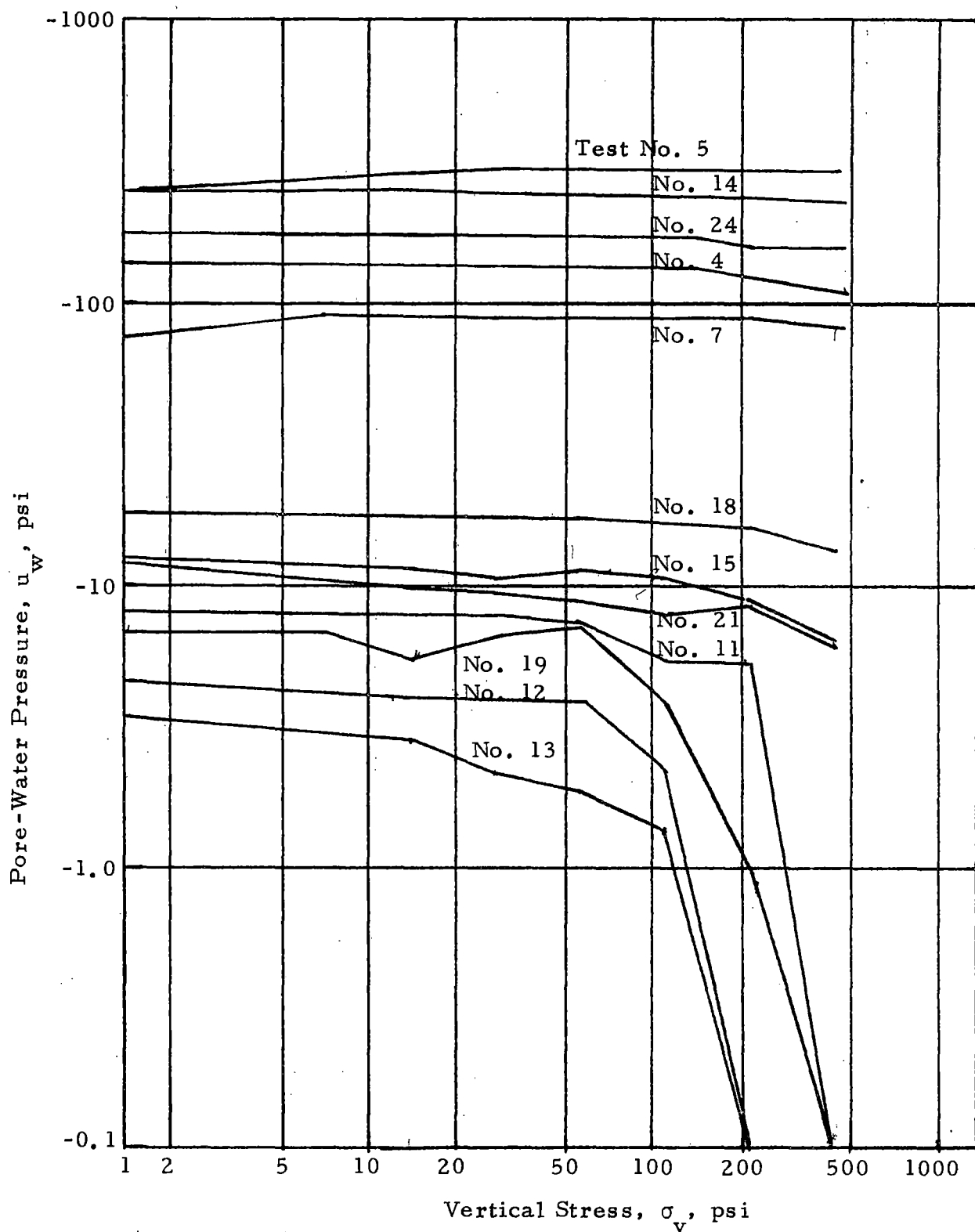


Fig. 4.7 Pore-Water Pressure vs Vertical Stress During Confined Compression

increases, whereas in over-consolidated clays the pore-water pressure decreases. Since shear strains of significant magnitude are produced during confined compression and the loess specimens were undrained in that the water content was constant, a change in pore-water pressure was to be expected. The reason that no change was observed is of interest. It is possible that the measurement system was not responsive. However, this is believed to be unlikely because of the excellent response observed for different initial water contents and for the predictable increase in pore-water pressure as saturation was approached. The most likely explanation is that the volume of clay which underwent shear strains was only that at the particle contacts and thus was a small part of the total clay volume. Because of the slow loading rate, pore-water pressures generated at the contacts could be dissipated by drainage to or from the remaining saturated clay voids. If this amount of drainage is small, as it is believed to be, then little or no pressure change will be produced in the pore-water filling the clay voids.

The relation between the pore-water pressure and the collapse stress σ_{vc} is shown in Fig. 4.8. The collapse stress increases rapidly with decreasing pore-water pressure but the rate diminishes when the pore-water pressure decreases below -100 psi. The collapse stress appears to approach a limiting value of 90 psi to 100 psi at a pore-water pressure of about -300 psi.

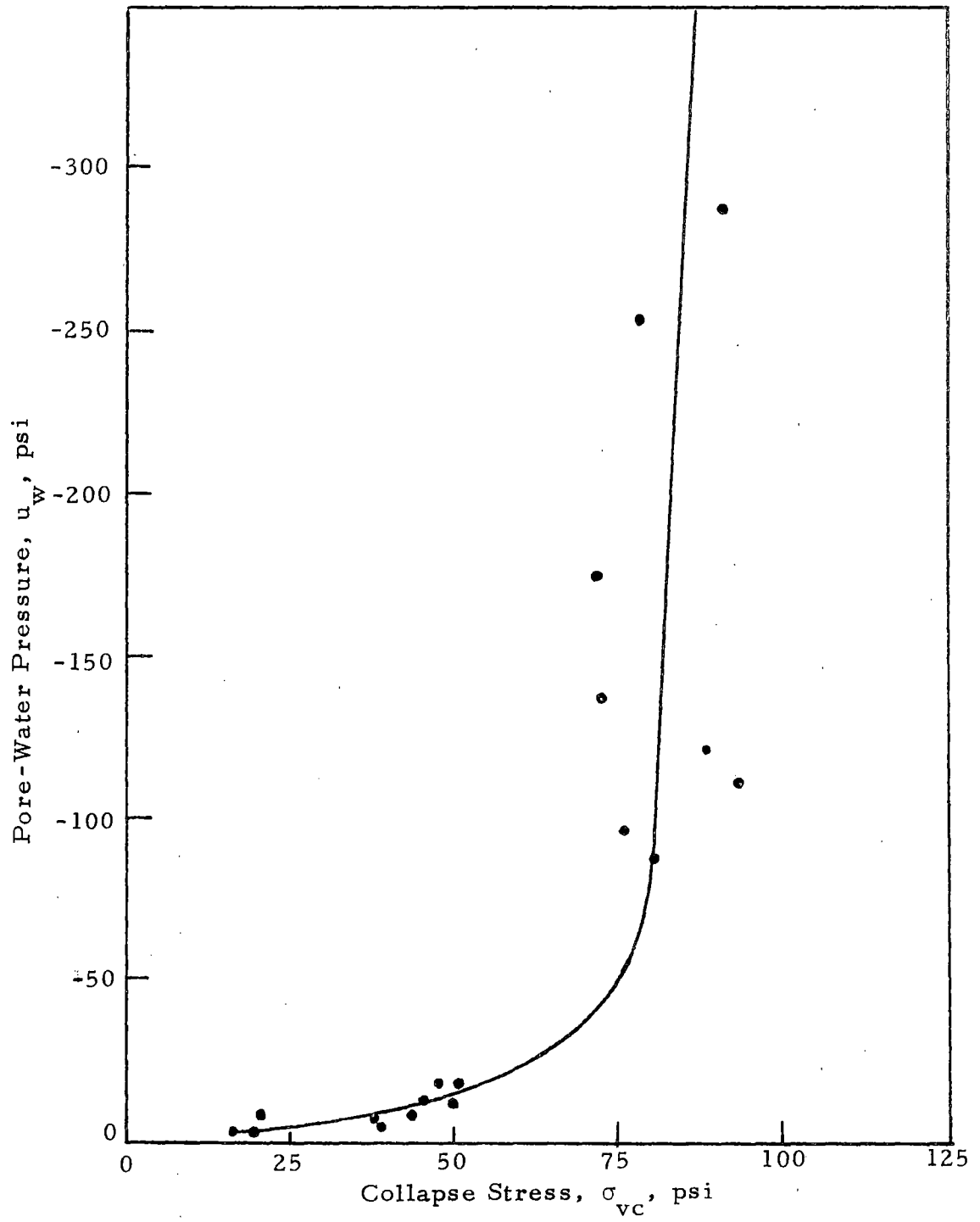


Fig. 4.8 Pore-Water Pressure vs Collapse Stress

4.4 Special Tests

The special confined compression tests were run by altering the water content of the specimen by known amounts while the specimen was under a vertical stress. The purpose of these tests was to inter-relate two or more of the void ratio-log stress curves in Fig. 4.1. The hypothesis to be tested was that at a low stress level, collapse would not occur upon wetting, whereas at a higher level, collapse would occur.

Three of the special tests are compared with appropriate tests from the basic series in Fig. 4.9. In Fig. 4.9 (c), it was necessary to adjust the void ratios for Test No. 22 because its initial void ratio (0.85) was significantly higher than the other two tests (0.80 and 0.81). The curves for the special tests do, in general, follow those for the basic tests having similar water contents. However the amount of compression that occurred upon wetting is greater than that indicated by the basic test curves. This may be due to the test procedure whereby the specimen was wetted from the bottom stone. It is possible that the water content of the lower part of the specimen was greater than the upper part before the water distributed itself uniformly through the specimen. If this were the case, the lower part of the specimen would compress more than the amount expected on the basis of the average water content. It was not possible to check this independently.

The vertical compressive strain that occurred as a result of the increase in water content depended on the magnitude of the vertical stress

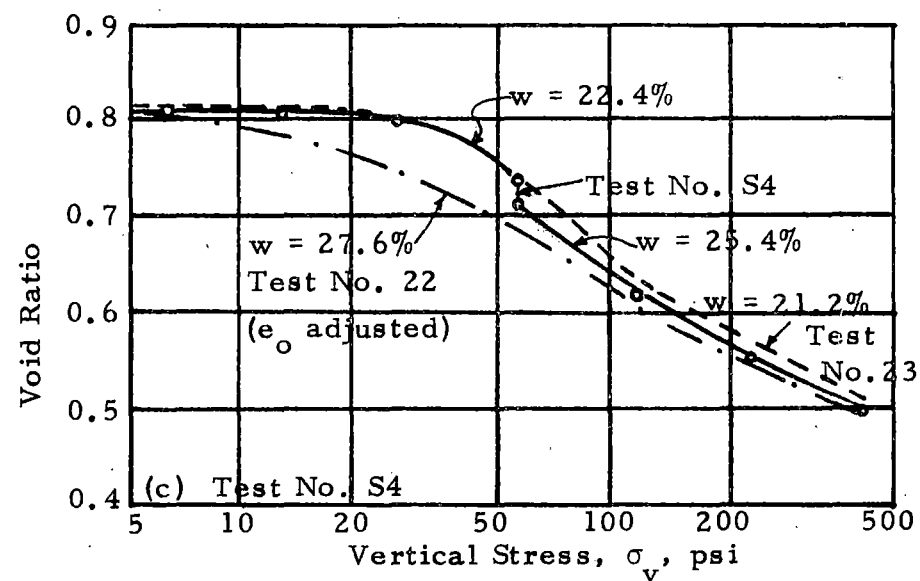
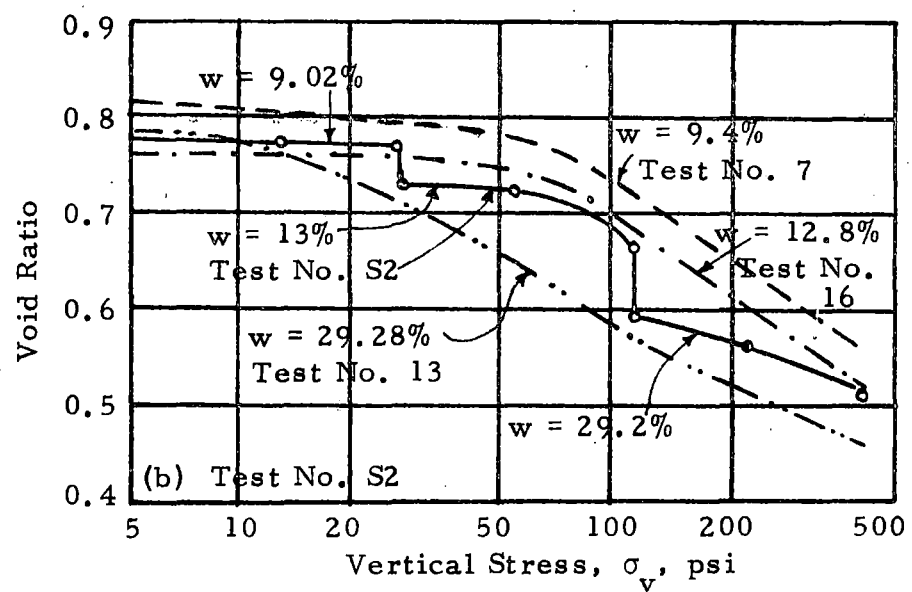
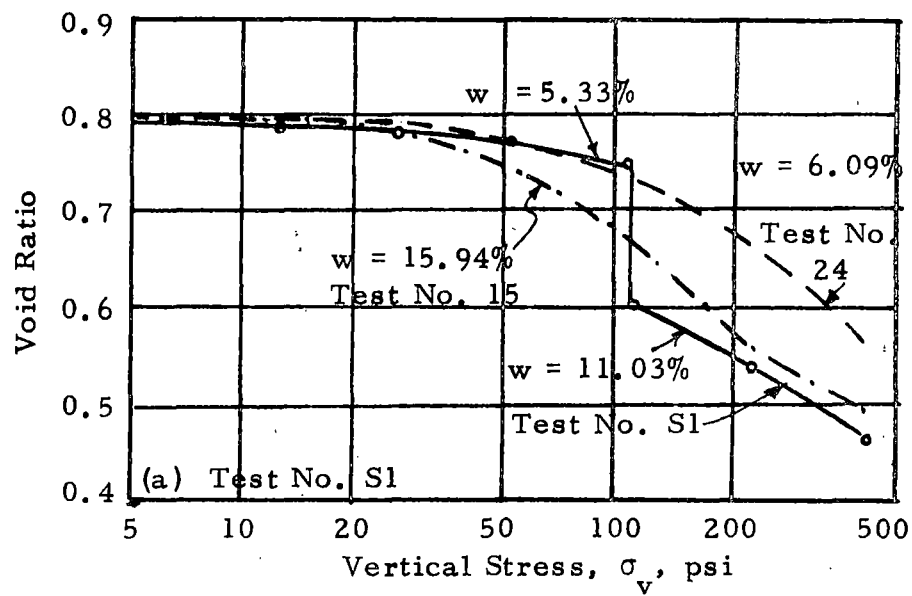


Fig. 4.9 Comparison of Special with Basic Confined Compression Tests

acting during the wetting as well as on the water content before and after wetting. Table 4.1 lists these values and also lists, for each water content, a collapse stress σ_{vc} computed using Eq. 4.1. During wetting, this collapse stress decreases. Large compressive strains occur only when the acting vertical σ_v is approximately equal to the collapse stress σ_{vc} , that is, when $\sigma_v / \sigma_{vc} = 1$. This is shown in Fig. 4.10 where the increase in strain due to wetting is plotted against the initial and final ratios of acting vertical stress to estimated collapse stress. When the acting stress is less than half the collapse stress after wetting ($\sigma_v / \sigma_{vc} < 0.5$), the additional strains are small. The additional strains are also small if the acting stress exceeds the collapse stress before wetting ($\sigma_v / \sigma_{vc} > 1$). In this case, the soil has already collapsed as evidenced by the large strains before wetting. The maximum strain during wetting occurs when the collapse stress is greater than the acting vertical stress before wetting, but smaller afterwards, that is, when $\sigma_v / \sigma_{vc} = 1$ at some point during wetting. This condition existed in Test No. S-5 in which the compressive strain increased from 2.0% to 8.5% during wetting.

4.5 Summary

The conclusions developed in the preceeding discussion are summarized as follows:

- a. With increasing initial water contents, the maximum compression index C_c and the collapse stress σ_{vc} (Fig. 3.28) decrease.

TABLE 4.1 STRAINS DUE TO WETTING

Test No.	σ_v , Vertical Stress During Wetting psi	w %	σ_{vc} psi	σ_v/σ_{vc}	w %	σ_{vc} psi	σ_v/σ_{vc}	$\Delta \epsilon_v$ Increase in Strain %	Δw Increase in Water Content %
S1	111.1	5.3	84.6	1.31	8.2	75.8	1.47	4.87	2.9
	111.1	8.2	75.8	1.47	11.0	67.4	1.64	3.16	2.8
S2 a.	27.8	9.0	73.4	0.38	13.0	61.4	0.45	2.15	4.0
b.	111.1	13.0	61.4	1.81	17.0	49.3	2.27	1.82	4.0
c.	111.1	17.0	49.3	2.27	22.5	32.8	3.39	2.31	5.5
S3	13.9	15.1	55.1	0.25	19.0	43.3	0.32	0.25	3.9
S4	55.6	22.4	33.1	1.68	25.4	24.1	2.30	1.20	3.0
S5	55.6	11.8	65.0	0.86	15.5	53.8	1.03	6.53	3.7
S6	27.8	10.7	68.3	0.41	14.5	56.9	0.49	0.80	3.8
S7	111.1	10.8	68.0	1.63	14.5	56.9	1.95	2.10	3.7

Note: The collapse stresses σ_{vc} have been computed using Eq. 4.1.

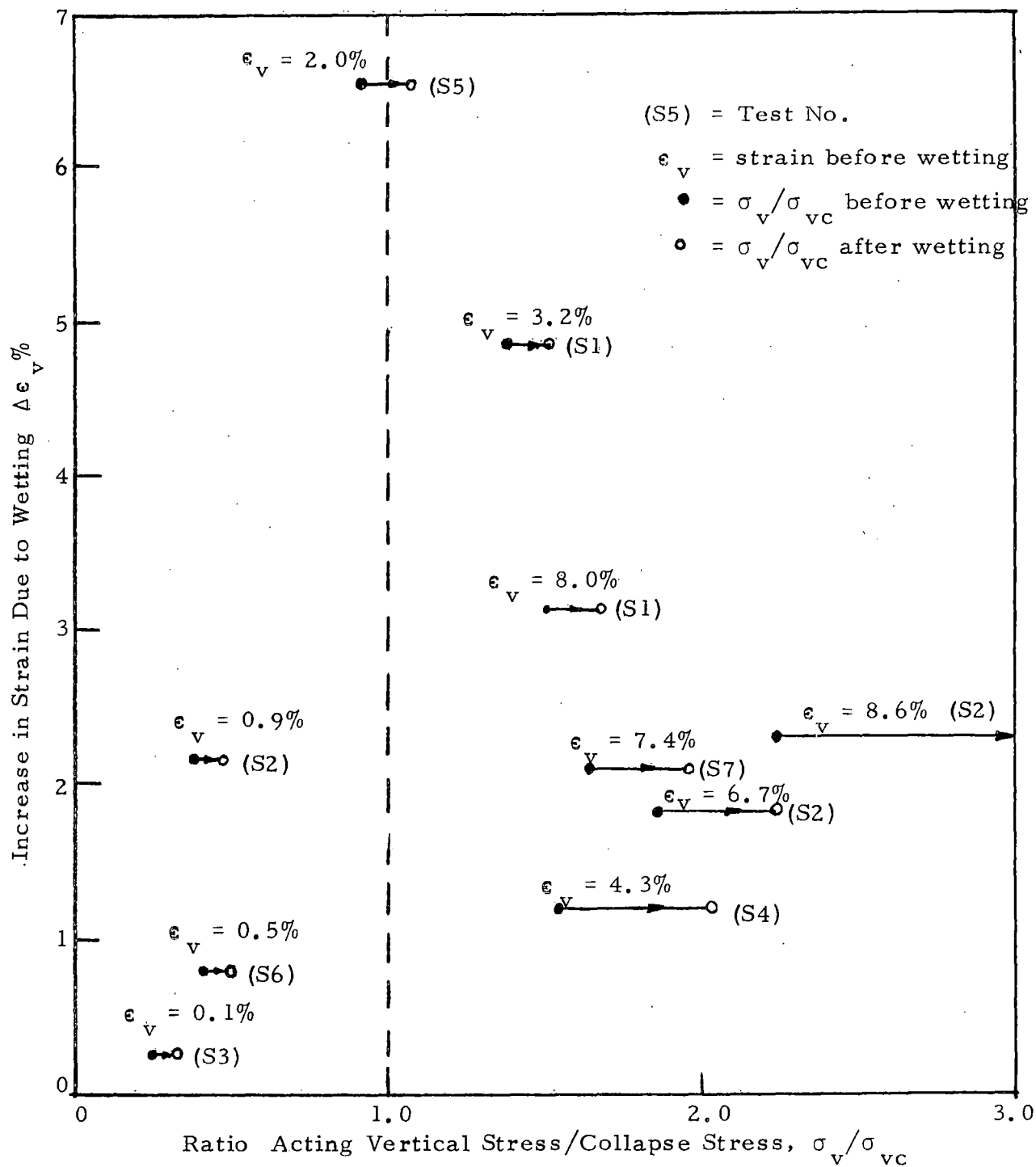


Fig. 4.10 Compressive Strains Due to Wetting

b. The stress at a compressive strain of 2% is approximately equal to the collapse stress, σ_{vc} .

c. The pore-water pressure is related to the water content through the empirical equation

$$u_w \text{ (psi)} = - \left(\frac{44}{w\%} \right)^{2.6} \quad (\text{Eq. 4.2})$$

d. At a given water content, the pore-water pressure is independent of the degree of saturation S_r except for $S_r > 90\%$.

e. The important parameter describing the susceptibility to collapse during wetting is the ratio of the acting stress to the collapse stress σ_v/σ_{vc} and not the amount of wetting.

f. The maximum collapse strains occur when $\sigma_v/\sigma_{vc} = 1$ at some point during wetting. If σ_v/σ_{vc} remains less than 1.0 during wetting, the soil does not collapse. On the other hand, if σ_v/σ_{vc} is greater than 1.0 before wetting, the soil has already collapsed and the additional strains are relatively small.

CHAPTER 5

ANALYSIS OF MECHANICAL BEHAVIOR

5.1 Introduction

During confined compression, the vertical stress σ_v is increased and the radial or horizontal stress σ_h increases sufficiently to maintain the condition of zero lateral strain. The stress path method of representing the successive states of stress (Lambe, 1964) forms the basis for the analysis of the behavior of the soil in the following sections. In this method, the state of stress is represented by a stress point on a $p - q$ diagram in which $p = (\sigma_v + \sigma_h)/2$ and $q = (\sigma_v - \sigma_h)/2$. Successive stress points are connected to form the stress path for a loading. The stress path may be drawn using either total stresses or effective stresses.

The stress path for the confined compression of a soil with a constant negative pore pressure is shown in Fig. 5.1 to illustrate the method. Also shown in this figure is the K_f -line, which connects the effective stress points for failure conditions.

The stress path method is particularly useful in this analysis because it can show the relationship between the stresses in confined compression and the failure stresses. For example, when the compression illustrated by stress path $\overline{A B}$ in Fig. 5.1 is continued, the path will intersect the K_f -line at point C. Since this point represents

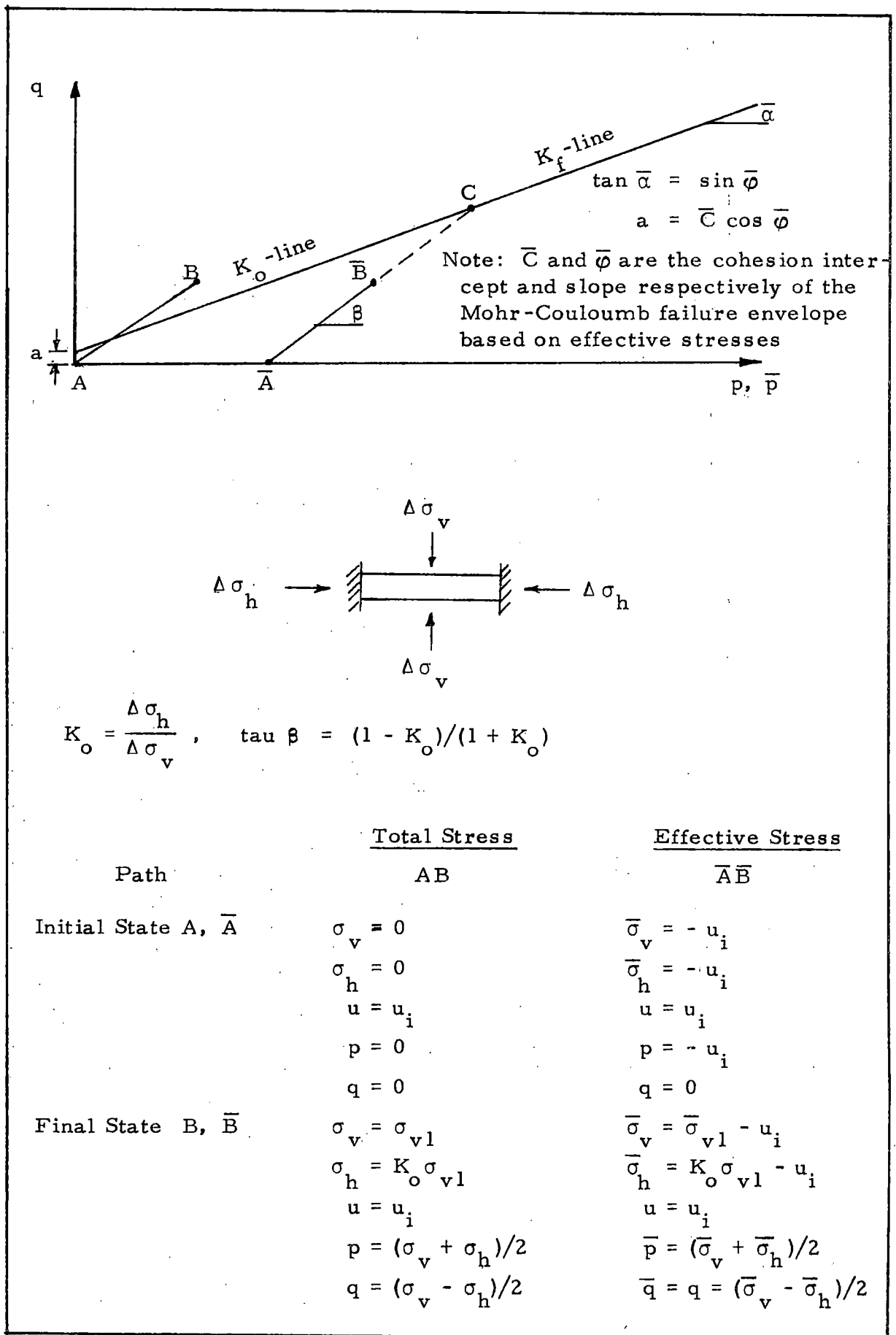


Fig. 5.1 Stress Path for Confined Compression

failure conditions, the stress path must change direction as the stress is increased further. The balance of this chapter is concerned with the mechanisms associated with the changes in the stress path before and after failure.

5.2 Effective Stresses

The effective stress, in the most general sense, is the stress which controls changes in either the volume or the strength of a soil (Skempton, 1961). For partially saturated soils, the expression for effective stress $\bar{\sigma}$ is (Bishop, 1960):

$$\bar{\sigma} = \sigma - [u_a - x(u_a - u_w)] \quad (\text{Eq. 5.1})$$

where σ is the total stress, u_a is the pore-air pressure, u_w is the pore-water pressure, and x is an experimentally determined coefficient. If the expression within the brackets is designated as the equivalent pore pressure u (as distinguished from the pore-water pressure u_w), then Eq. 5.1 may be written

$$\bar{\sigma} = \sigma - u \quad (\text{Eq. 5.2})$$

where

$$u = u_a - x(u_a - u_w) \quad (\text{Eq. 5.3})$$

Several special cases are of interest. If $u_a = 0$, then $u = x u_w$ and

$$\bar{\sigma} = \sigma - x u_w \quad (\text{Eq. 5.4})$$

The coefficient x depends on the degree of saturation and is not necessarily the same value for volume change and shear strength (Skempton,

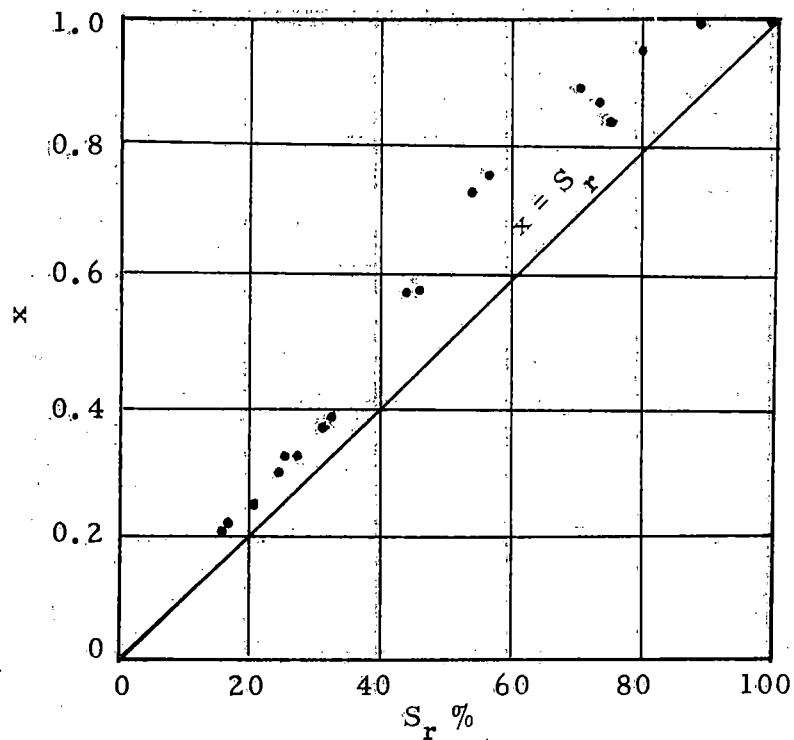
1961). A definition of x , simplified in that surface tension forces are neglected, is the ratio of the cross-sectional area occupied by water to the total area. Thus, when the soil is saturated, $x = 1$ and $\bar{\sigma} = \sigma - u_w$, and when the soil is dry $x = 0$ and $\bar{\sigma} = \sigma$. The determination of x at intermediate degrees of saturation has been the subject of several studies.

Aitchison (1961) has presented an expression for the pore pressure in a capillary model of cohesionless ideal spherical particles representing an incompressible soil. The expression leads to the following equation for x when $u_w = (u_w)_1$ and $S_r = (S_r)_1$:

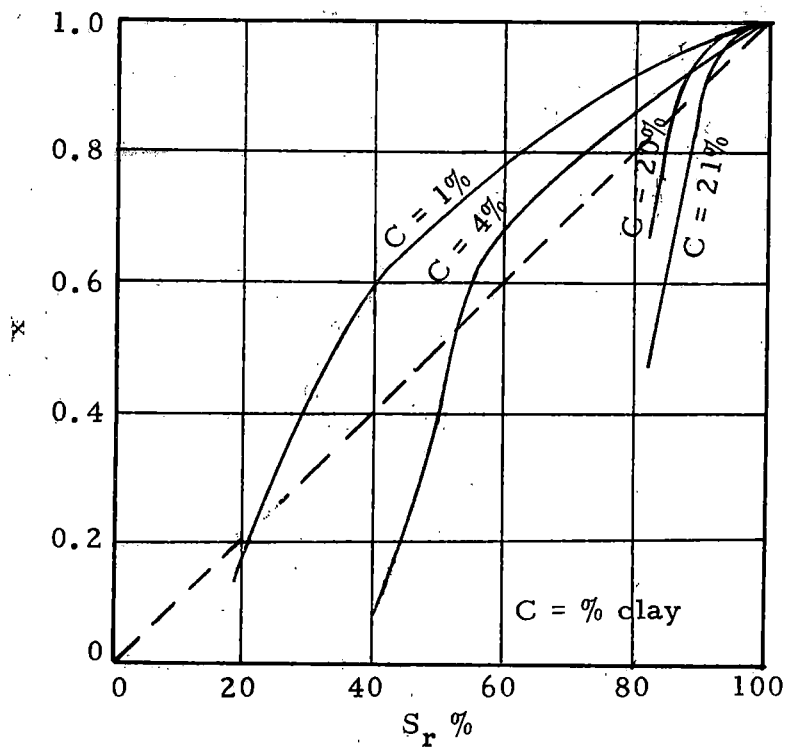
$$x = \frac{(S_r)_1}{100} + \frac{0.3}{(u_w)_1} \sum_{0}^{(u_w)_1} S_r u_w \quad (\text{Eq. 5.5})$$

The summation term is obtained from a curve of S_r vs u_w . No other analytical expressions for x have been published. The loess under investigation in this study is markedly different from the soil on which Eq. 5.5 is based, but for comparative purposes, this equation has been used to compute x for the initial values of S_r and u_w measured in each of the confined compression tests (Table 3.1). The resulting x -values are plotted against S_r in Fig. 5.2 (a) and the parameter x is seen to exceed S_r for all values of S_r . However, this is inconsistent with measurements on cohesive soils as shown in the following paragraph.

Bishop and Blight (1963) have presented four x vs S_r curves for compacted specimens with clay contents from 1% to 21%. These experimental curves are shown in Fig. 5.2 (b) and it is evident that the clay



(a) Results for Oakdale Loess Calculated from Eq. 5.5



(b) Experimental Results for Typical Compacted Soils (Bishop and Blight, 1963)

Fig. 5.2 Relations Between x and S_r

content has an important influence on the relationship. A comparison of Fig. 5.2 (a) and (b) indicates that Eq. 5.5 cannot be used for a soil such as Oakdale loess which has a clay content of 13%. The values of x in Fig. 5.2 (b) were obtained in the following manner. The K_f -line (Fig. 5.1) for the soil was determined from triaxial compression tests on saturated samples. Partially saturated samples were tested similarly and the pore-water pressure u_w and total failure stresses p_f and q_f were measured. For the measured failure stress q_f , the effective failure stress \bar{p}_f was found on the K_f -line. Finally, $u = p_f - \bar{p}_f$ and $x = u/u_w$ were computed.

The procedure for determining the K_f -line from tests on saturated samples cannot be used for an undisturbed loess because of the sensitivity of loess to saturation. The structure of a saturated loess would collapse under a small confining stress and the triaxial failure envelope would not be applicable to the loose natural structure. The following section describes the procedure used here to overcome this difficulty thus leading to the determination of the x vs S_r relations for the Oakdale loess under study.

5.3 Effective Stresses at Collapse During Confined Compression

The understanding of the collapse phenomenon in loess during confined compression in terms of effective stresses requires the knowledge of the intercept \underline{a} and the slope $\bar{\alpha}$ of the K_f -line (Fig. 5.1). In

addition, because the lateral stress was not measured in the confined compression tests, K_0 must be known in order to construct the stress path. The method for selecting these parameters is presented in the next paragraphs.

The triaxial compression test results (Table 3.4) were used in the determination of \underline{a} and $\bar{\alpha}$. Tests 9 and 10 were eliminated from consideration because the structure had already collapsed prior to the application of the deviator stress. In these tests, the volumetric strain due to the cell pressure alone was greater than 7%. The failure envelope therefore is based on the remaining tests, Nos. 1 through 8. The total failure stresses, p_f and q_f , are known for these tests but the pore pressure u is unknown since u is given by the expression $u = x u_w$. Two assumptions were made in order to determine u . First, since the degree of saturation was high (approximately 75%) for all samples, it was assumed that $x = 1$ is a good approximation. The subsequent determination of x supports this. Second, u_w , while not measured for the test samples, was determined using Eq. 4.2 (Fig. 4.5). This estimate is valid since u_w is a function of water content rather than degree of saturation for $S_r < 90\%$ (Chapter 4). The pore pressure $u = x u_w$ calculated on the basis of these assumptions ranged from -4.8 psi to -5.3 psi. The measured q_f and calculated $\bar{p}_f = p_f - u$ are plotted in Fig. 5.3; a least square fit gives the intercept $\underline{a} = 1.4$ psi and the slope $\bar{\alpha} = 23.7^\circ$. The corresponding \bar{c} - and $\bar{\phi}$ - values are 1.6 psi and 26.0° . The above

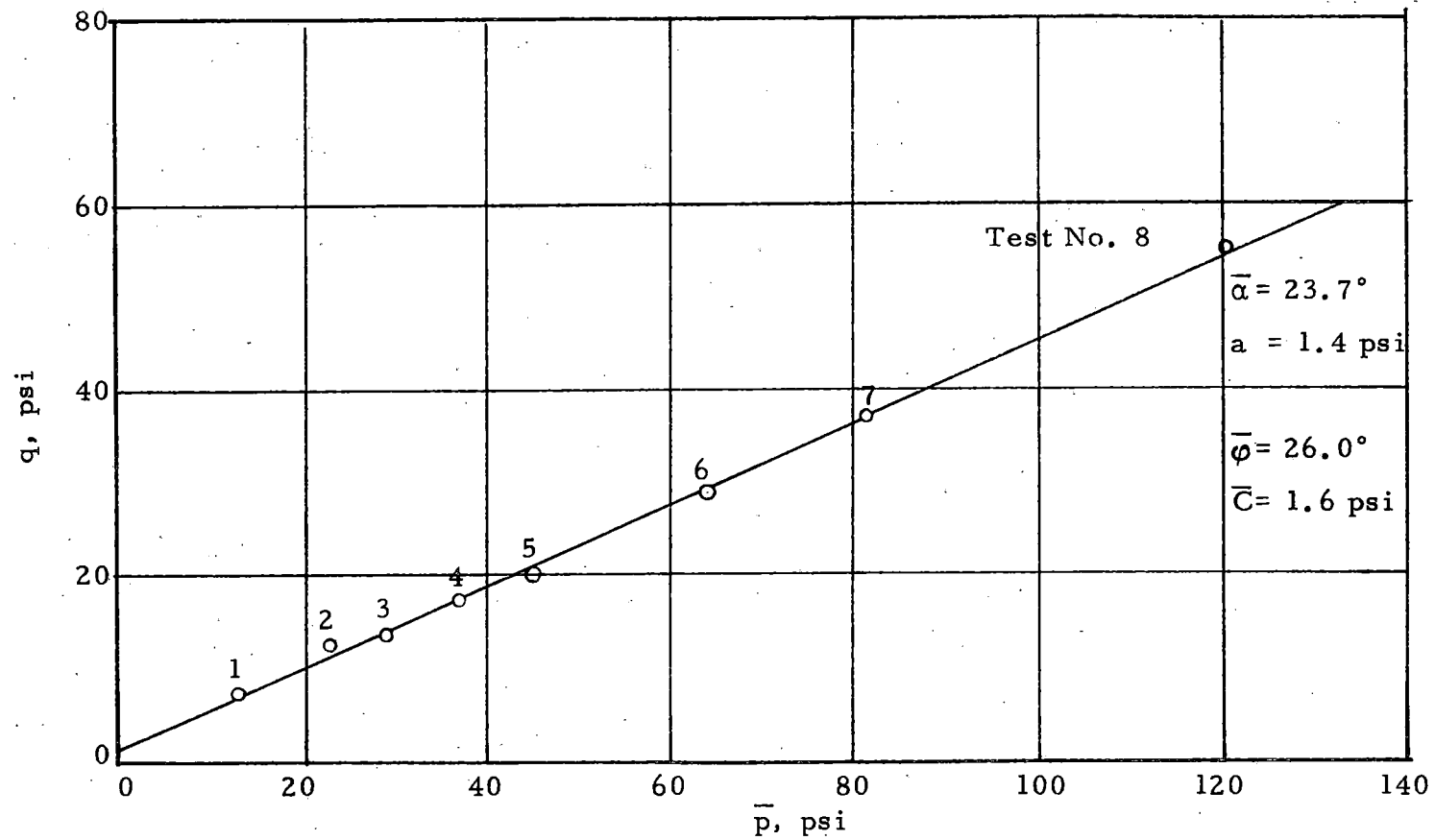


Fig. 5.3 Failure Envelope for Oakdale Loess Based on Effective Stresses

interpretation assumes that the pore-air pressure is atmospheric, that is, that there is no entrapped air. Since the air-voids in compacted clay are interconnected for degrees of saturation up to about 90% (Yoshimi and Osterberg, 1963), this assumption is certainly valid for loess when its natural open structure is intact.

Tests for the lateral stress ratio K_o were described in Chapter 3 and the results summarized in Table 3.3. For the following analysis, the average measured values of K_o have been used: $K_{oi} = 0.23$ before collapse and $K_{of} = 0.54$ after collapse. It should be noted that K_o is defined here on the basis of the total stresses σ_h / σ_v .

The method for determining x is illustrated in Fig. 5.4. At the collapse stress σ_{vc} in the confined compression test, the full shear strength of the soil is mobilized. The corresponding failure stresses p_f and q_f are computed from σ_{vc} and K_{oi} . The total stress path during loading is AC in Fig. 5.4, and the pore pressure u is the stress difference from C to \bar{C} on the K_f -line. The pore water pressure u_w has been taken as the initial value since only small changes occurred prior to collapse (Fig. 4.6a). With u and u_w known, $x = u/u_w$ may be computed.

The test results can be utilized in this method in two different ways: first, measured σ_{vc} and u_w from the individual tests can be used, and second, the average values of σ_{vc} and u_w may be computed from equations 4.1 and 4.2 respectively.

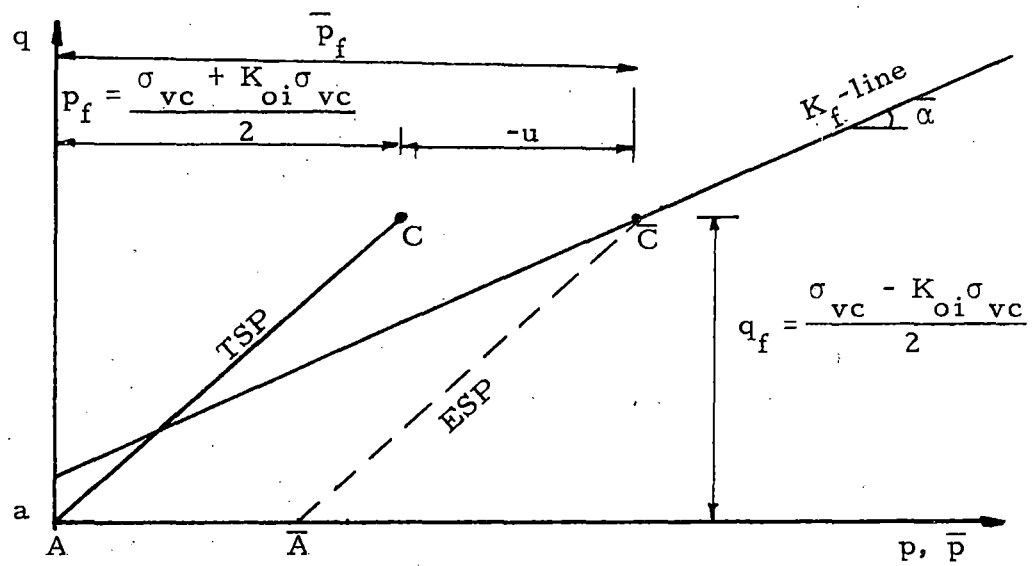


Fig. 5.4 Procedure for Determining the Pore Pressure u

The x vs S_r relations based on the individual tests are shown in Fig. 5.5. For $S_r \leq 70\%$, the points fall on a curve similar to those for compacted soils in Fig. 5.2 (b). When $S_r > 70\%$, there is a large scatter. This is due to the small measured pore-water pressures (-3 psi to -4 psi) which cause the ratio u/u_w to be very sensitive to small differences in u_w . It is also possible that positive air pressures exist at the higher S_r -values. Neglecting a positive u_a results in a computed x -value lower than it should be. In spite of the scatter for $S_r > 70\%$, it is clear from the remaining portion of the curve that x is approximately equal to unity when S_r exceeds 70%. This finding verifies the assumption to this effect used above to obtain the K_f -line.

Fig. 5.6 shows the x vs S_r curve determined by the average σ_{vc} - and u_w -values. For selected values of S_r , the water content was calculated ($e = 0.8$ was assumed) and then σ_{vc} and u_w were determined from Fig. 4.1 and 4.2 respectively. The value of x was then found as in the preceding case. The curve in Fig. 5.6 follows that in Fig. 5.5 to $S_r = 70\%$. When $S_r > 70\%$ the curve turns down indicating that the average σ_{vc} - and u_w -values are inconsistent since x must approach unity. The sensitivity of x to small differences in u and u_w , as in the case of the individual points, precludes an accurate curve in this region and the dashed curve is drawn to fit the known end value for x .

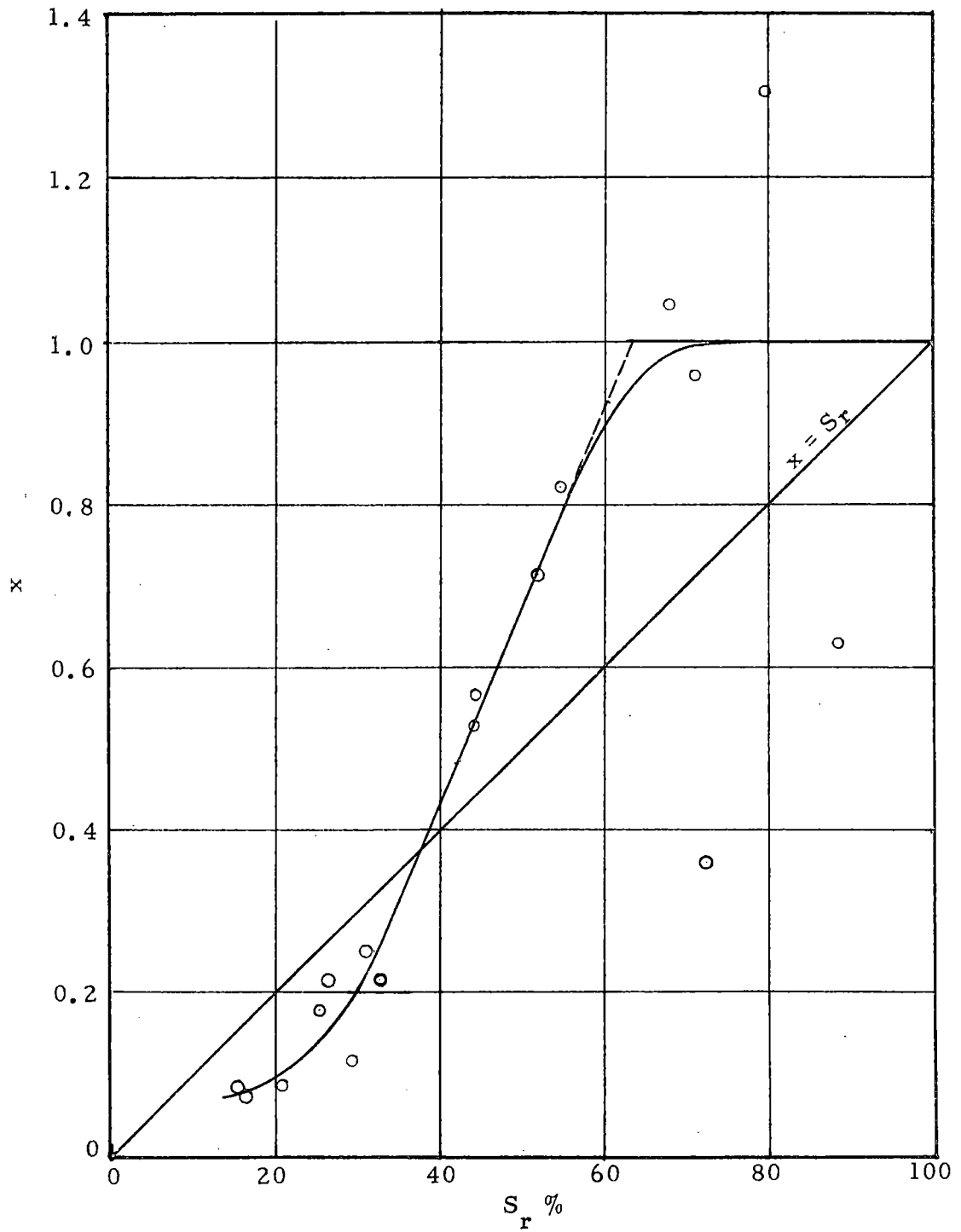


Fig. 5.5 x vs S_r for Oakdale Loess Based on Individual Test Results

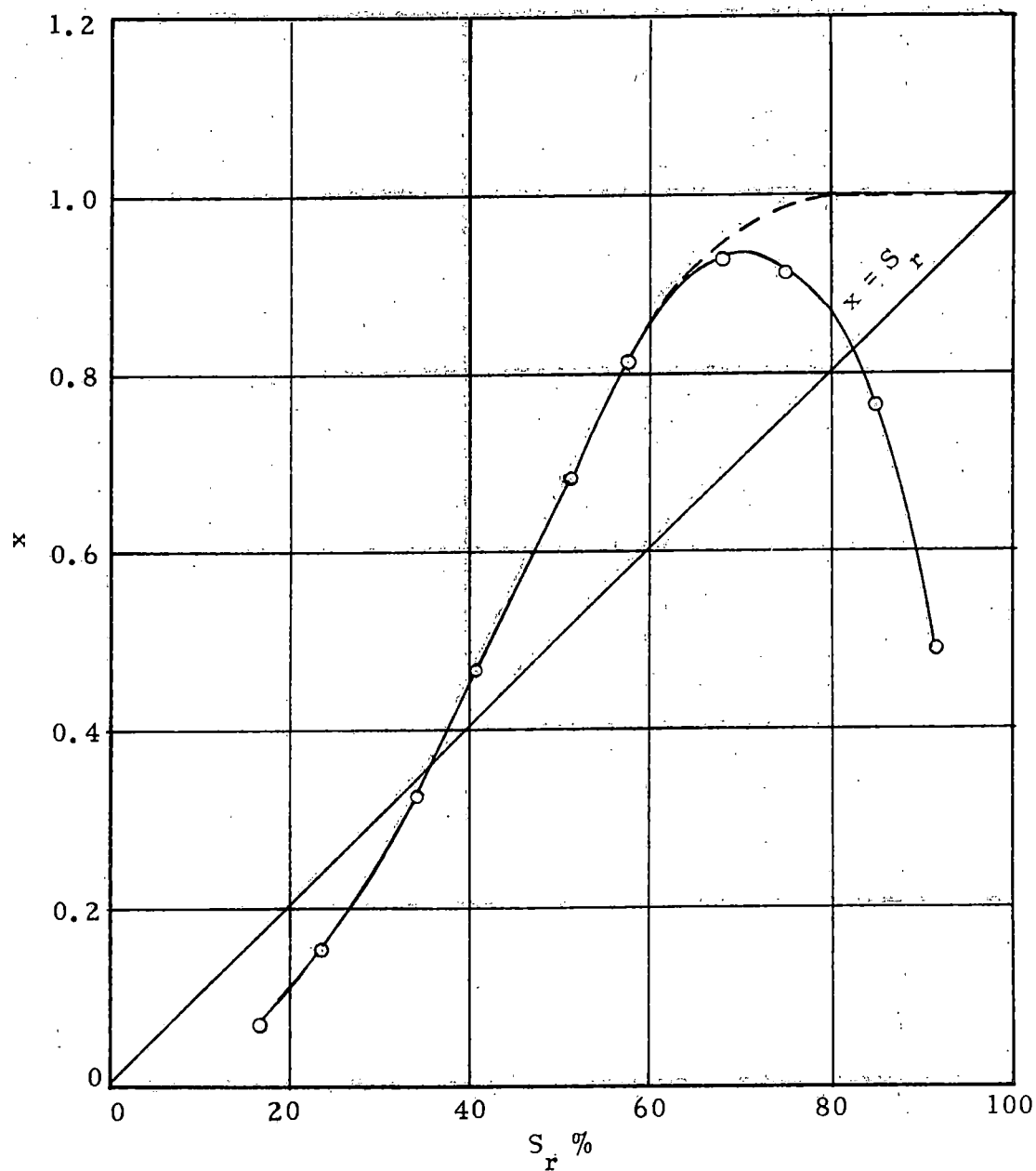


Fig. 5.6 x vs S_r for Oakdale Loess Based on Average Test results

5.4 Effective Stress Paths

In this section, the effective stress paths for representative tests are presented. To provide a basis for interpreting these diagrams, the general character of effective stress paths for the confined compression of loess is shown in Fig. 5.7. Four particular test conditions are considered in this figure: (a) loading without wetting, (b) wetting before collapse, (c) wetting after collapse and (d) collapse due to wetting. The first condition corresponds to the basic test series and the last three to conditions which existed during the special tests.

In the case of loading without wetting, Fig. 5.7 (a), the effective stress path for loading prior to collapse is AC. This path is the same as \overline{AC} in Fig. 5.4 and its slope is determined by the value of K_{oi} . At point C, the full shearing resistance at the particle contacts is mobilized and a further increase in σ_v causes slippage between particles. As a result, the soil compresses and new structural configurations develop. Collapse may be considered to have concluded when the particles lock in new stable positions at which point $K_o = K_{of}$, point D. The transition from $\sigma_v = K_{oi} \sigma_v$ to $\sigma_h = K_{of} \sigma_v$ occurs with $\Delta \sigma_h = \Delta \sigma_v$, that is, the stress path CD is horizontal. This conclusion is based on the measurements obtained from the K_o -tests, Appendix IV. The path for loading after collapse is DF and its slope is determined by the value of K_{of} .

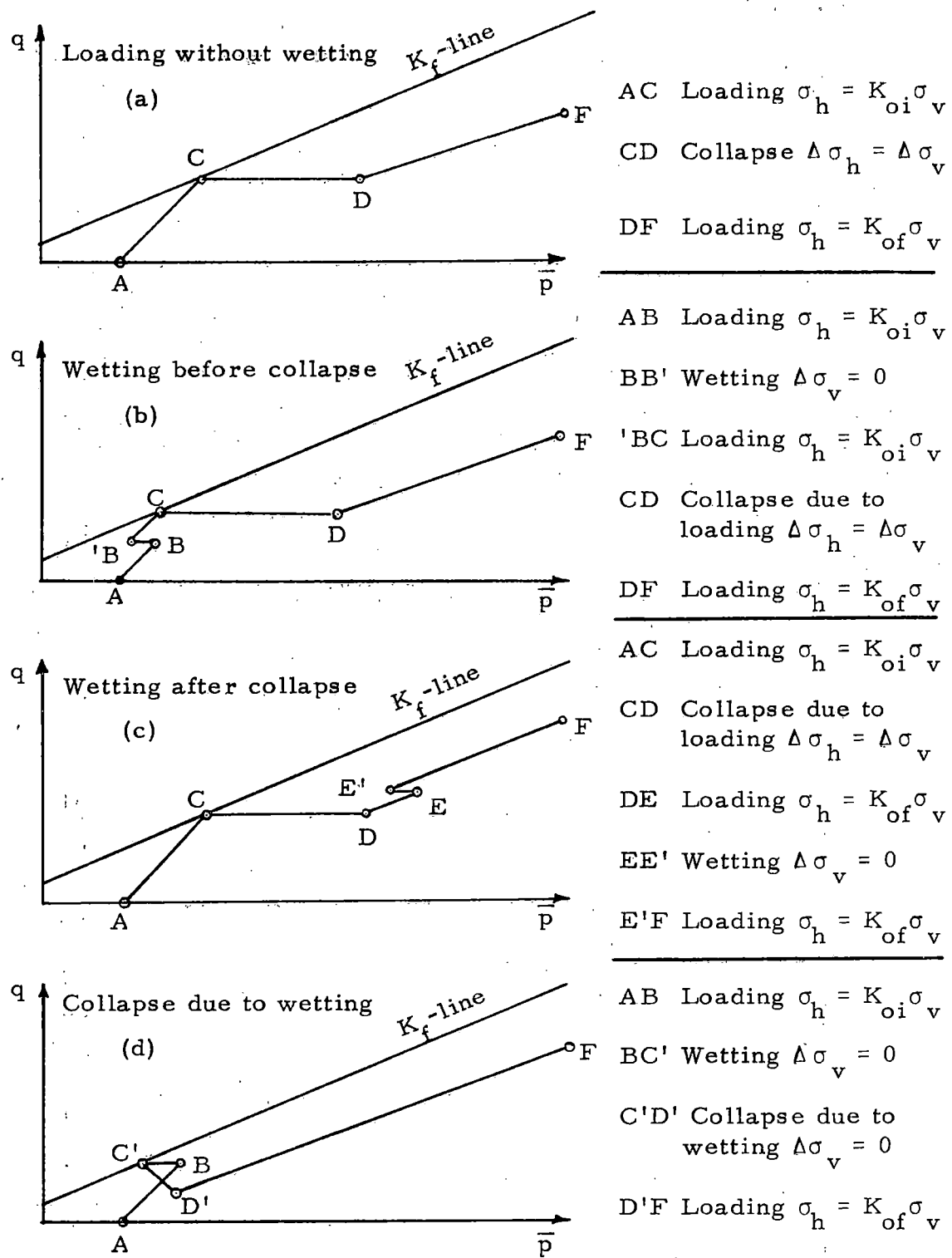


Fig. 5.7 Effective Stress Paths for Confined Compression of Loess

If, during the course of the test, the loess is wetted, the stress paths are changed in the manner shown in Figs. 5.7 (b), (c), and (d). Wetting under a constant σ_v reduces the negative pore pressure and thus \bar{p} decreases while q remains constant. The stress path during wetting is horizontal (BB' and EE'). If, during wetting, the stress path intersects the K_f -line, as for path BC' in Fig. 5.7 (d), collapse occurs as a result of wetting. In this case, σ_v remains constant during collapse but σ_h increases because K_o increases from K_{oi} to K_{of} . The stress path C'D' slopes downward from the K_f -line at a slope of 45 degrees if the pore pressure remains constant during collapse.

The effective stress paths for representative confined compression tests have been determined by computations based on the data obtained from the individual tests: the vertical stress σ_v , the pore-water pressure u_w , the strain ϵ_v , the water content w , and the degree of saturation S_r . Two additional parameters were obtained from other tests. First, the value of x for use in the expression $u = x u_w$ was obtained from the average x vs S_r curve Fig. 5.6. Second, the values of K_o for use in the computation of $\sigma_h = K_o \sigma_v$ are $K_{oi} = 0.23$ and $K_{of} = 0.54$ before and after collapse respectively; this is in accordance with the discussion in the preceeding section. The point of collapse has been taken as the point at which a disproportionate increase in strain occurs either upon the addition of more stress or upon wetting.

Stress paths for five of the basic tests, Nos. 7, 9, 11, 12, and 14, are shown in Figs. 5.8 through 5.12 respectively. The initial water contents for these tests range from 4.6% to 25.1%. The stress paths follow the idealized stress path in Fig. 5.7 (a) and the corresponding points are shown by the same letter designations. At each data point the vertical strain is given. Because of the relatively wide spacing of the data points, the collapse stress at point C is not precisely known. The portion of the stress path during the collapse of the structure is shown by a dashed line and drawn so that either point C or D is a data point and the line CD is horizontal. Point C is not on the K_f -line in all cases, as it is in Fig. 5.7 (a), because the collapse stress is not precisely known and because the K_f -line represents an average strength. However, it is evident from these figures that (1) there is a disproportionately high increase in strain as the path extends from C to D (since the load doubles, doubling the strain is proportionate), indicating a structural collapse, and (2) point C, where this collapse initiates, is near the K_f -line. Thus the test data substantiate the idealized concept for the effective stress path shown in Fig. 5.7 (a).

Stress paths for three of the special tests, Nos. S2, S1, and S5, are shown in Figs. 5.13, 5.14, and 5.15 respectively. The path for S2 follows the paths in Figs. 5.7 (b) and (c), since it was wetted both before and after collapse, and the points are lettered accordingly.

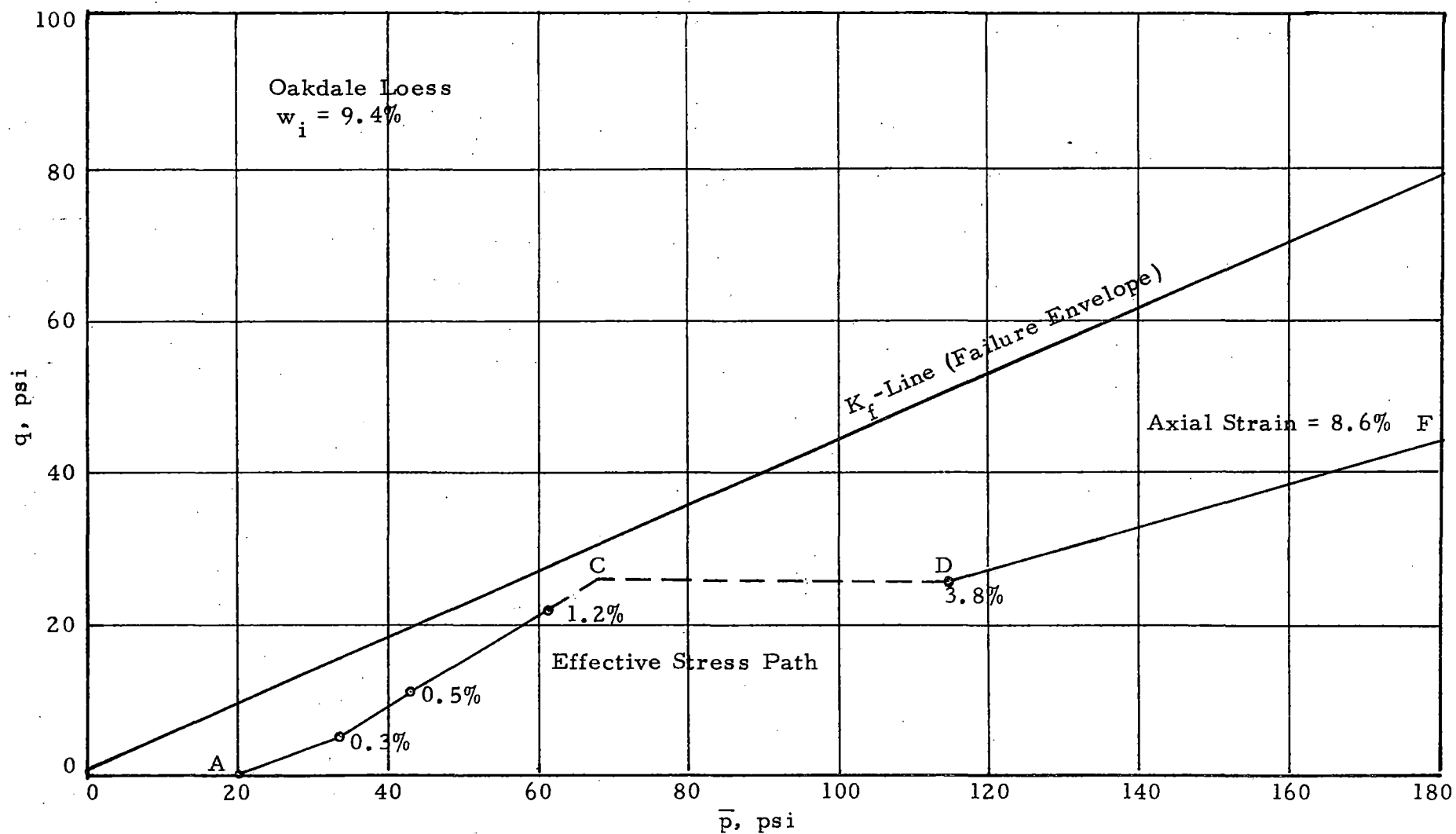


Fig. 5.8 Effective Stress Path for Confined Compression Test No. 7

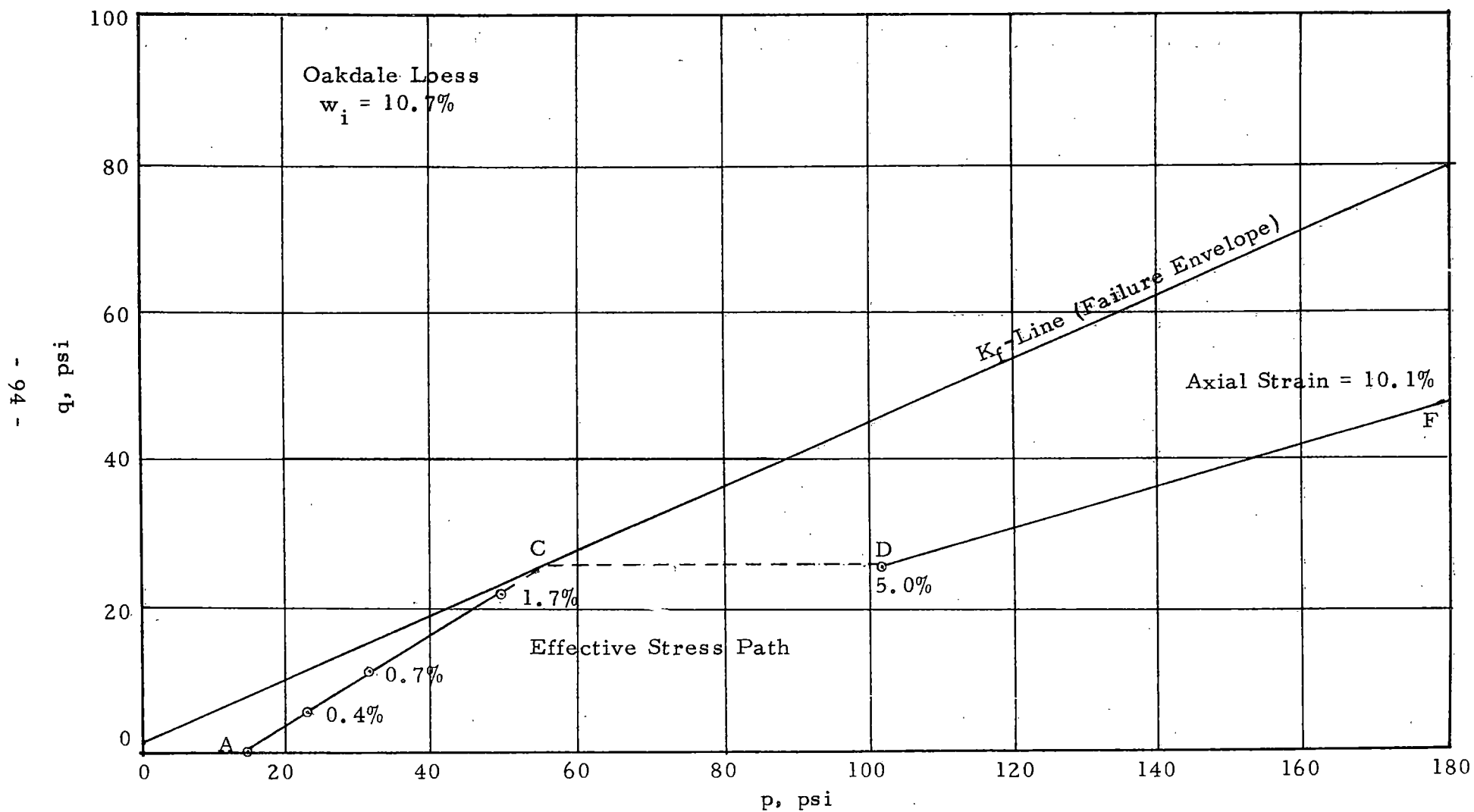


Fig. 5.9 Effective Stress Path for Confined Compression Test No. 9

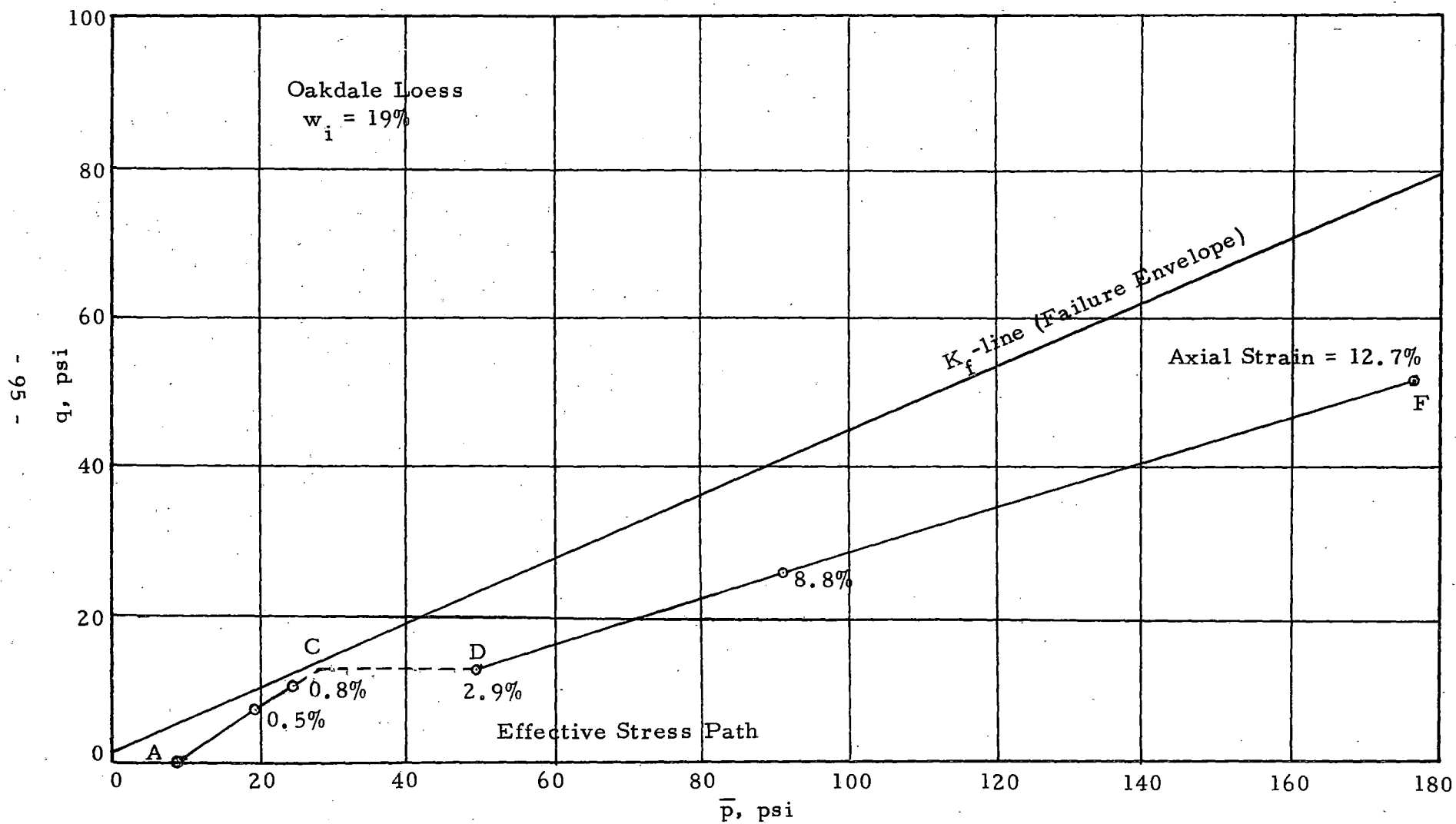


Fig. 5.10 Effective Stress Path for Confined Compression Test No. 11

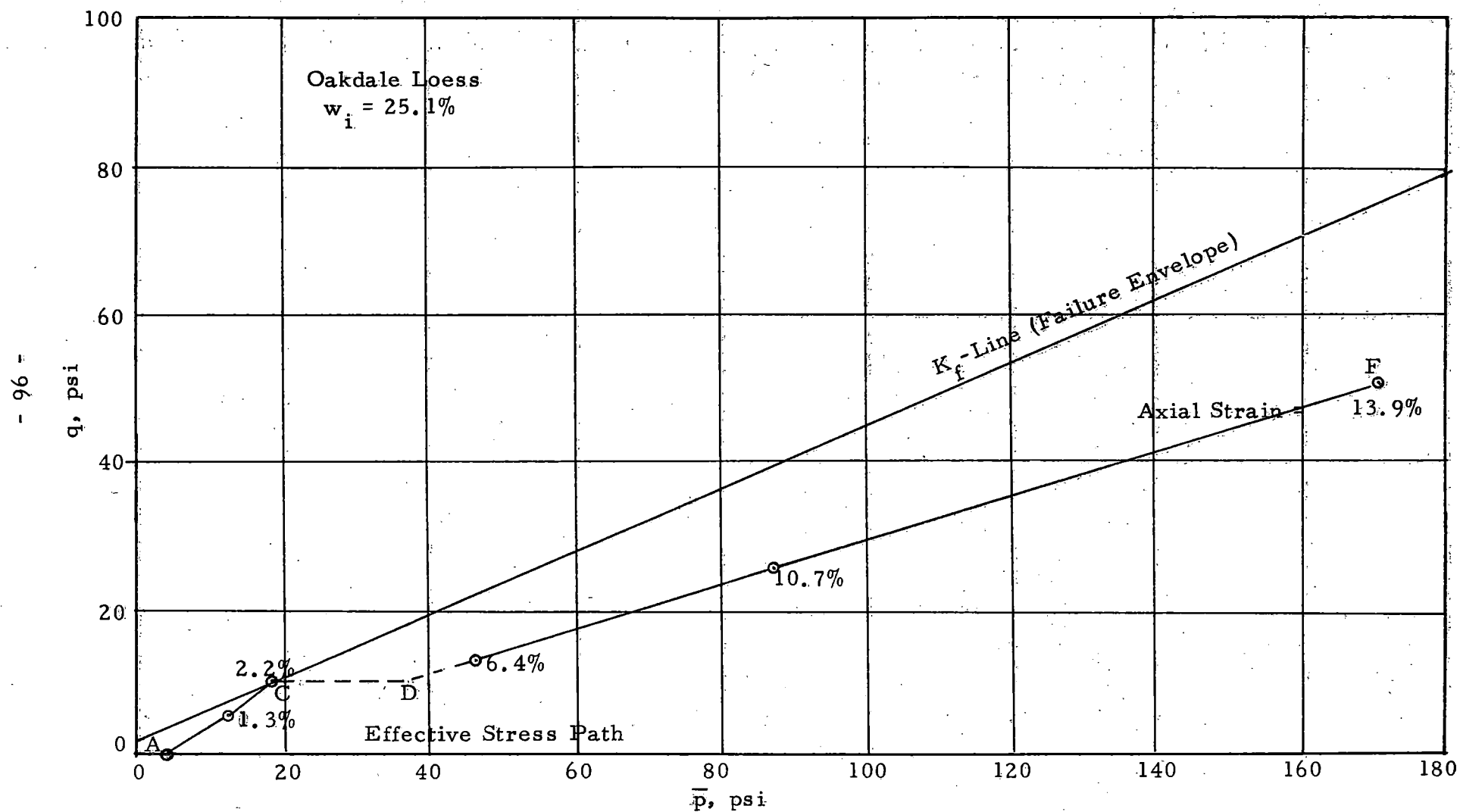


Fig. 5.11 Effective Stress Path for Confined Compression Test No. 12

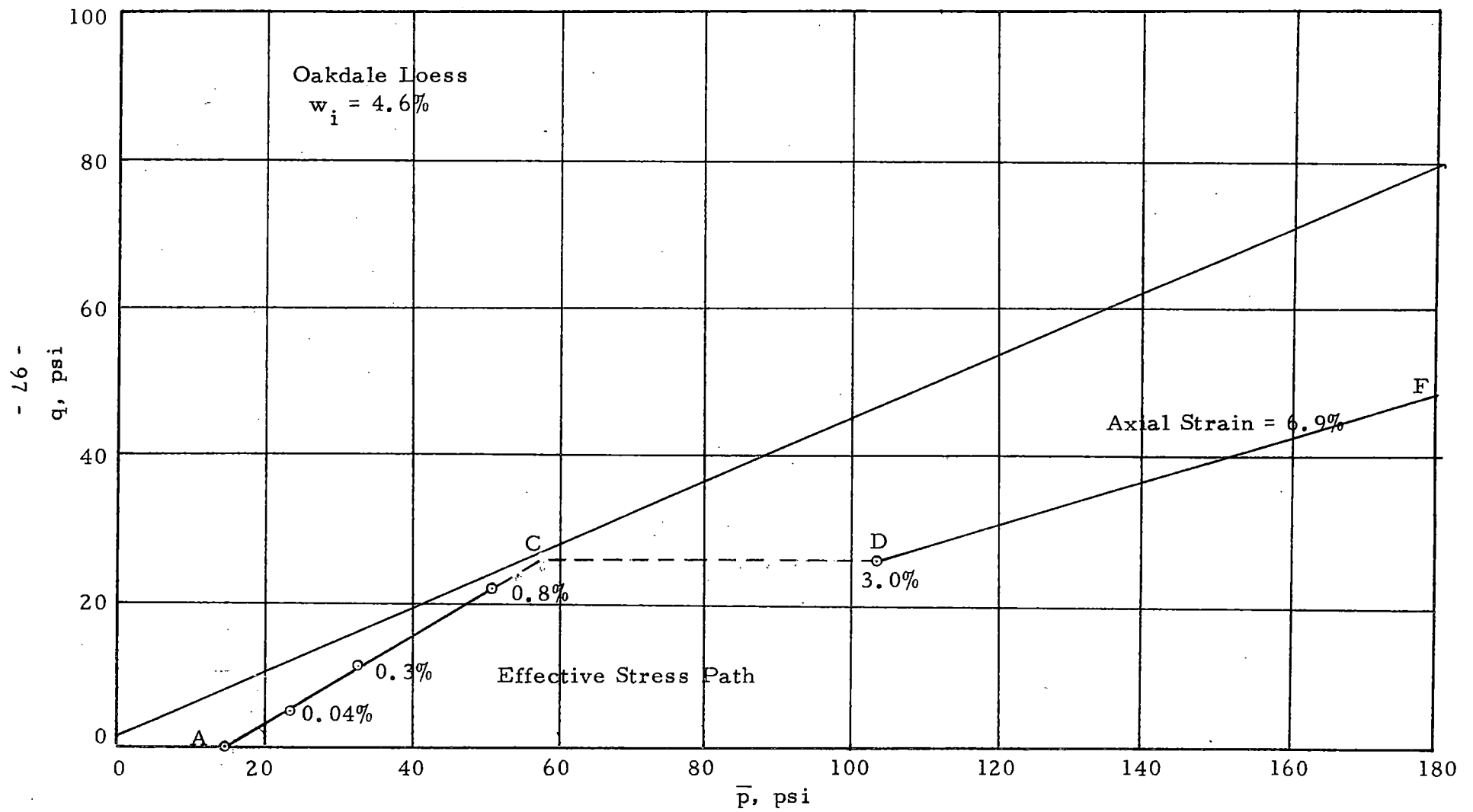


Fig. 5.12 Effective Stress Path for Confined Compression Test No. 14

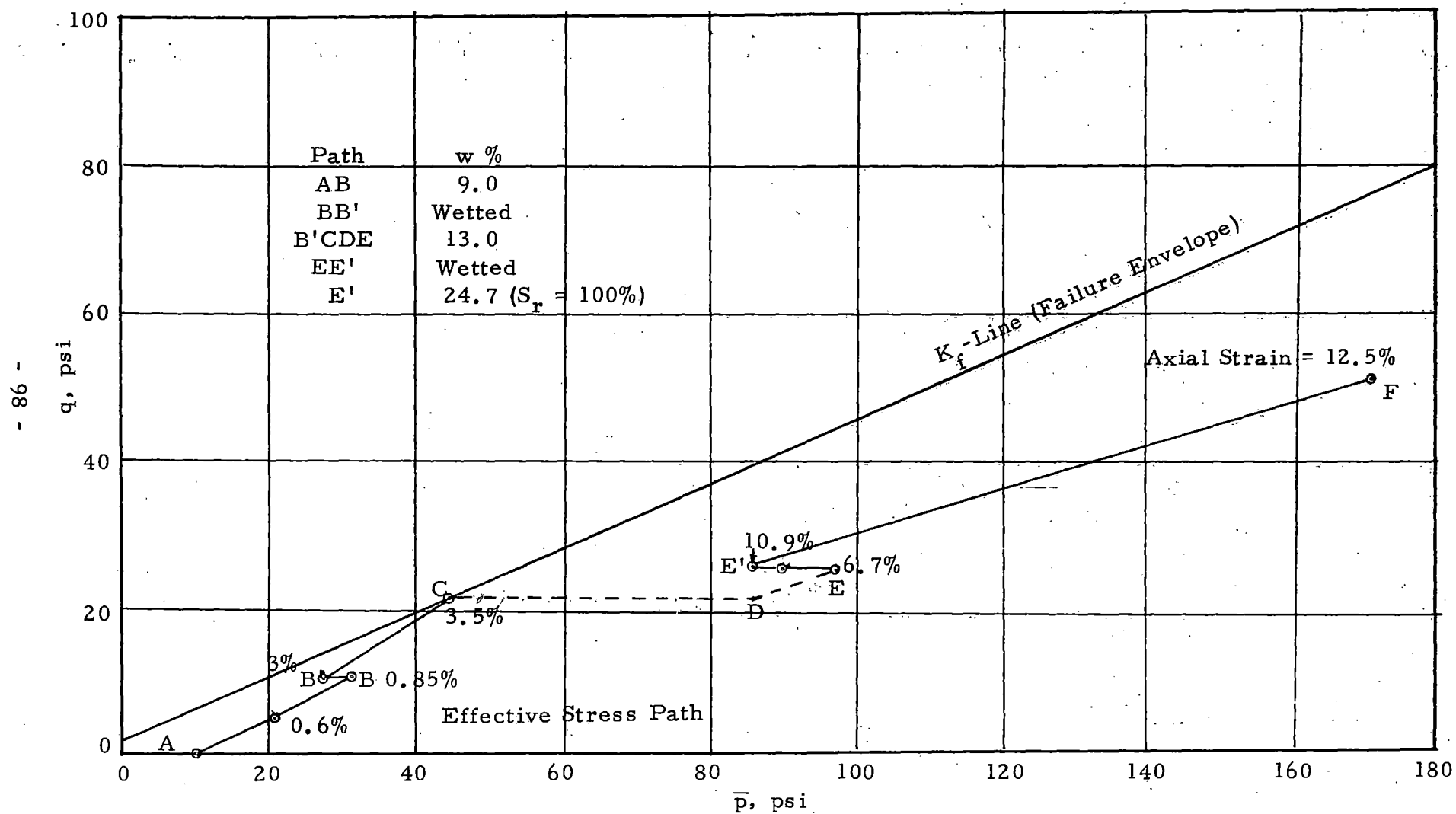


Fig. 5.13 Effective Stress Path for Confined Compression Test No. S2

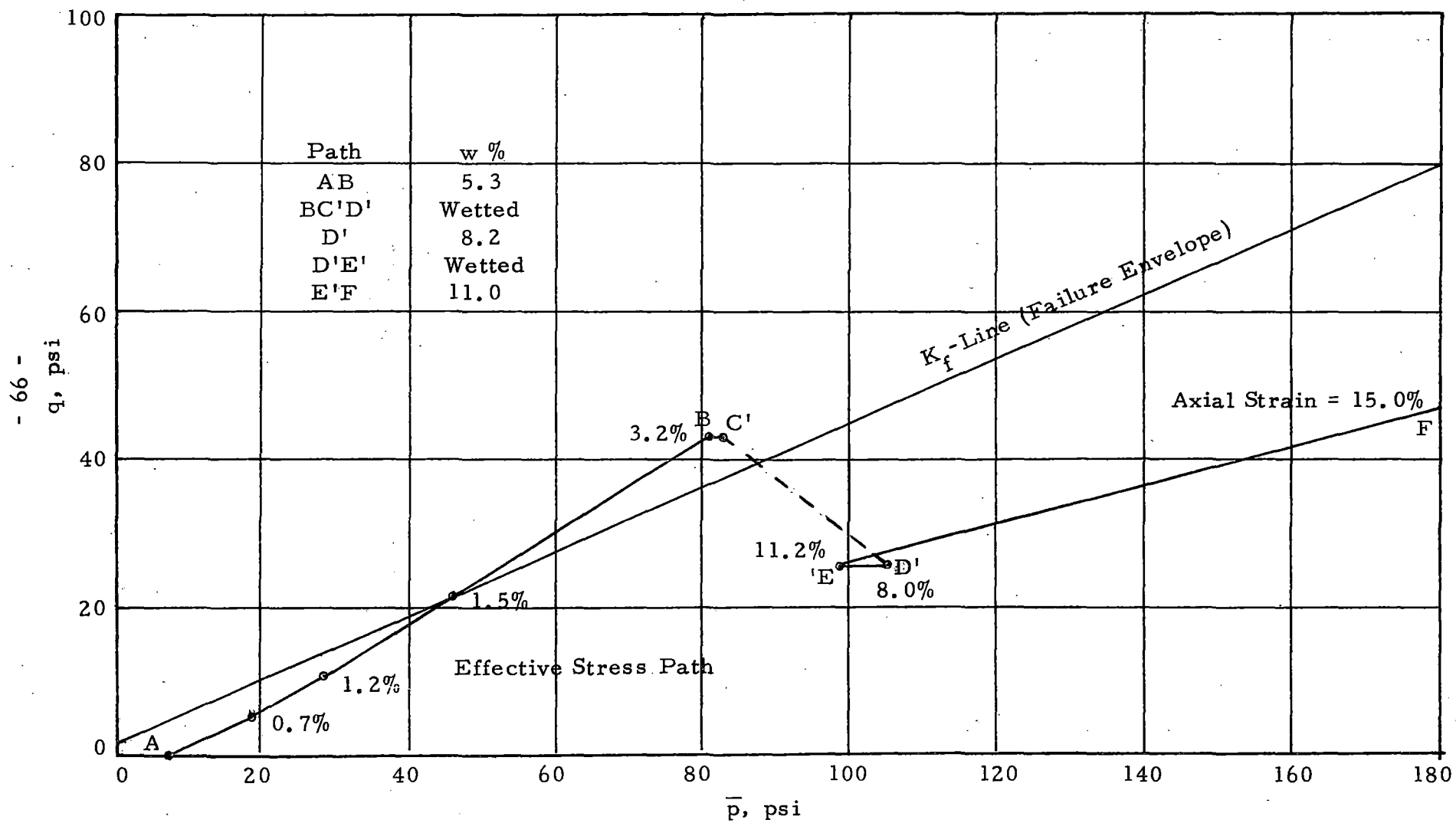


Fig. 5.14 Effective Stress Path for Confined Compression Test No. S1

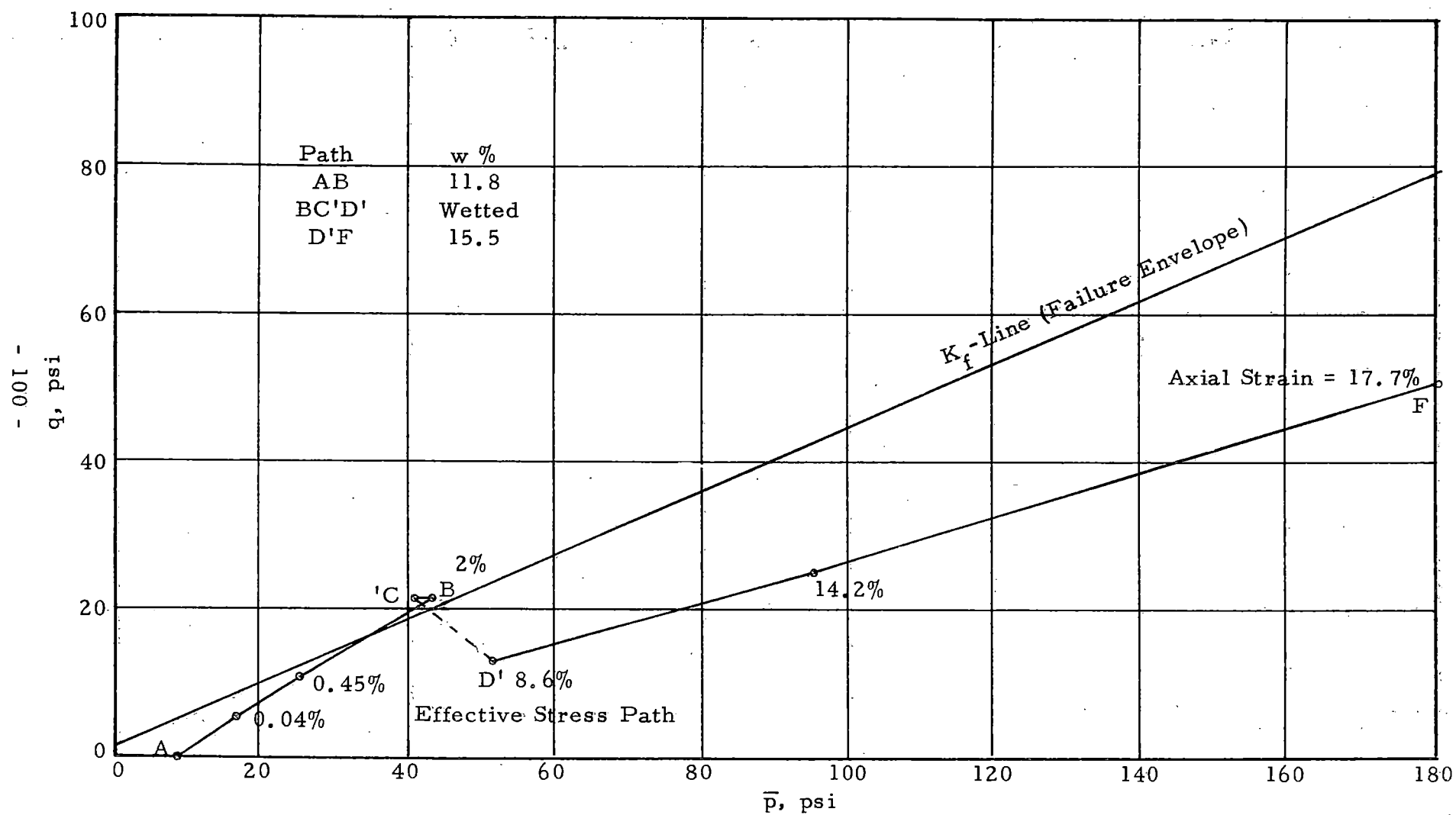


Fig. 5.15 Effective Stress Path for Confined Compression Test No. S5

The increase in strain during wetting BB' (0.8% to 3.0%) is relatively high and, while it has not been taken to indicate collapse, it may in fact so indicate. However the subsequent strain due to loading B'C is only an additional 0.5% and it is believed that the high strain during BB' is due to non-uniform wetting. The paths for S1 and S5 follow the path in Fig. 5.7 (d) which describes collapse due to wetting. In both tests, the strain increases to 8.0% or more (path C'D') due to wetting alone with no increase in stress. An anomaly exists in S1 during wetting path BC'. The increased x -value after wetting, due to the higher degree of saturation, has a greater influence than the reduced negative pore-water pressure u_w on the new pore pressure $x u_w$. As a result, the computations show a lower (more negative) pore pressure after wetting than before and the path BC' (Fig. 5.14) is in the direction of increasing effective stress. This implies an increased strength upon wetting which cannot be correct, and can only be due to errors in the measured pore-water pressure and in the average x vs S_r curve.

With the exceptions noted above, the stress paths for the special tests agree with and support the concepts illustrated by the stress paths in Fig. 5.7 (b), (c), and (d).

CHAPTER 6

SUMMARY AND CONCLUSIONS

6.1 Summary

The primary purpose of this study is to describe quantitatively the mechanisms involved in the confined compression of loess. To this end, the pore-water pressure, void ratio, water content, and applied stress have been measured in a basic test series on a soil having initial water contents ranging from air-dry to saturation. A special series of tests in which the water content was increased by known increments while the soil was under a constant stress was also run. These tests required the construction of a special confined compression cell which permitted the measurement of negative pore-water pressures as small as -300 psi during the course of the confined compression test.

Two additional tests were run to provide supporting data: K_o tests in which the lateral stress ratio was measured, and strength tests to determine the failure envelope.

An effective stress analysis was used to interpret the results. This analysis lead to the establishment of a curve showing x vs. S_r , and to the construction of quantitative effective stress paths for the basic tests and for the special tests in which the water content was increased.

6.2 Conclusions

The discussions and analysis of the test results in Chapters 4 and 5 lead to the following conclusions:

a. The collapse stress σ_{vc} , defined in Fig. 3.28, is a significant parameter in describing the stress-strain relations for the soil. An approximate linear decrease in σ_{vc} occurs with increasing initial water contents; that is, the wetter the soil, the lower the stress level at which collapse occurs, which is, of course, to be expected. The stress σ_{vc} is approximately equal to the stress causing a compressive strain of 2%.

b. The initial pore-water pressure was related to the water content through the empirical equation

$$u_w \text{ (psi)} = - \left(\frac{44}{w\%} \right)^{2.6} \quad (\text{Eq. 4.2})$$

During compression, no significant change in the pore water pressure occurred except when the degree of saturation S_r exceeded 85% to 90%. Thus, with this exception, the pore-water pressure is independent of the degree of saturation, and Eq. 4.2 is applicable to more than the initial conditions.

c. For stresses below the collapse stress, the lateral stress ratio for confined compression K_o was found to be small in comparison with values commonly measured in other soils. The average measured value for the loess tested was 0.23; in contrast, sands

have K_o -values from 0.4 to 0.6 for dense to loose densities respectively. After collapse, however, K_o was found to be 0.54 which compares favorably with values for other soils. Thus the structural change during collapse has a marked effect on the soil properties.

d. The interpretation of the test results permitted important qualitative conclusions. The collapse mechanism of the soil in confined compression is a shear phenomenon; that is, the collapse stress is determined by the shear strength expressed as a function of effective stresses. The behavior of the soil before, during, and after collapse can be illustrated by use of effective stress path diagrams (Fig. 5.7).

Loading in confined compression causes the shear stresses to increase and, because of the low K_o -value prior to collapse, the stress path approaches the K_f -line. When the path reaches the K_f -line, the shear stresses equal the strength and collapse occurs. K_o then increases as a result of the structural rearrangement during collapse and the stress path for subsequent loading has a flatter slope than the K_f -line.

Wetting the soil under a constant confined compressive stress reduces the negative pore pressure, thereby reducing the vertical and horizontal effective stresses and the strength. As a result, the stress path for wetting is horizontal and approaches the K_f -line. If the path intersects the K_f -line, collapse occurs.

e. The compressive strains and, therefore, settlements which accompany wetting depend on the amount of wetting and on the stress acting at the time of wetting. The strains are small when the acting stresses are smaller than the strength as reduced by wetting. The strains are also small if the collapse stress has been exceeded prior to wetting. Maximum compressive strains occur when the soil collapses during wetting, that is, when the strength as reduced by wetting diminishes to the level of the existing stresses.

f. The quantitative application of the above qualitative conclusions requires the knowledge of several soil properties which cannot be evaluated by routine soil tests. These properties are (1) the effective stress strength parameters \bar{c} and $\bar{\phi}$, (2) the pore-water pressure u_w expressed as a function of the water content of the soil, (3) the parameter x expressed as a function of the degree of saturation, and (4) the lateral stress ratio K_o before and after collapse. When these properties have been evaluated, the effective stress path for compressive loading can be constructed. Further studies may demonstrate that some of the necessary soil properties have a small variation or are related to easily measured quantities. For the present, however, special tests must be run to evaluate them and the test procedures described in this report may be followed.

APPENDIX I

REFERENCES

- Aitchison, G. D., (1961), "Relationships of Moisture Stress and Effective Stress Functions in Unsaturated Soils," Pore Pressure and Suction in Soils, Butterworths, London, pp. 47-52.
- Bally, R. J., (1961), "Data on the Homogeneity and Compressibility of Loesses Treated with the Help of Statistical Methods," Studii de Geotehnica, Fundatii si Constructii Hidrotehnice, Vol. 3, I.S.C.H., Bucharest.
- Berezantzev, V. G., A. A. Mustafayev, N. N. Sidorov, I. V. Kovalyov, and S. K. Aliev, (1969), "On the Strength of Some Soils," Proceedings, 7th International Conference on Soil Mechanics and Foundation Engineering, Mexico, Vol. 1, pp. 11-19.
- Bishop, A. W., (1960), "The Principle of Effective Stress," Publication No. 32, Norwegian Geotechnical Institute, Oslo, pp. 1-5.
- Bishop, A. W., and G. E. Blight, (1963), "Some Aspects of Effective Stress in Saturated and Partly Saturated Soils," Geotechnique, Vol. 13, No. 3, September, pp. 177-197.
- Burland, J. B., (1965), "Some Aspects of the Mechanical Behavior of Partly Saturated Soils," Moisture Equilibria and Moisture Changes in Soils Beneath Covered Areas, Butterworths, Sidney, pp. 270-278.
- Gibbs, H. J., and W. Y. Holland, (1960), "Petrographic and Engineering Properties of Loess," Engineering Monograph No. 28, U.S. Bureau of Reclamation, Denver, Colorado.
- Holtz, W. G., and H. J. Gibbs, (1951), "Consolidation and Related Properties of Loessial Soils," Symposium on Consolidation Testing of Soils - 1951, American Society for Testing Materials, Special Technical Publication No. 126, pp. 9-26.
- Lambe, T. W., (1964), "Methods of Estimating Settlement," Journal of the Soil Mechanics and Foundations Division, ASCE, Vol. 90, No. SM5, pp. 43-67.

- Larionov, A. K., (1965), "Structural Characteristics of Loess Soils for Evaluating Their Constructional Properties," Proceedings, 6th International Conference on Soil Mechanics and Foundation Engineering, Montreal, Vol. 1, pp. 64-68.
- Lyon, C. A., R. L. Handy, and D. T. Davidson, (1954), "Property Variations in the Wisconsin Loess of East-Central Iowa," Iowa Academy of Science Proceedings, Vol. 61, pp. 291-312. (Reprinted in Bulletin No. 20, Iowa Highway Research Board, December 1960, pp. 44-64).
- Northey, R. D., (1969), "Engineering Properties of Loess and Other Collapsible Soils," Proceedings, 7th International Conference on Soil Mechanics and Foundation Engineering, Mexico, Vol. 3, pp. 445-452.
- Olson, R. E., and L. J. Langfelder, (1965), "Pore Water Pressures in Unsaturated Soils," Journal of the Soil Mechanics and Foundations Division, ASCE, Vol. 91, No. SM4, pp. 127-150.
- Seed, H. B., R. J. Woodward, and R. Lundgren, (1962), "Prediction of Swelling Potential for Compacted Clays," Journal of the Soil Mechanics and Foundations Division, ASCE, Vol. 88, No. SM3, pp. 53-87.
- Sheeler, J. B., (1968), "Summarization and Comparison of Engineering Properties of Loess in the United States," Highway Research Record No. 212, Highway Research Board, pp. 1-9.
- Skempton, A. W., (1961), "Effective Stress in Soils, Concrete and Rocks," Pore Pressure and Suction in Soils, Butterworths, London, pp. 4-16.
- Yoshimi, Y., and J. O. Osterberg, (1963), "Compression of Partially Saturated Cohesive Soils," Journal of the Soil Mechanics and Foundations Division, ASCE, Vol. 89, No. SM4, pp. 1-24.

APPENDIX II

NOTATION

The following symbols are used in this report:

a	Intercept of q_f vs \bar{p}_f diagram on q -axis
\bar{c}	Cohesion intercept based on effective stresses
C	Clay content
C_c	Compression index, Fig. 3.28
e	Void ratio
e_i	Initial void ratio
K_o	Lateral stress ratio for one-dimensional strain = $\Delta\sigma_h / \Delta\sigma_v$
K_{oi}	Initial K_o -value before collapse
K_{of}	Final K_o -value after collapse
p	$(\sigma_v + \sigma_h) / 2$
p_f	p at failure
\bar{p}	$(\bar{\sigma}_v + \bar{\sigma}_h) / 2$
\bar{p}_f	\bar{p} at failure
q	$(\sigma_v - \sigma_h) / 2$
q_f	q at failure
S_r	Degree of saturation
S_{ri}	Initial degree of saturation
u	Equivalent pore pressure

u_a	Pore-air pressure
u_w	Pore-water pressure
w	Water content
w_i	Initial water content
x	Coefficient in Eq. 5.1
$\bar{\alpha}$	Slope of q_f vs \bar{p}_f diagram
β	Slope of K_o -line
Δ	Change or increment in appended quantity
ϵ_v	Vertical strain
σ	Normal stress
$\bar{\sigma}$	Effective normal stress
$\sigma_h, \bar{\sigma}_h$	Horizontal normal stress
$\sigma_v, \bar{\sigma}_v$	Vertical normal stress
σ_{vc}	Collapse stress, Fig. 3.28
$(\sigma_v)_2$	σ_v at $\epsilon_v = 2\%$
$(\sigma_v - \sigma_h)_f$	Deviator stress at failure in triaxial compression test
$\bar{\phi}$	Angle of shearing resistance based on effective stresses

APPENDIX III

CONFINED COMPRESSION TEST RESULTS

This appendix contains tabulated test data for each of the confined compression tests. A description of the tabulated quantities and assumptions used in the computations follows.

<u>Column</u>	<u>Description</u>
1,2 LOAD	Applied vertical stress (units given).
3 MACH CORR	Compression (in.) in machine due to loading without soil specimen.
4 DIAL READ	Reading (in.) on 0.0001-in. compression dial indicator. Add MACH CORR to obtain corrected dial reading.
5 WATER CONTENT	Water content (%) is assumed to remain constant until sample becomes saturated and is computed from initial wet weight. Thereafter sample is assumed to remain saturated and water content is calculated from void ratio.
6 DEG. SAT.	Degree of saturation (%) is computed for initial conditions using initial void ratio and water content. The initial water content is used with void ratios after loading until 100% saturation is achieved, after which sample is assumed to remain saturated.
7 DRY DEN.	Dry density (units given).
8 NEG. P-PR	Negative pore-water pressure measured (units given).
CHECK ON FINAL W/C MEASURED	Water content computed from final wet weight.

<u>Column</u>	<u>Description</u>
CALCULATED FROM D/R	Final water content in column 5.
9, 10 LOAD	Applied vertical stress (σ_v).
11 VOID RATIO	Void ratio (e) computed using initial volume, volume change found from change in corrected dial readings, dry weight, and specific gravity.
12 STRAIN	Vertical strain (ϵ_v) computed from change in corrected dial readings and original specimen height.
13 COEFF. COMPR.	$= (e_1 - e_2) / (\sigma_{v2} - \sigma_{v1})$ at σ_{v2}
14 CONSTR MODULUS	$= (\sigma_{v2} - \sigma_{v1}) / (\epsilon_2 - \epsilon_1)$ at σ_{v2}
15 COMPR INDEX	$= (e_1 - e_2) / \log (\sigma_{v2} / \sigma_{v1})$ at σ_{v2}

Note: (σ_{v1} , e_1 , ϵ_{v1}) and (σ_{v2} , e_2 , ϵ_{v2}) are for successive load increments.

THE UNIVERSITY OF IOWA
SOIL MECHANICS LABORATORY
ONE-DIMENSIONAL CONSOLIDATION TEST
WITH NEGATIVE PORE PRESSURE MEASUREMENTS

SAMPLE NO A2-8 SPECIMEN NO 3 TYPE NATURAL
DATE PLACED 05-06-70 DATE REMOVED 05-07-70 SP.GR. 2.72
SPECIMEN DIAMETER= 2.50 IN SPECIMEN HEIGHT= 0.752 IN

WT. OF RING + COVER PLATES + WET SOIL 184.3000 GM.
WT. OF RING + COVER PLATES 83.1200 GM.
D/R WITH SEATING LOAD ON SPECIMEN 0.2500
WET WT. OF SPECIMEN + CONTAINER (FINAL) 240.79 GM.
DRY WT. OF SPECIMEN + CONTAINER (FINAL) 232.23 GM.
WT. OF CONTAINER FOR W/C TEST 139.82 GM.
TEST PERFORMED ON CONSOLIDOMETER NO. 101

LOAD TSF	LOAD PSI	MACH CORR	DIAL READ	WATER CONTENT	DEG. SAT.	DRY DEN. GMCC	NEG. P-PR PSI.
0.03	0.44	0.0000	0.2500	9.49	33.07	1.53	78.0
1.00	13.89	0.0057	0.2356	9.49	33.97	1.55	96.5
2.00	27.78	0.0073	0.2312	9.49	34.27	1.55	97.2
4.00	55.55	0.0096	0.2234	9.49	34.87	1.56	96.9
8.00	111.11	0.0111	0.2004	9.49	37.45	1.61	93.0
16.00	222.22	0.0156	0.1613	9.49	42.50	1.69	89.1
32.00	444.45	0.0209	0.1205	9.49	49.32	1.79	84.2
8.00	111.11	0.0116	0.1526	9.49	44.71	1.72	84.2
2.00	27.78	0.0070	0.1847	9.49	40.18	1.66	84.8
0.03	0.44	0.0040	0.2167	9.49	36.30	1.59	85.0

CHECK ON FINAL W/C MEASURED= 9.263
CALCULATED FROM D/R= 9.490

LOAD TSF	LOAD KG./ SQCM	VOID RATIO	STRAIN PERCENT	COEFF. COMPR. CM ² /KG	CONSTR MODULUS KG/CM ²	COMPR INDEX
0.03	0.03	0.780	0.000	0.00000	0.000	0.000
1.00	0.98	0.760	1.157	0.02177	81.770	0.014
2.00	1.95	0.753	1.529	0.00679	262.159	0.022
4.00	3.91	0.740	2.261	0.00667	267.018	0.043
8.00	7.81	0.689	5.120	0.01303	136.613	0.169
16.00	15.62	0.607	9.721	0.01049	169.792	0.272
32.00	31.25	0.523	14.441	0.00538	330.962	0.279
8.00	7.81	0.577	11.410	0.00230	772.981	0.090
2.00	1.95	0.642	7.753	0.01111	160.209	0.108
0.03	0.03	0.711	3.896	0.03572	49.843	0.038

THE UNIVERSITY OF IOWA
SOIL MECHANICS LABORATORY
ONE-DIMENSIONAL CONSOLIDATION TEST
WITH NEGATIVE PORE PRESSURE MEASUREMENTS

SAMPLE NO A2-5 SPECIMEN NO 4 TYPE NATURAL
DATE PLACED 05-08-70 DATE REMOVED 05-09-70 SP.GR. 2.72
SPECIMEN DIAMETER= 2.50 IN SPECIMEN HEIGHT=0.752 IN

WT. OF RING + COVER PLATES + WET SOIL 183.2400 GM.
WT. OF RING + COVER PLATES 83.1100 GM.
D/R WITH SEATING LOAD ON SPECIMEN 0.2500
WET WT. OF SPECIMEN + CONTAINER (FINAL) 296.99 GM.
DRY WT. OF SPECIMEN + CONTAINER (FINAL) 289.30 GM.
WT. OF CONTAINER FOR W/C TEST 197.04 GM.
TEST PERFORMED ON CONSOLIDOMETER NO. 101

LOAD TSF	LOAD PSI	MACH CORR.	DIAL READ	WATER CONTENT	DEG. SAT.	DRY DEN. GMCC	NEG. P-PR PSI.
0.03	0.44	0.0000	0.2500	8.53	29.62	1.53	136.5
1.00	13.89	0.0057	0.2404	8.53	29.97	1.53	136.8
2.00	27.78	0.0073	0.2330	8.53	30.51	1.55	137.3
4.00	55.55	0.0096	0.2222	8.53	31.34	1.56	134.0
8.00	111.11	0.0111	0.1994	8.53	33.64	1.61	132.0
16.00	222.22	0.0156	0.1657	8.53	37.40	1.68	128.7
32.00	444.45	0.0209	0.1224	8.53	43.75	1.78	110.0
8.00	111.11	0.0116	0.1310	8.53	43.89	1.78	116.0
2.00	27.78	0.0070	0.1363	8.53	43.75	1.78	117.0
0.03	0.44	0.0040	0.1412	8.53	43.38	1.77	117.0

CHECK ON FINAL W/C MEASURED= 8.335
CALCULATED FROM D/R= 8.530

LOAD TSF	LOAD KG. / SQCM	VOID RATIO	STRAIN PERCENT	COEFF. COMPR. CM2/KG	CONSTR MODULUS KG/CM2	COMPR INDEX
0.03	0.03	0.783	0.000	0.00000	0.000	0.000
1.00	0.98	0.774	0.519	0.00978	182.410	0.006
2.00	1.95	0.760	1.290	0.01409	126.561	0.046
4.00	3.91	0.740	2.420	0.01032	172.775	0.067
8.00	7.81	0.690	5.253	0.01293	137.896	0.168
16.00	15.62	0.620	9.136	0.00886	201.192	0.230
32.00	31.25	0.530	14.189	0.00577	309.188	0.299
8.00	7.81	0.529	14.282	*****	*****	-0.003
2.00	1.95	0.530	14.189	0.00028	6293.543	0.003
0.03	0.03	0.535	13.936	0.00234	760.777	0.002

THE UNIVERSITY OF IOWA
SOIL MECHANICS LABORATORY
ONE-DIMENSIONAL CONSOLIDATION TEST
WITH NEGATIVE PORE PRESSURE MEASUREMENTS

SAMPLE NO A2-2 SPECIMEN NO 5 TYPE NATURAL
DATE PLACED 6-10-70 DATE REMOVED 6-11-70 SP.GR. 2.72
SPECIMEN DIAMETER= 2.50IN SPECIMEN HEIGHT=0.752IN

WT. OF RING + COVER PLATES + WET SOIL 177.8300GM.
WT. OF RING + COVER PLATES 83.1100 GM.
D/R WITH SEATING LOAD ON SPECIMEN 0.2500
WET WT. OF SPECIMEN + CONTAINER (FINAL) 273.50 GM.
DRY WT. OF SPECIMEN + CONTAINER (FINAL) 269.60 GM.
WT. OF CONTAINER FOR W/C TEST 179.05 GM.
TEST PERFORMED ON CONSOLIDOMETER NO. 101

LOAD TSF	LOAD PSI	MACH CORR	DIAL READ	WATER CONTENT	DEG. SAT.	DRY DEN. GMCC	NEG. P-PR PSI.
0.03	0.44	0.0000	0.2500	4.61	15.33	1.50	242.0
1.00	13.89	0.0057	0.2433	4.61	15.38	1.50	289.0
2.00	27.78	0.0073	0.2412	4.61	15.40	1.50	300.0
4.00	55.55	0.0096	0.2368	4.61	15.50	1.50	300.0
8.00	111.11	0.0111	0.2261	4.61	15.93	1.52	300.0
16.00	222.22	0.0156	0.1955	4.61	17.32	1.58	300.0
32.00	444.45	0.0209	0.1411	4.61	20.72	1.70	300.0
8.00	111.11	0.0116	0.1515	4.61	20.63	1.69	300.0
2.00	27.78	0.0070	0.1565	4.61	20.60	1.69	300.0
0.03	0.44	0.0040	0.1610	4.61	20.48	1.69	300.0

CHECK ON FINAL W/C MEASURED= 4.307
CALCULATED FROM D/R= 4.605

LOAD TSF	LOAD KG./ SQCM	VOID RATIO	STRAIN PERCENT	COEFF. COMPR. CM ² /KG	CONSTR MODULUS KG/CM ²	COMPR INDEX
0.03	0.03	0.817	0.000	0.00000	0.000	0.000
1.00	0.98	0.815	0.133	0.00255	711.412	0.002
2.00	1.95	0.813	0.199	0.00124	1467.854	0.004
4.00	3.91	0.808	0.479	0.00260	699.356	0.017
8.00	7.81	0.786	1.702	0.00569	319.259	0.074
16.00	15.62	0.723	5.173	0.00807	225.088	0.209
32.00	31.25	0.604	11.702	0.00759	239.291	0.394
8.00	7.81	0.607	11.556	0.00011	*****	0.004
2.00	1.95	0.608	11.503	0.00016	*****	0.002
0.03	0.03	0.612	11.303	0.00189	963.640	0.002

CORE USAGE OBJECT CODE= 9624 BYTES, ARRAY AREA= 8400 BYTES, TOTAL AREA
COMPILE TIME= 1.03 SEC, EXECUTION TIME= 6.56 SEC, WATFOR - VERSION 1 LEVE

THE UNIVERSITY OF IOWA
SOIL MECHANICS LABORATORY
ONE-DIMENSIONAL CONSOLIDATION TEST
WITH NEGATIVE PORE PRESSURE MEASUREMENTS

SAMPLE NO A2-4 SPECIMEN NO 6 TYPE NATURAL
DATE PLACED 6-12-70 DATE REMOVED 6-15-70 SP.GR. 2.72
SPECIMEN DIAMETER= 2.50 IN SPECIMEN HEIGHT=0.752 IN

WT. OF RING + COVER PLATES + WET SOIL 181.4100 GM.
WT. OF RING + COVER PLATES 83.1100 GM.
D/R WITH SEATING LOAD ON SPECIMEN 0.2500
WET WT. OF SPECIMEN + CONTAINER (FINAL) 243.59 GM.
DRY WT. OF SPECIMEN + CONTAINER (FINAL) 236.56 GM.
WT. OF CONTAINER FOR W/C TEST 145.21 GM.
TEST PERFORMED ON CONSOLIDOMETER NO. 101

LOAD TSF	LOAD PSI	MACH CORR	DIAL READ	WATER CONTENT	DEG. SAT.	DRY DEN. GMCC	NEG. P-PR PSI.
0.03	0.44	0.0000	0.2500	7.61	25.83	1.51	112.0
1.00	13.89	0.0057	0.2434	7.61	25.90	1.51	113.0
2.00	27.78	0.0073	0.2391	7.61	26.11	1.52	111.0
4.00	55.55	0.0096	0.2233	7.61	27.22	1.55	110.0
8.00	111.11	0.0111	0.2103	7.61	28.25	1.57	106.0
16.00	222.22	0.0156	0.1781	7.61	31.06	1.63	102.0
32.00	444.45	0.0209	0.1345	7.61	36.02	1.73	94.7
8.00	111.11	0.0116	0.1429	7.61	36.15	1.73	95.0
2.00	27.78	0.0070	0.1479	7.61	36.09	1.73	96.0
0.03	0.44	0.0040	0.1515	7.61	36.00	1.73	96.0

CHECK ON FINAL W/C MEASURED= 7.696
CALCULATED FROM D/R= 7.608

LOAD TSF	LOAD KG./ SQCM	VOID RATIO	STRAIN PERCENT	COEFF. COMPR. CM2/KG	CONSTR MODULUS KG/CM2	COMPR INDEX
0.03	0.03	0.801	0.000	0.00000	0.000	0.000
1.00	0.98	0.799	0.120	0.00228	790.408	0.001
2.00	1.95	0.793	0.479	0.00663	271.869	0.021
4.00	3.91	0.760	2.274	0.01656	108.785	0.107
8.00	7.81	0.733	3.803	0.00705	255.408	0.091
16.00	15.62	0.666	7.487	0.00849	212.087	0.220
32.00	31.25	0.575	12.580	0.00587	306.767	0.305
8.00	7.81	0.572	12.699	*****	*****	-0.004
2.00	1.95	0.573	12.646	0.00016	*****	0.002
0.03	0.03	0.575	12.566	0.00075	2409.120	0.001

THE UNIVERSITY OF IOWA
SOIL MECHANICS LABORATORY
ONE-DIMENSIONAL CONSOLIDATION TEST
WITH NEGATIVE PORE PRESSURE MEASUREMENTS

SAMPLE NO A2-6 SPECIMEN NO 7 TYPE NATURAL
DATE PLACED 6-18-70 DATE REMOVED 6-19-70 SP.GR. 2.72
SPECIMEN DIAMETER= 2.50 IN SPECIMEN HEIGHT=0.752 IN

WT. OF RING + COVER PLATES + WET SOIL 182.8300 GM.
WT. OF RING + COVER PLATES 83.1000 GM.
D/R WITH SEATING LOAD ON SPECIMEN 0.2500
WET WT. OF SPECIMEN + CONTAINER (FINAL) 238.48 GM.
DRY WT. OF SPECIMEN + CONTAINER (FINAL) 230.96 GM.
WT. OF CONTAINER FOR W/C TEST 139.80 GM.
TEST PERFORMED ON CONSOLIDOMETER NO. 101

LOAD TSF	LOAD PSI	MACH CORR	DIAL READ	WATER CONTENT	DEG. SAT.	DRY DEN. GMCC	NEG. P-PR PSI.
0.03	0.44	0.0000	0.2500	9.40	31.77	1.51	72.0
1.00	13.89	0.0057	0.2422	9.40	31.97	1.51	89.0
2.00	27.78	0.0073	0.2387	9.40	32.15	1.52	89.0
4.00	55.55	0.0096	0.2314	9.40	32.65	1.53	89.4
8.00	111.11	0.0111	0.2103	9.40	34.73	1.57	88.5
16.00	222.22	0.0156	0.1694	9.40	39.41	1.65	89.3
32.00	444.45	0.0209	0.1241	9.40	46.25	1.75	86.2
8.00	111.11	0.0116	0.1333	9.40	46.27	1.75	90.0
2.00	27.78	0.0070	0.1392	9.40	46.01	1.75	90.0
0.03	0.44	0.0040	0.1490	9.40	44.70	1.73	90.0

CHECK ON FINAL W/C MEASURED= 8.249
CALCULATED FROM D/R= 9.401

LOAD TSF	LOAD KG. / SQCM	VOID RATIO	STRAIN PERCENT	COEFF. COMPR. CM2/KG	CONSTR MODULUS KG/CM2	COMPR INDEX
0.03	0.03	0.805	0.000	0.00000	0.000	0.000
1.00	0.98	0.800	0.279	0.00533	338.760	0.003
2.00	1.95	0.795	0.532	0.00467	386.333	0.015
4.00	3.91	0.783	1.197	0.00614	293.722	0.040
8.00	7.81	0.736	3.803	0.01204	149.856	0.156
16.00	15.62	0.649	8.644	0.01118	161.395	0.290
32.00	31.25	0.553	13.963	0.00614	293.729	0.319
8.00	7.81	0.553	13.976	*****	*****	-0.000
2.00	1.95	0.556	13.803	0.00053	3389.103	0.005
0.03	0.03	0.572	12.899	0.00849	212.567	0.009

THE UNIVERSITY OF IOWA
SOIL MECHANICS LABORATORY
ONE-DIMENSIONAL CONSOLIDATION TEST
WITH NEGATIVE PORE PRESSURE MEASUREMENTS

SAMPLE NO A4-6 SPECIMEN NO 11 TYPE NATURAL
DATE PLACED 6-26-70 DATE REMOVED 6-26-70 SP.GR. 2.72
SPECIMEN DIAMETER= 2.50IN SPECIMEN HEIGHT=0.752IN

WT. OF RING + COVER PLATES + WET SOIL 194.6000GM.
WT. OF RING + COVER PLATES 83.1100 GM.
D/R WITH SEATING LOAD ON SPECIMEN 0.2500
WET WT. OF SPECIMEN + CONTAINER (FINAL) 251.59 GM.
DRY WT. OF SPECIMEN + CONTAINER (FINAL) 233.50 GM.
WT. OF CONTAINER FOR W/C TEST 139.79 GM.
TEST PERFORMED ON CONSOLIDOMETER NO. 101

LOAD TSF	LOAD PSI	MACH CORR	DIAL READ	WATER CONTENT	DEG. SAT.	DRY DEN. GMCC	NEG. P-PR PSI.
0.03	0.44	0.0000	0.2500	18.97	68.28	1.55	8.0
1.00	13.89	0.0057	0.2409	18.97	69.01	1.56	8.0
2.00	27.78	0.0073	0.2369	18.97	69.53	1.56	8.0
4.00	55.55	0.0096	0.2185	18.97	73.24	1.60	7.1
8.00	111.11	0.0111	0.1731	18.97	85.70	1.70	5.4
16.00	222.22	0.0156	0.1386	18.97	96.99	1.78	5.4
32.00	444.45	0.0209	0.1001	16.71	100.00	1.87	0.0
8.00	111.11	0.0116	0.1090	16.68	100.00	1.87	0.0
2.00	27.78	0.0070	0.1149	16.79	100.00	1.87	0.0
0.03	0.44	0.0040	0.1245	17.36	100.00	1.85	0.0

CHECK ON FINAL W/C MEASURED=19.304
CALCULATED FROM D/R=17.357

LOAD TSF	LOAD KG./ SQCM	VOID RATIO	STRAIN PERCENT	COEFF. COMPR. CM2/KG	CONSTR MODULUS KG/CM2	COMPR INDEX
0.03	0.03	0.756	0.000	0.00000	0.000	0.000
1.00	0.98	0.748	0.452	0.00839	209.232	0.005
2.00	1.95	0.742	0.771	0.00574	305.852	0.019
4.00	3.91	0.705	2.912	0.01925	91.217	0.125
8.00	7.81	0.602	8.750	0.02624	66.906	0.340
16.00	15.62	0.532	12.739	0.00897	195.827	0.233
32.00	31.25	0.455	17.154	0.00496	353.890	0.258
8.00	7.81	0.454	17.207	*****	*****	-0.002
2.00	1.95	0.457	17.035	0.00052	3389.140	0.005
0.03	0.03	0.472	16.157	0.00802	219.009	0.009

THE UNIVERSITY OF IOWA
SOIL MECHANICS LABORATORY
ONE-DIMENSIONAL CONSOLIDATION TEST
WITH NEGATIVE PORE PRESSURE MEASUREMENTS

SAMPLE NO A4-8 SPECIMEN NO 13 TYPE NATURAL
DATE PLACED 6-12-70 DATE REMOVED 6-30-70 SP.GR. 2.72
SPECIMEN DIAMETER= 2.50IN SPECIMEN HEIGHT=0.752IN

WT. OF RING + COVER PLATES + WET SOIL 201.0900GM.
WT. OF RING + COVER PLATES 83.1100 GM.
D/R WITH SEATING LOAD ON SPECIMEN 0.2500
WET WT. OF SPECIMEN + CONTAINER (FINAL) 259.91 GM.
DRY WT. OF SPECIMEN + CONTAINER (FINAL) 240.53 GM.
WT. OF CONTAINER FOR W/C TEST 148.56 GM.
TEST PERFORMED ON CONSOLIDOMETER NO. 101

LOAD TSF	LOAD PSI	MACH CORR	DIAL READ	WATER CONTENT	DEG. SAT.	DRY DEN. GMCC	NEG. P-PR PSI.
0.03	0.44	0.0000	0.2500	28.28	97.50	1.52	3.4
1.00	13.89	0.0057	0.2345	28.15	100.00	1.54	2.8
2.00	27.78	0.0073	0.2127	26.38	100.00	1.58	2.2
4.00	55.55	0.0096	0.1824	23.93	100.00	1.65	1.9
8.00	111.11	0.0111	0.1504	21.27	100.00	1.72	1.4
16.00	222.22	0.0156	0.1216	19.14	100.00	1.79	0.0
32.00	444.45	0.0209	0.0901	16.85	100.00	1.87	0.0
8.00	111.11	0.0116	0.0990	16.82	100.00	1.87	0.0
2.00	27.78	0.0070	0.1048	16.92	100.00	1.86	0.0
0.03	0.44	0.0040	0.1165	17.68	100.00	1.84	0.0

CHECK ON FINAL W/C MEASURED=21.072
CALCULATED FROM D/R=17.681

LOAD TSF	LOAD KG./ SQCM	VOID RATIO	STRAIN PERCENT	COEFF. COMPR. CM2/KG	CONSTR MODULUS KG/CM2	COMPR INDEX
0.03	0.03	0.789	0.000	0.00000	0.000	0.000
1.00	0.98	0.766	1.303	0.02464	72.592	0.016
2.00	1.95	0.718	3.989	0.04923	36.339	0.160
4.00	3.91	0.651	7.713	0.03411	52.450	0.221
8.00	7.81	0.578	11.769	0.01858	96.301	0.241
16.00	15.62	0.521	15.000	0.00740	241.761	0.192
32.00	31.25	0.458	18.484	0.00399	448.442	0.207
8.00	7.81	0.457	18.537	*****	*****	-0.002
2.00	1.95	0.460	18.378	0.00049	3671.431	0.005
0.03	0.03	0.481	17.221	0.01077	166.144	0.011

THE UNIVERSITY OF IOWA
SOIL MECHANICS LABORATORY
ONE-DIMENSIONAL CONSOLIDATION TEST
WITH NEGATIVE PORE PRESSURE MEASUREMENTS

SAMPLE NO A4-1 SPECIMEN NO 14 TYPE NATURAL
DATE PLACED 7-01-70 DATE REMOVED 7-02-70 SP.GR. 2.72
SPECIMEN DIAMETER= 2.50 IN SPECIMEN HEIGHT=0.752 IN

WT. OF RING + COVER PLATES + WET SOIL 180.8500 GM.
WT. OF RING + COVER PLATES 83.1100 GM.
D/R WITH SEATING LOAD ON SPECIMEN 0.2500
WET WT. OF SPECIMEN + CONTAINER (FINAL) 238.33 GM.
DRY WT. OF SPECIMEN + CONTAINER (FINAL) 233.20 GM.
WT. OF CONTAINER FOR W/C TEST 139.80 GM.
TEST PERFORMED ON CONSOLIDOMETER NO. 101

LOAD TSF	LOAD PSI	MACH CORR	DIAL READ	WATER CONTENT	DEG. SAT.	DRY DEN. GMCC	NEG. P-PR PSI.
0.03	0.44	0.0000	0.2500	4.65	16.60	1.54	248.0
1.00	13.89	0.0057	0.2440	4.65	16.61	1.54	255.0
2.00	27.78	0.0073	0.2404	4.65	16.71	1.55	245.5
4.00	55.55	0.0096	0.2344	4.65	16.91	1.56	243.3
8.00	111.11	0.0111	0.2165	4.65	17.82	1.59	243.0
16.00	222.22	0.0156	0.1826	4.65	19.74	1.66	242.3
32.00	444.45	0.0209	0.1392	4.65	22.94	1.75	231.0
8.00	111.11	0.0116	0.1485	4.65	22.94	1.75	231.0
2.00	27.78	0.0070	0.1540	4.65	22.85	1.75	231.0
0.03	0.44	0.0040	0.1720	4.65	21.49	1.71	231.0

CHECK ON FINAL W/C MEASURED= 5.493
CALCULATED FROM D/R= 4.647

LOAD TSF	LOAD KG./ SQCM	VOID RATIO	STRAIN PERCENT	COEFF. COMPR. CM ² /KG	CONSTR MODULUS KG/CM ²	COMPR INDEX
0.03	0.03	0.762	0.000	0.00000	0.000	0.000
1.00	0.98	0.761	0.040	0.00074	2371.437	0.000
2.00	1.95	0.756	0.306	0.00480	367.022	0.016
4.00	3.91	0.748	0.798	0.00444	396.913	0.029
8.00	7.81	0.709	2.979	0.00984	179.096	0.128
16.00	15.62	0.640	6.888	0.00882	199.824	0.229
32.00	31.25	0.551	11.955	0.00571	308.377	0.296
8.00	7.81	0.551	11.955	0.00000	*****	0.000
2.00	1.95	0.553	11.835	0.00036	4895.520	0.004
0.03	0.03	0.588	9.840	0.01828	96.364	0.019

THE UNIVERSITY OF IOWA
SOIL MECHANICS LABORATORY
ONE-DIMENSIONAL CONSOLIDATION TEST
WITH NEGATIVE PORE PRESSURE MEASUREMENTS

SAMPLE NO A4-5 SPECIMEN NO 15 TYPE NATURAL
DATE PLACED 7-03-70 DATE REMOVED 7-03-70 SP.GR. 2.72
SPECIMEN DIAMETER= 2.50 IN SPECIMEN HEIGHT=0.752 IN

WT. OF RING + COVER PLATES + WET SOIL 187.4600 GM.
WT. OF RING + COVER PLATES 83.1100 GM.
D/R WITH SEATING LOAD ON SPECIMEN 0.2500
WET WT. OF SPECIMEN + CONTAINER (FINAL) 243.95 GM.
DRY WT. OF SPECIMEN + CONTAINER (FINAL) 229.80 GM.
WT. OF CONTAINER FOR W/C TEST 139.80 GM.
TEST PERFORMED ON CONSOLIDOMETER NO. 101

LOAD TSF	LOAD PSI	MACH CORR	DIAL READ	WATER CONTENT	DEG. SAT.	DRY DEN. GMCC	NEG. P-PR PSI.
0.03	0.44	0.0000	0.2500	15.94	52.37	1.49	12.5
1.00	13.89	0.0057	0.2459	15.94	52.12	1.48	11.6
2.00	27.78	0.0073	0.2418	15.94	52.51	1.49	10.6
4.00	55.55	0.0096	0.2276	15.94	54.41	1.51	11.2
8.00	111.11	0.0111	0.1878	15.94	61.61	1.60	10.9
16.00	222.22	0.0156	0.1459	15.94	70.75	1.69	8.9
32.00	444.45	0.0209	0.1167	15.94	78.15	1.75	6.4
8.00	111.11	0.0116	0.1272	15.94	77.75	1.75	9.2
2.00	27.78	0.0070	0.1334	15.94	77.21	1.74	10.5
0.03	0.44	0.0040	0.1409	15.94	75.73	1.73	12.5

CHECK ON FINAL W/C MEASURED=15.722
CALCULATED FROM D/R=15.944

LOAD TSF	LOAD KG./ SQCM	VOID RATIO	STRAIN PERCENT	COEFF. COMPR. CM2/KG	CONSTR MODULUS KG/CM2	COMPR INDEX
0.03	0.03	0.828	0.000	0.00000	0.000	0.000
1.00	0.98	0.832	-0.213	*****	-444.634	-0.003
2.00	1.95	0.826	0.120	0.00623	293.624	0.020
4.00	3.91	0.797	1.702	0.01481	123.411	0.096
8.00	7.81	0.704	6.795	0.02384	76.689	0.309
16.00	15.62	0.613	11.769	0.01164	157.080	0.302
32.00	31.25	0.555	14.947	0.00372	491.597	0.193
8.00	7.81	0.558	14.787	0.00012	*****	0.005
2.00	1.95	0.562	14.574	0.00066	2753.538	0.006
0.03	0.03	0.573	13.976	0.00569	321.215	0.006

THE UNIVERSITY OF IOWA
SOIL MECHANICS LABORATORY
ONE-DIMENSIONAL CONSOLIDATION TEST
WITH NEGATIVE PORE PRESSURE MEASUREMENTS

SAMPLE NO A4-3 SPECIMEN NO 16 TYPE NATURAL
DATE PLACED 7-06-70 DATE REMOVED 7-07-70 SP.GR. 2.72
SPECIMEN DIAMETER= 2.50IN SPECIMEN HEIGHT=0.752IN

WT. OF RING + COVER PLATES + WET SOIL 187.8700GM.
WT. OF RING + COVER PLATES 83.1100 GM.
D/R WITH SEATING LOAD ON SPECIMEN 0.2500
WET WT. OF SPECIMEN + CONTAINER (FINAL) 253.06 GM.
DRY WT. OF SPECIMEN + CONTAINER (FINAL) 241.47 GM.
WT. OF CONTAINER FOR W/C TEST 148.58 GM.
TEST PERFORMED ON CONSOLIDOMETER NO. 101

LOAD TSF	LOAD PSI	MACH CORR	DIAL READ	WATER CONTENT	DEG. SAT.	DRY DEN. GMCC	NEG. P-PR PSI.
0.03	0.44	0.0000	0.2500	12.78	45.06	1.54	18.0
1.00	13.89	0.0057	0.2432	12.78	45.22	1.54	17.7
2.00	27.78	0.0073	0.2395	12.78	45.51	1.54	18.0
4.00	55.55	0.0096	0.2319	12.78	46.27	1.55	18.0
8.00	111.11	0.0111	0.2014	12.78	50.89	1.62	17.4
16.00	222.22	0.0156	0.1619	12.78	57.88	1.70	16.8
32.00	444.45	0.0209	0.1210	12.78	67.27	1.79	14.9
8.00	111.11	0.0116	0.1302	12.78	67.30	1.79	15.4
2.00	27.78	0.0070	0.1365	12.78	66.79	1.79	18.0
0.03	0.44	0.0040	0.1440	12.78	65.45	1.78	18.0

CHECK ON FINAL W/C MEASURED=12.477
CALCULATED FROM D/R=12.778

LOAD TSF	LOAD KG./ SQCM	VOID RATIO	STRAIN PERCENT	COEFF. COMPR. CM2/KG	CONSTR MODULUS KG/CM2	COMPR INDEX
0.03	0.03	0.771	0.000	0.00000	0.000	0.000
1.00	0.98	0.769	0.146	0.00274	646.731	0.002
2.00	1.95	0.764	0.426	0.00507	349.543	0.016
4.00	3.91	0.751	1.130	0.00639	277.093	0.041
8.00	7.81	0.683	4.987	0.01749	101.282	0.227
16.00	15.62	0.601	9.641	0.01055	167.852	0.274
32.00	31.25	0.517	14.375	0.00537	330.033	0.279
8.00	7.81	0.516	14.388	*****	*****	-0.000
2.00	1.95	0.520	14.162	0.00068	2591.663	0.007
0.03	0.03	0.531	13.564	0.00551	321.213	0.006

THE UNIVERSITY OF IOWA
SOIL MECHANICS LABORATORY
ONE-DIMENSIONAL CONSOLIDATION TEST
WITH NEGATIVE PORE PRESSURE MEASUREMENTS

SAMPLE NO A6-6 SPECIMEN NO 17 TYPE NATURAL
DATE PLACED 7-17-70 DATE REMOVED 7-18-70 SP.GR. 2.72
SPECIMEN DIAMETER= 2.50 IN SPECIMEN HEIGHT=0.752 IN

WT. OF RING + COVER PLATES + WET SOIL 195.5200 GM.
WT. OF RING + COVER PLATES 83.1000 GM.
D/R WITH SEATING LOAD ON SPECIMEN 0.2500
WET WT. OF SPECIMEN + CONTAINER (FINAL) 240.02 GM.
DRY WT. OF SPECIMEN + CONTAINER (FINAL) 220.88 GM.
WT. OF CONTAINER FOR W/C TEST 130.10 GM.
TEST PERFORMED ON CONSOLIDOMETER NO. 101

LOAD TSF	LOAD PSI	MACH CORR	DIAL READ	WATER CONTENT	DEG. SAT.	DRY DEN. GMCC	NEG. P-PR PSI.
0.03	0.44	0.0000	0.2500	23.84	79.81	1.50	5.4
0.50	6.95	0.0041	0.2452	23.84	79.97	1.50	5.1
1.00	13.89	0.0057	0.2434	23.84	80.02	1.50	5.0
2.00	27.78	0.0073	0.2337	23.84	82.00	1.52	4.4
4.00	55.55	0.0096	0.2071	23.84	88.55	1.57	3.9
8.00	111.11	0.0111	0.1656	23.37	100.00	1.66	0.9
16.00	222.22	0.0156	0.1339	20.96	100.00	1.73	0.0
32.00	444.45	0.0209	0.1036	18.75	100.00	1.80	0.0
8.00	111.11	0.0116	0.1128	18.74	100.00	1.80	0.0
2.00	27.78	0.0070	0.1186	18.85	100.00	1.80	0.0
0.50	6.95	0.0055	0.1235	19.15	100.00	1.79	0.0
0.03	0.44	0.0040	0.1300	19.59	100.00	1.77	0.0

CHECK ON FINAL W/C MEASURED=21.084
CALCULATED FROM D/R=19.591

LOAD TSF	LOAD KG./ SQCM	VOID RATIO	STRAIN PERCENT	COEFF. COMPR. CM2/KG	CONSTR MODULUS KG/CM2	COMPR INDEX
0.03	0.03	0.812	0.000	0.00000	0.000	0.000
0.50	0.49	0.811	0.093	0.00369	491.590	0.001
1.00	0.98	0.810	0.120	0.00099	1836.599	0.002
2.00	1.95	0.791	1.197	0.02000	90.624	0.065
4.00	3.91	0.732	4.428	0.02999	60.436	0.195
8.00	7.81	0.636	9.747	0.02468	73.429	0.320
16.00	15.62	0.570	13.364	0.00839	215.985	0.218
32.00	31.25	0.510	16.689	0.00386	469.967	0.200
8.00	7.81	0.510	16.702	*****	*****	-0.000
2.00	1.95	0.513	16.543	0.00049	3671.420	0.005
0.50	0.49	0.521	16.090	0.00560	323.922	0.014
0.03	0.03	0.533	15.426	0.02633	68.827	0.010

THE UNIVERSITY OF IOWA
SOIL MECHANICS LABORATORY
ONE-DIMENSIONAL CONSOLIDATION TEST
WITH NEGATIVE PORE PRESSURE MEASUREMENTS

SAMPLE NO A6-5 SPECIMEN NO 18 TYPE NATURAL
DATE PLACED 7-20-70 DATE REMOVED 7-21-70 SP.GR. 2.72
SPECIMEN DIAMETER= 2.50 IN SPECIMEN HEIGHT=0.752 IN

WT. OF RING + COVER PLATES + WET SOIL 187.5000 GM.
WT. OF RING + COVER PLATES 83.1000 GM.
D/R WITH SEATING LOAD ON SPECIMEN 0.2500
WET WT. OF SPECIMEN + CONTAINER (FINAL) 266.65 GM.
DRY WT. OF SPECIMEN + CONTAINER (FINAL) 255.12 GM.
WT. OF CONTAINER FOR W/C TEST 162.48 GM.
TEST PERFORMED ON CONSOLIDOMETER NO. 101

LOAD TSF	LOAD PSI	MACH CORR	DIAL READ	WATER CONTENT	DEG. SAT.	DRY DEN. GMCC	NEG. P-PR PSI.
0.03	0.44	0.0000	0.2500	12.69	44.49	1.53	18.0
1.00	13.89	0.0057	0.2440	12.69	44.53	1.53	17.7
2.00	27.78	0.0073	0.2407	12.69	44.76	1.54	17.7
4.00	55.55	0.0096	0.2327	12.69	45.56	1.55	17.6
8.00	111.11	0.0111	0.2032	12.69	49.91	1.61	17.0
16.00	222.22	0.0156	0.1614	12.69	57.20	1.70	16.4
32.00	444.45	0.0209	0.1226	12.69	65.83	1.78	13.5
8.00	111.11	0.0116	0.1301	12.69	66.36	1.79	13.5
2.00	27.78	0.0070	0.1354	12.69	66.15	1.79	16.5
0.03	0.44	0.0040	0.1410	12.69	65.39	1.78	18.0

CHECK ON FINAL W/C MEASURED=12.446
CALCULATED FROM D/R=12.694

LOAD TSF	LOAD KG./ SQCM	VOID RATIO	STRAIN PERCENT	COEFF. COMPR. CM2/KG	CONSTR MODULUS KG/CM2	COMPR INDEX
0.03	0.03	0.776	0.000	0.00000	0.000	0.000
1.00	0.98	0.775	0.040	0.00075	2371.382	0.000
2.00	1.95	0.771	0.266	0.00411	431.787	0.013
4.00	3.91	0.758	1.024	0.00689	257.647	0.045
8.00	7.81	0.692	4.747	0.01693	104.899	0.220
16.00	15.62	0.604	9.707	0.01128	157.502	0.293
32.00	31.25	0.525	14.162	0.00506	350.721	0.263
8.00	7.81	0.520	14.402	*****	*****	-0.007
2.00	1.95	0.522	14.309	0.00028	6293.941	0.003
0.03	0.03	0.528	13.963	0.00319	555.950	0.003

THE UNIVERSITY OF IOWA
SOIL MECHANICS LABORATORY
ONE-DIMENSIONAL CONSOLIDATION TEST
WITH NEGATIVE PORE PRESSURE MEASUREMENTS

SAMPLE NO A5-2 SPECIMEN NO 19 TYPE NATURAL
DATE PLACED 7-21-70 DATE REMOVED 7-22-70 SP.GR. 2.72
SPECIMEN DIAMETER= 2.50IN SPECIMEN HEIGHT=0.752IN

WT. OF RING + COVER PLATES + WET SOIL 193.2700GM.
WT. OF RING + COVER PLATES 83.1000 GM.
D/R WITH SEATING LOAD ON SPECIMEN 0.2500
WET WT. OF SPECIMEN + CONTAINER (FINAL) 272.00 GM.
DRY WT. OF SPECIMEN + CONTAINER (FINAL) 253.10 GM.
WT. OF CONTAINER FOR W/C TEST 162.25 GM.
TEST PERFORMED ON CONSOLIDOMETER NO. 101

LOAD TSF	LOAD PSI	MACH CORR	DIAL READ	WATER CONTENT	DEG. SAT.	DRY DEN. GMCC	NEG. P-PR PSI.
0.03	0.44	0.0000	0.2500	21.27	71.32	1.50	7.0
0.50	6.95	0.0041	0.2450	21.27	71.51	1.50	6.9
1.00	13.89	0.0057	0.2405	21.27	72.13	1.51	5.6
2.00	27.78	0.0073	0.2132	21.27	78.16	1.56	6.7
4.00	55.55	0.0096	0.1994	21.27	81.20	1.59	7.1
8.00	111.11	0.0111	0.1652	21.27	91.30	1.67	4.0
16.00	222.22	0.0156	0.1334	20.88	100.00	1.73	1.0
32.00	444.45	0.0209	0.0974	18.16	100.00	1.82	0.0
8.00	111.11	0.0116	0.1063	18.12	100.00	1.82	0.0
2.00	27.78	0.0070	0.1125	18.26	100.00	1.82	0.0
0.50	6.95	0.0055	0.1175	18.57	100.00	1.81	0.0
0.03	0.44	0.0040	0.1230	18.93	100.00	1.80	0.0

CHECK ON FINAL W/C MEASURED=20.803
CALCULATED FROM D/R=18.928

LOAD TSF	LOAD KG./ SQCM	VOID RATIO	STRAIN PERCENT	COEFF. COMPR. CM2/KG	CONSTR MODULUS KG/CM2	COMPR INDEX
0.03	0.03	0.811	0.000	0.00000	0.000	0.000
0.50	0.49	0.809	0.120	0.00474	382.365	0.002
1.00	0.98	0.802	0.505	0.01430	126.642	0.023
2.00	1.95	0.740	3.923	0.06341	28.563	0.206
4.00	3.91	0.712	5.452	0.01418	127.704	0.092
8.00	7.81	0.634	9.801	0.02016	89.822	0.262
16.00	15.62	0.568	13.431	0.00842	215.195	0.218
32.00	31.25	0.494	17.513	0.00473	382.709	0.246
8.00	7.81	0.493	17.566	*****	*****	-0.002
2.00	1.95	0.497	17.354	0.00066	2753.557	0.006
0.50	0.49	0.505	16.888	0.00576	314.666	0.014
0.03	0.03	0.515	16.356	0.02105	86.033	0.008

THE UNIVERSITY OF IOWA
SOIL MECHANICS LABORATORY
ONE-DIMENSIONAL CONSOLIDATION TEST
WITH NEGATIVE PORE PRESSURE MEASUREMENTS

SAMPLE NO A6-12 SPECIMEN NO 20 TYPE NATURAL
DATE PLACED 7-23-70 DATE REMOVED 7-24-70 SP.GR. 2.72
SPECIMEN DIAMETER= 2.50 IN SPECIMEN HEIGHT=0.752 IN

WT. OF RING + COVER PLATES + WET SOIL 184.0700 GM.
WT. OF RING + COVER PLATES 83.1000 GM.
D/R WITH SEATING LOAD ON SPECIMEN 0.2500
WET WT. OF SPECIMEN + CONTAINER (FINAL) 281.70 GM.
DRY WT. OF SPECIMEN + CONTAINER (FINAL) 274.64 GM.
WT. OF CONTAINER FOR W/C TEST 180.67 GM.
TEST PERFORMED ON CONSOLIDOMETER NO. 101

LOAD TSF	LOAD PSI	MACH CORR	DIAL READ	WATER CONTENT	DEG. SAT.	DRY DEN. GMCC	NEG. P-PR PSI.
0.03	0.44	0.0000	0.2500	7.45	26.98	1.55	101.0
1.00	13.89	0.0057	0.2421	7.45	27.17	1.56	112.0
2.00	27.78	0.0073	0.2393	7.45	27.27	1.56	122.0
4.00	55.55	0.0096	0.2343	7.45	27.50	1.57	116.0
8.00	111.11	0.0111	0.2244	7.45	28.25	1.58	115.0
16.00	222.22	0.0156	0.1933	7.45	30.92	1.64	114.0
32.00	444.45	0.0209	0.1496	7.45	35.81	1.74	98.0
8.00	111.11	0.0116	0.1575	7.45	36.02	1.74	100.0
2.00	27.78	0.0070	0.1623	7.45	35.99	1.74	101.0
0.03	0.44	0.0040	0.1694	7.45	35.39	1.73	101.0

CHECK ON FINAL W/C MEASURED= 7.513
CALCULATED FROM D/R= 7.449

LOAD TSF	LOAD KG./ SQCM	VOID RATIO	STRAIN PERCENT	COEFF. COMPR. CM2/KG	CONSTR MODULUS KG/CM2	COMPR INDEX
0.03	0.03	0.751	0.000	0.00000	0.000	0.000
1.00	0.98	0.746	0.293	0.00541	323.361	0.003
2.00	1.95	0.743	0.452	0.00286	611.703	0.009
4.00	3.91	0.737	0.811	0.00322	543.929	0.021
8.00	7.81	0.717	1.928	0.00501	349.663	0.065
16.00	15.62	0.655	5.465	0.00793	220.857	0.206
32.00	31.25	0.566	10.572	0.00572	305.968	0.297
8.00	7.81	0.563	10.758	*****	*****	-0.005
2.00	1.95	0.563	10.731	0.00008	*****	0.001
0.03	0.03	0.573	10.186	0.00497	352.553	0.005

THE UNIVERSITY OF IOWA
SOIL MECHANICS LABORATORY
ONE-DIMENSIONAL CONSOLIDATION TEST
WITH NEGATIVE PORE PRESSURE MEASUREMENTS

SAMPLE NO A6-7 SPECIMEN NO 21 TYPE NATURAL
DATE PLACED 7-24-70 DATE REMOVED 7-25-70 SP.GR. 2.72
SPECIMEN DIAMETER= 2.50IN SPECIMEN HEIGHT=0.752IN

WT. OF RING + COVER PLATES + WET SOIL 188.8000GM.
WT. OF RING + COVER PLATES 83.1000 GM.
D/R WITH SEATING LOAD ON SPECIMEN 0.2500
WET WT. OF SPECIMEN + CONTAINER (FINAL) 277.78 GM.
DRY WT. OF SPECIMEN + CONTAINER (FINAL) 262.87 GM.
WT. OF CONTAINER FOR W/C TEST 172.21 GM.
TEST PERFORMED ON CONSOLIDOMETER NO. 101

LOAD TSF	LOAD PSI	MACH CORR	DIAL READ	WATER CONTENT	DEG. SAT.	DRY DEN. GMCC	NEG. P-PR PSI.
0.03	0.44	0.0000	0.2500	16.59	55.38	1.50	12.0
0.50	6.95	0.0041	0.2448	16.59	55.56	1.50	10.4
1.00	13.89	0.0057	0.2417	16.59	55.81	1.50	10.0
2.00	27.78	0.0073	0.2392	16.59	55.96	1.51	9.5
4.00	55.55	0.0096	0.2303	16.59	57.08	1.52	8.8
8.00	111.11	0.0111	0.1894	16.59	64.89	1.60	7.9
16.00	222.22	0.0156	0.1460	16.59	75.02	1.70	8.6
32.00	444.45	0.0209	0.1096	16.59	85.71	1.78	6.2
8.00	111.11	0.0116	0.1187	16.59	85.79	1.78	8.0
2.00	27.78	0.0070	0.1249	16.59	85.16	1.78	8.8
0.50	6.95	0.0055	0.1289	16.59	84.21	1.77	9.2
0.03	0.44	0.0040	0.1333	16.59	83.12	1.76	9.4

CHECK ON FINAL W/C MEASURED=16.446
CALCULATED FROM D/R=16.589

LOAD TSF	LOAD KG. / SQCM	VOID RATIO	STRAIN PERCENT	COEFF. COMPR. CM2/KG	CONSTR MODULUS KG/CM2	COMPR INDEX
0.03	0.03	0.815	0.000	0.00000	0.000	0.000
0.50	0.49	0.812	0.146	0.00580	312.832	0.002
1.00	0.98	0.809	0.346	0.00741	244.848	0.012
2.00	1.95	0.806	0.465	0.00223	815.589	0.007
4.00	3.91	0.790	1.343	0.00816	222.515	0.053
8.00	7.81	0.695	6.582	0.02434	74.548	0.316
16.00	15.62	0.602	11.755	0.01202	151.023	0.312
32.00	31.25	0.526	15.891	0.00480	377.786	0.249
8.00	7.81	0.526	15.918	*****	*****	-0.001
2.00	1.95	0.530	15.705	0.00066	2753.660	0.006
0.50	0.49	0.536	15.372	0.00412	440.529	0.010
0.03	0.03	0.543	14.987	0.01529	118.667	0.006

THE UNIVERSITY OF IOWA
SOIL MECHANICS LABORATORY
ONE-DIMENSIONAL CONSOLIDATION TEST
WITH NEGATIVE PORE PRESSURE MEASUREMENTS

SAMPLE NO A6-9 SPECIMEN NO 22 TYPE NATURAL
DATE PLACED 7-27-7 DATE REMOVED 7-28-70 SP.GR. 2.72
SPECIMEN DIAMETER= 2.50IN SPECIMEN HEIGHT=0.752IN

WT. OF RING + COVER PLATES + WET SOIL 196.6200GM.
WT. OF RING + COVER PLATES 83.1000 GM.
D/R WITH SEATING LOAD ON SPECIMEN 0.2500
WET WT. OF SPECIMEN + CONTAINER (FINAL) 255.78 GM.
DRY WT. OF SPECIMEN + CONTAINER (FINAL) 237.22 GM.
WT. OF CONTAINER FOR W/C TEST 148.28 GM.
TEST PERFORMED ON CONSOLIDOMETER NO. 101

LOAD TSF	LOAD PSI	MACH CORR	DIAL READ	WATER CONTENT	DEG. SAT.	DRY DEN. GMCC	NEG. P-PR PSI.
0.03	0.44	0.0000	0.2500	27.64	88.44	1.47	3.4
0.50	6.95	0.0041	0.2385	27.64	90.38	1.48	3.0
1.00	13.89	0.0057	0.2305	27.64	92.12	1.50	2.8
2.00	27.78	0.0073	0.2132	27.64	96.70	1.53	2.8
4.00	55.55	0.0096	0.1833	26.08	100.00	1.59	2.5
8.00	111.11	0.0111	0.1514	23.33	100.00	1.66	2.2
16.00	222.22	0.0156	0.1229	21.16	100.00	1.73	1.7
32.00	444.45	0.0209	0.0959	19.20	100.00	1.79	0.0
8.00	111.11	0.0116	0.1047	19.16	100.00	1.79	0.0
2.00	27.78	0.0070	0.1105	19.26	100.00	1.78	0.0
0.50	6.95	0.0055	0.1151	19.54	100.00	1.78	0.0
0.03	0.44	0.0040	0.1207	19.92	100.00	1.76	0.0

CHECK ON FINAL W/C MEASURED=20.868
CALCULATED FROM D/R=19.916

LOAD TSF	LOAD KG./ SQCM	VOID RATIO	STRAIN PERCENT	COEFF. COMPR. CM2/KG	CONSTR MODULUS KG/CM2	COMPR INDEX
0.03	0.03	0.850	0.000	0.00000	0.000	0.000
0.50	0.49	0.832	0.984	0.03978	46.504	0.015
1.00	0.98	0.816	1.835	0.03224	57.385	0.052
2.00	1.95	0.777	3.923	0.03957	46.755	0.128
4.00	3.91	0.709	7.593	0.03477	53.210	0.226
8.00	7.81	0.635	11.636	0.01915	96.618	0.248
16.00	15.62	0.576	14.827	0.00756	244.783	0.196
32.00	31.25	0.522	17.713	0.00342	541.435	0.177
8.00	7.81	0.521	17.779	*****	*****	-0.002
2.00	1.95	0.524	17.620	0.00050	3671.632	0.005
0.50	0.49	0.532	17.207	0.00521	355.260	0.013
0.03	0.03	0.542	16.662	0.02204	83.936	0.008

THE UNIVERSITY OF IOWA
SOIL MECHANICS LABORATORY
ONE-DIMENSIONAL CONSOLIDATION TEST
WITH NEGATIVE PORE PRESSURE MEASUREMENTS

SAMPLE NO A6-8 SPECIMEN NO 23 TYPE NATURAL
DATE PLACED 7-28-7 DATE REMOVED 7-29-70 SP.GR. 2.72
SPECIMEN DIAMETER= 2.50 IN SPECIMEN HEIGHT=0.752 IN

WT. OF RING + COVER PLATES + WET SOIL 194.1000 GM.
WT. OF RING + COVER PLATES 83.1000 GM.
D/R WITH SEATING LOAD ON SPECIMEN 0.2500
WET WT. OF SPECIMEN + CONTAINER (FINAL) 251.28 GM.
DRY WT. OF SPECIMEN + CONTAINER (FINAL) 231.94 GM.
WT. OF CONTAINER FOR W/C TEST 140.34 GM.
TEST PERFORMED ON CONSOLIDOMETER NO. 101

LOAD TSF	LOAD PSI	MACH CORR	DIAL READ	WATER CONTENT	DEG. SAT.	DRY DEN. GMCC	NEG. P-PR PSI.
0.03	0.44	0.0000	0.2500	21.18	72.35	1.51	9.0
0.50	6.95	0.0041	0.2453	21.18	72.48	1.52	3.4
1.00	13.89	0.0057	0.2441	21.18	72.39	1.51	3.6
2.00	27.78	0.0073	0.2374	21.18	73.52	1.53	3.0
4.00	55.55	0.0096	0.2075	21.18	80.27	1.58	1.8
8.00	111.11	0.0111	0.1638	21.18	93.39	1.68	1.5
16.00	222.22	0.0156	0.1347	20.52	100.00	1.75	1.2
32.00	444.45	0.0209	0.0999	17.93	100.00	1.83	0.0
8.00	111.11	0.0116	0.1122	18.19	100.00	1.82	0.0
2.00	27.78	0.0070	0.1186	18.35	100.00	1.81	0.0
0.50	6.95	0.0055	0.1230	18.60	100.00	1.81	0.0
0.03	0.44	0.0040	0.1295	19.04	100.00	1.79	0.0

CHECK ON FINAL W/C MEASURED=21.114
CALCULATED FROM D/R=19.043

LOAD TSF	LOAD KG./ SQCM	VOID RATIO	STRAIN PERCENT	COEFF. COMPR. CM2/KG	CONSTR MODULUS KG/CM2	COMPR INDEX
0.03	0.03	0.796	0.000	0.00000	0.000	0.000
0.50	0.49	0.795	0.080	0.00313	573.520	0.001
1.00	0.98	0.796	0.027	*****	-918.198	-0.003
2.00	1.95	0.784	0.705	0.01248	143.933	0.040
4.00	3.91	0.718	4.375	0.03376	53.210	0.219
8.00	7.81	0.617	9.987	0.02581	69.601	0.335
16.00	15.62	0.558	13.258	0.00752	238.813	0.195
32.00	31.25	0.488	17.181	0.00451	398.277	0.234
8.00	7.81	0.495	16.782	0.00031	5874.578	0.012
2.00	1.95	0.499	16.543	0.00073	2447.661	0.007
0.50	0.49	0.506	16.157	0.00473	379.766	0.012
0.03	0.03	0.518	15.492	0.02610	68.828	0.010

THE UNIVERSITY OF IOWA
SOIL MECHANICS LABORATORY
ONE-DIMENSIONAL CONSOLIDATION TEST
WITH NEGATIVE PORE PRESSURE MEASUREMENTS

SAMPLE NO A6-2 SPECIMEN NO 24 TYPE NATURAL
DATE PLACED 7-29-70 DATE REMOVED 7-30-70 SP.GR. 2.72
SPECIMEN DIAMETER= 2.50IN SPECIMEN HEIGHT=0.752IN

WT. OF RING + COVER PLATES + WET SOIL 180.2000GM.
WT. OF RING + COVER PLATES 83.1000 GM.
D/R WITH SEATING LOAD ON SPECIMEN 0.2500
WET WT. OF SPECIMEN + CONTAINER (FINAL) 245.32 GM.
DRY WT. OF SPECIMEN + CONTAINER (FINAL) 239.83 GM.
WT. OF CONTAINER FOR W/C TEST 148.30 GM.
TEST PERFORMED ON CONSOLIDOMETER NO. 101

LOAD TSF	LOAD PSI	MACH CORR	DIAL READ	WATER CONTENT	DEG. SAT.	DRY DEN. GMCC	NEG. P-PR PSI.
0.03	0.44	0.0000	0.2500	6.09	20.75	1.51	175.0
1.00	13.89	0.0057	0.2440	6.09	20.77	1.51	174.0
2.00	27.78	0.0073	0.2417	6.09	20.81	1.52	173.5
4.00	55.55	0.0096	0.2319	6.09	21.29	1.53	172.7
8.00	111.11	0.0111	0.2112	6.09	22.63	1.57	172.0
16.00	222.22	0.0156	0.1808	6.09	24.72	1.63	161.5
32.00	444.45	0.0209	0.1355	6.09	28.84	1.73	160.0
8.00	111.11	0.0116	0.1488	6.09	28.37	1.72	160.0
2.00	27.78	0.0070	0.1525	6.09	28.48	1.72	160.0
0.03	0.44	0.0040	0.1598	6.09	27.98	1.71	160.0

CHECK ON FINAL W/C MEASURED= 5.998
CALCULATED FROM D/R= 6.085

LOAD TSF	LOAD KG./ SQCM	VOID RATIO	STRAIN PERCENT	COEFF. COMPR. CM2/KG	CONSTR MODULUS KG/CM2	COMPR INDEX
0.03	0.03	0.798	0.000	0.00000	0.000	0.000
1.00	0.98	0.797	0.040	0.00076	2371.216	0.000
2.00	1.95	0.795	0.133	0.00171	1048.592	0.006
4.00	3.91	0.777	1.130	0.00918	195.812	0.060
8.00	7.81	0.731	3.684	0.01175	152.978	0.152
16.00	15.62	0.669	7.128	0.00793	226.827	0.206
32.00	31.25	0.574	12.447	0.00612	293.729	0.318
8.00	7.81	0.583	11.915	0.00041	4405.996	0.016
2.00	1.95	0.581	12.035	*****	*****	-0.004
0.03	0.03	0.592	11.463	0.00535	336.151	0.006

THE UNIVERSITY OF IOWA
SOIL MECHANICS LABORATORY
ONE-DIMENSIONAL CONSOLIDATION TEST
WITH NEGATIVE PORE PRESSURE MEASUREMENTS

SAMPLE NO A2-1 SPECIMEN NO S1 TYPE NATURAL
DATE PLACED 5-27-7 DATE REMOVED 5-29-70 SP. GR. 2.72
SPECIMEN DIAMETER= 2.50 IN SPECIMEN HEIGHT=0.752 IN

WT. OF RING + COVER PLATES + WET SOIL 178.7200 GM.
WT. OF RING + COVER PLATES 83.1000 GM.
D/R WITH SEATING LOAD ON SPECIMEN 0.2500
WET WT. OF SPECIMEN + CONTAINER (FINAL) 249.36 GM.
DRY WT. OF SPECIMEN + CONTAINER (FINAL) 239.35 GM.
WT. OF CONTAINER FOR W/C TEST 148.57 GM.
TEST PERFORMED ON CONSOLIDOMETER NO. 101

LOAD TSF	LOAD PSI	MACH CORR	DIAL READ	WATER CONTENT	DEG. SAT.	DRY DEN. GMCC	NEG. P-PR PSI.
0.03	0.44	0.0000	0.2500	5.33	17.85	1.50	109.0
1.00	13.89	0.0057	0.2390	5.33	18.13	1.51	130.0
2.00	27.78	0.0057	0.2355	5.33	18.33	1.52	140.5
4.00	55.55	0.0096	0.2293	5.33	18.46	1.52	138.7
8.00	111.11	0.0111	0.2151	5.33	19.21	1.55	137.0
8.00	111.11	0.0111	0.1785	8.18	33.36	1.63	63.8
8.00	111.11	0.0111	0.1547	11.03	49.22	1.69	19.5
16.00	222.22	0.0156	0.1216	11.03	55.50	1.77	22.5
32.00	444.45	0.0209	0.0862	11.03	64.10	1.85	22.9
8.00	111.11	0.0116	0.0965	11.03	63.77	1.85	29.3
2.00	27.78	0.0070	0.1021	11.03	63.45	1.85	32.7
0.03	0.44	0.0040	0.1080	11.03	62.52	1.84	36.0

CHECK ON FINAL W/C MEASURED=11.027
CALCULATED FROM D/R=11.030

LOAD TSF	LOAD KG. / SQCM	VOID RATIO	STRAIN PERCENT	COEFF. COMPR. CM ² /KG	CONSTR MODULUS KG/CM ²	COMPR INDEX
0.03	0.03	0.812	0.000	0.00000	0.000	0.000
1.00	0.98	0.800	0.705	0.01350	134.227	0.009
2.00	1.95	0.791	1.170	0.00864	209.727	0.028
4.00	3.91	0.786	1.476	0.00284	638.531	0.018
8.00	7.81	0.755	3.165	0.00784	231.273	0.102
8.00	7.81	0.667	8.032	0.00000	0.000	0.000
8.00	7.81	0.610	11.197	0.00000	0.000	0.000
16.00	15.62	0.541	15.000	0.00882	205.413	0.229
32.00	31.25	0.468	19.003	0.00464	390.338	0.241
8.00	7.81	0.470	18.870	0.00010	*****	0.004
2.00	1.95	0.473	18.737	0.00041	4405.555	0.004
0.03	0.03	0.480	18.351	0.00364	498.440	0.004

THE UNIVERSITY OF IOWA
SOIL MECHANICS LABORATORY
ONE-DIMENSIONAL CONSOLIDATION TEST
WITH NEGATIVE PORE PRESSURE MEASUREMENTS

SAMPLE NO A6-3 SPECIMEN NO S2 TYPE NATURAL
DATE PLACED 7-13-7 DATE REMOVED 7-15-70 SP.GR. 2.72
SPECIMEN DIAMETER= 2.50IN SPECIMEN HEIGHT=0.752IN

WT. OF RING + COVER PLATES + WET SOIL 183.2200GM.
WT. OF RING + COVER PLATES 83.1000 GM.
D/R WITH SEATING LOAD ON SPECIMEN 0.2500
WET WT. OF SPECIMEN + CONTAINER (FINAL) 292.27 GM.
DRY WT. OF SPECIMEN + CONTAINER (FINAL) 272.51 GM.
WT. OF CONTAINER FOR W/C TEST 180.67 GM.
TEST PERFORMED ON CONSOLIDOMETER NO. 101

LOAD TSF	LOAD PSI	MACH CORR	DIAL READ	WATER CONTENT	DEG. SAT.	DRY DEN. GMCC	NEG. P-PR PSI
0.03	0.44	0.0000	0.2500	9.02	30.98	1.52	38.0
1.00	13.89	0.0057	0.2402	9.02	31.37	1.53	45.0
2.00	27.78	0.0073	0.2363	9.02	31.59	1.53	52.0
2.00	27.78	0.0073	0.2201	13.00	47.93	1.57	17.1
4.00	55.55	0.0096	0.2141	13.00	48.51	1.57	16.3
8.00	111.11	0.0111	0.1882	13.00	52.72	1.63	16.2
8.00	111.11	0.0111	0.1745	17.00	72.46	1.66	12.4
8.00	111.11	0.0111	0.1666	21.00	92.23	1.68	4.5
8.00	111.11	0.0111	0.1604	24.66	100.00	1.70	1.1
8.00	111.11	0.0111	0.1571	24.66	100.00	1.70	0.8
16.00	222.22	0.0156	0.1393	20.77	100.00	1.74	0.2
32.00	444.45	0.0209	0.1109	18.75	100.00	1.80	0.0
8.00	111.11	0.0116	0.1260	19.26	100.00	1.79	0.0
2.00	27.78	0.0070	0.1414	20.20	100.00	1.76	0.0
0.03	0.44	0.0040	0.1575	21.35	100.00	1.72	0.0

CHECK ON FINAL W/C MEASURED=21.516
CALCULATED FROM D/R=21.349

LOAD TSF	LOAD KG./ SQCM	VOID RATIO	STRAIN PERCENT	COEFF. COMPR. CM ² /KG	CONSTR MODULUS KG/CM ²	COMPR INDEX
0.03	0.03	0.792	0.000	0.00000	0.000	0.000
1.00	0.98	0.782	0.545	0.01033	173.510	0.007
2.00	1.95	0.776	0.851	0.00561	319.154	0.018
2.00	1.95	0.738	3.005	0.00000	0.000	0.000
4.00	3.91	0.729	3.497	0.00451	396.921	0.029
8.00	7.81	0.671	6.742	0.01488	120.376	0.193
8.00	7.81	0.638	8.564	0.00000	0.000	0.000
8.00	7.81	0.619	9.614	0.00000	0.000	0.000
8.00	7.81	0.605	10.439	0.00000	0.000	0.000
8.00	7.81	0.597	10.878	0.00000	0.000	0.000
16.00	15.62	0.565	12.646	0.00406	441.713	0.105
32.00	31.25	0.510	15.718	0.00352	508.621	0.183
8.00	7.81	0.524	14.947	0.00059	3038.609	0.023
2.00	1.95	0.549	13.511	0.00439	407.941	0.043
0.03	0.03	0.581	11.769	0.01624	110.340	0.017

THE UNIVERSITY OF IOWA
SOIL MECHANICS LABORATORY
ONE-DIMENSIONAL CONSOLIDATION TEST
WITH NEGATIVE PORE PRESSURE MEASUREMENTS

SAMPLE NO A6-4 SPECIMEN NO S3 TYPE NATURAL
DATE PLACED 8-04-7 DATE REMOVED 8-05-70 SP.GR. 2.72
SPECIMEN DIAMETER= 2.50 IN SPECIMEN HEIGHT=0.752 IN

WT. OF RING + COVER PLATES + WET SOIL 186.7800 GM.
WT. OF RING + COVER PLATES 83.1000 GM.
D/R WITH SEATING LOAD ON SPECIMEN 0.2500
WET WT. OF SPECIMEN + CONTAINER (FINAL) 255.26 GM.
DRY WT. OF SPECIMEN + CONTAINER (FINAL) 238.35 GM.
WT. OF CONTAINER FOR W/C TEST 148.26 GM.
TEST PERFORMED ON CONSOLIDOMETER NO. 101

LOAD TSF	LOAD PSI	MACH CORR	DIAL READ	WATER CONTENT	DEG. SAT.	DRY DEN. GMCC	NEG. P-PR PSI.
0.03	0.44	0.0000	0.2500	15.08	49.65	1.49	21.0
1.00	13.89	0.0057	0.2438	15.08	49.73	1.49	20.7
1.00	13.89	0.0057	0.2419	19.00	62.99	1.49	19.8
2.00	27.78	0.0073	0.2388	19.00	63.27	1.50	19.9
4.00	55.55	0.0096	0.2336	19.00	63.82	1.50	19.8
8.00	111.11	0.0111	0.1937	19.00	72.12	1.58	19.5
16.00	222.22	0.0156	0.1631	19.00	79.12	1.65	18.8
32.00	444.45	0.0209	0.1348	19.00	86.52	1.70	14.7
8.00	111.11	0.0116	0.1446	19.00	86.34	1.70	16.6
2.00	27.78	0.0070	0.1495	19.00	86.24	1.70	18.8
0.03	0.44	0.0040	0.1570	19.00	84.70	1.69	19.0

CHECK ON FINAL W/C MEASURED=18.770
CALCULATED FROM D/R=19.000

LOAD TSF	LOAD KG./ SQCM	VOID RATIO	STRAIN PERCENT	COEFF. COMPR. CM ² /KG	CONSTR MODULUS KG/CM ²	COMPR INDEX
0.03	0.03	0.826	0.000	0.00000	0.000	0.000
1.00	0.98	0.825	0.066	0.00128	1422.719	0.001
1.00	0.98	0.821	0.319	0.00000	0.000	0.000
2.00	1.95	0.817	0.519	0.00373	489.345	0.012
4.00	3.91	0.810	0.904	0.00361	506.418	0.023
8.00	7.81	0.717	6.011	0.02388	76.489	0.310
16.00	15.62	0.653	9.481	0.00811	225.088	0.211
32.00	31.25	0.597	12.540	0.00358	510.833	0.186
8.00	7.81	0.599	12.473	0.00005	*****	0.002
2.00	1.95	0.599	12.434	0.00012	*****	0.001
0.03	0.03	0.610	11.835	0.00569	321.216	0.006

THE UNIVERSITY OF IOWA
SOIL MECHANICS LABORATORY
ONE-DIMENSIONAL CONSOLIDATION TEST
WITH NEGATIVE PORE PRESSURE MEASUREMENTS

SAMPLE NO A5-2 SPECIMEN NO S4 TYPE NATURAL
DATE PLACED 8-06-7 DATE REMOVED 8-07-70 SP.GR. 2.72
SPECIMEN DIAMETER= 2.50IN SPECIMEN HEIGHT=0.752IN

WT. OF RING + COVER PLATES + WET SOIL 194.3200GM.
WT. OF RING + COVER PLATES 83.1000 GM.
D/R WITH SEATING LOAD ON SPECIMEN 0.2500
WET WT. OF SPECIMEN + CONTAINER (FINAL) 266.62 GM.
DRY WT. OF SPECIMEN + CONTAINER (FINAL) 247.44 GM.
WT. OF CONTAINER FOR W/C TEST 156.57 GM.
TEST PERFORMED ON CONSOLIDOMETER NO. 101

LOAD TSF	LOAD PSI	MACH CORR	DIAL READ	WATER CONTENT	DEG. SAT.	DRY DEN. GMCC	NEG. P-PR PSI.
0.03	0.44	0.0000	0.2500	22.39	75.14	1.50	4.6
0.50	6.95	0.0041	0.2450	22.39	75.34	1.50	4.6
1.00	13.89	0.0057	0.2411	22.39	75.86	1.51	4.6
2.00	27.78	0.0073	0.2373	22.39	76.37	1.51	4.5
4.00	55.55	0.0096	0.2078	22.39	83.20	1.57	3.4
4.00	55.55	0.0096	0.1988	25.40	97.24	1.59	0.9
8.00	111.11	0.0111	0.1588	22.71	100.00	1.68	0.7
16.00	222.22	0.0156	0.1286	20.44	100.00	1.75	0.0
32.00	444.45	0.0209	0.0984	18.23	100.00	1.82	0.0
8.00	111.11	0.0116	0.1081	18.27	100.00	1.82	0.0
2.00	27.78	0.0070	0.1144	18.42	100.00	1.81	0.0
0.50	6.95	0.0055	0.1205	18.83	100.00	1.80	0.0
0.03	0.44	0.0040	0.1264	19.22	100.00	1.79	0.0

CHECK ON FINAL W/C MEASURED=21.107
CALCULATED FROM D/R=19.216

LOAD TSF	LOAD KG./ SQCM	VOID RATIO	STRAIN PERCENT	COEFF. COMPR. CM2/KG	CONSTR MODULUS KG/CM2	COMPR INDEX
0.03	0.03	0.811	0.000	0.00000	0.000	0.000
0.50	0.49	0.808	0.120	0.00474	382.365	0.002
1.00	0.98	0.803	0.426	0.01134	159.682	0.018
2.00	1.95	0.798	0.718	0.00543	333.653	0.018
4.00	3.91	0.732	4.335	0.03354	53.992	0.218
4.00	3.91	0.710	5.532	0.00000	0.000	0.000
8.00	7.81	0.618	10.652	0.02373	76.290	0.308
16.00	15.62	0.556	14.069	0.00792	228.591	0.206
32.00	31.25	0.496	17.380	0.00384	471.854	0.199
8.00	7.81	0.497	17.327	0.00004	*****	0.002
2.00	1.95	0.501	17.101	0.00070	2591.562	0.007
0.50	0.49	0.512	16.489	0.00756	239.419	0.018
0.03	0.03	0.523	15.904	0.02315	78.213	0.009

THE UNIVERSITY OF IOWA
SOIL MECHANICS LABORATORY
ONE-DIMENSIONAL CONSOLIDATION TEST
WITH NEGATIVE PORE PRESSURE MEASUREMENTS

SAMPLE NO: A5-3 SPECIMEN NO S5 TYPE NATURAL
DATE PLACED 8-10-7 DATE REMOVED 8-11-70 SP. GR. 2.72
SPECIMEN DIAMETER= 2.50IN SPECIMEN HEIGHT=0.752IN

WT. OF RING + COVER PLATES + WET SOIL 174.2200GM.
WT. OF RING + COVER PLATES 83.1000 GM.
D/R WITH SEATING LOAD ON SPECIMEN 0.2500
WET WT. OF SPECIMEN + CONTAINER (FINAL) 242.43 GM.
DRY WT. OF SPECIMEN + CONTAINER (FINAL) 229.76 GM.
WT. OF CONTAINER FOR W/C TEST 148.26 GM.
TEST PERFORMED ON CONSOLIDOMETER NO. 101

LOAD TSF	LOAD PSI	MACH CORR	DIAL READ	WATER CONTENT	DEG. SAT.	DRY DEN. GMCC	NEG. P-PR PSI.
0.03	0.44	0.0000	0.2500	11.80	31.51	1.35	30.0
1.00	13.89	0.0057	0.2440	11.80	31.54	1.35	30.0
2.00	27.78	0.0073	0.2395	11.80	31.78	1.35	29.7
4.00	55.55	0.0096	0.2252	11.80	32.83	1.38	30.0
4.00	55.55	0.0096	0.1761	15.50	49.82	1.47	13.6
8.00	111.11	0.0111	0.1320	15.50	57.61	1.57	12.2
16.00	222.22	0.0156	0.1010	15.50	63.81	1.64	10.4
32.00	444.45	0.0209	0.0557	15.50	76.19	1.75	8.0
8.00	111.11	0.0116	0.0658	15.50	75.90	1.75	12.5
2.00	27.78	0.0070	0.0708	15.50	75.75	1.75	14.3
0.03	0.44	0.0040	0.0782	15.50	74.18	1.73	16.8

CHECK ON FINAL W/C MEASURED=15.546
CALCULATED FROM D/R=15.500

LOAD TSF	LOAD KG. / SQCM	VOID RATIO	STRAIN PERCENT	COEFF. COMPR. CM2/KG	CONSTR MODULUS KG/CM2	COMPR INDEX
0.03	0.03	1.019	0.000	0.00000	0.000	0.000
1.00	0.98	1.018	0.040	0.00085	2369.944	0.001
2.00	1.95	1.010	0.426	0.00798	253.110	0.026
4.00	3.91	0.978	2.021	0.01650	122.385	0.107
4.00	3.91	0.846	8.551	0.00000	0.000	0.000
8.00	7.81	0.732	14.215	0.02928	68.948	0.380
16.00	15.62	0.661	17.739	0.00911	221.691	0.236
32.00	31.25	0.553	23.059	0.00687	293.729	0.357
8.00	7.81	0.555	22.952	0.00009	*****	0.004
2.00	1.95	0.557	22.899	0.00018	*****	0.002
0.03	0.03	0.568	22.314	0.00615	328.515	0.007

THE UNIVERSITY OF IOWA
SOIL MECHANICS LABORATORY
ONE-DIMENSIONAL CONSOLIDATION TEST
WITH NEGATIVE PORE PRESSURE MEASUREMENTS

SAMPLE NO A4-9 SPECIMEN NO S6 TYPE NATURAL
DATE PLACED 8-12-7 DATE REMOVED 8-13-70 SP.GR. 2.72
SPECIMEN DIAMETER= 2.50IN SPECIMEN HEIGHT=0.752IN

WT. OF RING + COVER PLATES + WET SOIL 183.7000GM.
WT. OF RING + COVER PLATES 83.1000 GM.
D/R WITH SEATING LOAD ON SPECIMEN 0.2500
WET WT. OF SPECIMEN + CONTAINER (FINAL) 244.05 GM.
DRY WT. OF SPECIMEN + CONTAINER (FINAL) 231.21 GM.
WT. OF CONTAINER FOR W/C TEST 140.35 GM.
TEST PERFORMED ON CONSOLIDOMETER NO. 101

LOAD TSF	LOAD PSI	MACH CORR	DIAL READ	WATER CONTENT	DEG. SAT.	DRY DEN. GMCC	NEG. P-PR PSI.
0.03	0.44	0.0000	0.2500	10.72	35.96	1.50	31.0
1.00	13.89	0.0057	0.2429	10.72	36.11	1.50	34.0
2.00	27.78	0.0073	0.2389	10.72	36.37	1.51	34.0
2.00	27.78	0.0073	0.2329	14.50	50.10	1.52	13.6
4.00	55.55	0.0096	0.2224	14.50	51.39	1.54	13.4
8.00	111.11	0.0111	0.1890	14.50	57.10	1.61	13.3
16.00	222.22	0.0156	0.1514	14.50	64.55	1.69	12.1
32.00	444.45	0.0209	0.1165	14.50	73.08	1.77	9.6
8.00	111.11	0.0116	0.1280	14.50	72.37	1.76	10.2
2.00	27.78	0.0070	0.1345	14.50	71.76	1.76	12.4
0.03	0.44	0.0040	0.1425	14.50	70.22	1.74	13.6

CHECK ON FINAL W/C MEASURED=14.132
CALCULATED FROM D/R=14.500

LOAD TSF	LOAD KG./ SQCM	VOID RATIO	STRAIN PERCENT	COEFF. COMPR. CM ² /KG	CONSTR MODULUS KG/CM ²	COMPR INDEX
0.03	0.03	0.811	0.000	0.00000	0.000	0.000
1.00	0.98	0.807	0.186	0.00356	508.148	0.002
2.00	1.95	0.802	0.505	0.00592	305.852	0.019
2.00	1.95	0.787	1.303	0.00000	0.000	0.000
4.00	3.91	0.768	2.394	0.01011	179.096	0.066
8.00	7.81	0.691	6.636	0.01967	92.074	0.255
16.00	15.62	0.611	11.037	0.01020	177.487	0.265
32.00	31.25	0.540	14.973	0.00456	396.931	0.237
8.00	7.81	0.545	14.681	0.00023	8010.906	0.009
2.00	1.95	0.550	14.428	0.00078	2318.792	0.008
0.03	0.03	0.562	13.763	0.00626	289.095	0.007

THE UNIVERSITY OF IOWA
SOIL MECHANICS LABORATORY
ONE-DIMENSIONAL CONSOLIDATION TEST
WITH NEGATIVE PORE PRESSURE MEASUREMENTS

SAMPLE NO A5-4 SPECIMEN NO S7 TYPE NATURAL
DATE PLACED 8-14-7 DATE REMOVED 8-17-70 SP.GR. 2.72
SPECIMEN DIAMETER= 2.50IN SPECIMEN HEIGHT=0.752IN

WT. OF RING + COVER PLATES + WET SOIL 182.5400GM.
WT. OF RING + COVER PLATES 83.1000 GM.
D/R WITH SEATING LOAD ON SPECIMEN 0.2500
WET WT. OF SPECIMEN + CONTAINER (FINAL) 299.38 GM.
DRY WT. OF SPECIMEN + CONTAINER (FINAL) 286.75 GM.
WT. OF CONTAINER FOR W/C TEST 196.99 GM.
TEST PERFORMED ON CONSOLIDOMETER NO. 101

LOAD TSF	LOAD PSI	MACH CORR	DIAL READ	WATER CONTENT	DEG. SAT.	DRY DEN. GMCC	NEG. P-PR PSI.
0.03	0.44	0.0000	0.2500	10.78	35.21	1.48	22.0
1.00	13.89	0.0057	0.2423	10.78	35.42	1.49	26.0
2.00	27.78	0.0073	0.2380	10.78	35.70	1.49	27.0
4.00	55.55	0.0096	0.2233	10.78	37.07	1.52	29.0
8.00	111.11	0.0111	0.1831	10.78	42.08	1.60	28.6
8.00	111.11	0.0111	0.1673	14.50	59.89	1.64	12.6
16.00	222.22	0.0156	0.1319	14.50	67.63	1.72	11.8
32.00	444.45	0.0209	0.0994	14.50	76.30	1.79	10.0
8.00	111.11	0.0116	0.1090	14.50	76.19	1.79	10.5
2.00	27.78	0.0070	0.1148	14.50	75.77	1.79	11.0
0.03	0.44	0.0040	0.1238	14.50	73.69	1.77	11.5

CHECK ON FINAL W/C MEASURED=14.071
CALCULATED FROM D/R=14.500

LOAD TSF	LOAD KG. / SQCM	VOID RATIO	STRAIN PERCENT	COEFF. COMPR. CM2/KG	CONSTR MODULUS KG/CM2	COMPR INDEX
0.03	0.03	0.833	0.000	0.00000	0.000	0.000
1.00	0.98	0.828	0.266	0.00515	355.691	0.003
2.00	1.95	0.822	0.625	0.00674	271.871	0.022
4.00	3.91	0.791	2.274	0.01548	118.435	0.100
8.00	7.81	0.697	7.420	0.02415	75.896	0.313
8.00	7.81	0.659	9.521	0.00000	0.000	0.000
16.00	15.62	0.583	13.630	0.00964	190.123	0.250
32.00	31.25	0.517	17.247	0.00424	431.954	0.220
8.00	7.81	0.518	17.207	0.00003	*****	0.001
2.00	1.95	0.521	17.048	0.00050	3671.601	0.005
0.03	0.03	0.535	16.250	0.00761	240.910	0.008

APPENDIX IV

K_o - TEST REPORT

The K_o -testing program was conducted as a separate study to provide special measurements for the interpretations presented in the body of this report. The pertinent results from this study have been summarized in Chapter 3.

The following report, which describes the K_o - tests in detail, was written as a thesis by Mr. Bharat Mathur in partial fulfillment of the requirements for the degree of Master of Science in Civil Engineering at the University of Iowa.

APPENDIX IV

AN EXPERIMENTAL STUDY OF STRESS-STRAIN
PARAMETERS FOR AN UNDISTURBED LOESS

by

Bharat Mathur

A thesis submitted in partial fulfillment of the
requirements for the degree of Master of Science
in the Department of Civil Engineering
in the Graduate College of
The University of Iowa

August, 1970

Thesis supervisor: Professor Harrison Kane

APPENDIX IV

ACKNOWLEDGMENTS

The work described in this thesis was supported by the Iowa State Highway Commission under research project HR-144, Consolidation of Loess.

I wish to express my sincere appreciation and gratitude to my advisor, Professor Harrison Kane, for his guidance and patience throughout the undertaking of this research.

I am also extremely grateful to Mr. Bruce Bailey and Mr. Altaf Rahman for their constant assistance, suggestions and encouragement.

Finally, I thank Mrs. Bonnie Browning for her indefatigable and meticulous typing of this thesis in a very short time.

APPENDIX IV

TABLE OF CONTENTS

Chapter		Page
	List of Tables	IV- v
	List of Figures	IV-vi
	Notation	IV-x
1.	INTRODUCTION	IV-1
1.1	Statement of Problem	IV-1
1.2	Review of Literature	IV-2
1.3	Objective and Scope	IV-5
2.	DESCRIPTION OF TEST PROCEDURE	IV-7
2.1	Field Sampling and Preparation of Triaxial Test Samples	IV-7
2.2	Types of Tests Conducted	IV-9
2.3	Test Equipment	IV-9
	2.3.1 Calibration of Strain Gages	IV-10
2.4	Test Conditions and Procedures	IV-13
	2.4.1 Confined Compression Tests - K_0 Tests	IV-13
	2.4.2 Triaxial Compression Tests	IV-16
2.5	Important Precautions During Testing	IV-17
3.	TESTS RESULTS AND INTERPRETATION	IV-19
3.1	Test Results	IV-19

APPENDIX IV

TABLE OF CONTENTS (cont'd.)

Chapter	Page
3.1.1 Confined Compression Tests - K _o Tests	IV-19
3.1.2 Triaxial Compression Tests	IV-46
3.2 Interpretation of Data	IV-72
4. SUMMARY AND CONCLUSIONS	IV-84
4.1 Summary	IV-84
4.2 Conclusions	IV-85
REFERENCES	IV-87

APPENDIX IV

LIST OF TABLES

Table		Page
1	SOIL INDEX PROPERTIES FOR OAKDALE LOESS	IV- 8
2	SUMMARY OF CONFINED COMPRESSION TESTS	IV- 20
3	SUMMARY OF TRIAXIAL TESTS	IV- 47
4	STRESS-STRAIN PARAMETERS FROM TRIAxIAL COMPRESSION TESTS	IV- 73
5	STRESS-STRAIN PARAMETERS FROM TRIAxIAL COMPRESSION TESTS	IV- 74
6	CALCULATED VALUES OF K_o FROM TRIAxIAL TESTS	IV- 79
7	VALUES OF CONSTRAINED MODULII (D) FROM K_o TESTS	IV- 82
8	CONSTRAINED MODULUS CALCULATED FROM TRIAXIAL TESTS	IV- 82

APPENDIX IV

LIST OF FIGURES

Figure		Page
2.1	Lateral Strain Indicator - Assembly	IV-11
2.2	Lateral Strain Indicator - Parts	IV-12
2.3	Calibration Curve for Lateral Strain Indicator	IV-14
2.4	Explanation of Sample Orientation	IV-15
3.1	Definitions of Parameters K_{oi} and K_{of}	IV-21
3.2	Lateral Stress versus Axial Stress, K_o -Test No. 1	IV-22
3.3	Lateral Stress versus Axial Stress, K_o -Test No. 2	IV-23
3.4	Lateral Stress versus Axial Stress, K_o -Test No. 3	IV-24
3.5	Lateral Stress versus Axial Stress, K_o -Test No. H-1	IV-25
3.6	Lateral Stress versus Axial Stress, K_o -Test No. H-2	IV-26
3.7	Lateral Stress versus Axial Stress, K_o -Test No. H-3	IV-27
3.8	Lateral Stress versus Axial Stress, up to 2% Strain, K_o -Test No. 1	IV-28
3.9	Lateral Stress versus Axial Stress, up to 2% Strain, K_o -Test No. 2	IV-29

APPENDIX IV

LIST OF FIGURES (cont'd.)

Figure		Page
3.10	Lateral Stress versus Axial Stress, up to 2% Strain, K_0 -Test No. 3	IV-30
3.11	Lateral Stress versus Axial Stress, up to 2% Strain, K_0 -Test No. H-1	IV-31
3.12	Lateral Stress versus Axial Stress, up to 2% Strain, K_0 -Test No. H-2	IV-32
3.13	Lateral Stress versus Axial Stress, up to 2% Strain, K_0 -Test No. H-3	IV-33
3.14	Stress-Strain Relations, K_0 -Test No. 1	IV-34
3.15	Stress-Strain Relations, K_0 -Test No. 2	IV-35
3.16	Stress-Strain Relations, K_0 -Test No. 3	IV-36
3.17	Stress-Strain Relations, K_0 -Test No. H-1	IV-37
3.18	Stress-Strain Relations, K_0 -Test No. H-2	IV-38
3.19	Stress-Strain Relations, K_0 -Test No. H-3	IV-39
3.20	Stress-Strain Relations up to 2% Strain, K_0 -Test No. 2	IV-40
3.21	Stress-Strain Relations up to 2% Strain, K_0 -Test No. 3	IV-41
3.22	Stress-Strain Relations up to 2% Strain, K_0 -Test No. H-1	IV-42
3.23	Stress-Strain Relations up to 2% Strain, K_0 -Test No. H-2	IV-43
3.24	Stress-Strain Relations up to 2% Strain, K_0 -Test No. H-3	IV-44
3.25	Stress-Strain Relations, Test Nos. 1 to 5	IV-50

APPENDIX IV

LIST OF FIGURES (cont'd.)

Figure		Page
3.26	Stress-Strain Relations, Test Nos. 6 to 8	IV-51
3.27	Stress-Strain Relations, Test Nos. 9 and 10	IV-52
3.28	Stress-Strain Relations, Test Nos. 12 to 17	IV-53
3.29	Axial Strain versus Lateral Strain, Test No. 1	IV-54
3.30	Axial Strain versus Lateral Strain, Test No. 2	IV-55
3.31	Axial Strain versus Lateral Strain, Test No. 3	IV-56
3.32	Axial Strain versus Lateral Strain, Test No. 4	IV-57
3.33	Axial Strain versus Lateral Strain, Test No. 5	IV-58
3.34	Axial Strain versus Lateral Strain, Test No. 6	IV-59
3.35	Axial Strain versus Lateral Strain, Test No. 7	IV-60
3.36	Axial Strain versus Lateral Strain, Test No. 8	IV-61
3.37	Axial Strain versus Lateral Strain, Test No. 9	IV-62
3.38	Axial Strain versus Lateral Strain, Test No. 10	IV-63
3.39	Axial Strain versus Lateral Strain, Test No. 12	IV-64
3.40	Axial Strain versus Lateral Strain, Test No. 13	IV-65
3.41	Axial Strain versus Lateral Strain, Test No. 14	IV-66
3.42	Axial Strain versus Lateral Strain, Test No. 15	IV-67
3.43	Axial Strain versus Lateral Strain, Test No. 16	IV-68
3.44	Axial Strain versus Lateral Strain, Test No. 17	IV-69
3.45	Definition of Parameters $(\sigma_1 - \sigma_3)_f$, $(\sigma_1 - \sigma_3)_{50}$, E_i , ϵ_o , ϵ_{50} , ϵ_f	IV-70

APPENDIX IV

LIST OF FIGURES (cont'd.)

Figures		Page
3.46	Definition of Parameters V_a , V_b , ϵ_{ab} , ϵ_{oa}	IV-71
3.47	Modified Mohr-Coulomb Diagram Triaxial Tests Nos. 1 to 10	IV-75
3.48	Stress paths for Triaxial Tests Nos. 1 to 3	IV-76
3.49	Initial Tangent Modulus versus Cell Pressure, Triaxial Tests	IV-80
3.50	Definition of Parameters D_i , D_c and D_f	IV-81

APPENDIX IV

NOTATION

\bar{a}	= intercept on y-axis of the Modified Mohr-Coulomb failure envelope
\bar{c}	= cohesion intercept of Conventional Mohr-Coulomb failure envelope
D_i	= constrained modulus before collapse or initial constrained modulus
D_c	= constrained modulus at collapse
D_f	= constrained modulus after collapse or final constrained modulus
e_o, e_i	= initial void ratio
e_c	= consolidated void ratio
E_i	= initial tangent modulus
K_o	= coefficient of earth pressure at rest
K_{oi}	= coefficient of earth pressure at rest before collapse
K_{of}	= coefficient of earth pressure at rest after collapse
S, S_{ri}	= initial degree of saturation
S_{rc}	= consolidated degree of saturation
w_i	= initial water content
w_n	= natural water content
$\bar{\alpha}$	= slope of modified Mohr-Coulomb envelope
ϵ_a	= axial strain

APPENDIX IV

ϵ_f	= strain corresponding to maximum deviator stress
ϵ_L	= lateral strain
ϵ_o	= axial strain at zero deviator stress in triaxial tests
ϵ_{50}	= strain corresponding to half the maximum deviator stress
ϵ_{oa}	= axial strain at which lateral strain begins to increase from zero, triaxial tests
ϵ_{ab}	= axial strain at which the graph of axial strain versus lateral strain changes slope
σ_1	= axial stress
σ_3	= lateral stress or cell pressure
$\sigma_1 - \sigma_3$	= deviator stress
$(\sigma_1 - \sigma_3)_f$	= maximum deviator stress
$(\sigma_1 - \sigma_3)_{50}$	= half the maximum deviator stress
γ_d	= natural dry density
$\bar{\phi}$	= angle of shearing resistance, slope of Mohr-Coulomb failure envelope
ν	= Poisson's ratio
ν_a	= initial Poisson's ratio
ν_b	= final Poisson's ratio

Chapter 1

INTRODUCTION

1.1 Statement of Problem

The Midwestern region of the United States including more than half of Iowa is abundantly covered with loess, a wind deposited, silt-sized material. The physical properties of loess in its natural undisturbed state are of immense interest to engineers who are engaged in the design and study of foundations, slopes, excavations and other engineering works with the in-situ soil. Since the properties of loess and the variations in these properties is not completely known, this soil presents innumerable problems to engineers. This uncertainty often results in uneconomical designs, failure of structures or both.

This investigation has been undertaken to determine and study some stress-strain parameters for an undisturbed loess. Two parameters of particular interest here are, (1) the coefficient of earth pressure at rest K_0 , defined as the ratio of the lateral to axial stress during one-dimensional compression (i.e., axial compression with zero lateral strain) and (2) Poisson's ratio ν , the ratio of lateral to axial strain during uni-axial compression. The importance of the coefficient of earth pressure at rest in the study of foundation

settlement, pressures against retaining walls and in the determination of Poisson's ratio which is used to determine stresses, is well known. Both parameters have been measured in this work and their relationship to other stress-strain parameters is discussed.

1.2 Review of Literature

In this section the work of earlier investigators has been listed chronologically.

The importance of K_0 , the coefficient of earth pressure at rest, has been recognized from the beginning of the science of Soil Mechanics. It is said that it was Donath who in 1891 introduced the term 'earth pressure at rest', and since then many investigators have designed various types of apparatus and conducted numerous experiments to measure and study this parameter for various types of soils.

One of the earliest experiments to measure K_0 was conducted by Terzaghi (1920) who determined K_0 to find pressures against retaining walls. In his set-up Terzaghi had thin metal strips placed horizontally and vertically in two different consolidation samples which were vertically loaded. After consolidation was completed the strips were pulled out and the forces required to do so measured. K_0 was then calculated as the ratio of the force required to pull out the strip horizontally oriented to the force required to pull out the vertically oriented strip. In further investigations Terzaghi showed

that K_0 depends on the relative density of the soil and the process by which the deposit was formed. He came up with a value of 0.42 for sands and for remoulded and reconsolidated clays his value for K_0 varied from 0.7 to 0.75.

In a series of 'one axial' compression tests with no lateral expansion, Kjellman (1936) determined K_0 for standard sand as varying from 0.5 during loading to 1.5 during unloading.

Tschebotarioff (1951), claimed by his experiments that Terzaghi's values were low for sand and high for clays. He tested samples 30 cm. in diameter and 45 cm. in height in his earth-pressure meter, by applying normal load at top and measuring corresponding lateral pressure and displacements at small increments throughout its depth. Experimenting with clay he obtained K_0 equal to 0.5. Because of the size of his sample his apparatus was not suited for undisturbed samples.

The next piece of research reported is that of Kjellman and Jakobson (1955) in Sweden. They used a big cylindrical soil sample 50 cm. in diameter and 100 cm. in height (to permit a grain size as big as 5 cm.). The specimen was applied a vertical pressure and was confined laterally by a wall which consisted of steel rings placed one above the other with gaps to allow axial strain. They conducted tests on pebbles and macadam and their determined value for K_0 was about 0.44. They showed that K_0 is constant during loading and

increasing in the unloading stage.

That K_o increases with initial porosity was exhibited by Chi-in (1957) and Bjerrum, Kringstad and Kunmenjee (1961). The latter conducted consolidation tests with zero lateral strain. K_o as determined by them varied from 0.25 for dense sand to 0.65 for sand in a loose state.

Tests using a modified consolidation cell were also done by Komornik and Zeitlin (1965). They introduced a thin wall section in the central portion of a consolidation apparatus and used electric strain wires to detect applied internal pressure.

A new type of apparatus was used by Kenney (1967) to determine the in-situ value of the coefficient of earth pressure at rest. He used a large hollow pipe fitted with earth pressure and water pressure gages. He experimented with different types of clays in different regions and concluded that: (1) K_o increases owing to the decrease in the thickness of the disturbed clay layer with depth, and (2) K_o decreases with decreasing depth.

At the same time, experimenting with swelling clays Ho (1967) found that K_o exceeds unity if swell is permitted or on rebound after compression.

A significant contribution to the study of K_o has been made by Bishop (1958). He studied this parameter at length and suggested in his work the various essential parts of an apparatus to measure K_o .

He also designed a mechanical apparatus, a lateral strain indicator using mercury, and observed changes in diameter to the order of 10^{-3} inches, (Bishop, 1957). His apparatus is, however, limited to 4 in. samples. Bishop also experimentally confirmed that K_o can be accurately predicted by the relation $K_o = 1 - \sin \bar{\phi}$ (where $\bar{\phi}$ is the angle of shearing resistance) an empirical expression proposed by Jaky. After a more recent review of measurement of K_o , Morgenstern and Eisenstein (1970) concluded that the Jaky equation "no longer appears to be a matter of contention."

1.3 Objective and Scope

The principal objective of this investigation was to determine experimentally the values of the coefficient of earth pressure at rest (K_o) and Poisson's ratio (ν). All the tests were performed on Oakdale loess at its natural water content.

Other stress-strain parameters were calculated and studied to understand the behavior of the soil more fully. Two types of tests were conducted: a) Confined or one-dimensional compression tests and, b) Triaxial compression tests with the measurement of lateral strain.

In the previous section a survey has been presented of the existing literature on the coefficient of earth pressure at rest. Chapter 2 deals with the procedures and conditions of actual experimental

Chapter 2

DESCRIPTION OF TEST PROCEDURE

2.1 Field Sampling and Preparation of Triaxial Test Samples

Undisturbed samples, 8 in. by 10 in. by 10 in. were hand-carved from a test pit in Oakdale, near Iowa City in Iowa. These were packed in boxes and at that time some loose soil was collected from each sample for moisture content determination.

In the laboratory these samples were broken down into smaller samples about 5 in. in length and 3 in. in diameter, suitable for 1-1/2 in. by 3 in. triaxial test samples. Kane (1968) has dealt with sampling procedures in detail. These small samples were wrapped in aluminum foil and sealed with wax, after some soil was taken off for moisture content determination. Each sample was weighed, appropriately labelled and stored in a humid chamber. The in-situ orientation of each sample was recorded.

The soil index properties for this Oakdale loess in the undisturbed state have been determined previously (Kane, 1969) and are listed in Table 1.

TABLE 1
SOIL INDEX PROPERTIES FOR OAKDALE LOESS

a. Whole Soil

Liquid Limit	27
Plastic Limit	23
Plasticity Index	4
Specific Gravity	2.72
Percentage Clay:	
Less than 0.005 mm	17
Less than 0.002 mm	13
Natural Dry Density, pcf	
Range	89.5 to 93.5
Average	91.5
Natural Water Content, %	
Range	21.5 to 23.5
Average	22.5

b. Clay Fraction Less than 0.002 mm

Liquid Limit	120
Plastic Limit	39
Plasticity Index	81
Percentage of Clay:	
Less than 0.002 mm	100

2.2 Types of Tests Conducted

Essentially, two series of tests were conducted on this soil. In the first series of tests the samples were subjected to vertical compression in a triaxial test machine. No lateral strain was allowed by controlling the cell pressure. These tests were drained and conducted on samples vertically and horizontally oriented in the cell. They have been called K_0 tests.

The second series consisted of consolidated-drained triaxial tests, together with the measurement of lateral strain. The pattern of sample orientation was as above.

2.3 Test Equipment

The equipment was the same for all the tests conducted. The two main items were the triaxial testing machine and the lateral strain indicator. The major elements of the former, manufactured by Wykeham Farrance Engineering Ltd., England, are:

- a. 5-ton capacity gear driven compression test machine
- b. Self-compensating constant pressure apparatus for applying cell pressures to 140 psi.
- c. Cell volume change measuring apparatus
- d. Triaxial cells for 1-1/2 in. diameter specimens with working pressure of 150 psi.

- e. Load rings for axial load measurement, of high strength steel with capacities of 500 and 1000 lbs.

The lateral strain indicator was used to detect lateral strains owing to axial compression. It was designed in the Soil Mechanics laboratory at the University of Iowa, and is shown in Figures 2.1 and 2.2. Two curved pads are pressed gently against the sample by a clock spring segment. The spring was selected to provide a pressure between the pads and the sample, of approximately 1.0 psi. On the inside and outside of the clock spring segment are glued strain gages with the following specifications:

SR-4 Strain Gages: Type FAE-25-12S6

Gage Factor (G.F.) = $2.04 \pm 1\%$

Resistance (Ohms) = 120.0 ± 0.2

Serial Number 3-A-GA, Lot Number 252

Manufactured by Baldwin-Lima-Hamilton, Massachusetts.

The wires from these strain gages (two from each) are passed through a watertight connection in the base of the triaxial cell. Strains were read on a Baldwin-Lima-Hamilton Type N strain indicator.

2.3.1 Calibration of Strain Gages

It was necessary to calibrate the strain gages so that lateral strain in per cent could be obtained from the strain reading (in micro inches per inch) on the B-L-H strain indicator. For this purpose, the

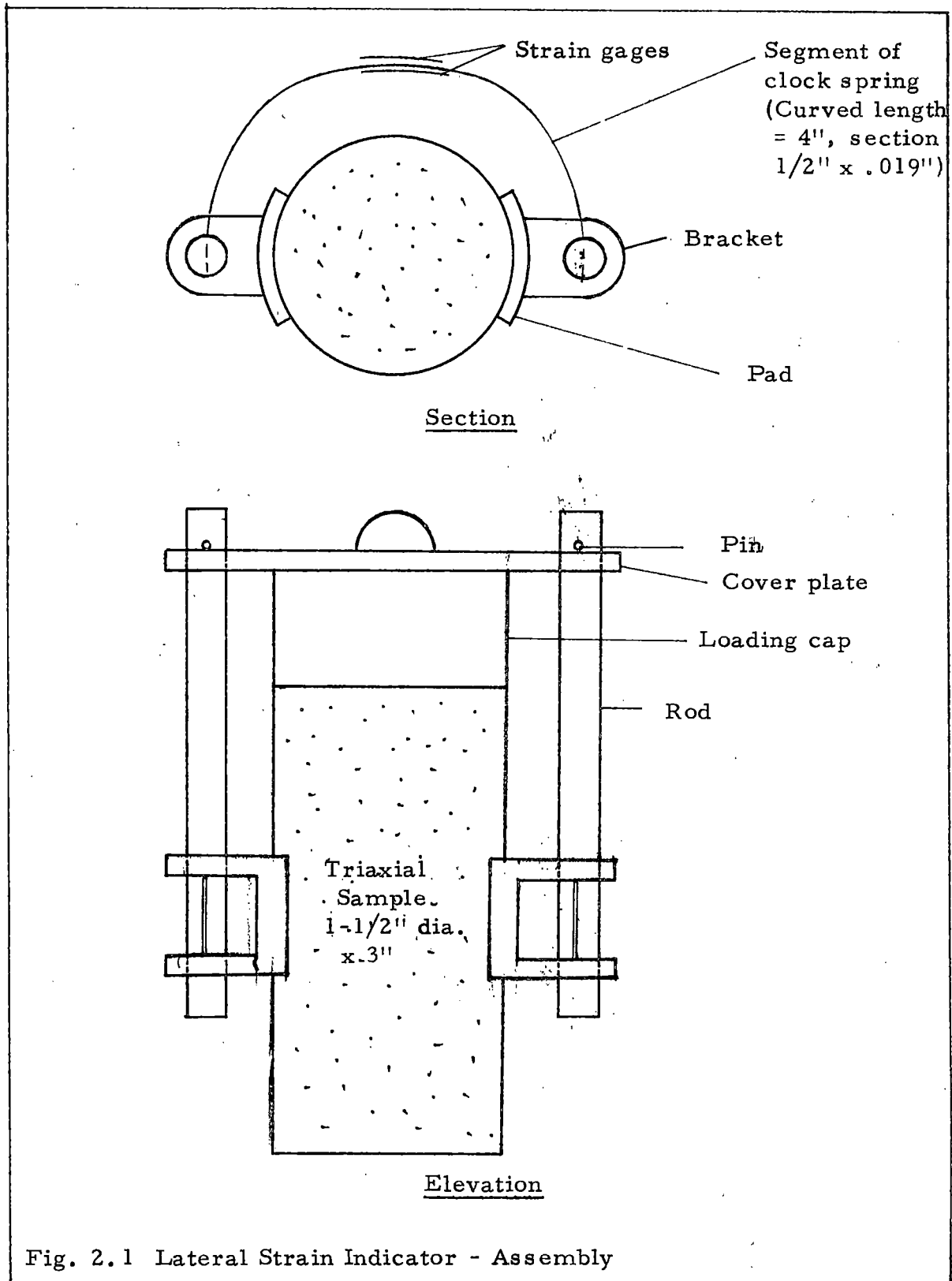
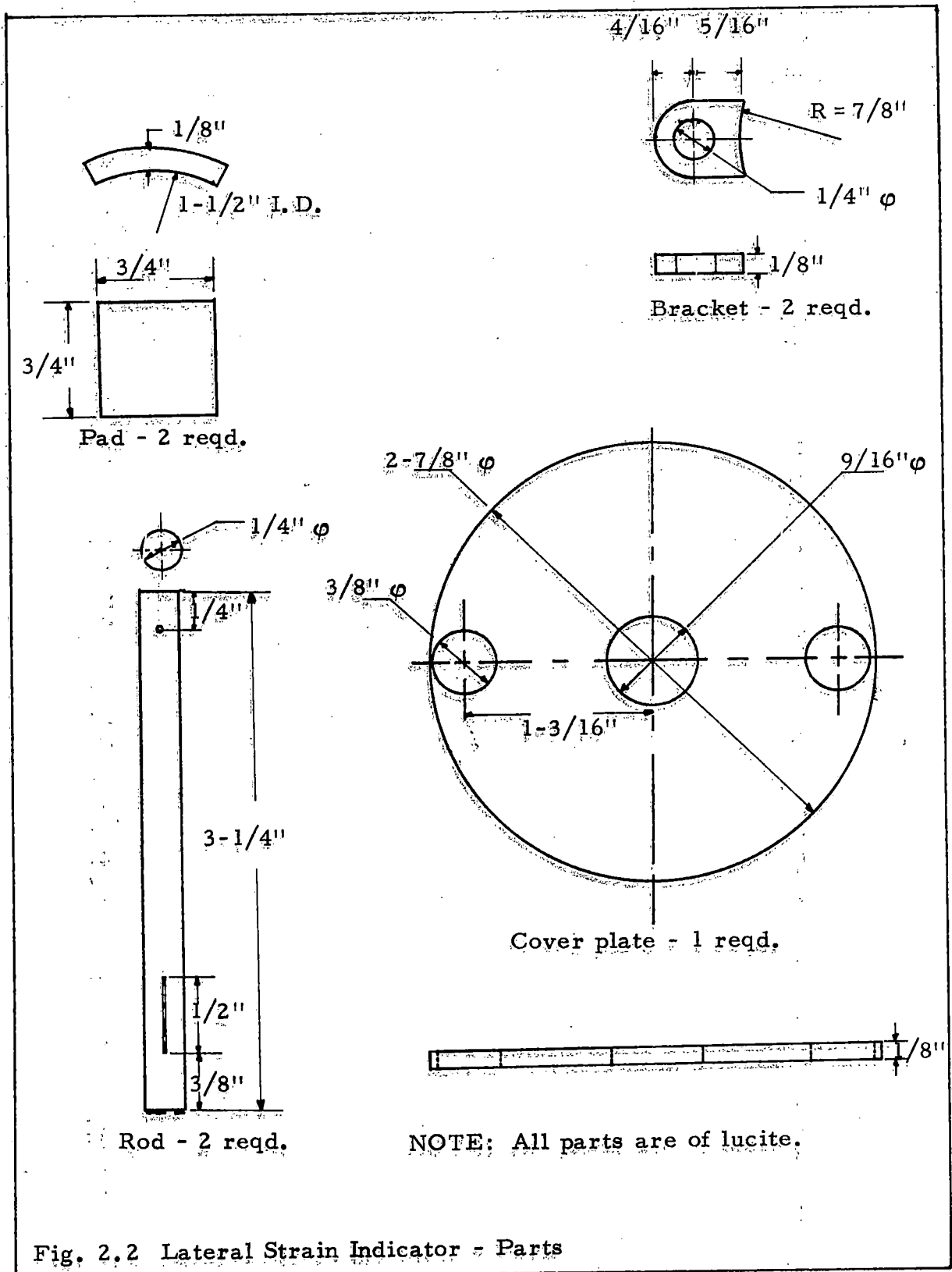


Fig. 2.1 Lateral Strain Indicator - Assembly



pads of the lateral strain indicator were initially separated by 1-1/2 in. (the diameter of a test sample). The distance between the pads was then increased by a known amount and the gage strain read off from the strain indicator. A curve was plotted between this gage strain and percentage lateral strain (obtained by dividing the change in distance between the pads by 1-1/2 in). This calibration curve is shown in Figure 2.3.

2.4 Test Conditions and Procedures

The test conditions were more or less the same for both series of tests. They have been described, along with various procedures adopted, separately for the K_0 tests and Triaxial tests. The orientation of the sample in-situ and in the cell is shown in Figure 2.4. The soil during field sampling was as in Figure 2.4 (a). Testing was done with the sample vertically and horizontally oriented as in Figure 2.4 (b). The pads were oriented along the x-axis for the vertical samples, and along the z- or y-axis for the horizontal samples. The orientations have been called P_1 , P_2 and P_3 respectively and will be referred to as such throughout this work.

2.4.1 Confined Compression Tests - K_0 Tests

The K_0 tests were conducted on the standard triaxial test machine. They were drained tests and no lateral expansion of the soil was allowed. Triaxial samples, 1-1/2 in. in diameter and

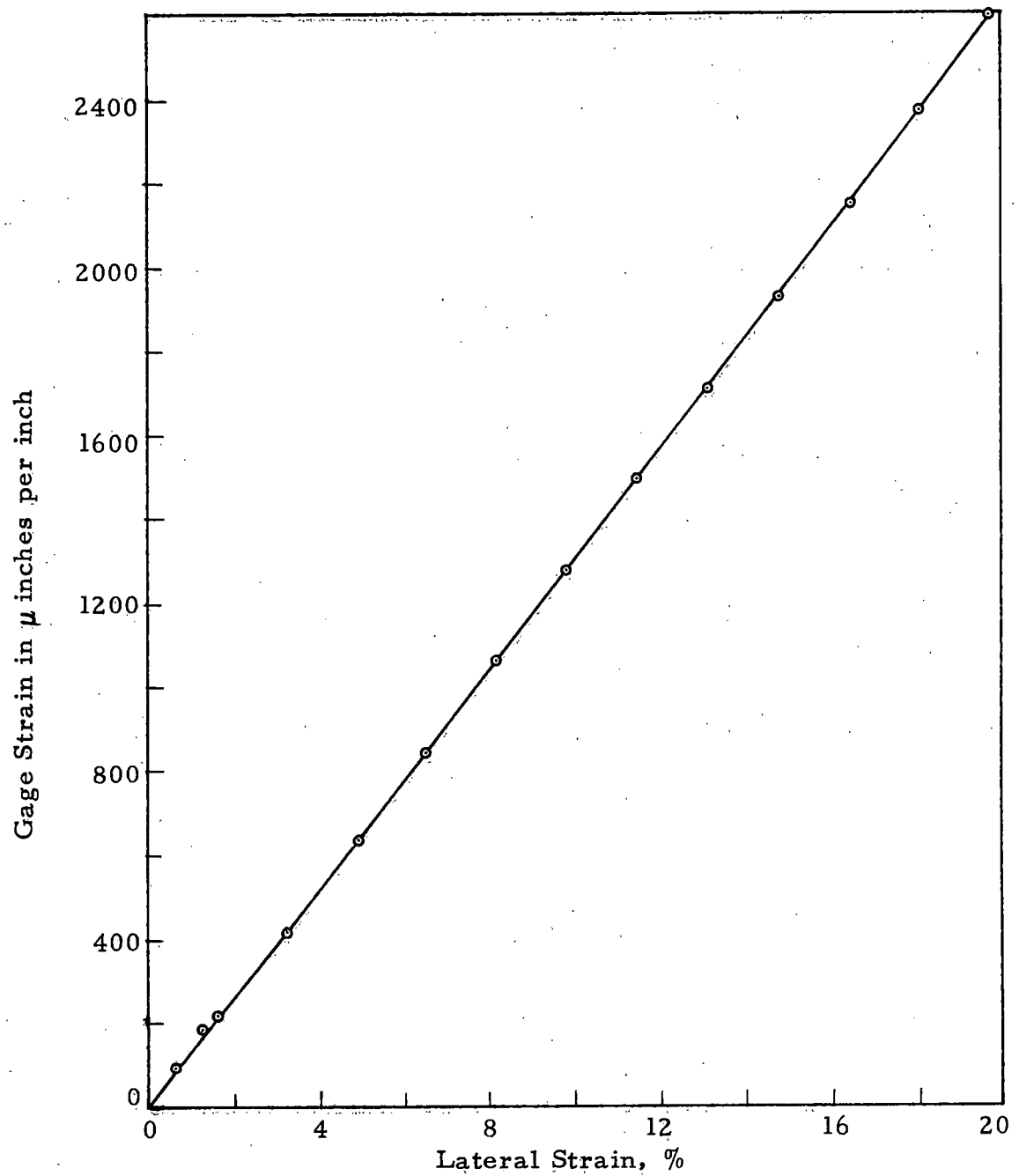


Fig. 2.3 Calibration Curve for Lateral Strain Indicator

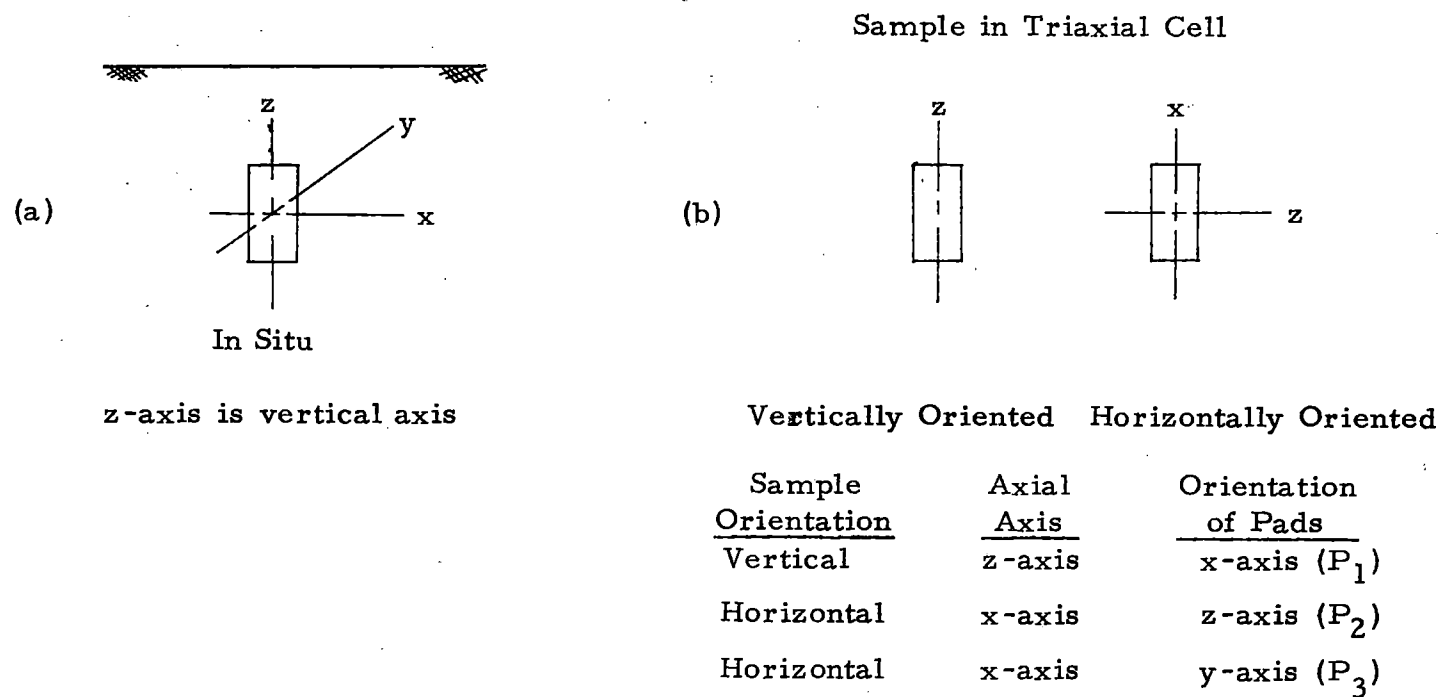


Fig. 2.4 Explanation of Sample Orientation

3 in. in height, were trimmed from samples previously carved out of field blocks. (See Section 2.1). During the trimming some soil was collected in tins for moisture content determination. Immediately after trimming the sample was weighed and placed on a **porous** stone on the pedestal of the triaxial cell. The sample was enclosed by a rubber membrane and a loading cap was placed on the top. A good seal between the membrane and the loading cap and pedestal was ensured by using 'O'-rings. The lateral strain indicator was then put around the sample with the pads oriented along the desired axis. The cell was then assembled and filled with water. The load ring (the 500 lb. ring was used here) and axial strain dial indicator were then fixed to the triaxial machine frame and a good seating accomplished between the loading ram and the top of the loading cap. With all the components adjusted the machine was started at a strain rate of 0.006 in. per minute. The cell pressure was increased constantly to maintain zero lateral strain. This was ensured by applying an increasing cell pressure when the B-L-H strain indicator needle moved from its null position. In each case the test was stopped when the cell pressure reached 150 psi. The parameters recorded were the axial strain, axial load and the cell pressure, all at one instant of time.

2.4.2 Triaxial Compression Tests

The triaxial compression tests also incorporated the measurement of lateral strain. They were consolidated-drained triaxial tests;

the samples were allowed to consolidate for a certain duration of time before application of any vertical load. The drainage was accomplished by inserting a porous stone between the pedestal and the sample. Tests were run with cell pressures varying from 0 to 140 psi for samples vertically oriented in the cell and from 0 to 20 psi for samples horizontally oriented (with pad orientation P_2 and P_3) in the cell. The trimming and setting up of the sample and the assembling of the apparatus was done in the same way as for the K_0 tests.

After the initial consolidation was completed the axial load was applied using a strain rate of 0.006 in per minute. The test was continued until the axial load dropped or, in the absence of any drop in the axial load, up to 20% axial strain. Gage strain readings on the B-L-H indicator were recorded at intervals of axial strain. Simultaneously, the axial load was also recorded. The percentage lateral strain in the sample corresponding to the gage strain readings was obtained from the calibration curve, Figure 2.3.

2.5 Important Precautions During Testing

Since the soil specimen is very sensitive certain precautions must be observed to achieve accuracy in the experimental results.

The main precautions are listed below:

- a. There should be no air in the system. This can be achieved to a certain extent by pouring water on the 'O' rings, between

the top surface of the loading cap and the bottom of the plate of the lateral strain indicator and all over the membrane. The valves of the triaxial cell must be flushed with water to expel air.

b. The pads of the lateral strain indicator must be diametrically opposite each other and the rods must be vertical.

c. Proper seating must be ensured between the loading ram and the top of the loading cap.

Chapter 3

TEST RESULTS AND INTERPRETATION

3.1 Test Results

The results of the confined compression tests and the triaxial tests are presented first.

3.1.1 Confined Compression Tests - K_o Tests

The results of the confined compression tests have been summarized in Table 2. For each test Table 2 gives the orientation of the sample and the pads, the natural water content, dry density, degree of saturation, the initial void ratio and the coefficient of earth pressure at rest in the initial and final stages. K_{oi} and K_{of} have been defined in Figure 3.1.

The data from the confined compression tests are plotted in Figures 3.2 to 3.24. In Figures 3.2 to 3.7 lateral stress has been plotted against axial stress for each test for the entire duration of the test. In Figures 3.8 to 3.13 the lateral stress is plotted against the axial stress up to 2% axial strain.

From Table 2 it is seen that all the samples are at more or less the same water content, the maximum variation being 1.5%. All the samples are nearly of the same density. The computed values

TABLE 2

SUMMARY OF CONFINED COMPRESSION TESTS

<u>Test No.</u>	<u>Orientation of Sample in Cell</u>	<u>Orientation of Pads</u>	<u>Natural Water Content w_n %</u>	<u>Dry Density γ_d pcf</u>
1	Vertical	P_1	22.6	89.86
2	Vertical	P_1	21.5	90.48
3	Vertical	P_1	22.9	91.42
H-1	Horizontal	P	22.6	90.36
H-2	Horizontal	P_2	22.7	91.69
H-3	Horizontal	P_3	23.0	92.29

<u>Test No.</u>	<u>Degree of Saturation S, %</u>	<u>Initial Void Ratio e_o</u>	<u>Coefficient of Earth Pressure at Rest</u>	
			<u>Initial K_{oi}</u>	<u>Final K_{of}</u>
1	69.3	0.883	0.25	0.52
2	67.5	0.862	0.22	0.56
3	73.1	0.851	0.15	0.54
H-1	70.2	0.871	0.23	0.54
H-2	72.6	0.848	0.33	0.56
H-3	74.8	0.833	0.17	0.50
Average			0.23	0.54

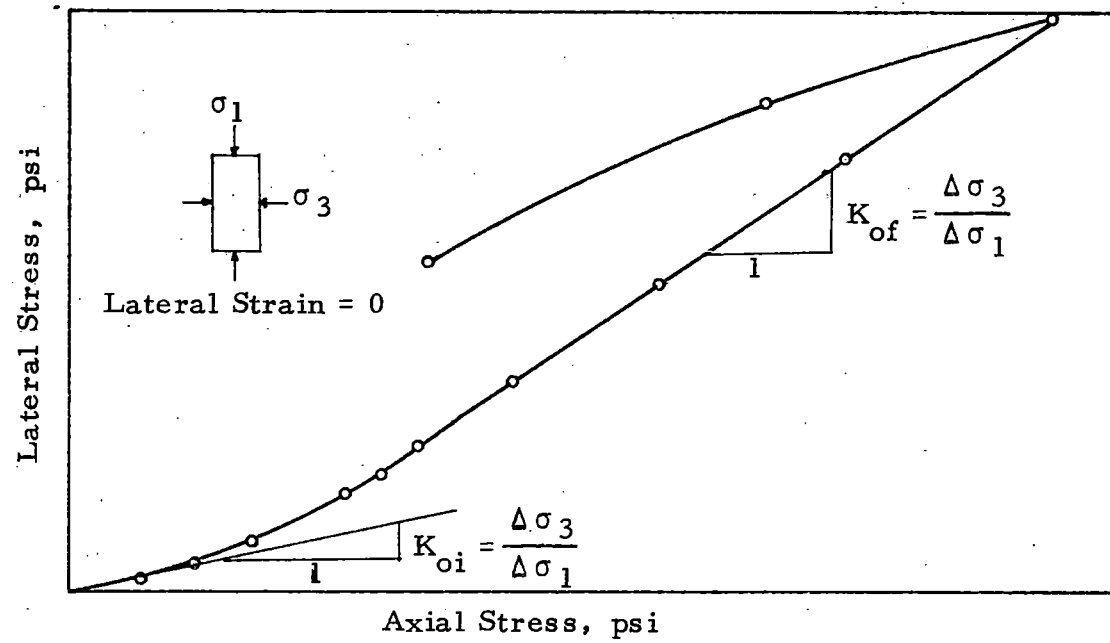


Fig. 3.1 Definition of Parameters K_{oi} and K_{of}

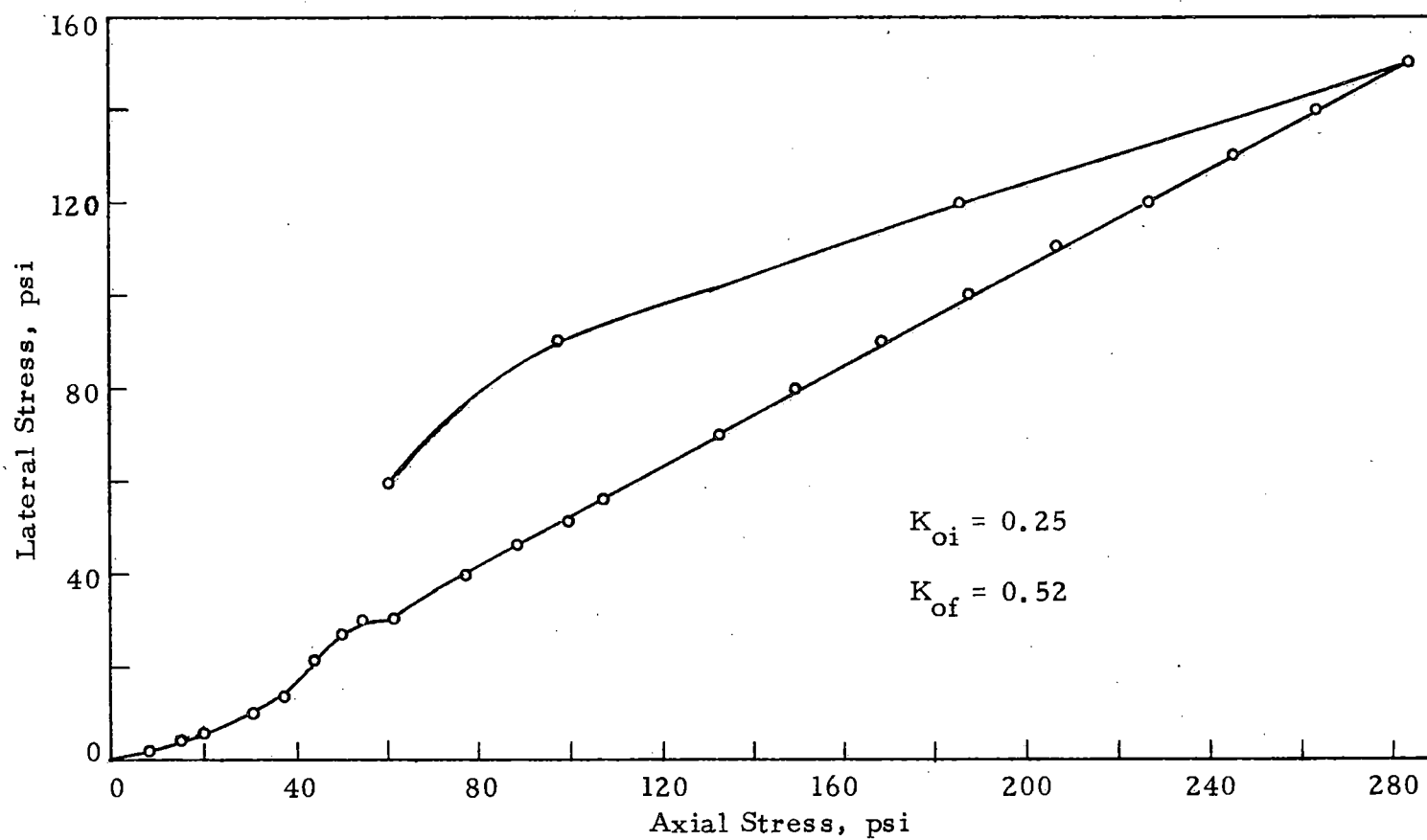


Fig. 3.2 Lateral Stress versus Axial Stress, K_O - Test No. 1

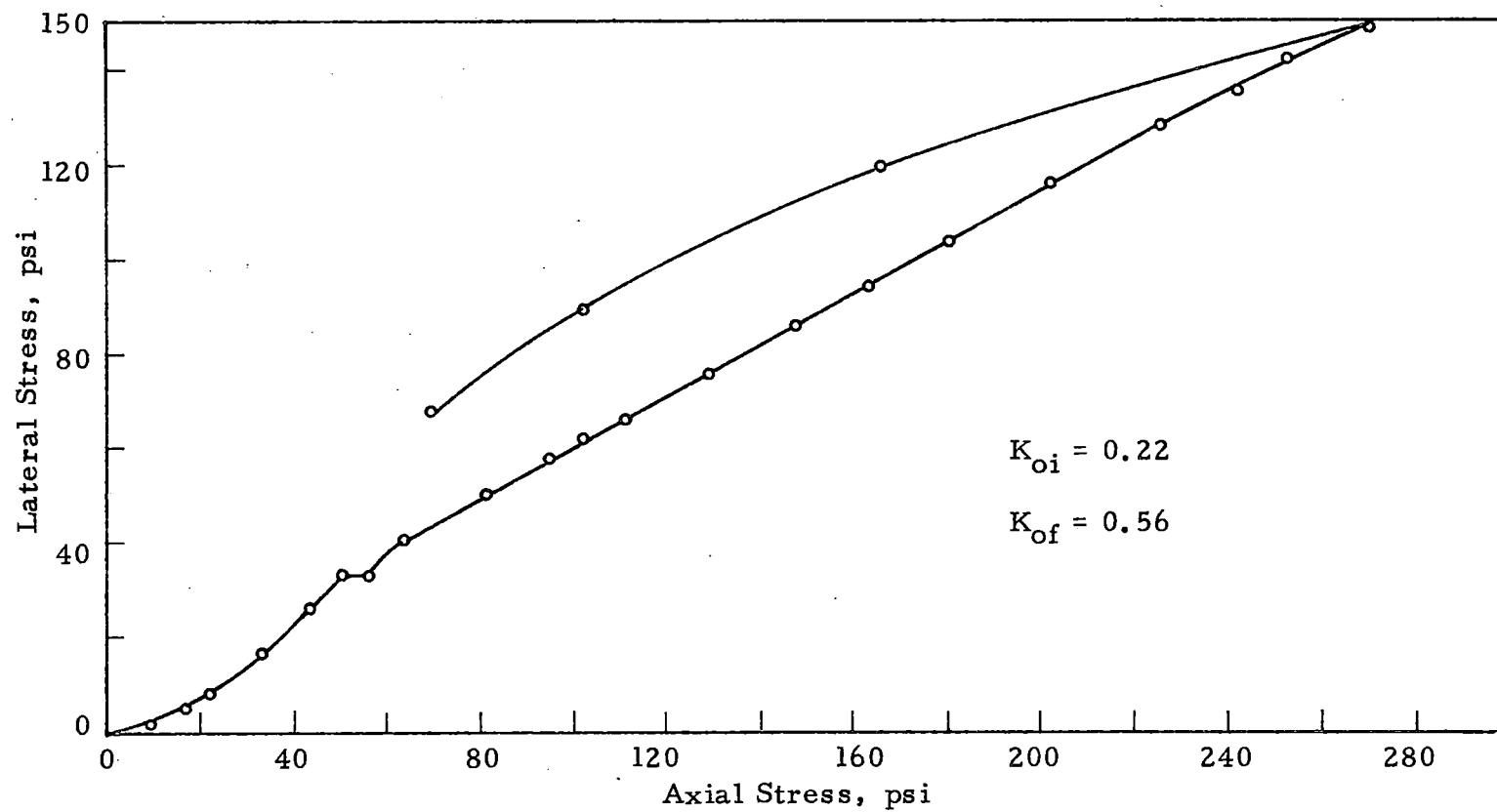


Fig. 3.3 Lateral Stress versus Axial Stress, K_O - Test No. 2

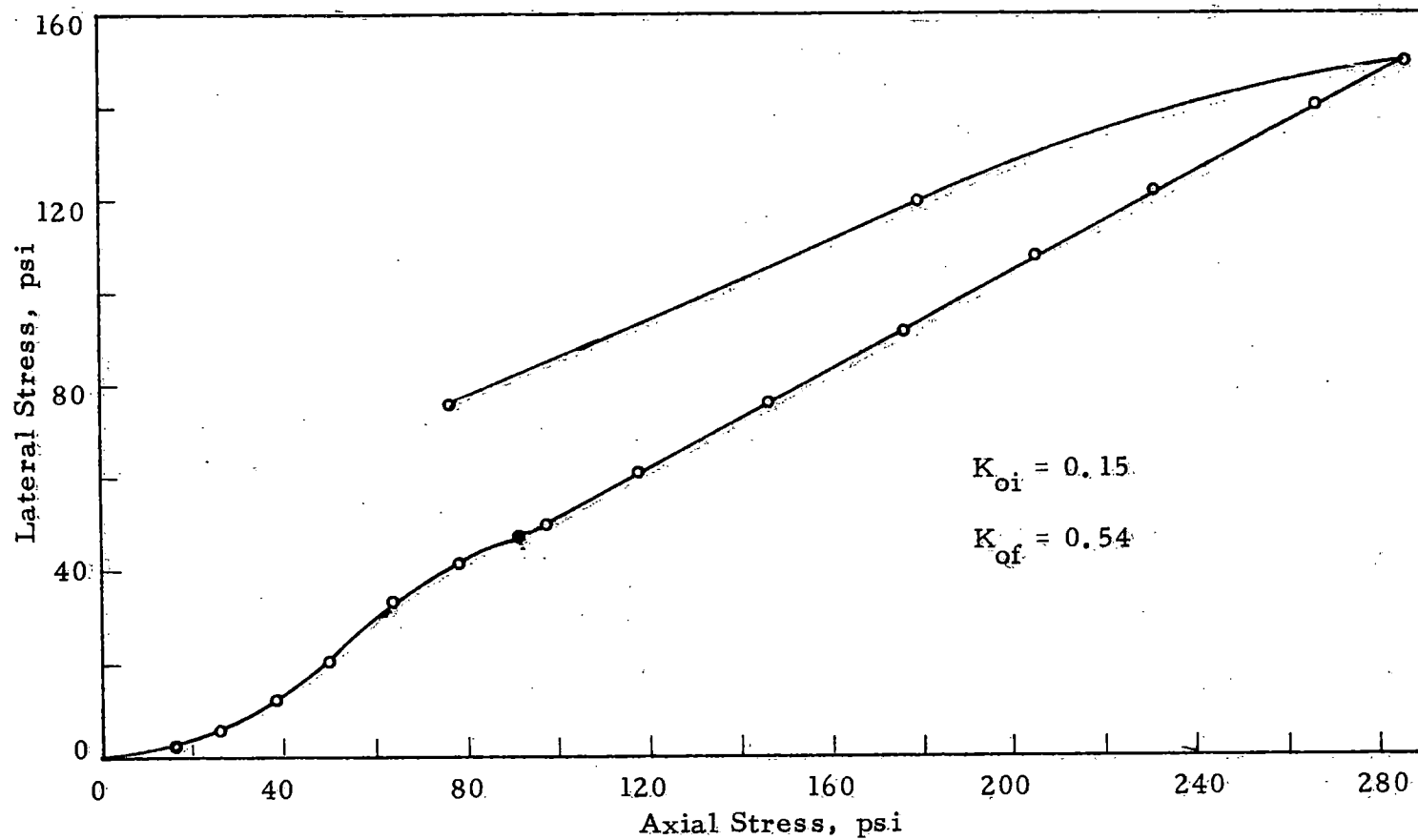


Fig. 3.4 Lateral Stress versus Axial Stress, K_o - Test No. 3

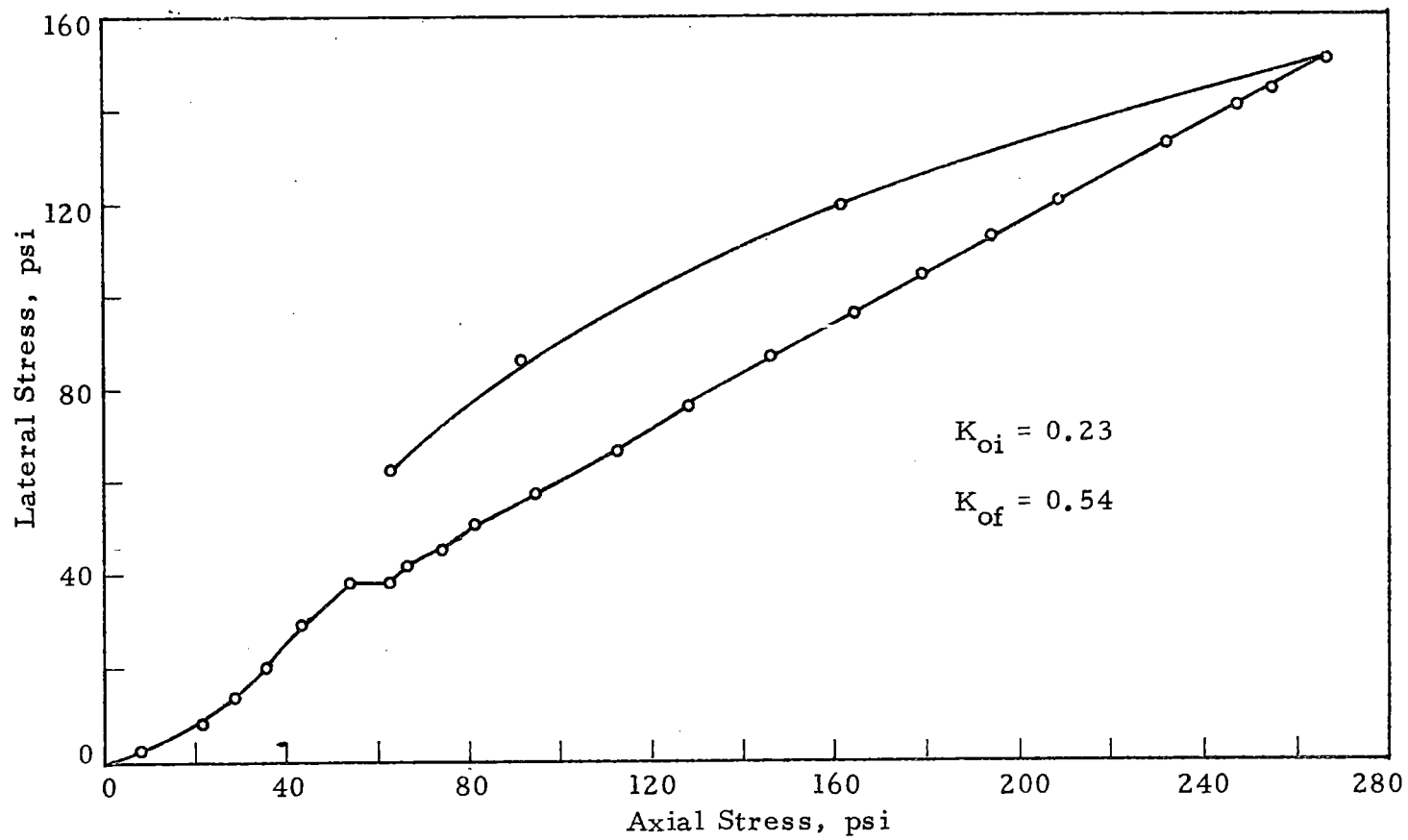


Fig. 3.5 Lateral Stress versus Axial Stress, K_o -Test No. H-1

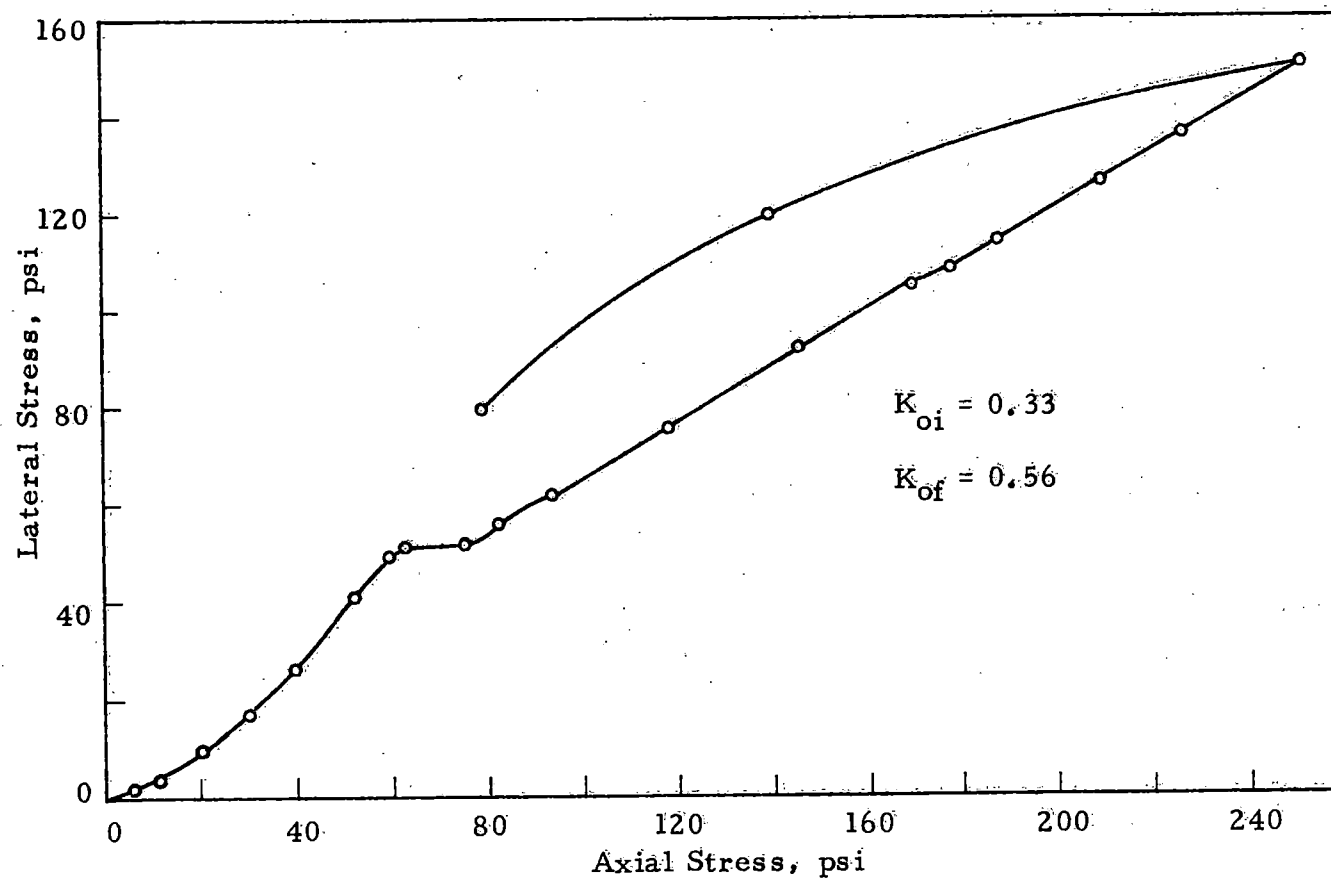


Fig. 3.6 Lateral Stress versus Axial Stress, K_o - Test No. H-2

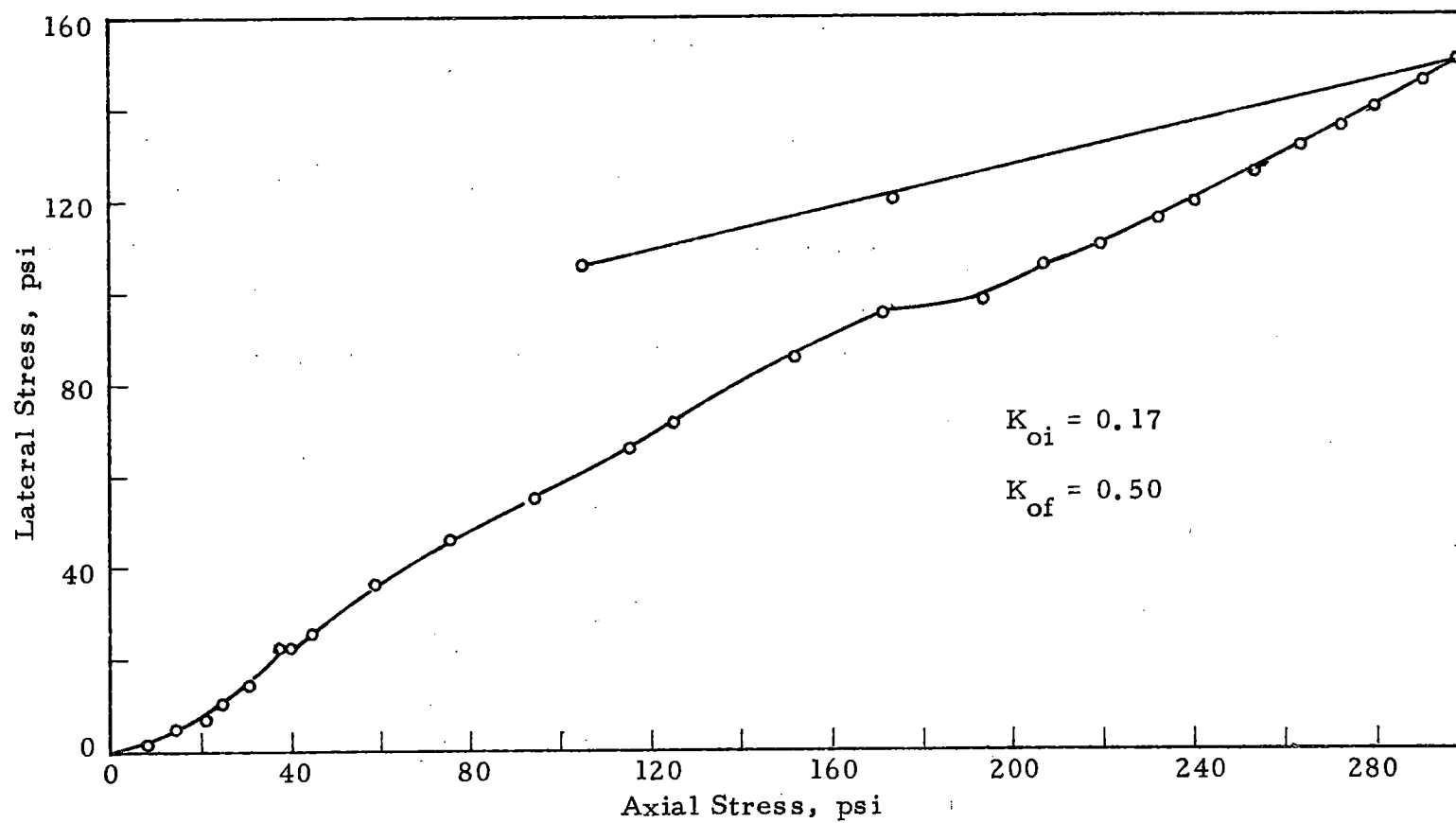


Fig. 3.7 Lateral Stress versus Axial Stress, K_o - Test No. H-3

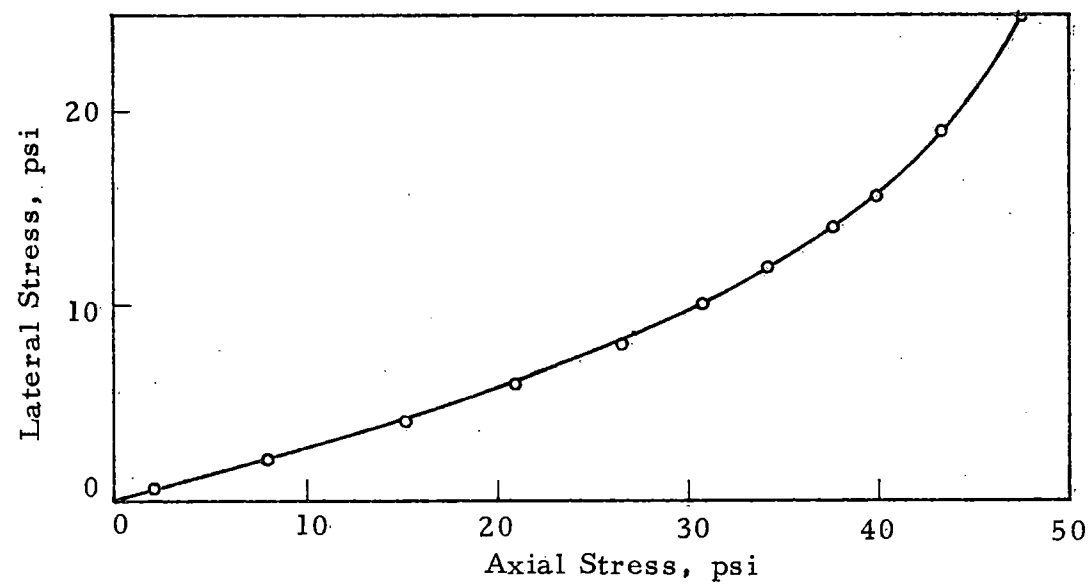


Fig. 3.8 Lateral Stress versus Axial Stress up to 2% Strain,
 K_0 - Test No. 1

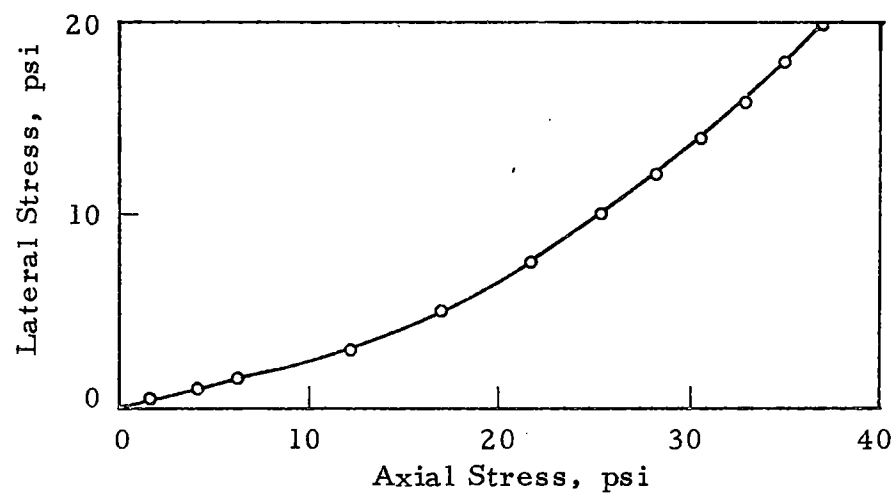


Fig. 3.9 Lateral Stress versus Axial Stress up to 2% Strain, K_o - Test No. 2

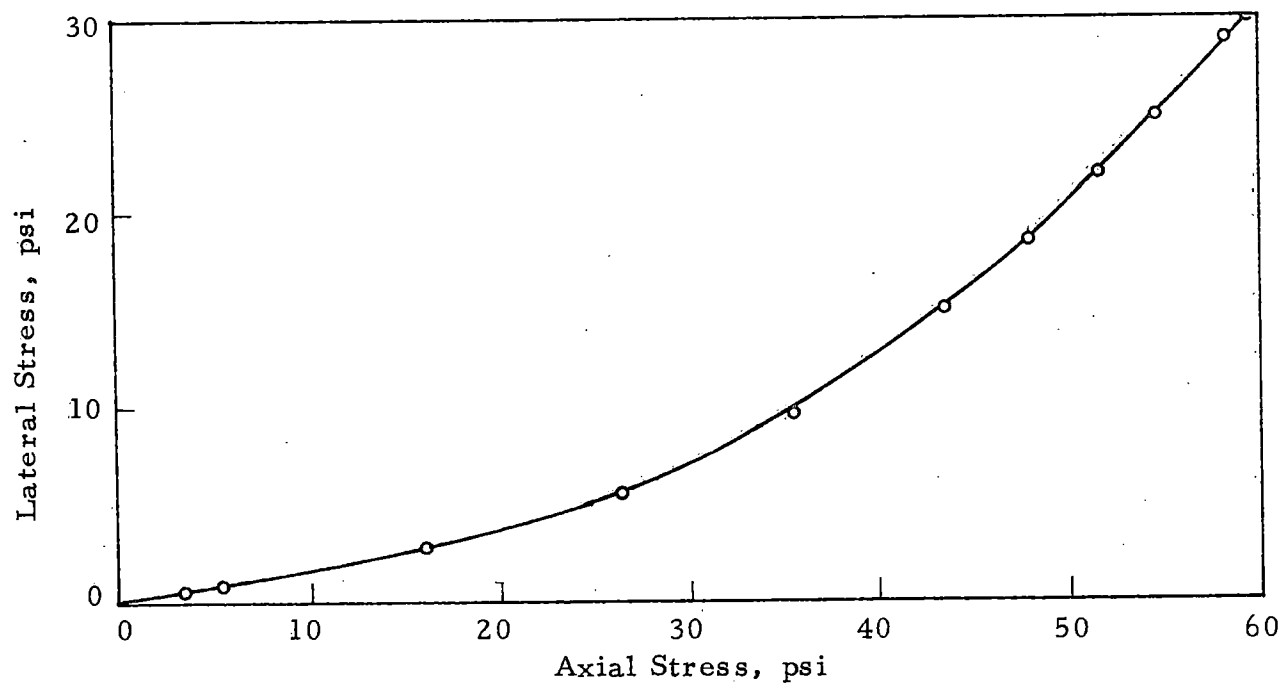


Fig. 3.10 Lateral Stress versus Axial Stress up to 2% Strain, K_0 - Test No. 3

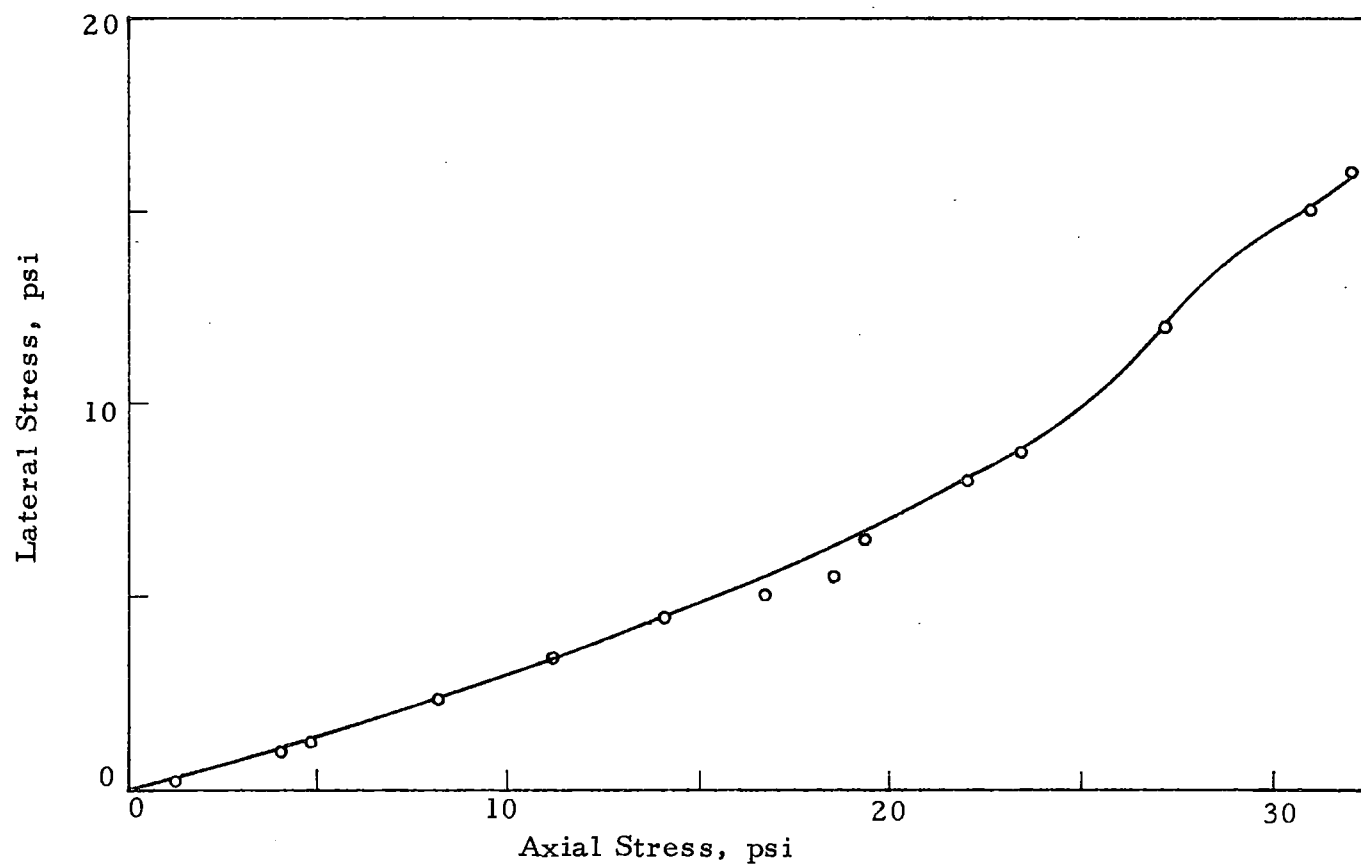


Fig. 3.11 Lateral Stress versus Axial Stress up to 2% Strain, K_0 - Test No. H-1

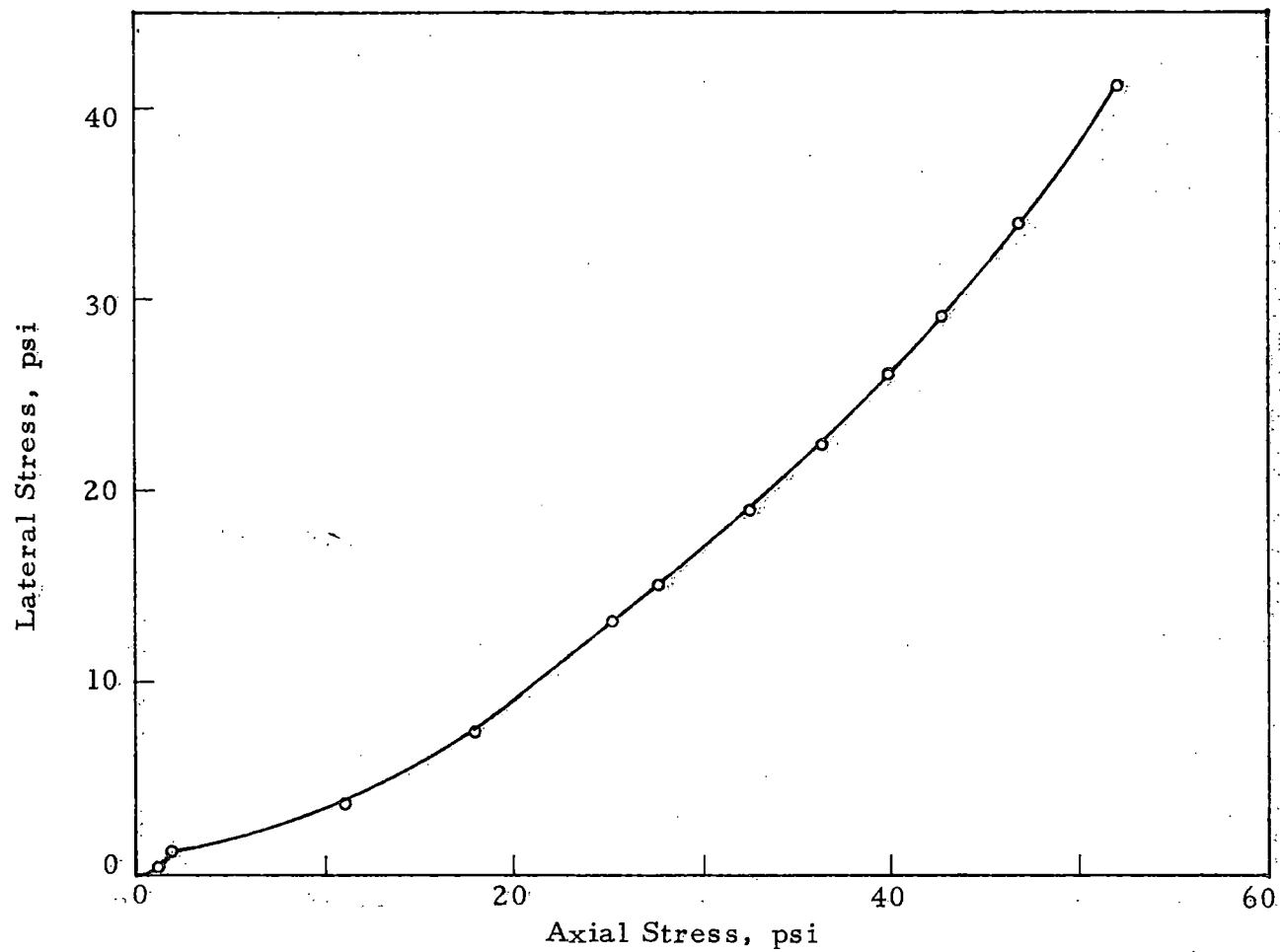


Fig. 3.12 Lateral Stress versus Axial Stress up to 2% Strain, K_0 - Test No. H-2

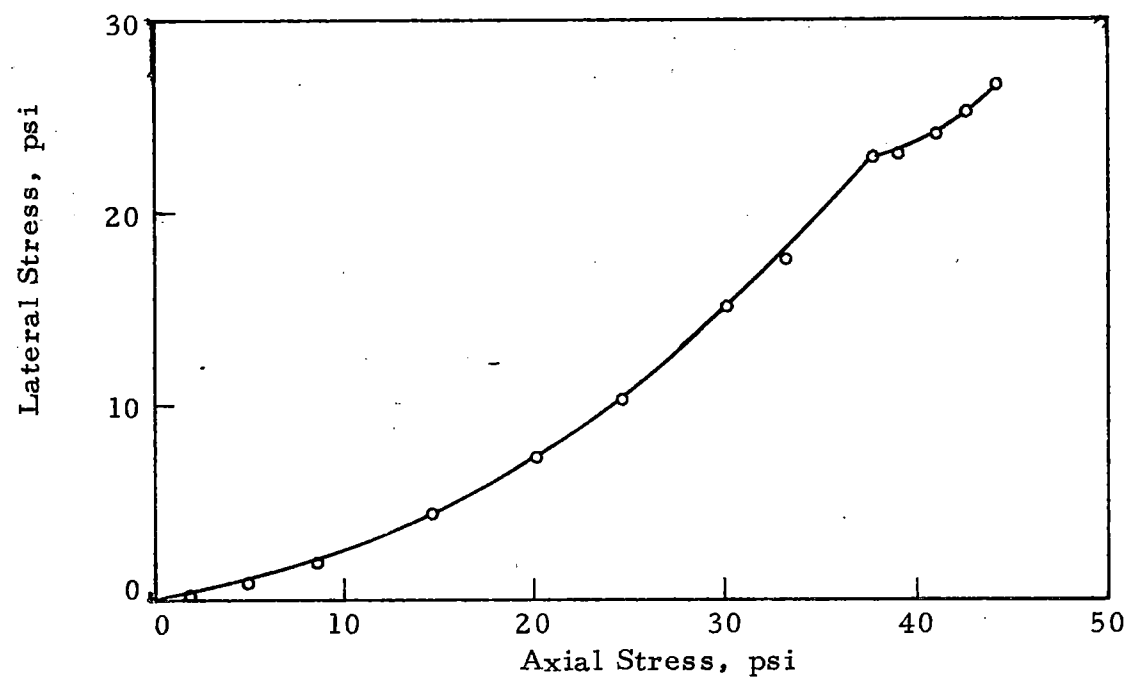


Fig. 3.13 Lateral Stress versus Axial Stress up to 2% Strain, K_0 -
Test No. H-3

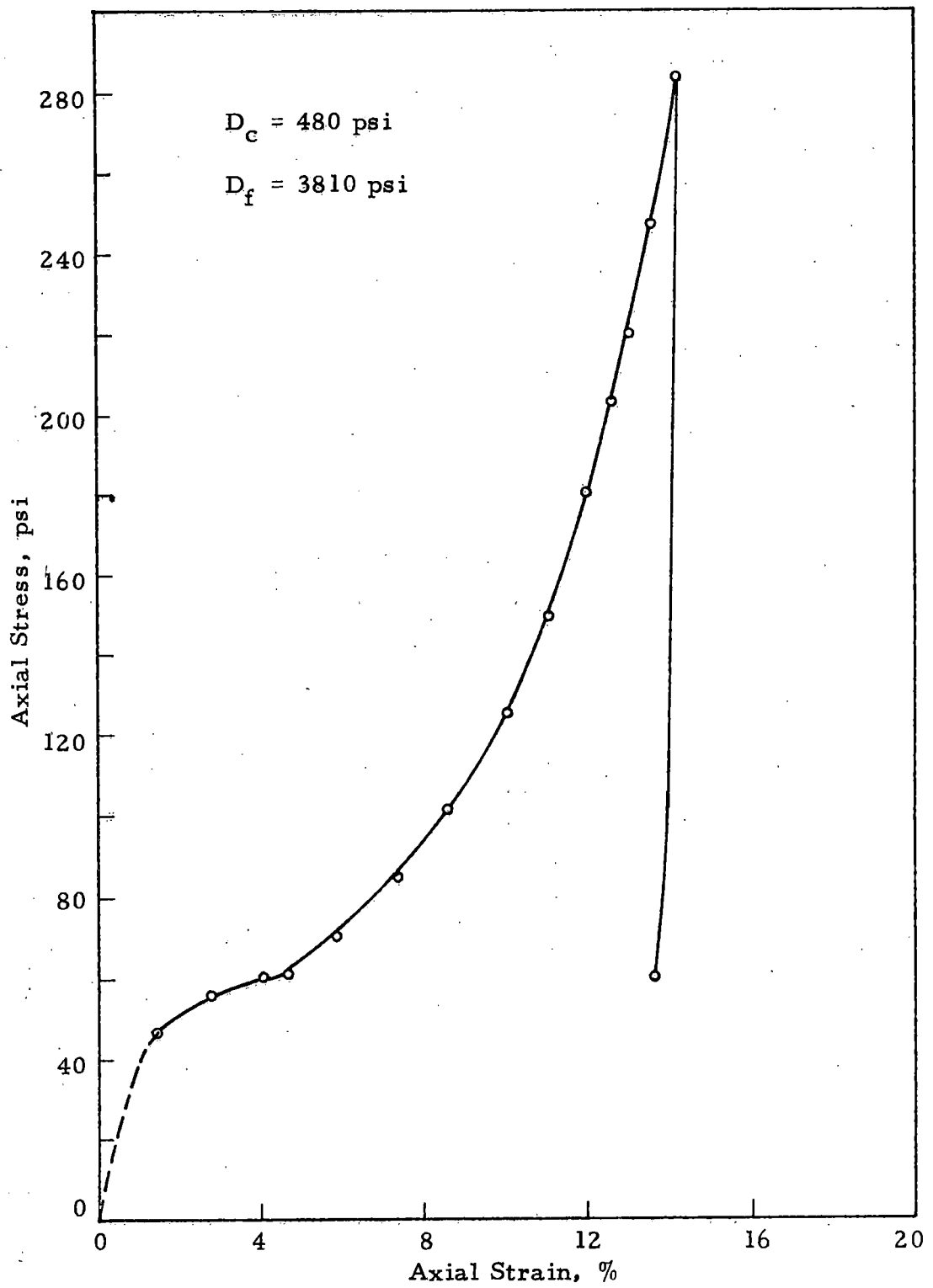
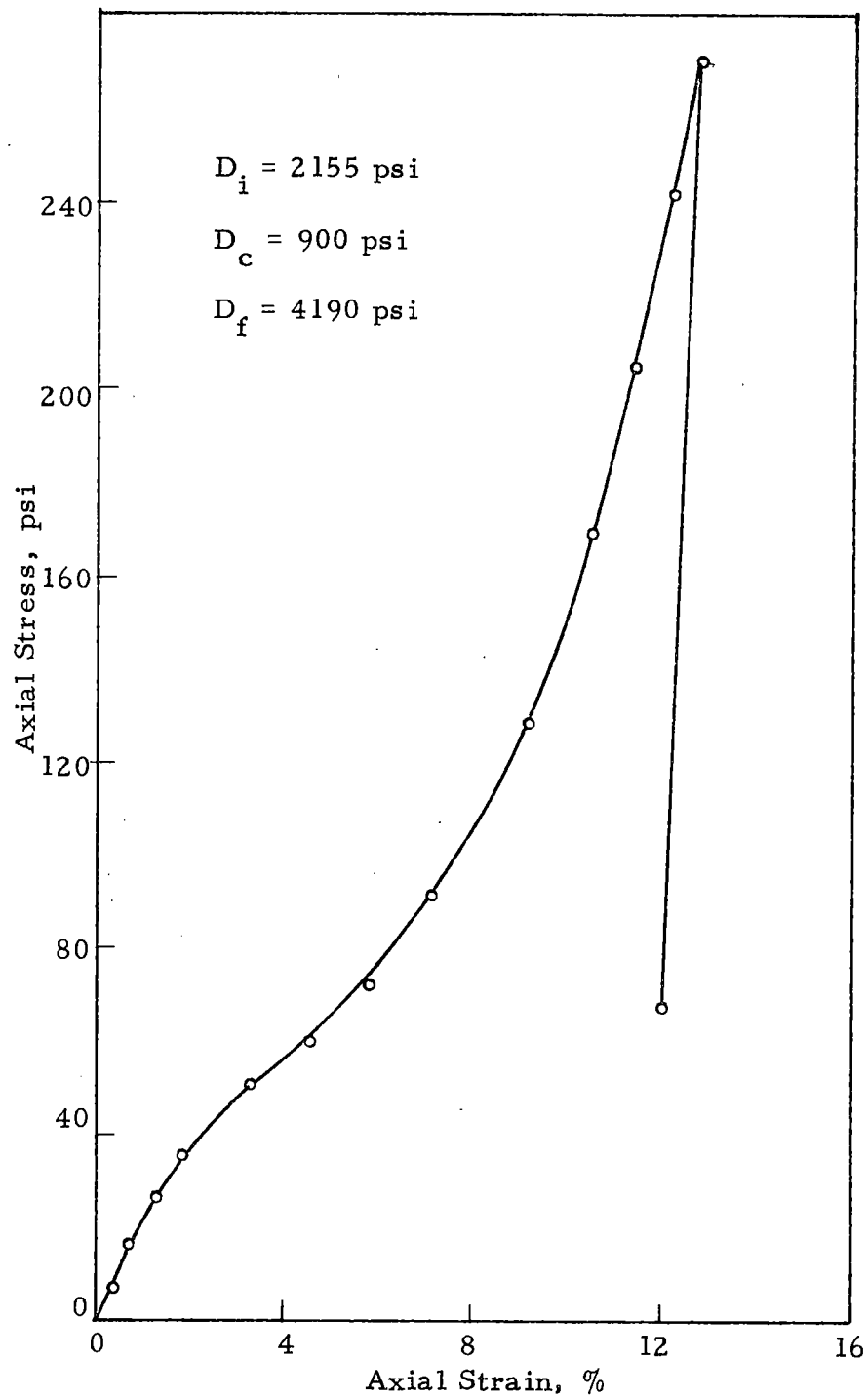


Fig. 3.14 Stress-Strain Relations, K_o - Test No. 1

Fig

Fig. 3.15 Stress-Strain Relations, K_o - Test No. 2

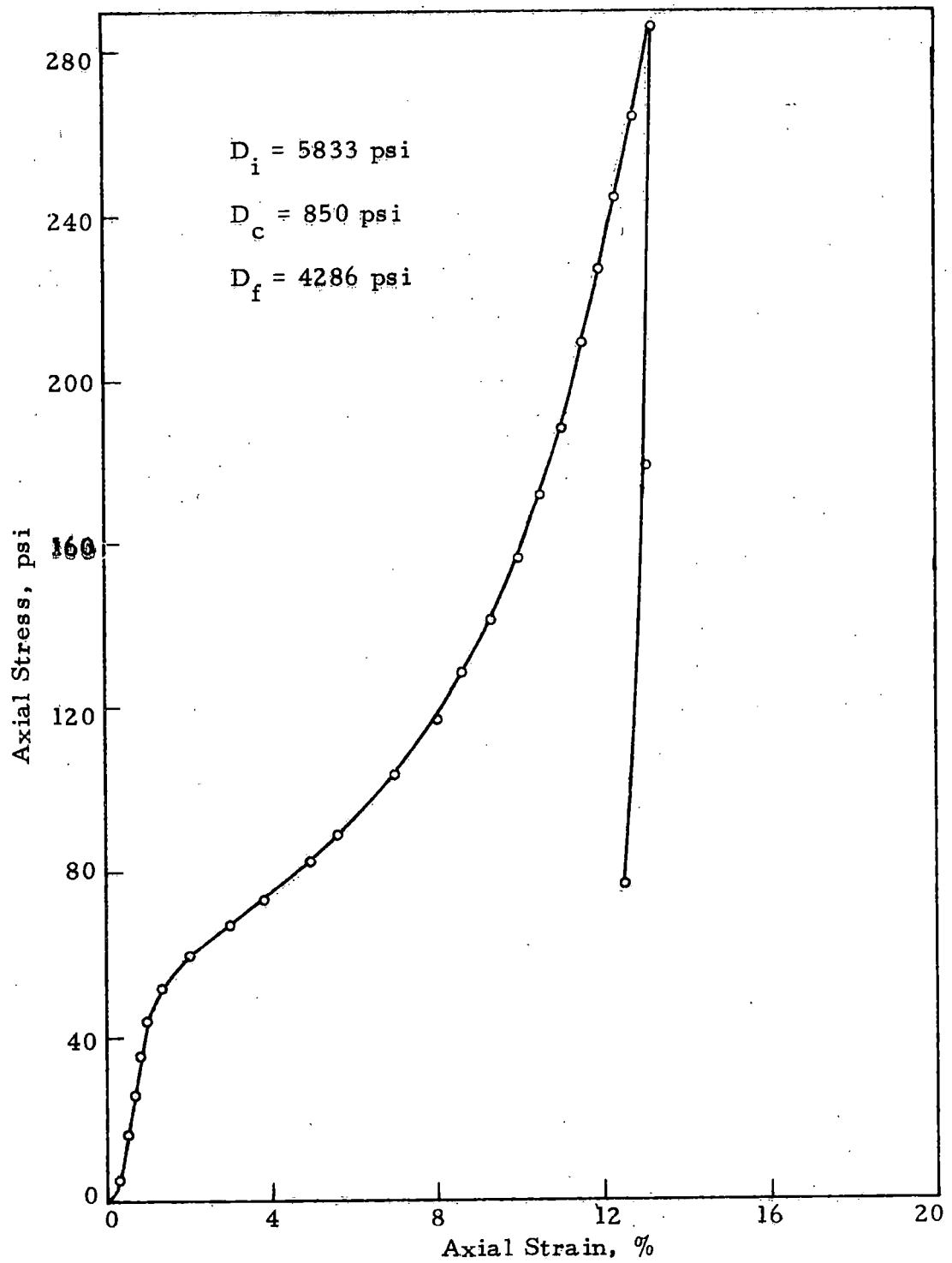


Fig. 3.16 Stress-Strain Relations, K_o - Test No. 3

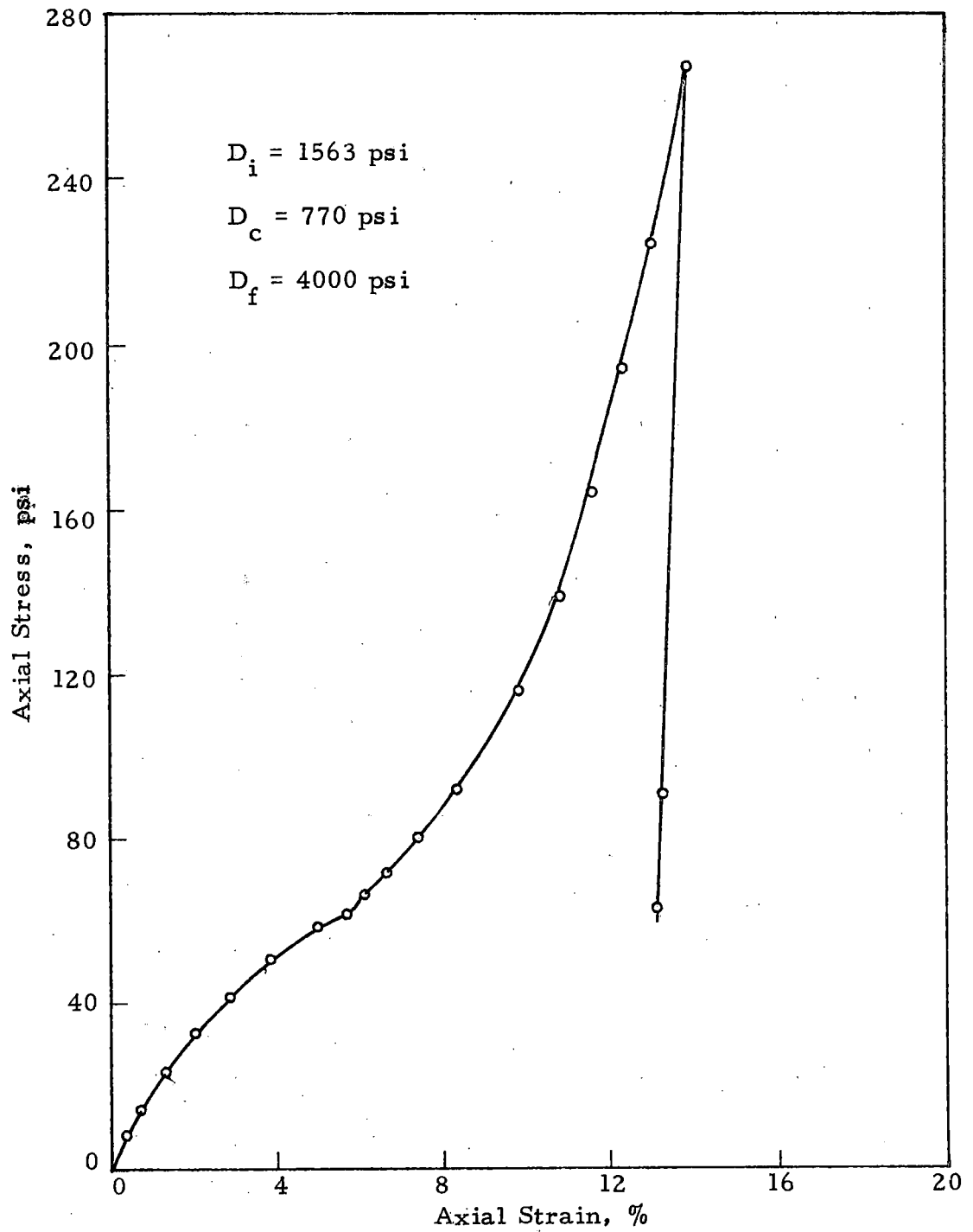


Fig. 3.17 Stress-Strain Relations, K_o - Test No. H-1

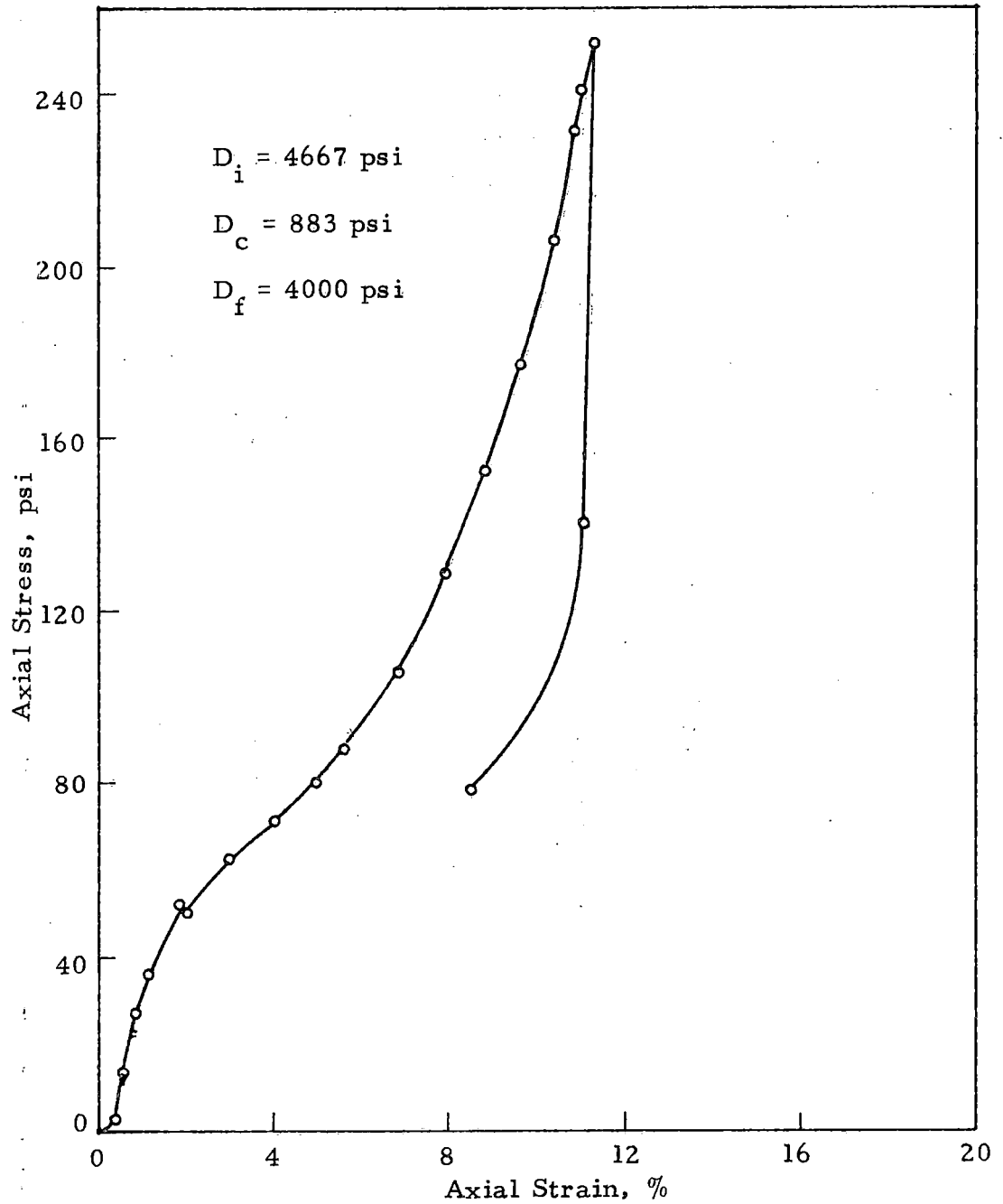


Fig. 3.18 Stress-Strain Relations, K_o - Test No. H-2

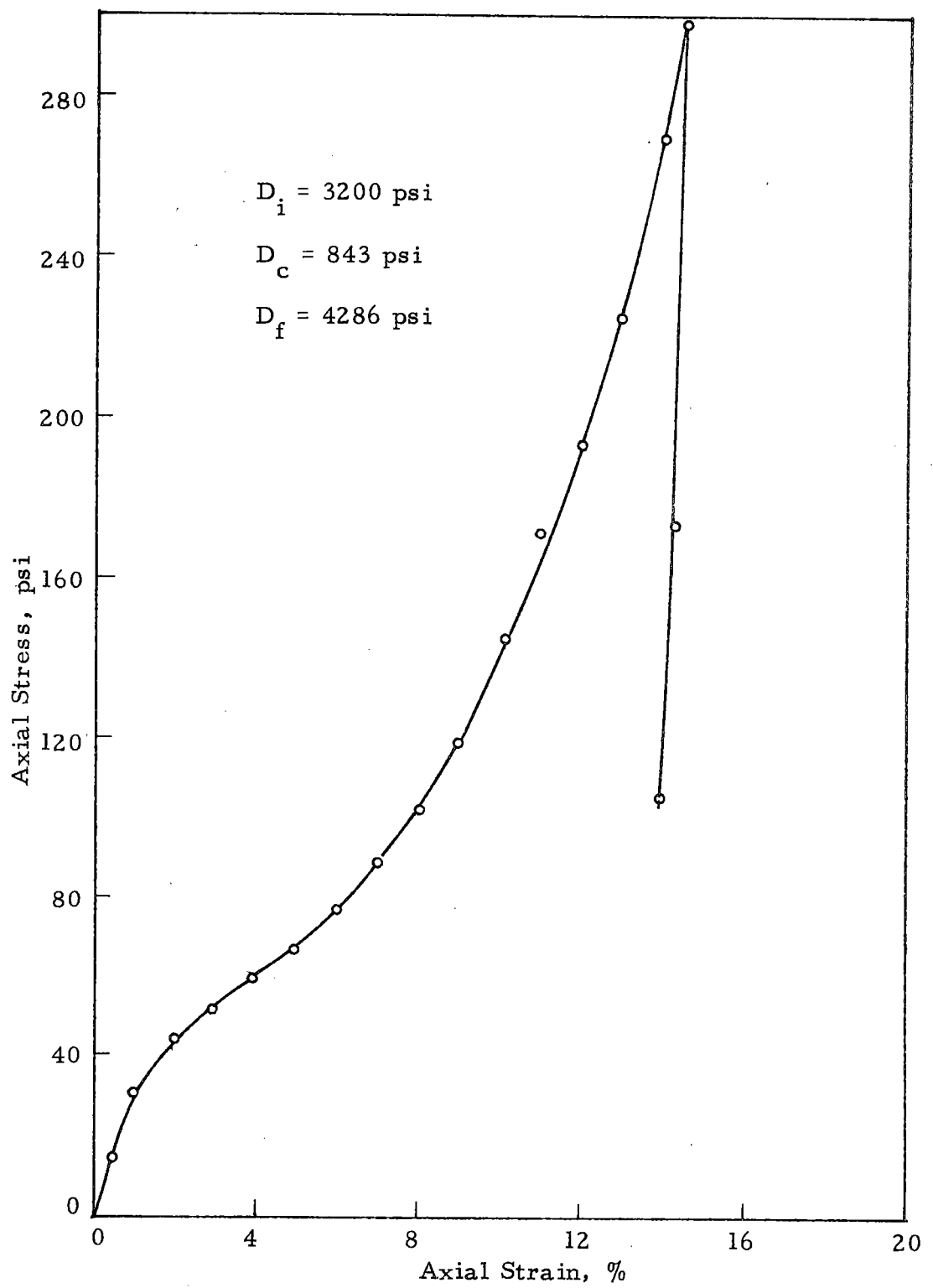


Fig. 3.19 Stress-Strain Relations, K_o - Test No. H-3

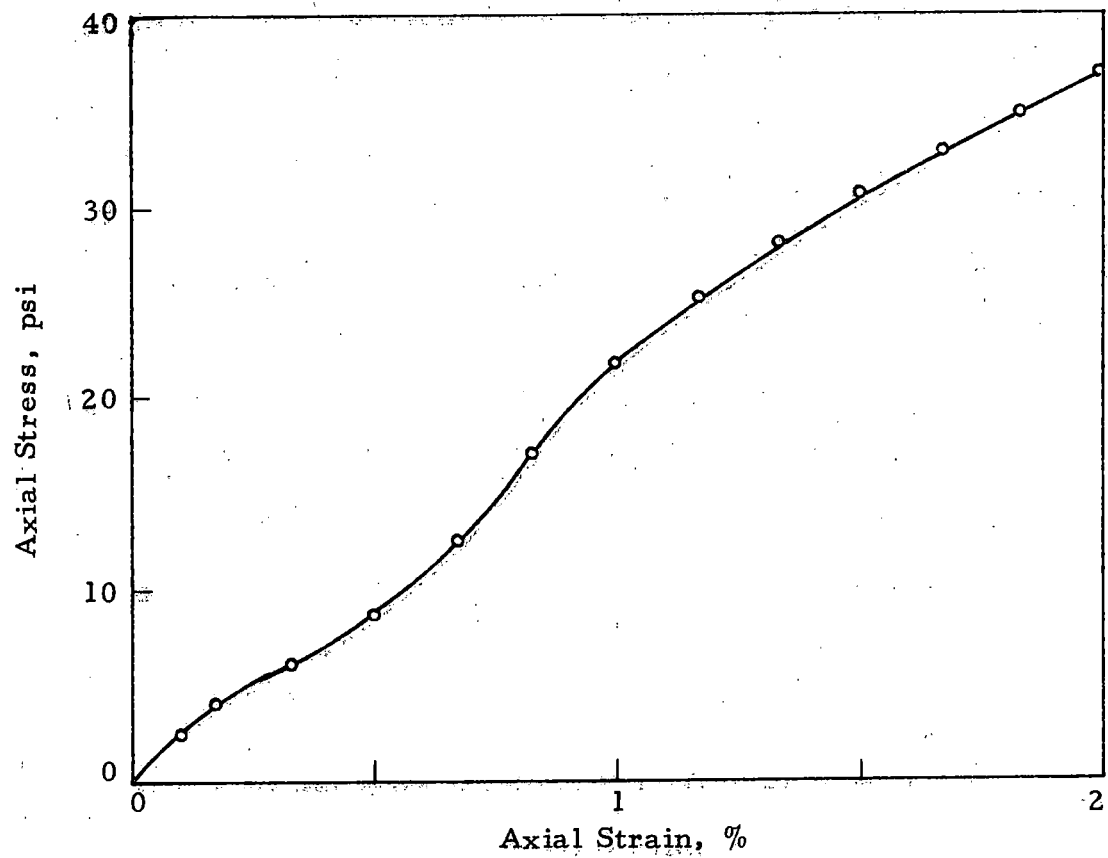


Fig. 3.20 Stress-Strain Relations up to 2% Strain, K_0 - Test No. 2

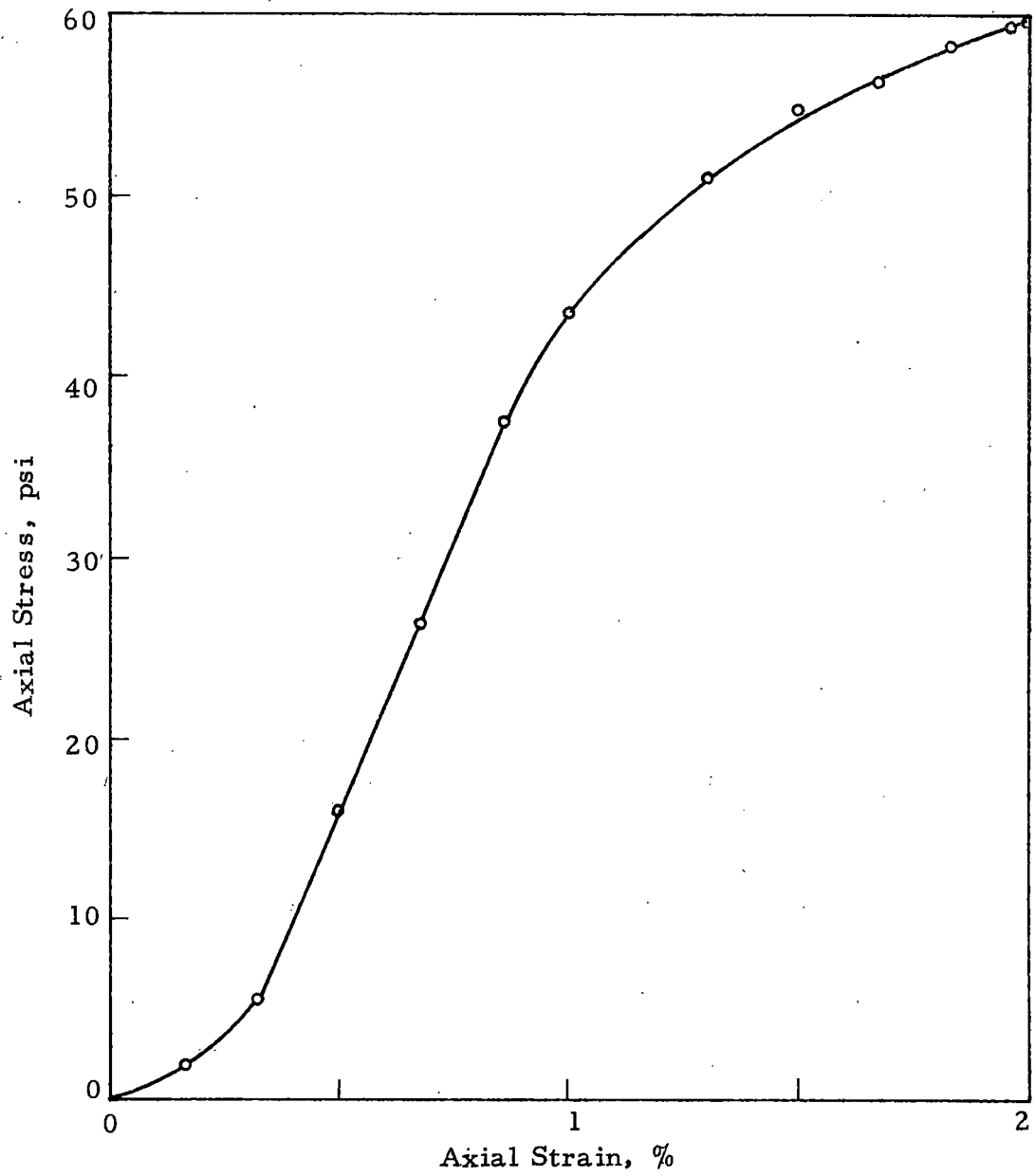


Fig. 3.21 Stress-Strain Relations up to 2% Strain, K_0 - Test No. 3

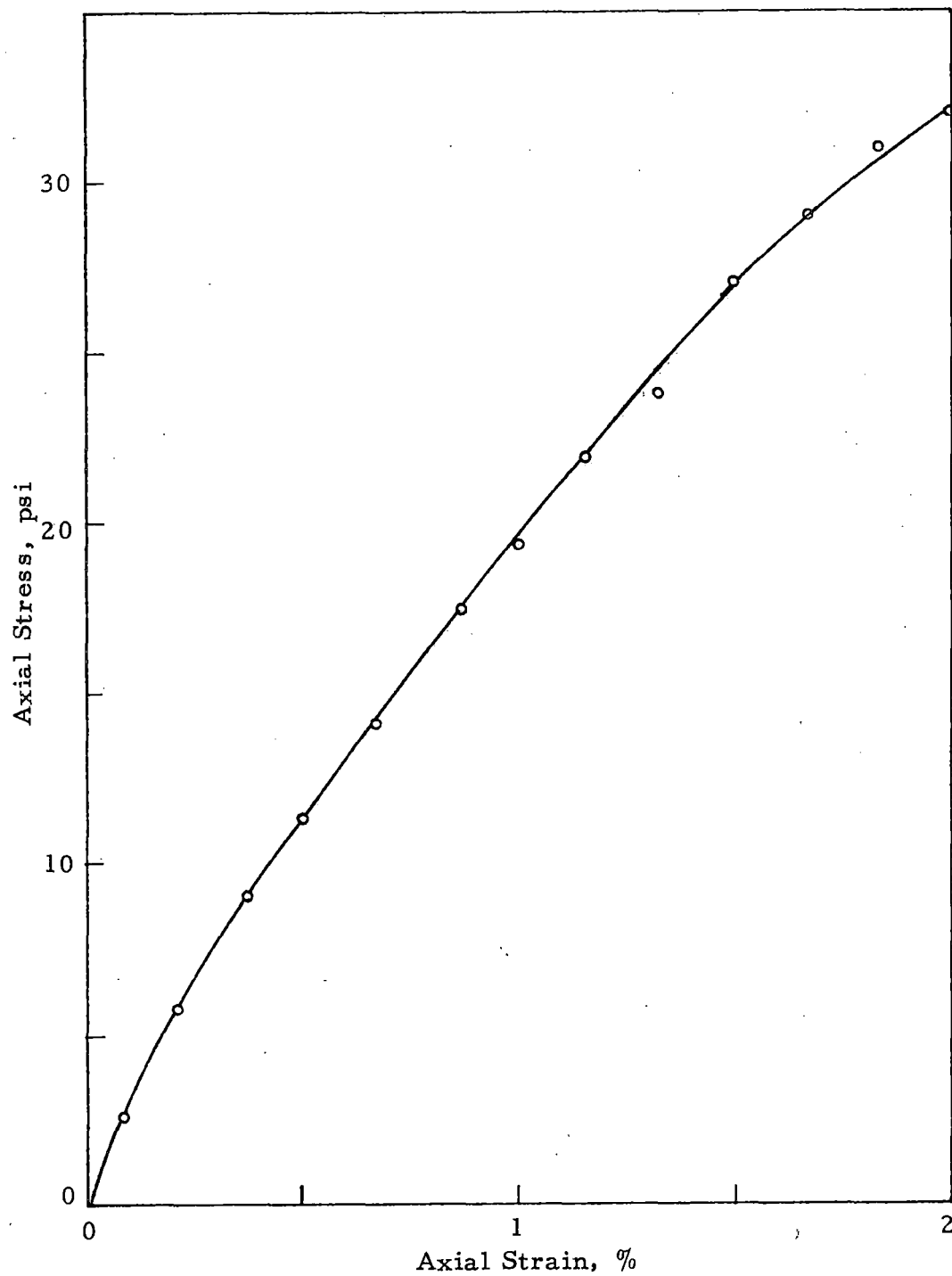


Fig. 3.22 Stress-Strain Relations up to 2% Strain, K_0 - Test No. H-1

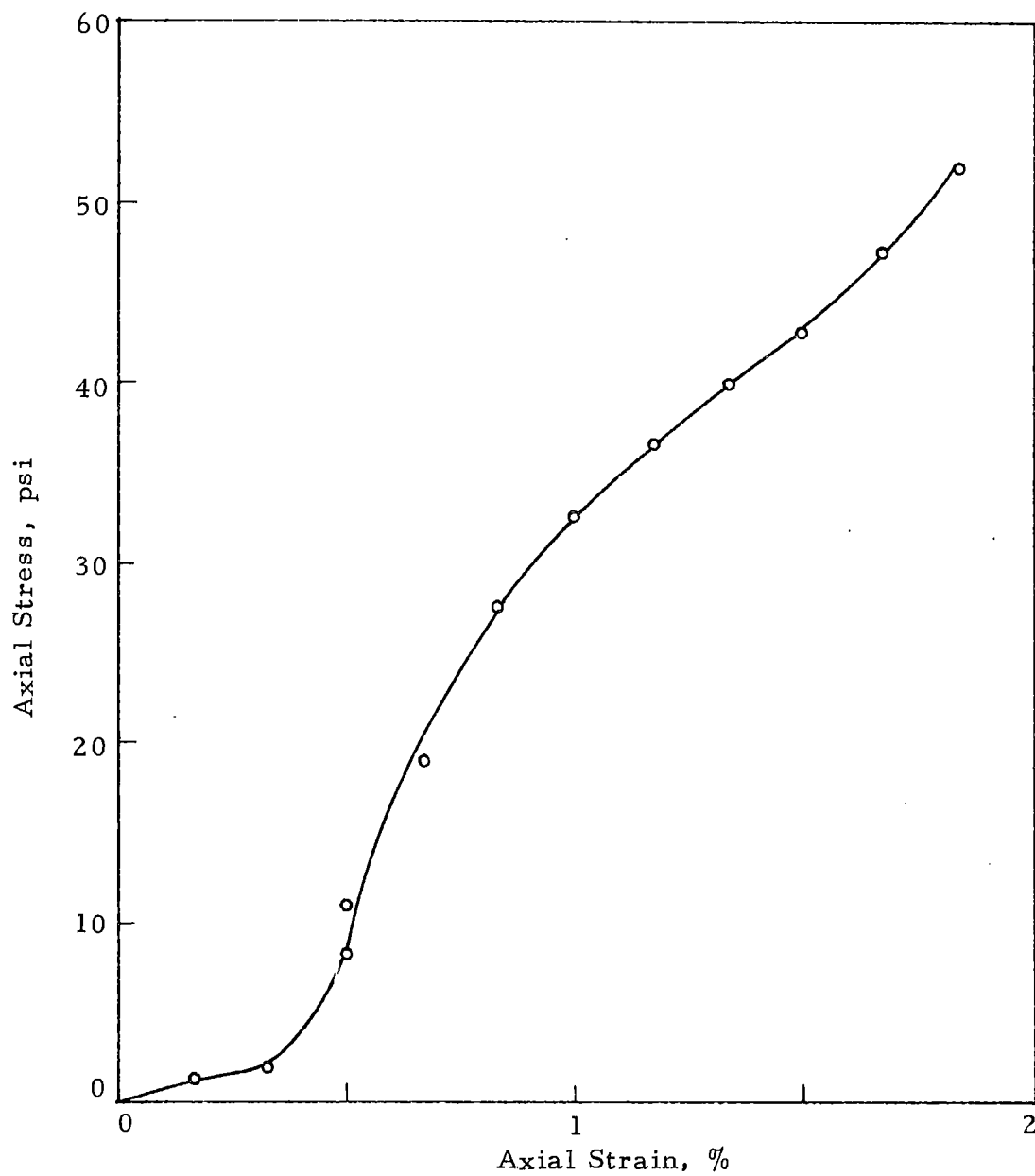


Fig. 3.23 Stress-Strain Relations up to 2% Strain, K_0 - Test No. H-2

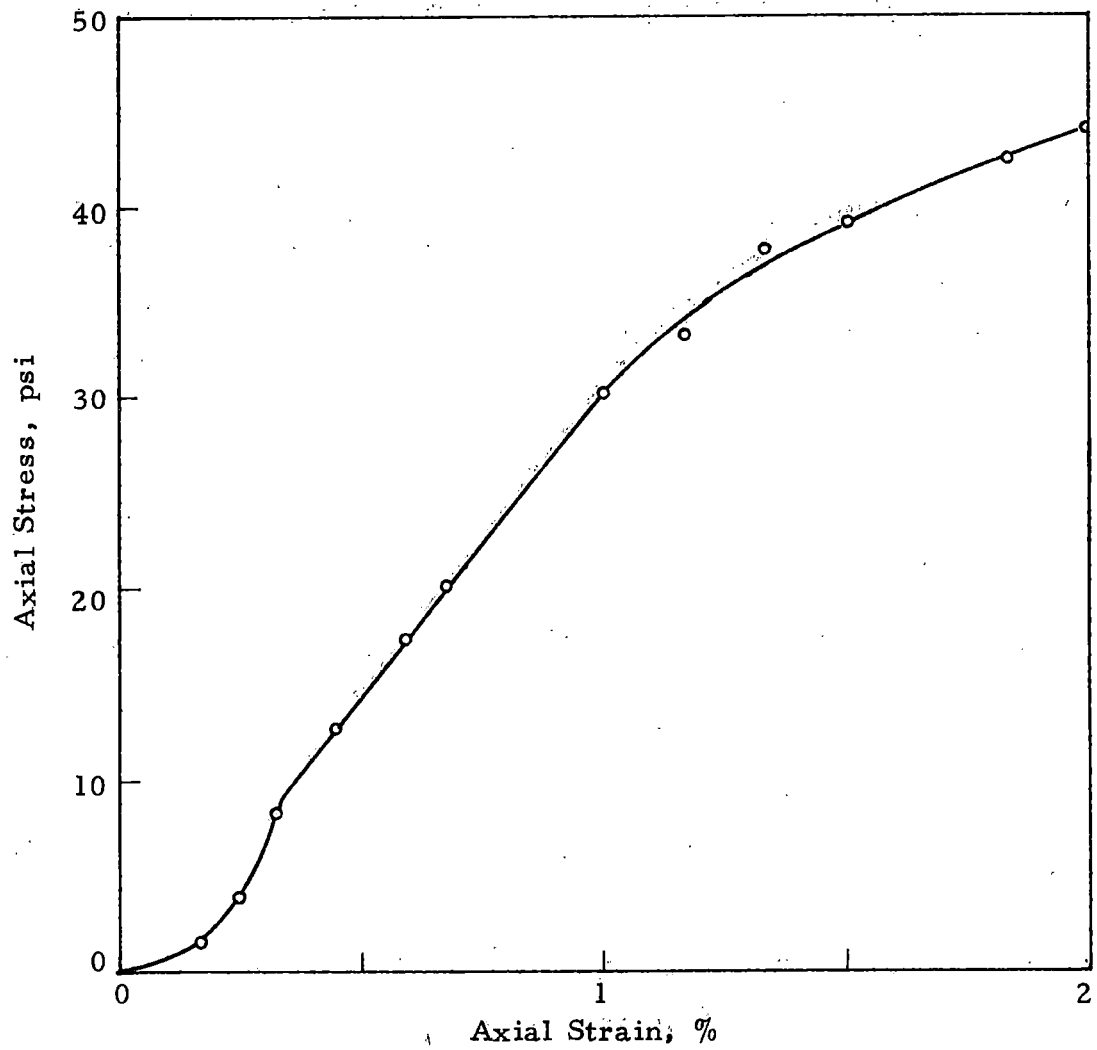


Fig. 3.24 Stress-Strain Relations up to 2% Strain, K_0 - Test No. H-3

of all the other parameters are also very nearly the same. Thus, it is evident that there is little or no variation in the samples and it is natural to expect similar values for the coefficient of earth pressure at rest in each case. The initial values of the coefficient of earth pressure at rest (K_{oi}), computed from Figures 3.8 to 3.13 have a maximum variation of 0.18. From Figures 3.2 to 3.7 it is seen that the K_o graph is curved in the initial stages and is a straight line in the final stages of loading. In each case a slight break in the curve is noticed between a lateral stress of 20 and 60 psi. It was noted during the experiment that within this range of confining pressure the sample underwent a compressive lateral strain. When this happened the confining pressure was maintained constant until the sample diameter increased to its original dimensions. A maximum variation of 0.06 in K_{of} suggests that the samples behaved in the same manner in the final loading stages. As expected, K_o has a higher value during unloading.

Axial stress has been plotted against axial strain for the entire duration of the test in Figures 3.14 to 3.19. Figures 3.20 to 3.24 show the same parameters plotted up to 2% axial strain. In these curves too, there is an obvious change in behavior at an axial stress ranging from 30 to 60 psi, (which corresponds approximately to a lateral stress between 20 and 40 psi). In the beginning of these

graphs there is a slight curve which may be attributed to improper seating between the loading ram and the top of the loading cap.

3.1.2 Triaxial Compression Tests

The results of the triaxial compression tests have been summarized in Table 3. The data from these tests have been plotted in Figures 3.25 to 3.44. The deviator stress ($\sigma_1 - \sigma_3$) has been plotted against axial strain in Figures 3.25 to 3.28. The axial strain is plotted against lateral strain in Figures 3.29 to 3.44. All the parameters measured in these tests have been defined in Figures 3.45 and 3.46.

The deviator stress-strain curves follow a set pattern, with the maximum deviator stress increasing with cell pressure. The pairs of curves with equal cell pressure are close. Figure 3.45 is a typical deviator stress-strain curve. By extending back the straight line portion of the graph, the magnitude of the axial strain, ϵ_0 , at zero stress is obtained as the intercept on the strain axis. The initial curvature and the strain, ϵ_0 , are not apparent in Figures 3.25 to 3.28 because of the scale. They may be attributed to faulty seating between the ram and the loading cap.

The graphs between axial strain and lateral strain have the same shape for all the tests. A typical shape of the initial portion of these graphs, greatly enlarged, is shown in Figure 3.46. The

TABLE 3

SUMMARY OF TRIAXIAL TESTS

<u>Test No.</u>	<u>Cell Pressure psi</u>	<u>Orientation of Sample in Cell</u>	<u>Orientation of Pads</u>	<u>Rate of Loading in/min</u>
1	0	Vertical	P ₁	
2	5	Vertical		
3	10	Vertical	up to test	
4	15	Vertical	No. 10	
5	20	Vertical		
6	30	Vertical		
7	40	Vertical		
8	60	Vertical		0.006
9	100	Vertical		
10	140	Vertical	P ₁	for all
12	0	Horizontal	P ₂	tests
13	0	Horizontal	P ₃	
14	10	Horizontal	P ₂	
15	10	Horizontal	P ₃	
16	20	Horizontal	P ₂	
17	20	Horizontal	P ₃	

TABLE 3 (cont'd.)

Test No.	Initial Void Ratio e_i	Consolidated Void Ratio e_c	Dry Density in pcf	Initial Tangent Modulus E_i in psi
1	0.817	-	93.4	3100
2	0.841	0.835	92.2	6140
3	0.856	0.845	91.4	5900
4	0.896	0.887	89.5	6200
5	0.842	0.838	92.2	6730
6	0.868	0.838	90.9	6170
7	0.856	0.822	91.4	8200
8	0.862	0.757	91.1	6680
9	0.819	0.695	93.3	11400
10	0.837	0.661	92.4	15900
12	0.837	-	92.4	3030
13	0.878	-	90.4	1920
14	0.846	0.837	92.0	5450
15	0.845	0.836	92.0	4250
16	0.853	0.842	91.6	4850
17	0.828	0.817	92.9	5150

TABLE 3 (cont'd.)

Test No.	Initial Water Content w_i %	Initial Degree of Saturation S_{ri} %	Consolidated Degree of Saturation S_{rc} %
1	23.4	77.9	-
2	23.3	75.4	76.4
3	23.2	73.6	74.6
4	23.5	71.3	72.0
5	23.4	75.5	75.9
6	23.4	73.2	75.8
7	24.0	76.3	-
8	23.3	73.5	-
9	23.2	77.1	-
10	23.5	76.5	-
12	22.8	74.2	-
13	22.7	70.4	-
14	23.1	74.2	74.9
15	22.5	72.5	73.2
16	22.7	72.4	73.3
17	22.9	75.2	76.1

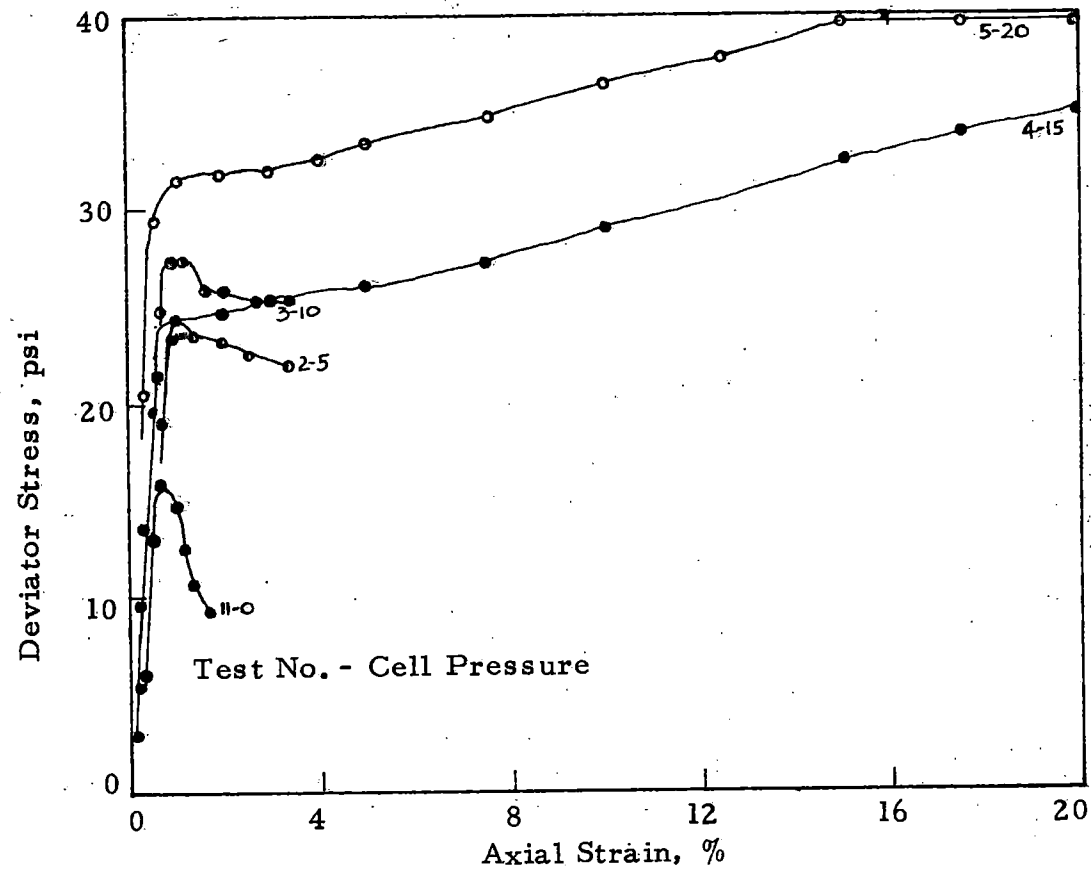


Fig. 3.25 Stress-Strain Relations, Test Nos. 1 to 5

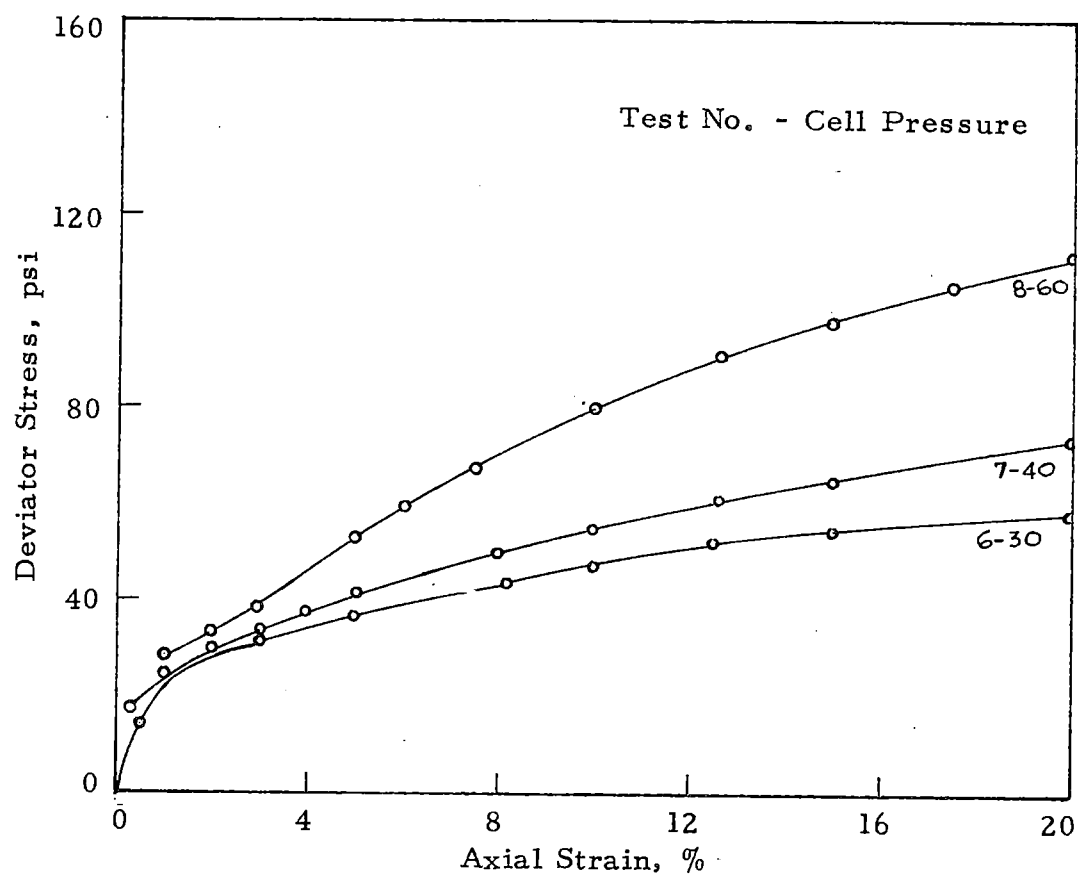


Fig. 3.26 Stress-Strain Relations, Test Nos. 6 to 8

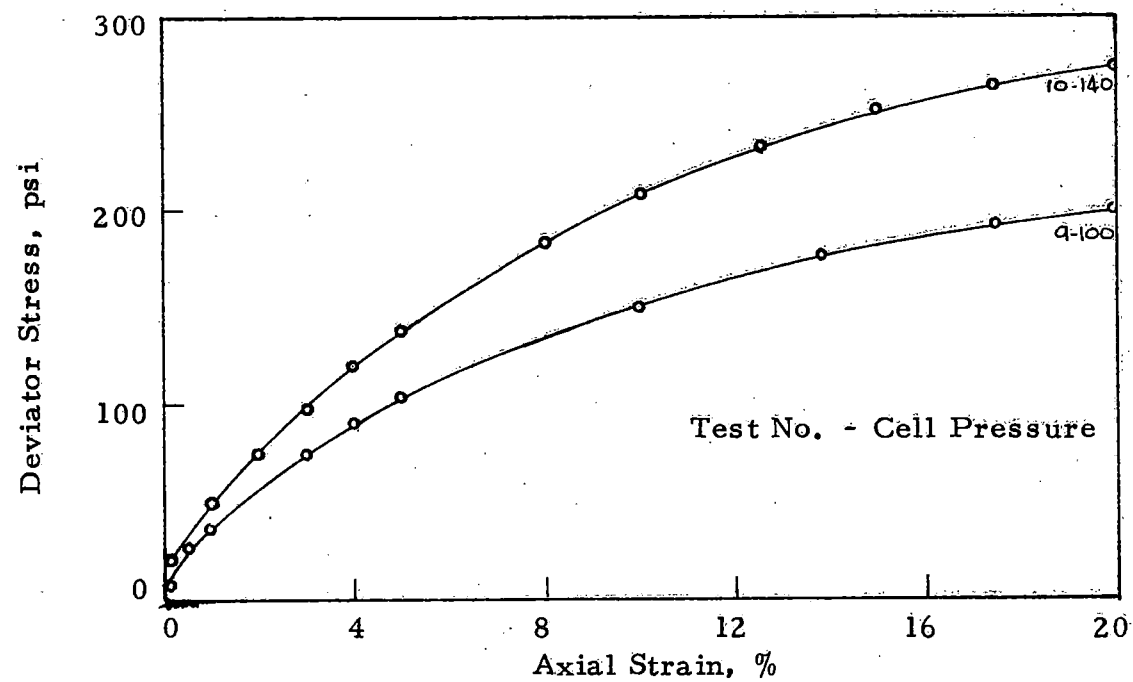


Fig. 3.27 Stress-Strain Relations, Test Nos. 9 and 10

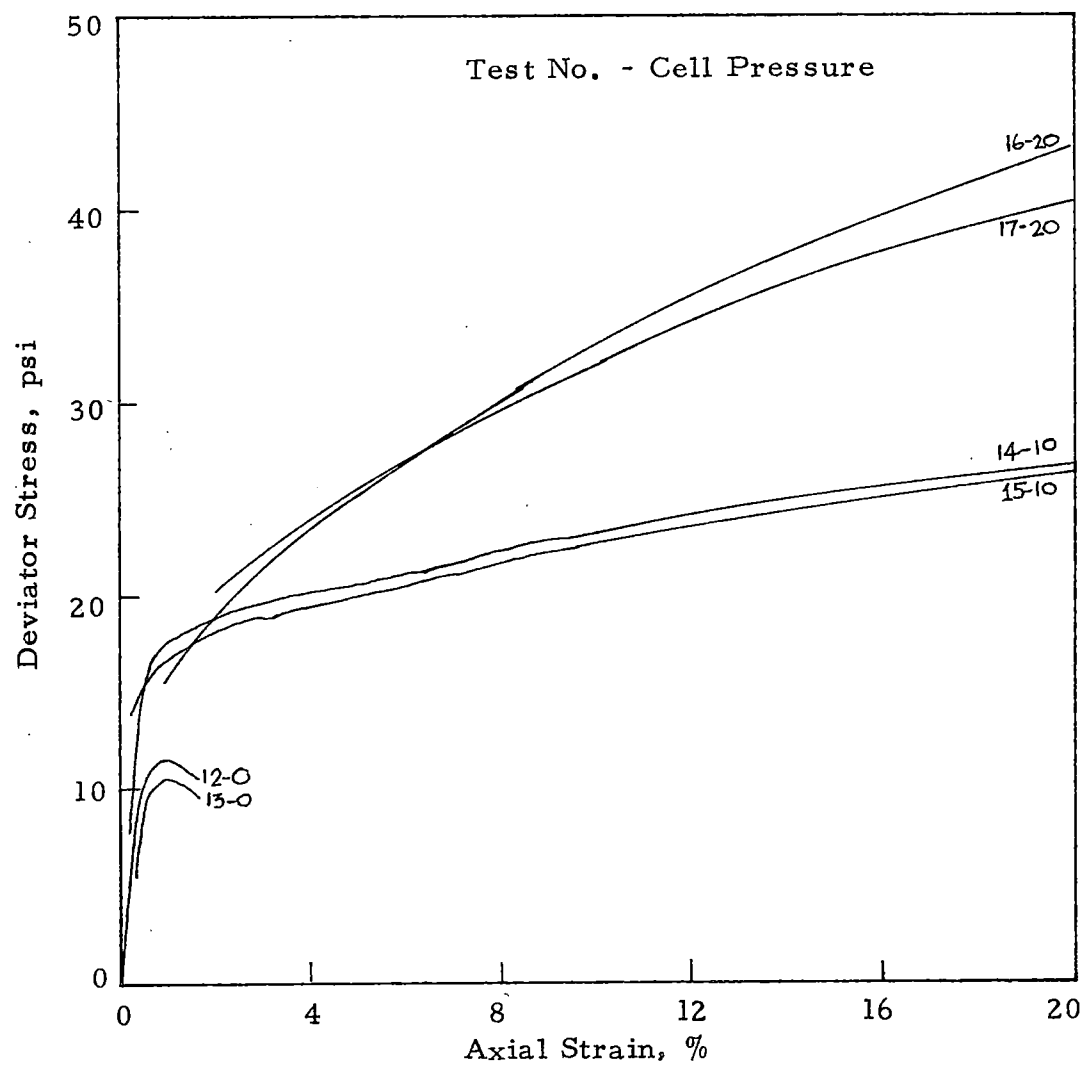


Fig. 3.28 Stress-Strain Relations, Test Nos. 12 to 17

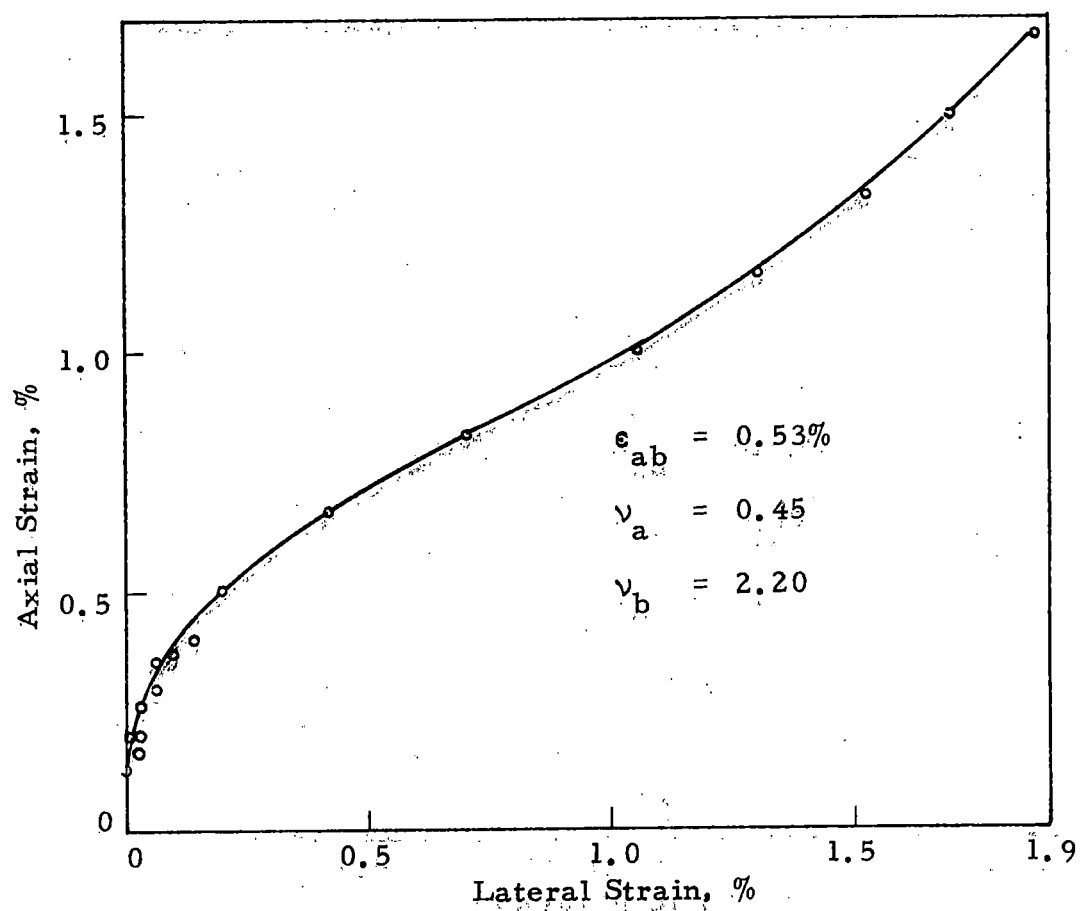


Fig. 3.29 Axial Strain versus Lateral Strain - Test No. 1

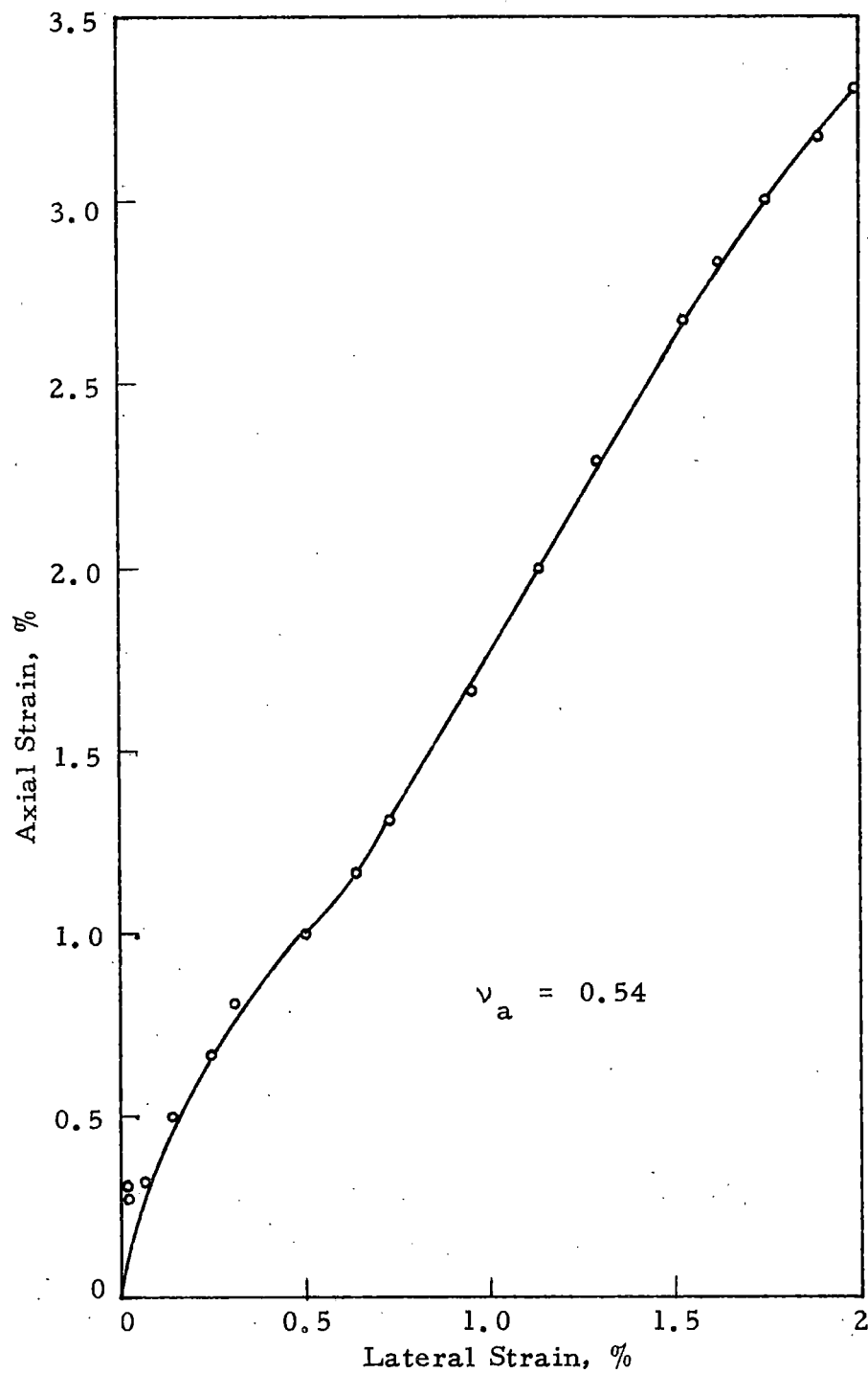


Fig. 3.30 Axial Strain versus Lateral Strain, Test No. 2

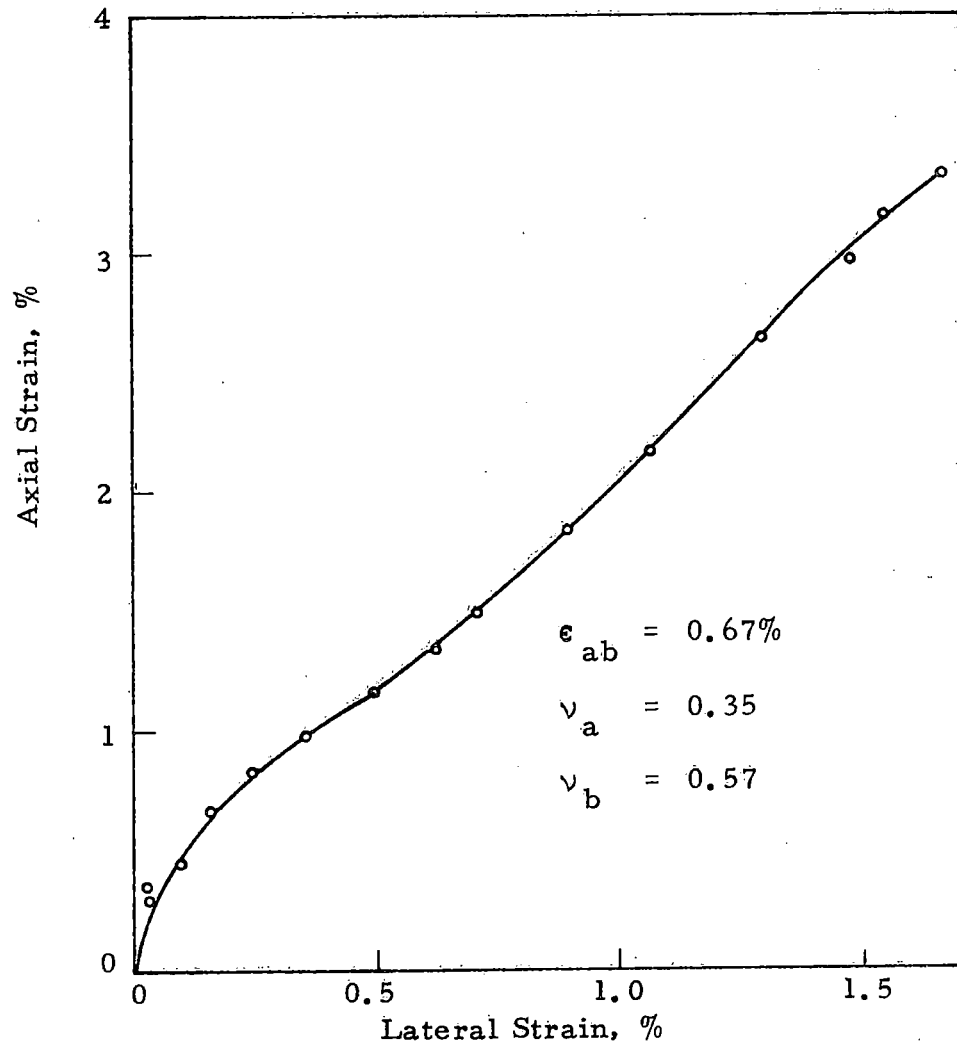


Fig. 3.31 Axial Strain versus Lateral Strain, Test No. 3

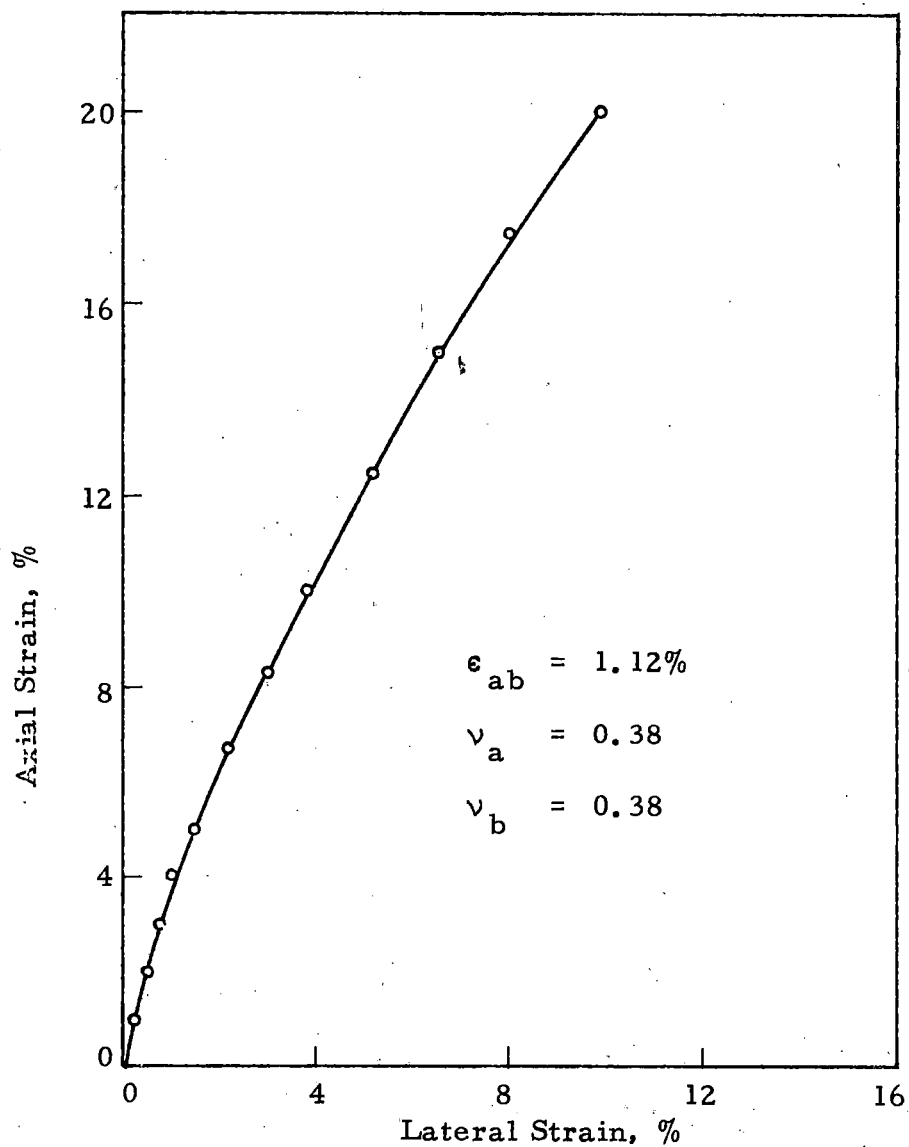


Fig. 3.32 Axial Strain versus Lateral Strain, Test No. 4

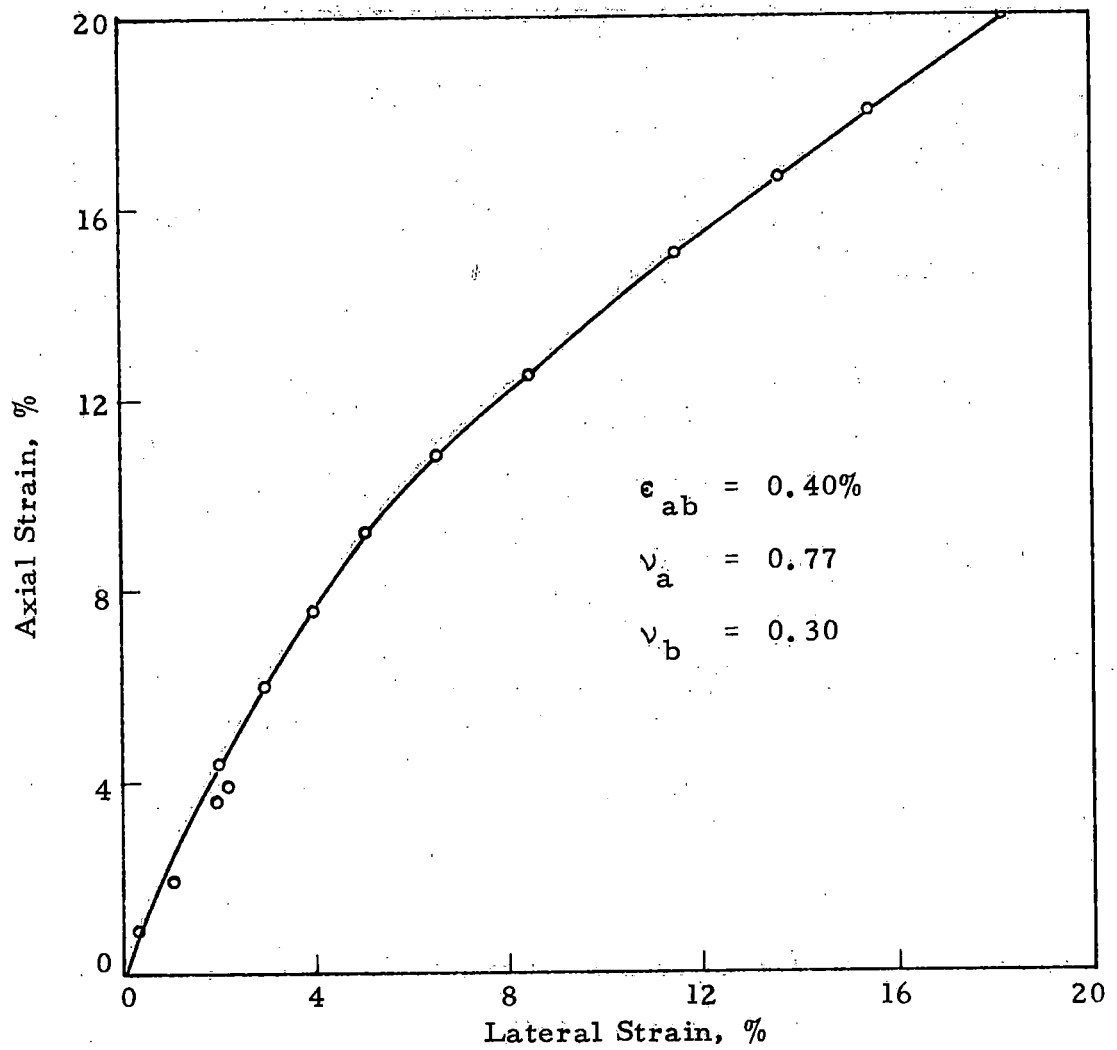


Fig. 3.33 Axial Strain versus Lateral Strain, Test No. 5

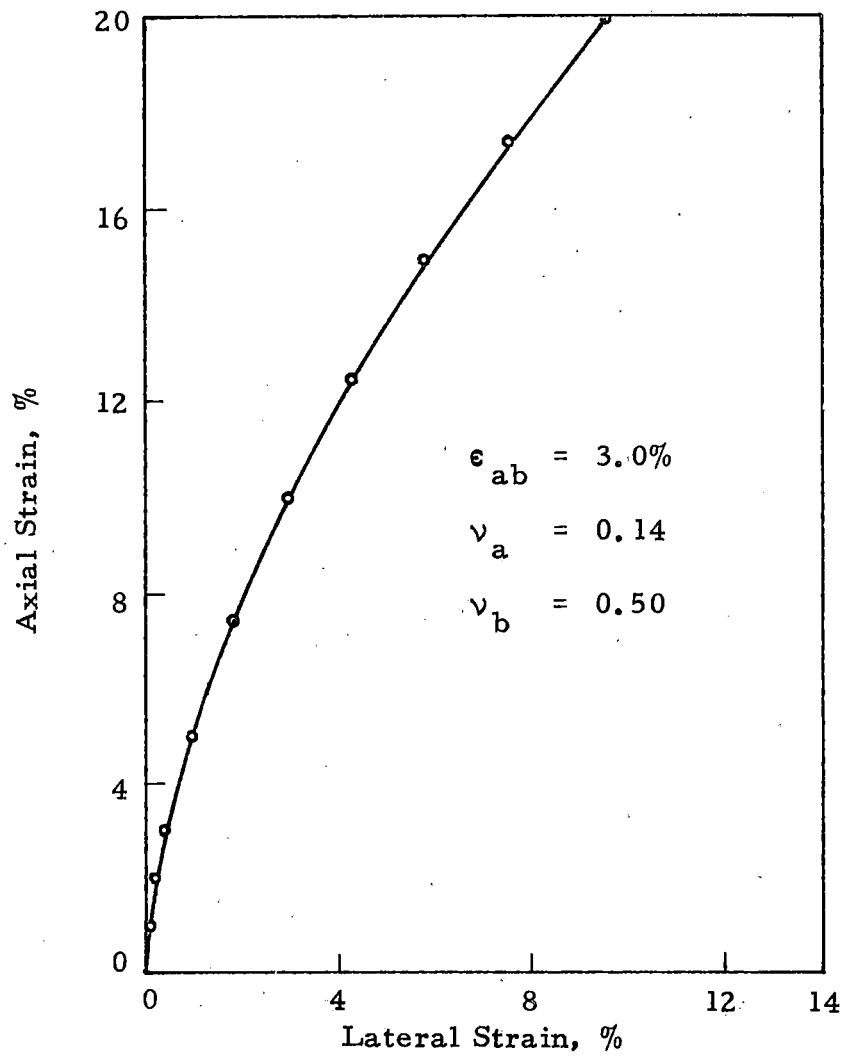


Fig. 3.34 Axial Strain versus Lateral Strain, Test No. 6

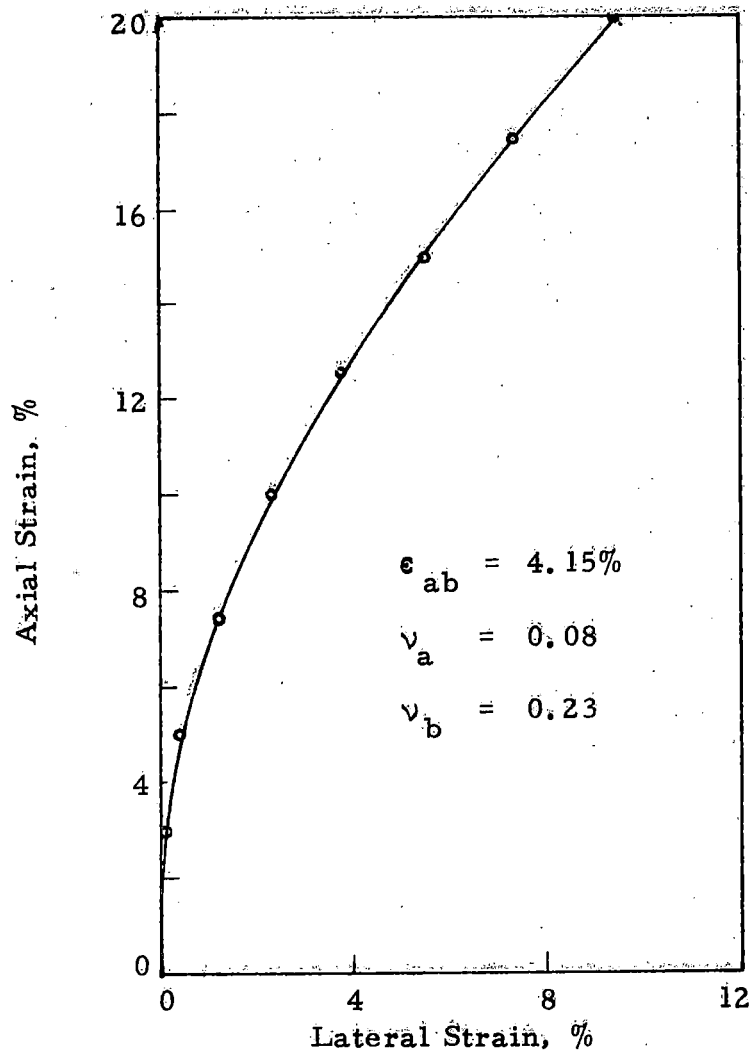


Fig. 3.35 Axial Strain versus Lateral Strain, Test No. 7

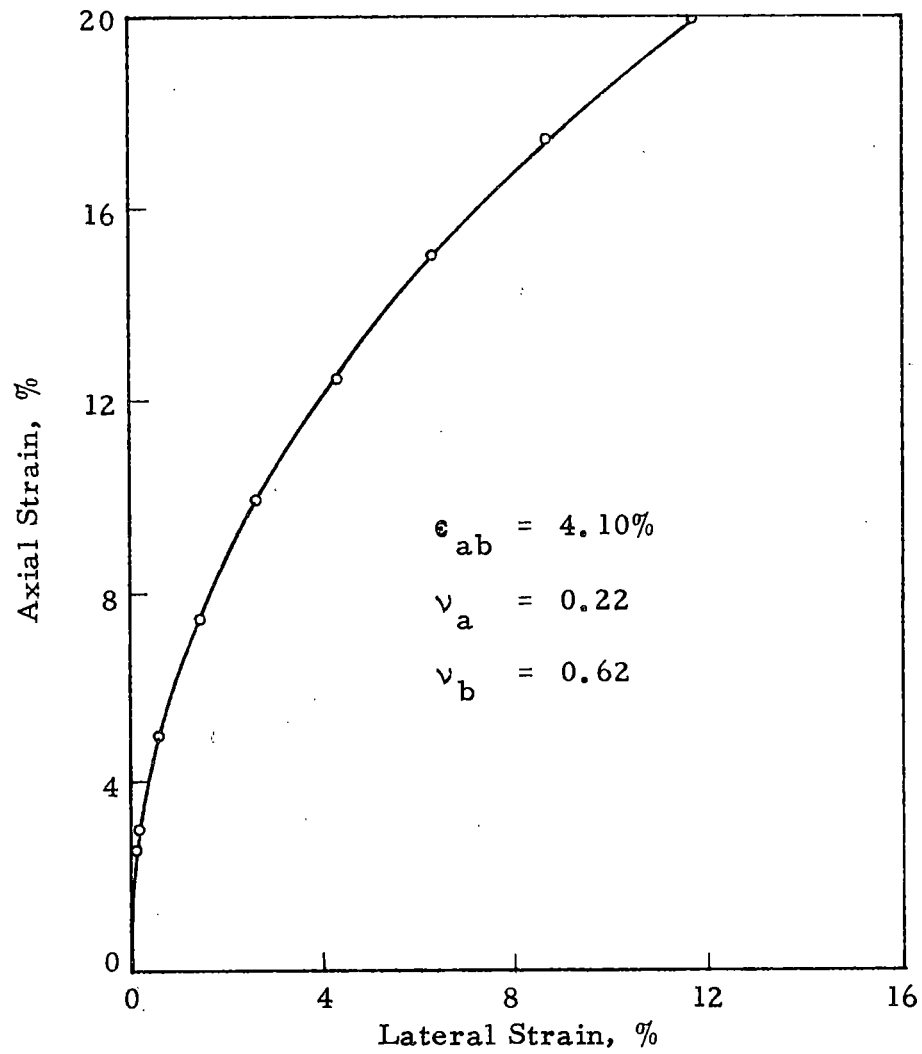


Fig. 3.36 Axial Strain versus Lateral Strain, Test No. 8

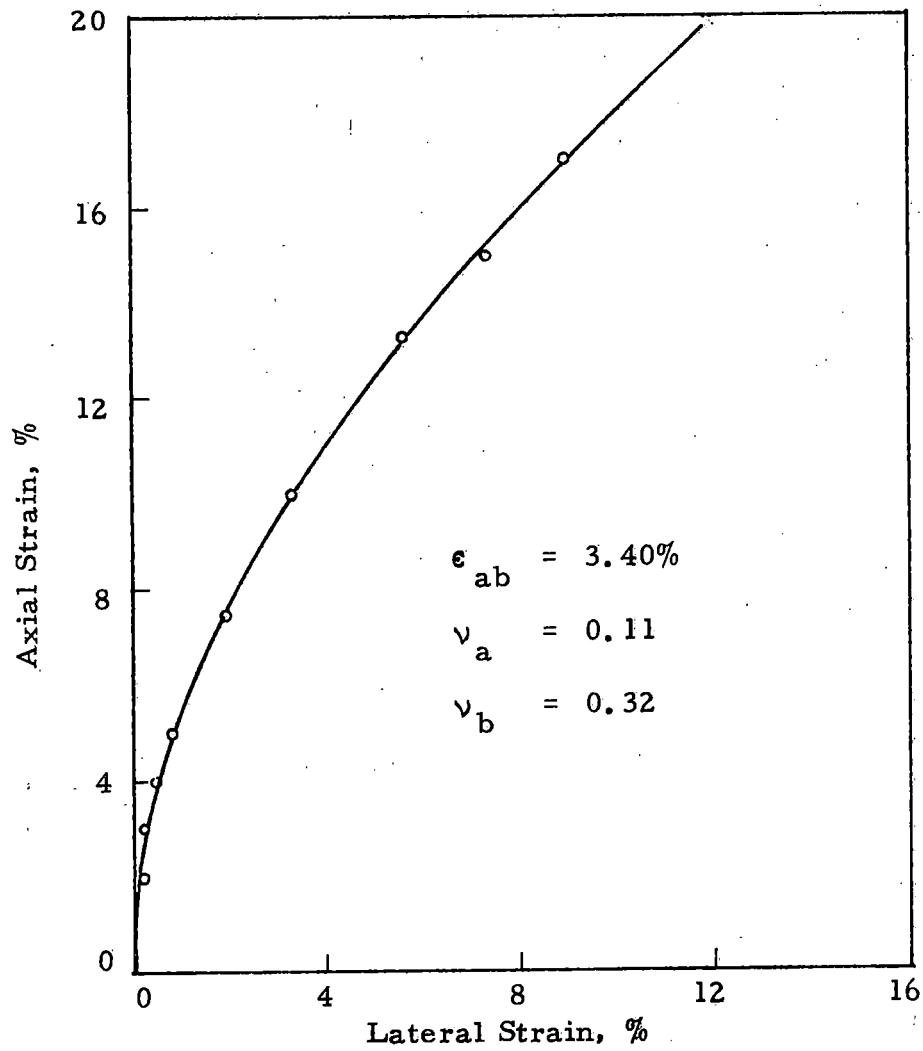


Fig. 3.37 Axial Strain versus Lateral Strain, Test No. 9

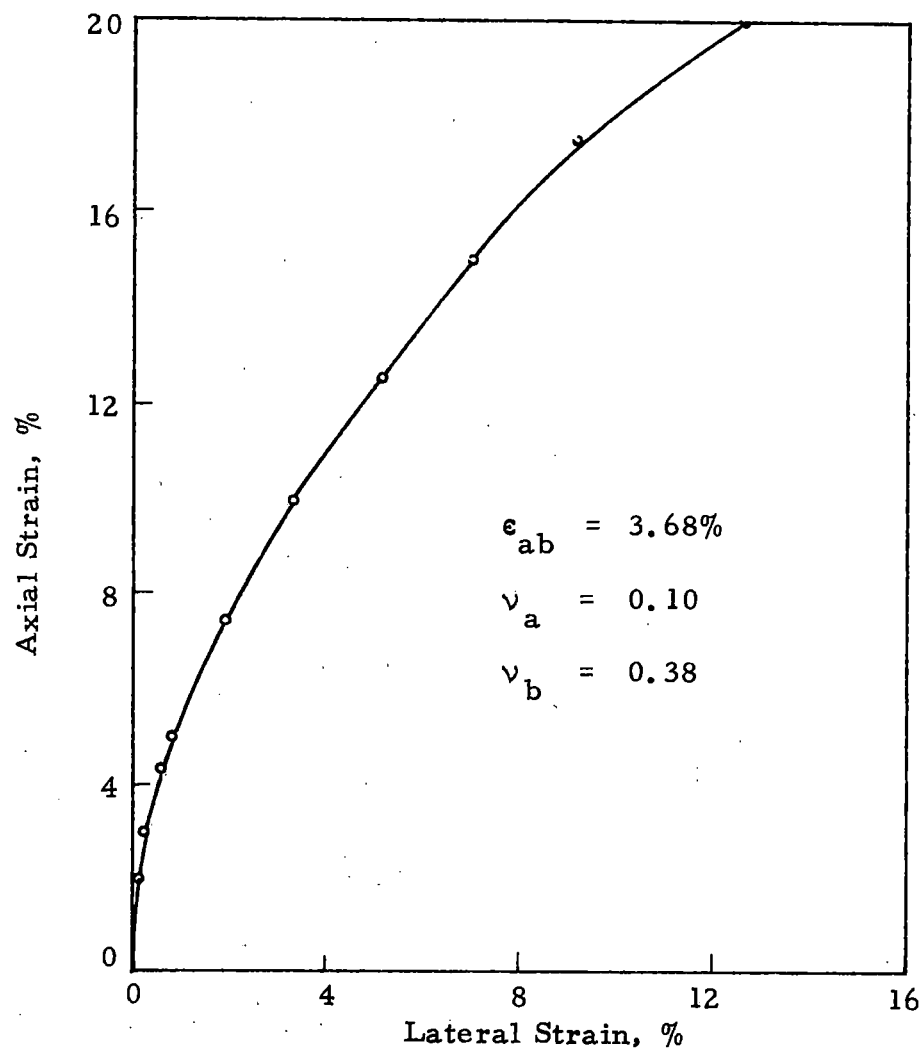


Fig. 3.38 Axial Strain versus Lateral Strain, Test No. 10

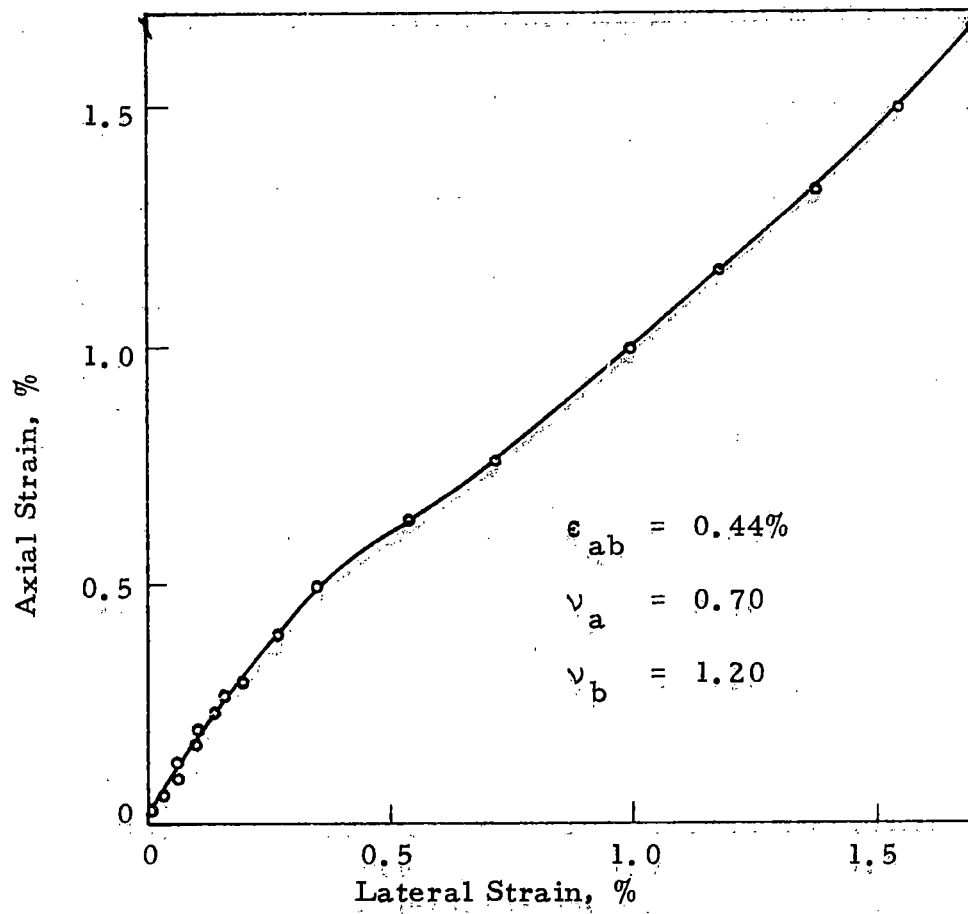


Fig. 3.39 Axial Strain versus Lateral Strain, Test No. 12

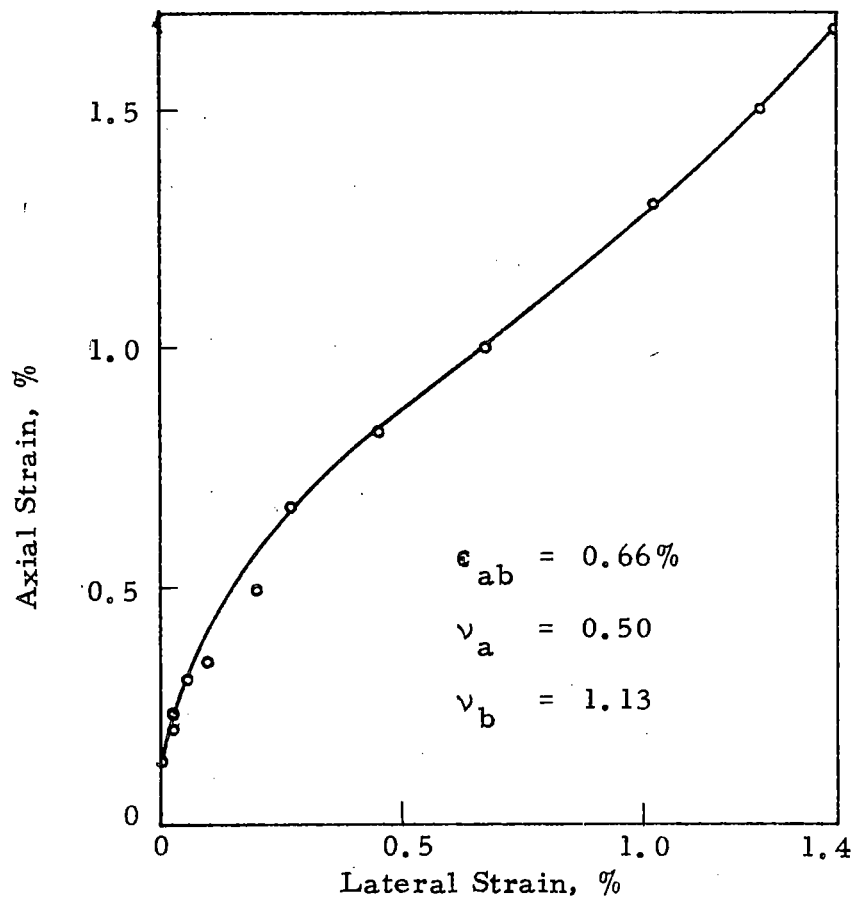


Fig. 3.40 Axial Strain versus Lateral Strain, Test No. 13

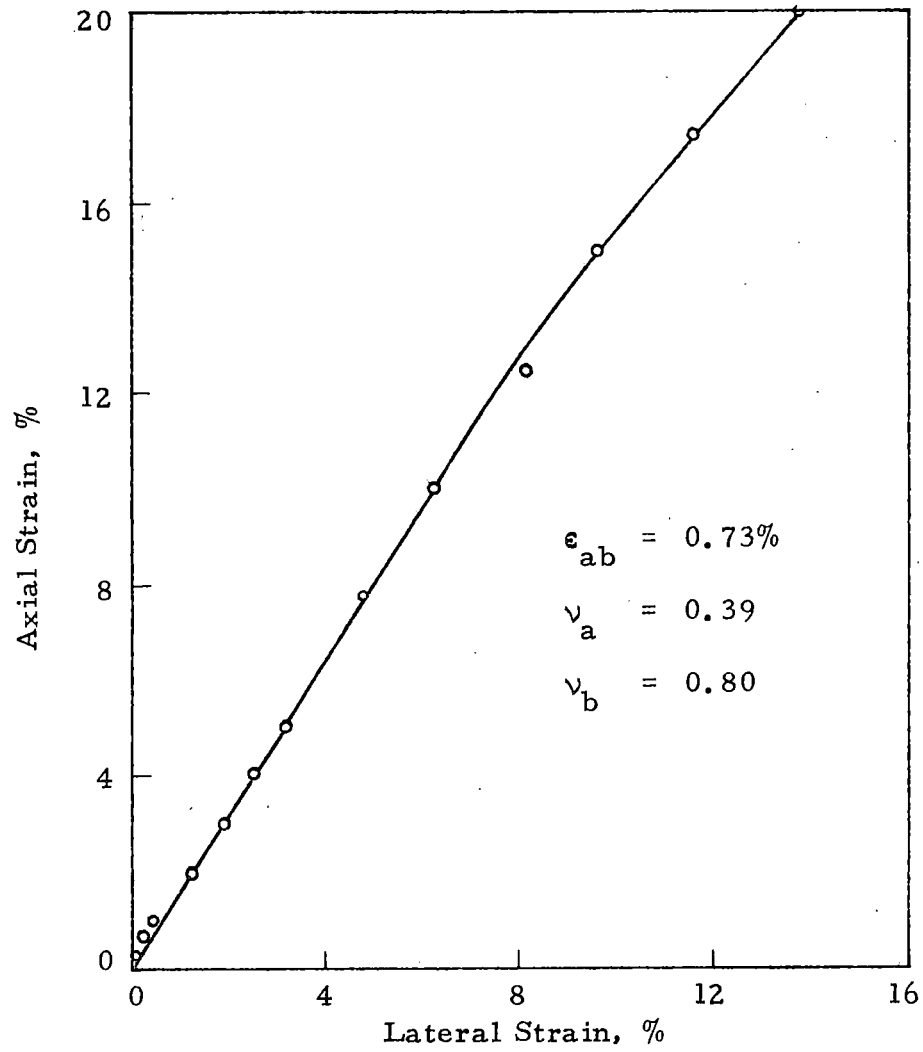


Fig. 3.41 Axial Strain versus Lateral Strain, Test No. 14

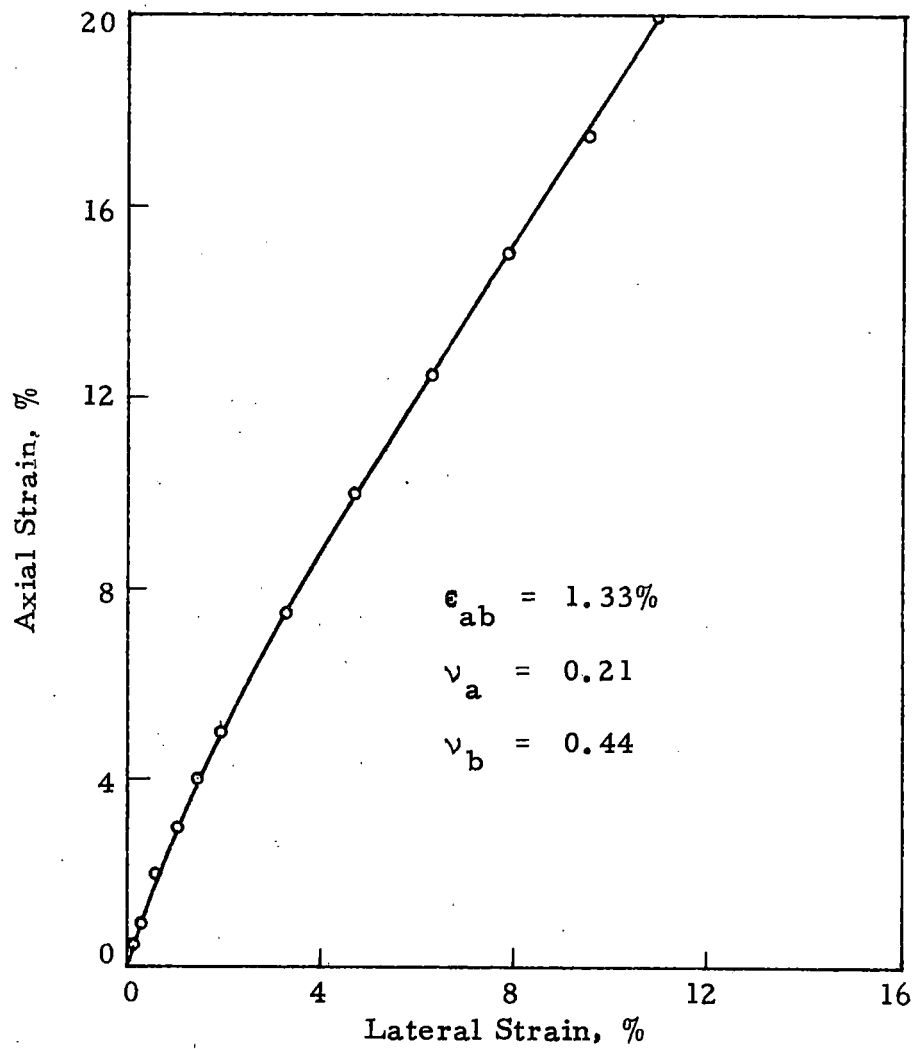


Fig. 3.42 Axial Strain versus Lateral Strain, Test No. 15

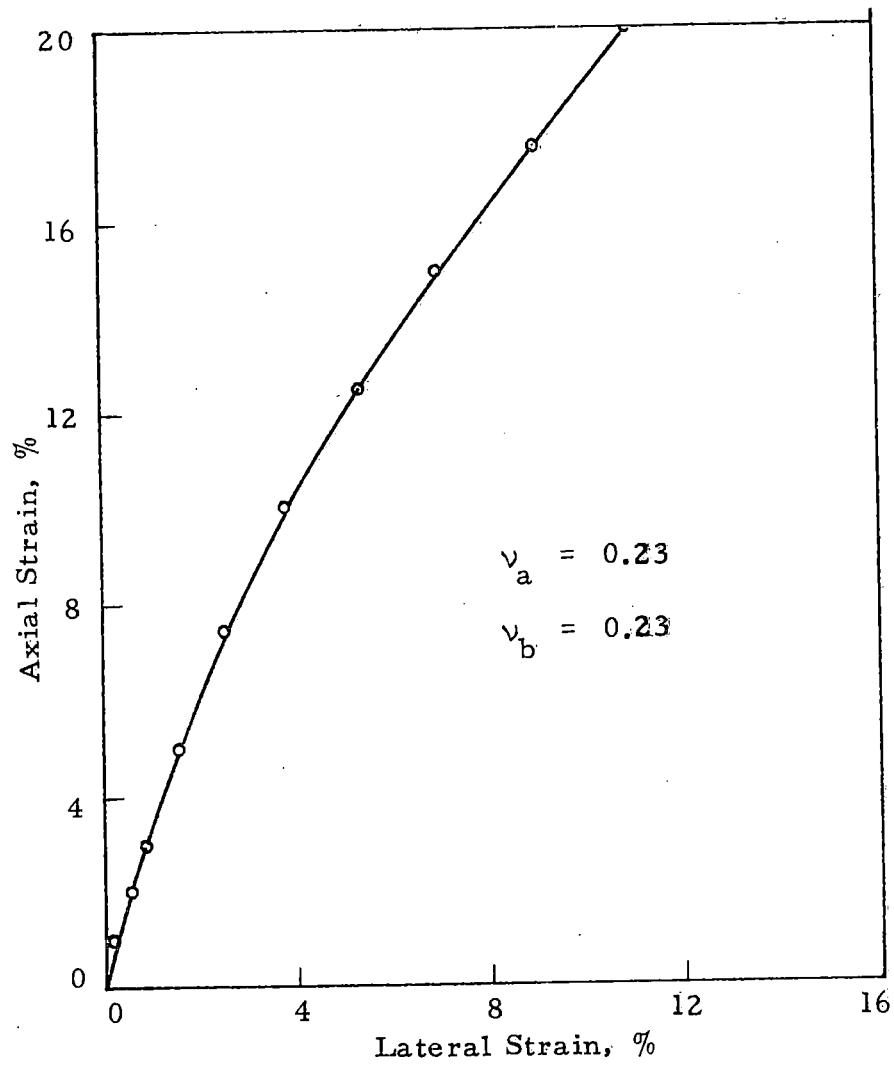


Fig. 3.43 Axial Strain versus Lateral Strain, Test No. 16

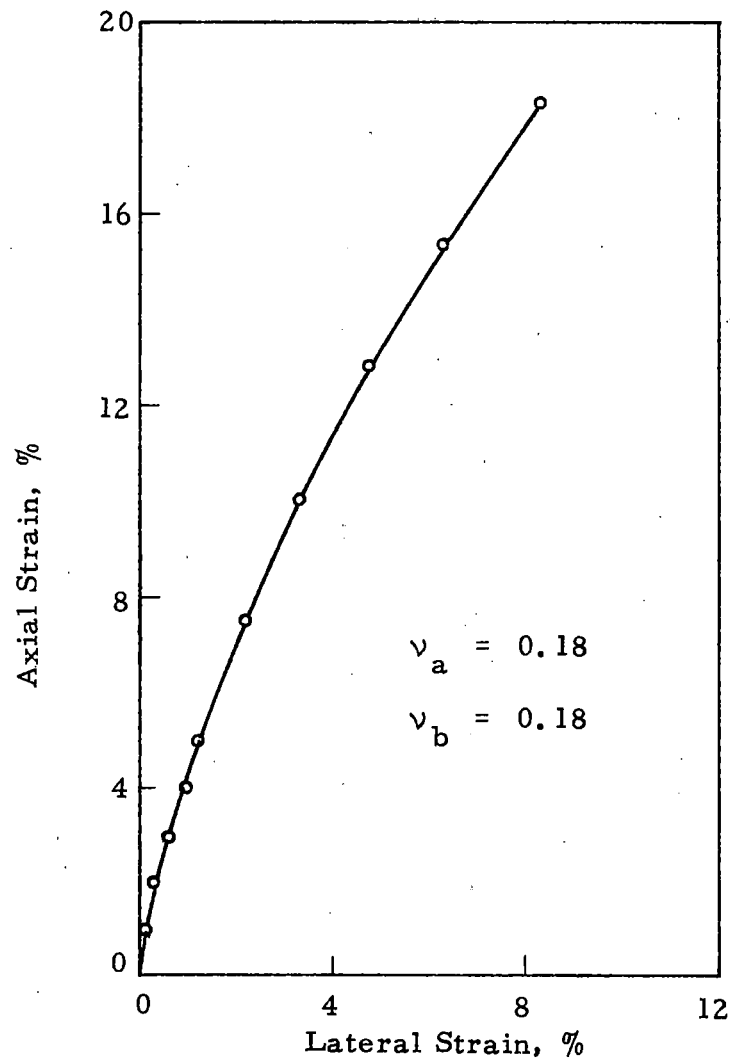


Fig. 3.44 Axial Strain versus Lateral Strain, Test No. 17

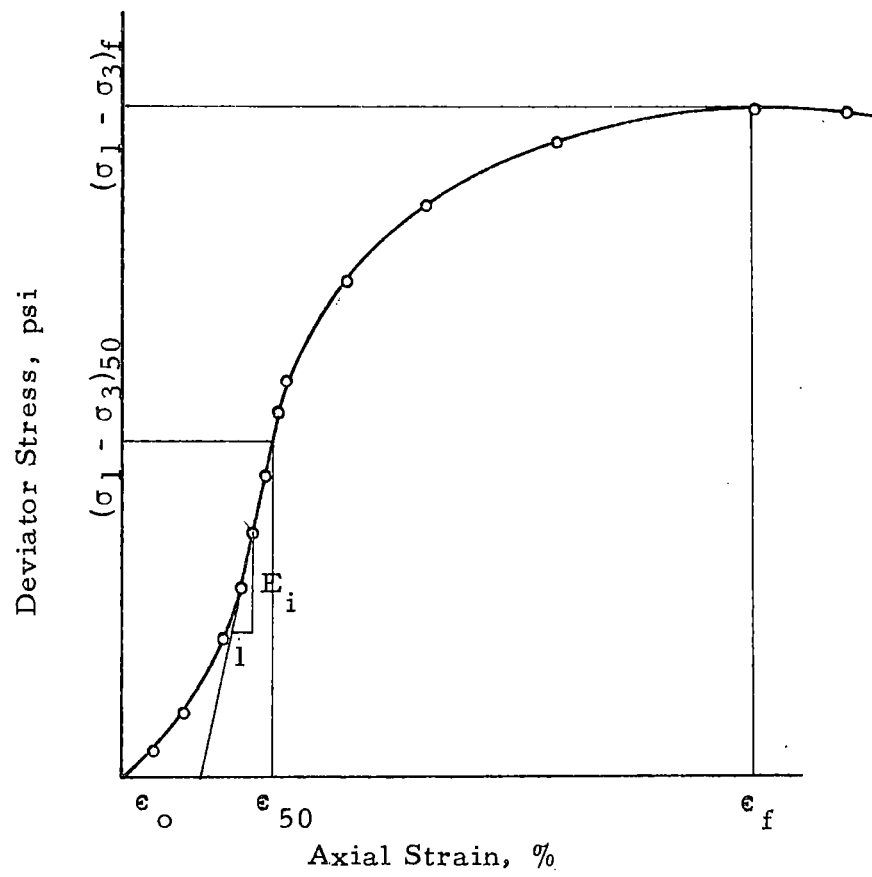


Fig. 3.45 Definition of Parameters, $(\sigma_1 - \sigma_3)_f$, $(\sigma_1 - \sigma_3)_{50}$, E_i , ϵ_0 , ϵ_{50} , ϵ_f

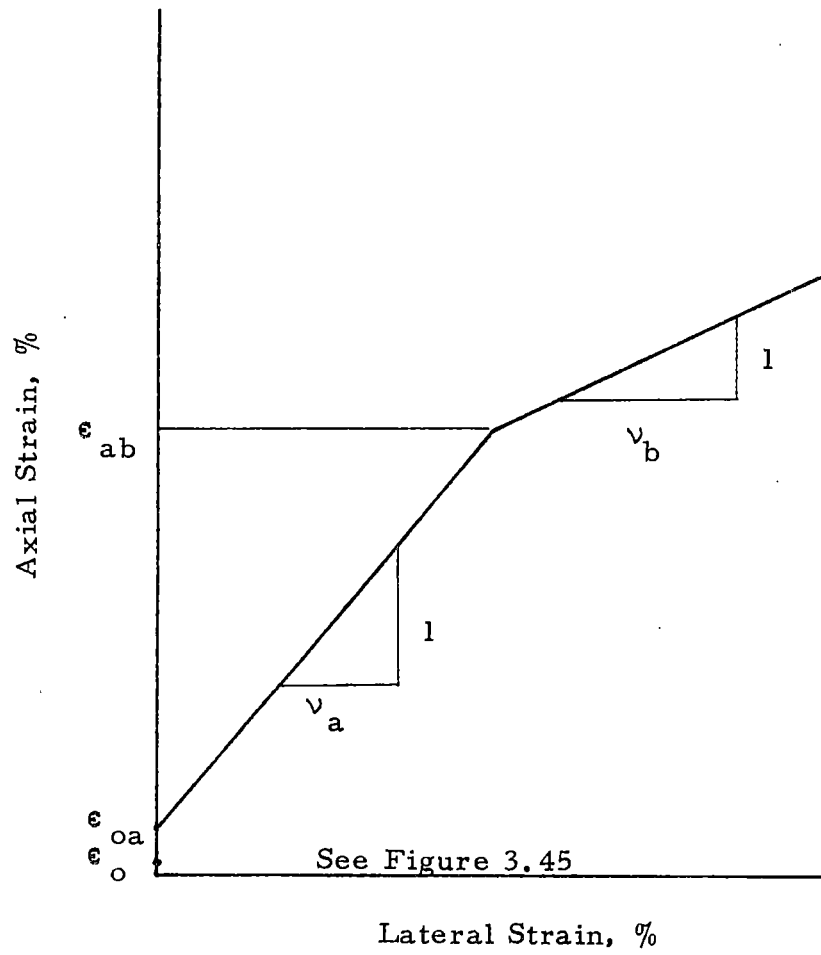


Fig. 3.46 Definition of Parameters, v_a , v_b , ϵ_{ab} , ϵ_{oa}

two straight lines with different slopes have been approximated and do not necessarily pass through each and every data point. From Figure 3.46 it is seen that the lateral strain begins to increase after axial strain has reached a certain magnitude (ϵ_{oa}). ϵ_{ab} is that value of axial strain at which the slope of the graph changes. Poisson's ratio, which is the ratio of the lateral strain to the axial strain, has been calculated for both straight line regions. All the parameters shown in Figures 3.45 and 3.46 have been tabulated in Tables 4 and 5, respectively.

3.2 Interpretation of Data

Interpretations have been made using data from both types of tests simultaneously.

Figure 3.47 is a modified Mohr-Coulomb diagram. Through the data points two straight lines have been fitted having intercepts \bar{a}_1 and \bar{a}_2 , and slopes $\bar{\alpha}_1$ and $\bar{\alpha}_2$, respectively. The intercept \bar{a} and the slope $\bar{\alpha}$ of these straight lines are related directly to the cohesion intercept \bar{c} and slope $\bar{\phi}$ of the conventional Mohr-Coulomb failure envelope.

Figure 3.48 is a plot of the stress paths for K_0 tests Nos. 1 to 3. The heavy straight line is the failure envelope obtained by

TABLE 4

STRESS-STRAIN PARAMETERS FROM TRIAXIAL COMPRESSION TESTS

<u>Test No.</u>	<u>$(\sigma_1 - \sigma_3)_f$ psi</u>	<u>$(\sigma_1 - \sigma_3)_{50}$ psi</u>	<u>ϵ_o in %</u>	<u>ϵ_{50} in %</u>	<u>ϵ_f in %</u>
1	15.60	7.80	0.02	0.25	0.68
2	24.40	12.20	0.08	0.30	0.83
3	27.30	13.65	0.16	0.39	1.00
4	34.80	17.40	0.24	0.55	20.00
5	40.00	20.00	0.02	0.30	15.80
6	57.90	28.90	0.25	2.45	20.00
7	73.60	36.80	-0.02	3.80	20.00
8	110.10	55.05	0.02	5.25	20.00
9	200.00	100.00	0.10	4.70	20.00
10	274.00	137.00	0.00	4.95	20.00
12	11.50	5.75	0.01	0.19	1.00
13	10.50	5.25	0.02	0.26	1.00
14	26.80	13.40	0.00	0.40	20.00
15	26.20	13.10	0.03	0.50	20.00
16	43.40	21.70	0.02	3.10	20.00
17	40.50	20.25	0.03	1.95	20.00

Note: Parameters are defined in Figure 3.45.

TABLE 5
STRESS-STRAIN PARAMETERS FROM TRIAXIAL TESTS

<u>Test No.</u>	ϵ_{oa} <u>in %</u>	ϵ_{ab} <u>in %</u>	ν_a	ν_b
1	0.16	0.53	0.45	2.20
2	0.22	-	0.54	-
3	0.22	0.67	0.35	0.57
4	0.37	1.12	0.38	0.38
5	0.10	0.40	0.77	0.30
6	0.50	3.00	0.14	0.50
7	1.17	4.15	0.08	0.23
8	1.50	4.10	0.22	0.62
9	1.00	3.40	0.11	0.32
10	0.10	3.68	0.10	0.38
12	0.04	0.44	0.70	1.20
13	0.15	0.66	0.50	1.13
14	0.10	0.73	0.39	0.80
15	0.05	1.33	0.21	0.44
16	0.17	-	0.23	0.23
17	0.00	-	0.18	0.18

Note: Parameters are defined in Figure 3.46.

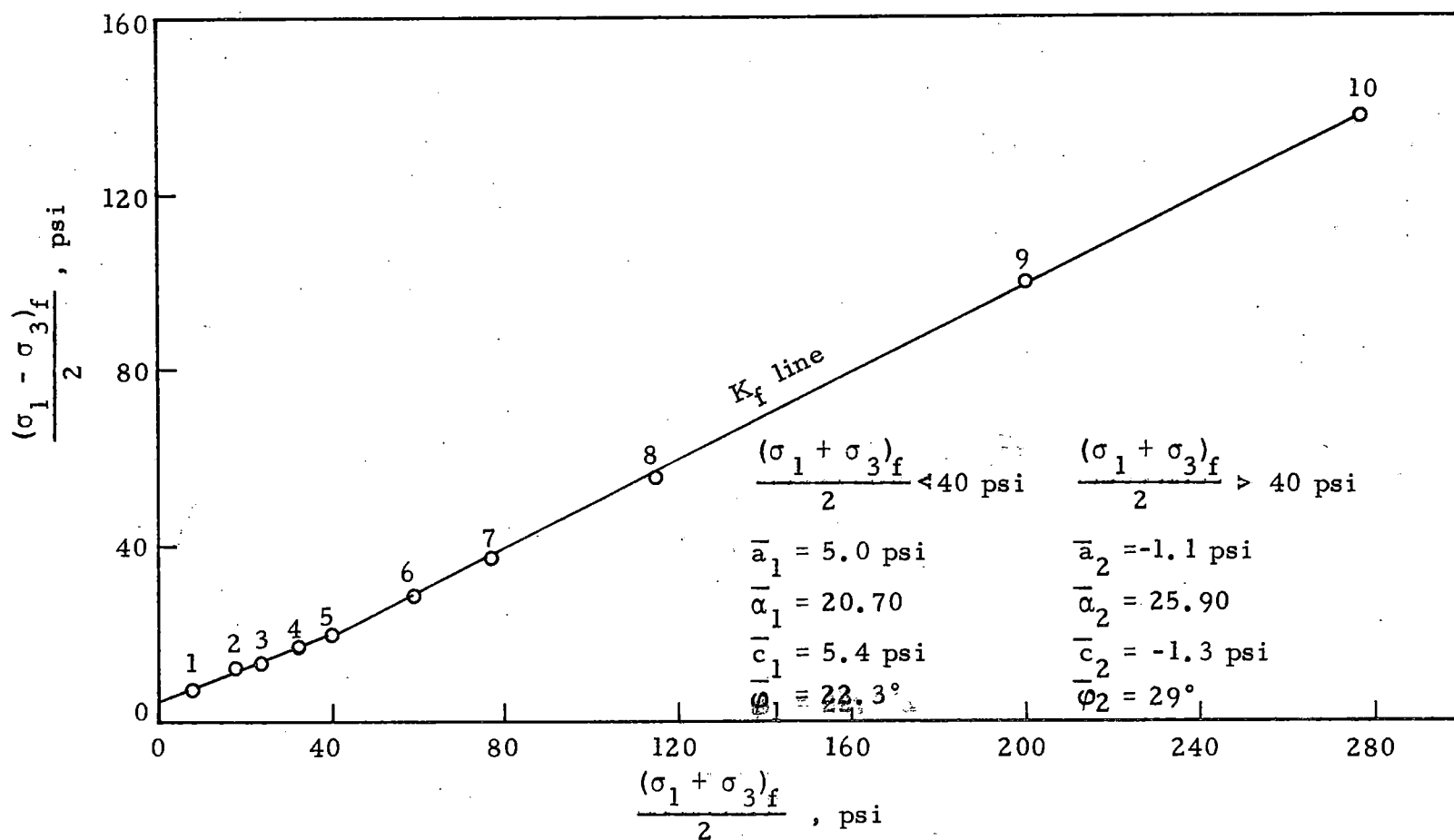


Fig. 3.47 Modified Mohr-Coulomb Diagram, Triaxial Tests Nos. 1 to 10.

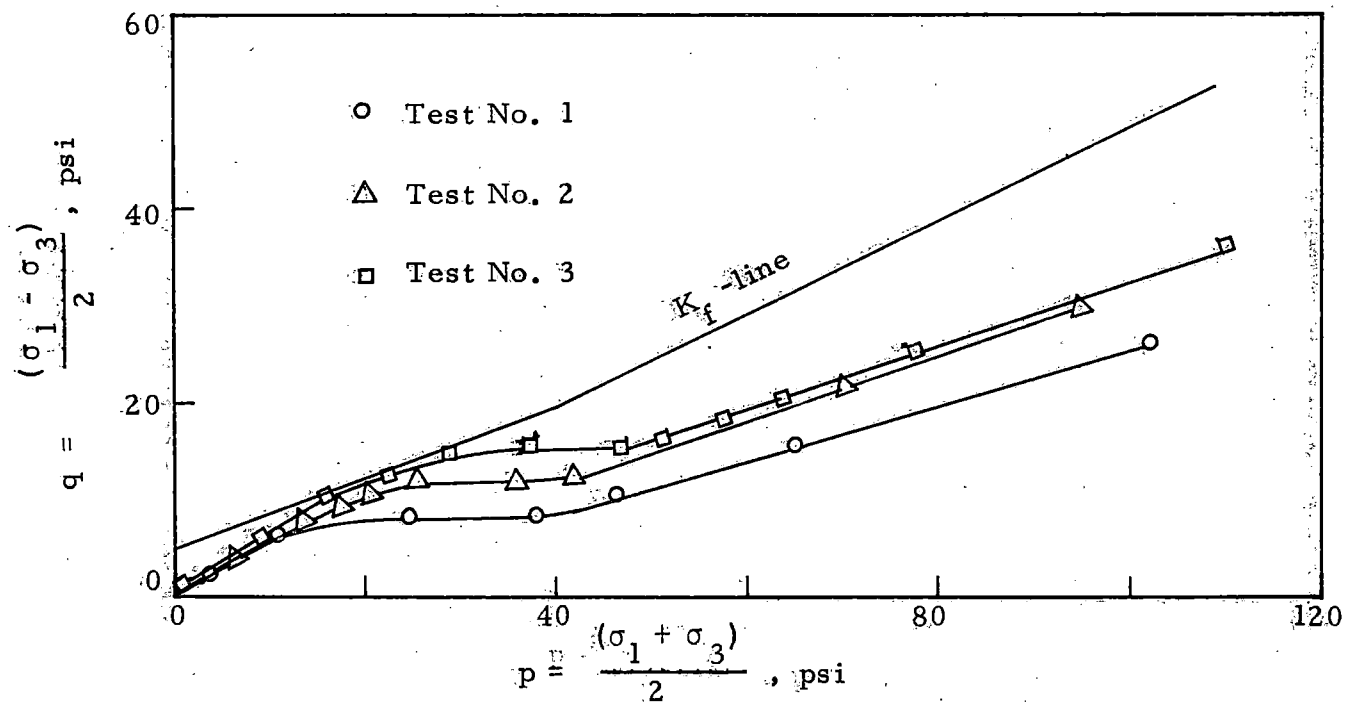


Fig. 3.48 Stress Paths for K_o - Tests Nos. 1 to 3

extending the line joining the data points for the triaxial tests 1 to 4.

This is, therefore, only the initial portion of the envelope in Figure

3.47. The plot for each K_o test is known as the K_o -line and the failure envelope is the K_f -line, (Lambe and Whitman, 1969). The K_o -line rises up from the origin and approaches the K_f -line. This region corresponds to K_{oi} . When the K_o -line intersects the K_f -line (or comes very close to it), K_o approaches unity, and the K_o -line becomes approximately horizontal between $p = 20$ and 30 psi. This represents a plastic behavior as the soil collapses. The K_o -line then increases to a slope corresponding to K_{of} .

The study of the soil can, therefore, be divided into three stages: 1) Before Collapse,

2) At Collapse and

3) After Collapse

Before Collapse

Before collapse of the soil occurs the average value of the coefficient of earth pressure at rest, K_{oi} , is 0.23 from Table 2. K_{oi} has been measured in that stage of behavior of the soil where the stress-strain curve is linear. Thus, the application of the elastic theory for any computations may be appropriate. Using the elastic theory K_o may be computed from the relation $K_o = \frac{\nu}{1 - \nu}$, where ν is Poisson's ratio in the elastic region, that is, in that stage of behavior where the stress-strain curve is linear. ν_a has been measured

in the region between ϵ_{oa} and ϵ_{ab} (Figure 3.46). From Tables 4 and 5 it is seen that the values for ϵ_{ab} are only slightly higher than, and in some cases less than, the corresponding values of ϵ_{50} . It may thus be inferred that ν_a has been measured in the region of linearity of the stress-strain curve and thus may be used in the above relation to compute K_o , the values for which have been listed in Table 6. The values range from 0.09 to 3.35. Excluding values of K_o equal to and greater than 1.0, average K_{oi} from Table 6 is 0.34, which agrees fairly well with the values from K_o tests. For most soils, good agreement exists between measured K_o values and those computed from Jaky's empirical expression $K_o = 1 - \sin \bar{\phi}$. In this case, for $\bar{\phi} = 29^\circ$, the computed K_o is 0.52, almost double the measured value. Thus the behavior of loess before collapse is unlike that of other soils.

Figure 3.49 is a plot between the initial tangent modulus (E_i) and the cell pressure. The increase in E_i with cell pressure is consistent with the behavior of other soils.

From the axial stress-strain curves for the confined compression tests, the constrained moduli D_i , D_c and D_f (defined in Figure 3.50) were measured. These are listed in Table 7. Taking advantage of the application of the elastic theory D_i was also calculated using the relation: $D_i = \frac{E_i(1-\nu)}{(1+\nu)(1-2\nu)}$ (Lambe and Whitman, 1969). The values for D_i are listed in Table 8. The values marked * indicate excessive lateral strain which may be due to irregularities and weak spots in

TABLE 6
CALCULATED VALUES OF K_o FROM TRIAXIAL TESTS

<u>Test No.</u>	<u>Initial Value of K_o, K_{oi}</u>
1	0.82
2	1.17*
3	0.54
4	0.61
5	3.35*
6	0.16
7	0.09
8	0.28
9	0.12
10	0.11
12	2.33*
13	1.00*
14	0.64
15	0.27
16	0.29
17	0.22

Average value of K_{oi} from above (excluding *) is equal to 0.34.

Average value of K_{oi} measured from K_o tests is equal to 0.23.

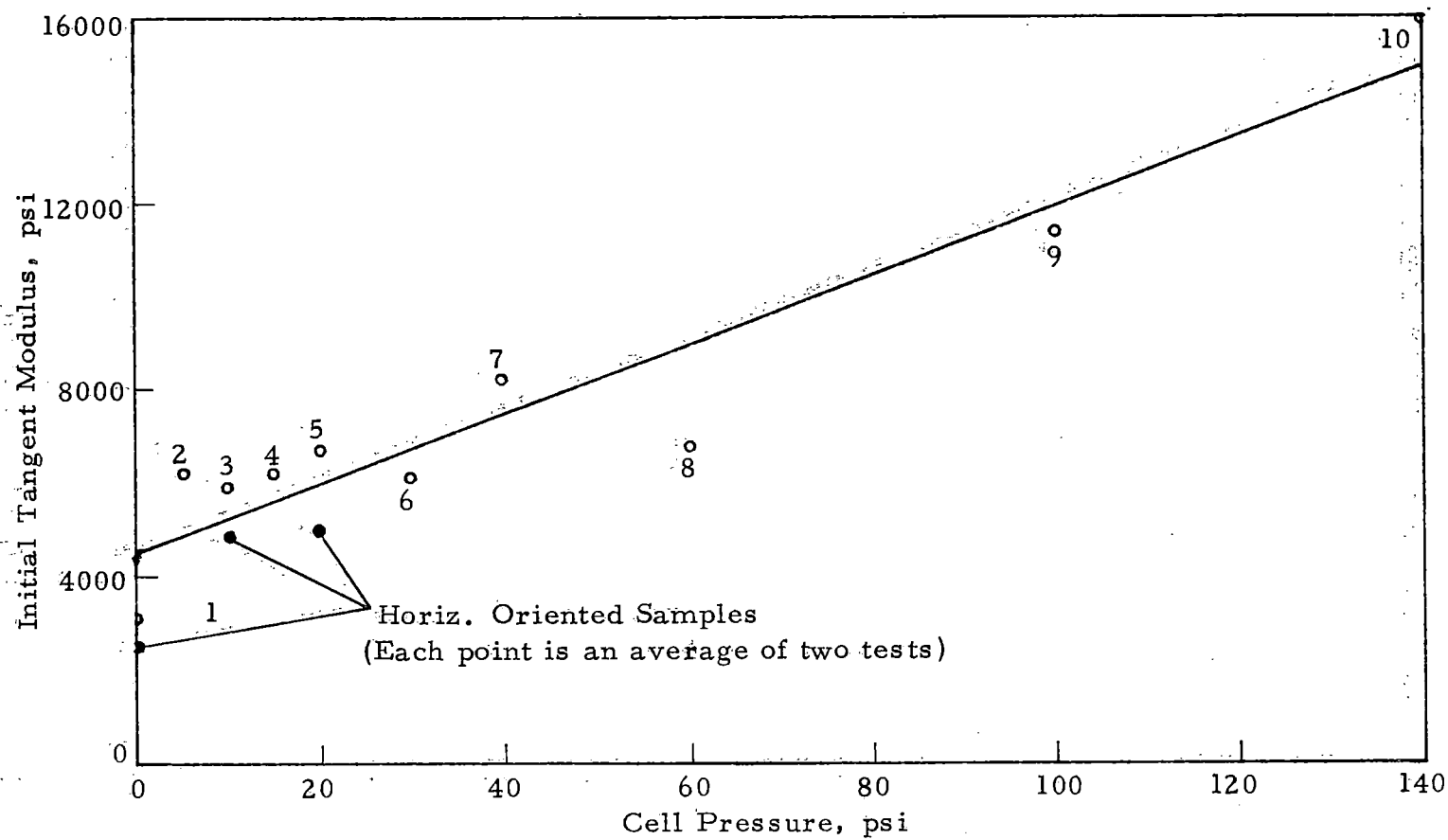


Fig. 3.49 Initial Tangent Modulus versus Cell Pressure, Triaxial Tests

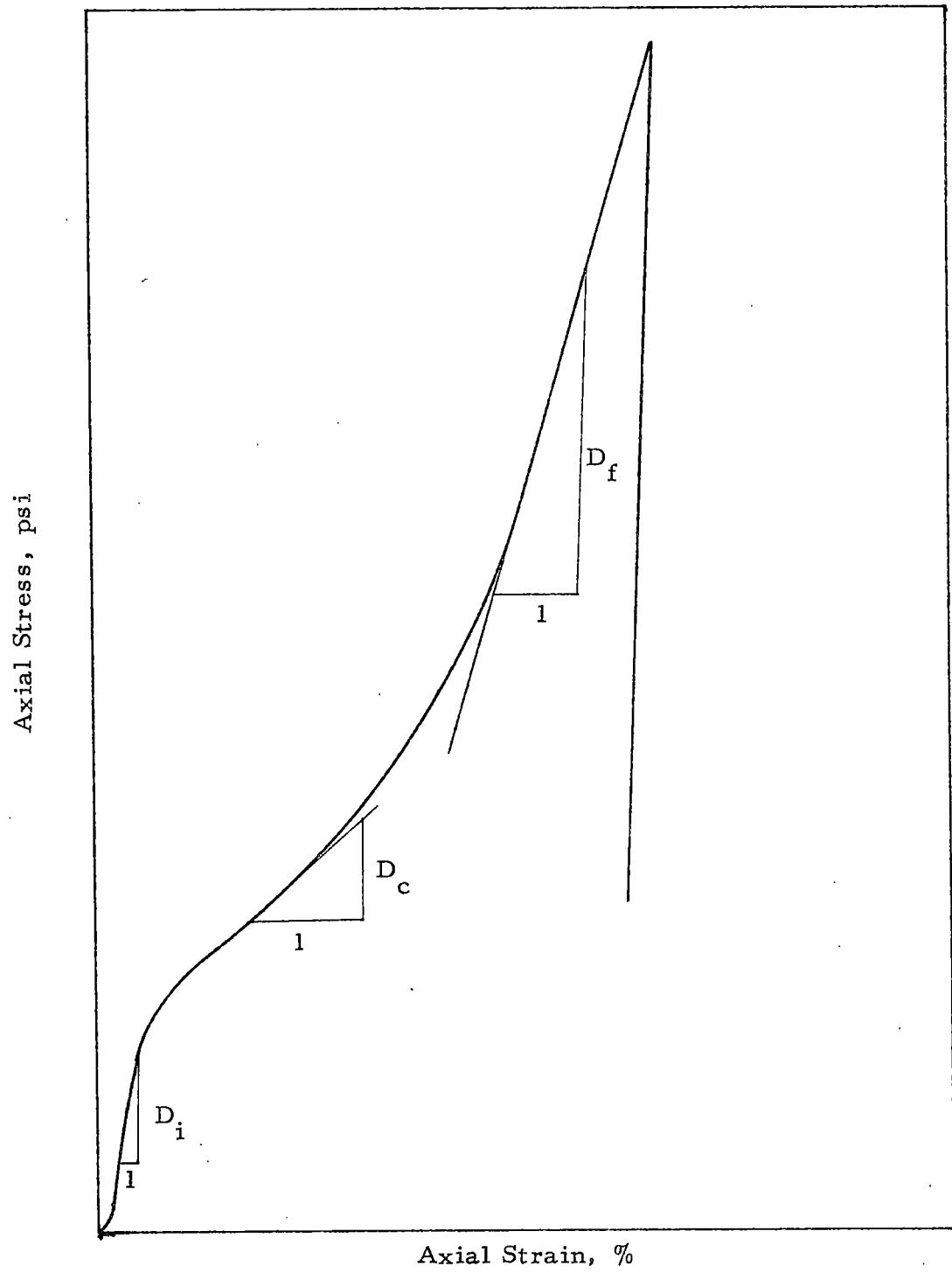


Fig. 3.50 Definition of Parameters, D_i , D_c and D_f

TABLE 7

VALUES OF CONSTRAINED MODULUS (D) FROM K_0 TESTS

<u>Test No.</u>	<u>Initial Constrained Modulus D_i, psi</u>	<u>Constrained Modulus at Collapse D_c, psi</u>	<u>Final Constrained Modulus D_f, psi</u>
1	1555	480	3810
2	2455	900	4190
3	5833	850	4286
H-1	1563	770	4000
H-2	4667	883	4000
H-3	3200	843	4286
Average	3484	787	4095

TABLE 8

CONSTRAINED MODULUS CALCULATED FROM TRIAXIAL TESTS

<u>Test No.</u>	<u>Initial Constrained Modulus D_i, psi</u>	<u>Test No.</u>	<u>Initial Constrained Modulus D_i, psi</u>
1	11759	9	11716
2	-22925*	10	16261
3	9469	12	-1337*
4	11613	13	∞ *
5	-1621*	14	10726
6	6471	15	4797
7	8382	16	5646
8	7662	17	5593

Average value of D_i from above (excluding *) is equal to 9174 psi.

the sample. The average D_i from Table 8, excluding values marked *, is 9122 psi., which is much higher than the D_i measured from the K_o tests. The difference may be due to the fact that calculated D_i is extremely sensitive to changes in Poisson's ratio.

At Collapse

Collapse of the sample occurred at about 30 to 60 psi axial stress, about 3.5 tsf on an average. This corresponds to an axial strain of 1 to 4%. The average value of the constrained modulus at collapse, D_c , was calculated to be 787 psi or 55 Kg/cm². From an earlier investigation conducted in this laboratory the constrained modulus determined at 4 tsf during a conventional consolidation test was found to be 56 Kg/cm², at the same water content. Since there is a considerable difference in the test conditions, the closeness in the values is very significant. As mentioned earlier, just before collapse the coefficient of earth pressure approaches unity and $K_o = 1$ at collapse.

After Collapse

The behavior of the soil changed after collapse. The constrained modulus increased as can be seen from Table 7. In this stage the value of the coefficient of earth pressure at rest K_{of} was obtained as 0.54. Using the angle of shearing resistance to determine K_o (from Jaky's empirical equation $K_o = 1 - \sin \bar{\phi}$), the value for the coefficient is 0.52, showing an excellent agreement. The behavior of loess in this stage is consistent with the behavior of most other soils.

Chapter 4

SUMMARY AND CONCLUSIONS

4.1 Summary

The primary purpose of this study on an undisturbed loess was to measure the coefficient of earth pressure at rest and the Poisson's ratio. A single deposit was used and the soil in all the tests was at its natural water content.

Drained confined compression tests and drained triaxial compression tests were conducted and their results are summarized in Tables 2 and 3 respectively. One of the original hypothesis was that the soil might behave differently depending upon the orientation of the pads of the lateral strain indicator. Thus, the experiments were conducted with the soil sample oriented vertically and horizontally in the cell and the pads oriented along each of the directions P_1 , P_2 and P_3 (see Figure 2.4).

Various other stress-strain parameters were measured and calculated and the data from the confined compression tests was compared with the data from the triaxial compression tests. Comparisons of data were also made with results from outside sources. All these data are tabulated in Tables 4 to 8.

4.2 Conclusions

The conclusions that follow are based on test results and interpretations given in Chapter 3. It must be borne in mind that only one loess deposit was used and all the tests were conducted at natural water content in which there was little variation. These conclusions are, therefore, drawn from tests on only one typical soil and any generalizations must be made with care. It is also significant to note that this work is a pilot study in this field and the number and type of tests conducted are not enough to make any narrow and definite conclusions.

1. Three stages of behavior could be observed. They were
 - a) Before collapse,
 - b) At collapse and
 - c) After collapse,

and the behavior was distinctly different in each stage.

2. Before collapse the average measured value of K_o was 0.23. This value compared well with a calculated value based on the elastic equation $K_o = \frac{\nu}{1 - \nu}$, where ν was measured in triaxial tests. On the other hand, the Jaky empirical equation $K_o = 1 - \sin \bar{\phi}$ predicted a value double the measured value.

3. At collapse $K_o = 1$. In the later stage, after collapse, $K_o = 0.54$. This compared well with the value 0.52 predicted by

Jaky's empirical equation. Thus, Jaky's equation is valid for loess, but only after collapse; that is, when axial strains are in excess of 4%.

4. The measured values of ν before collapse show a very wide scatter, the average value being 0.33. Because of this scatter there is poor agreement between the measured values of constrained modulus D_i , and those computed using E_i and ν_a , measured in the triaxial tests.

REFERENCES

1. Bishop, A. W., and Henkel, D. J., (1957), "The Measurement of Soil Properties in the Triaxial Test," Edward Arnold, London, 190 pp.
2. Bishop, A. W., (1958), "The Test Requirements for Measuring the Coefficient of Earth Pressure at Rest," Brussels Conference on Earth Pressure Problems, Vol. 1, pp. 2-14.
3. Bjerrum, L., Kringstad, S., and Kunmenaje, O., (1961), "The Shear Strength of a Fine Sand," Proceedings of the Fifth International Conference on Soil Mechanics and Foundation Engineering, Vol. 1, pp. 29-37.
4. Chi-In, H., (1957), "A New Apparatus for the Determination of the Coefficient of Lateral Earth Pressure at Rest," Scientia Sinica, Vol. VII, No. 6.
5. Ho, M. M. K., (1967), "The Effect of Swelling on Swelling Pressures," Proceedings, Third Asian Regional Conference on Soil Mechanics and Foundation Engineering, Haifa, pp. 90-93.
6. Kane, H., (1968), "A Mechanistic Explanation of the Physical Properties of Undisturbed Loess," Final Report, Research Project HR-126, Iowa State Highway Commission, February 1968, 113 pp.
7. Kane, H., (1969), "Consolidation of Two Loessial Soils," Highway Research Record, Highway Research Board.
8. Kenney, T. C., (1967), "Field Measurement of In-Situ Stresses in Quick Clays," Proceedings, Geotechnical Conference, Oslo, Norwegian Geotechnical Institute, Publication No. 76, pp. 15-21.

9. Kjellman, W., (1936), "Report on an Apparatus for Consummate Investigation of the Mechanical Properties of Soils," Proceedings, First International Conference on Soil Mechanics and Foundation Engineering, Cambridge, Vol. II, pp. 16-20.
10. Kjellman, W., and Jakobson, B., (1955), "Some Relations Between Stress and Strain in Coarse-Grained Cohesionless Materials," Bulletin No. 9, Proceedings of the Royal Swedish Geotechnical Institute, Stockholm.
11. Komornik, A., and Zeitlin, J. G., (1965), "An Apparatus for Measuring Lateral Soil Swelling Pressure in the Laboratory," Proceedings, Sixth International Conference on Soil Mechanics and Foundation Engineering, Vol. I, pp. 278-281.
12. Lambe, T. W., and Whitman, R. V., (1969), "Soil Mechanics," John Wiley and Sons, Inc., New York, 553 pp.
13. Morgenstern, N. R., and Eisenstein, Z., (1970), "Methods of Estimating Lateral Loads and Deformations," 1970 Specialty Conference, Lateral Stresses in the Ground and Design of Earth Retaining Structures, Sponsored by Soil Mechanics and Foundations Division, A.S.C.E., Ithaca, New York.
14. Terzaghi, K., (1920), "Old Earth-Pressure Theories and New Test Results," Engineering News Record, Vol. 85, No. 14, September 30, pp. 632-637.
15. Tschebotarioff, G. P., (1951), "Soil Mechanics, Foundations and Earth Structures," McGraw-Hill Book Co., Inc., New York, 655 pp.